LEABHARLANN CHOLÁISTE NA TRÍONÓIDE, BAILE ÁTHA CLIATH | TRINITY COLLEGE LIBRARY DUBLIN
Ollscoil Átha Cliath | The University of Dublin

Terms and Conditions of Use of Digitised Theses from Trinity College Library Dublin

Copyright statement

All material supplied by Trinity College Library is protected by copyright (under the Copyright and Related Rights Act, 2000 as amended) and other relevant Intellectual Property Rights. By accessing and using a Digitised Thesis from Trinity College Library you acknowledge that all Intellectual Property Rights in any Works supplied are the sole and exclusive property of the copyright and/or other IPR holder. Specific copyright holders may not be explicitly identified. Use of materials from other sources within a thesis should not be construed as a claim over them.

A non-exclusive, non-transferable licence is hereby granted to those using or reproducing, in whole or in part, the material for valid purposes, providing the copyright owners are acknowledged using the normal conventions. Where specific permission to use material is required, this is identified and such permission must be sought from the copyright holder or agency cited.

Liability statement

By using a Digitised Thesis, I accept that Trinity College Dublin bears no legal responsibility for the accuracy, legality or comprehensiveness of materials contained within the thesis, and that Trinity College Dublin accepts no liability for indirect, consequential, or incidental, damages or losses arising from use of the thesis for whatever reason. Information located in a thesis may be subject to specific use constraints, details of which may not be explicitly described. It is the responsibility of potential and actual users to be aware of such constraints and to abide by them. By making use of material from a digitised thesis, you accept these copyright and disclaimer provisions. Where it is brought to the attention of Trinity College Library that there may be a breach of copyright or other restraint, it is the policy to withdraw or take down access to a thesis while the issue is being resolved.

Access Agreement

By using a Digitised Thesis from Trinity College Library you are bound by the following Terms & Conditions. Please read them carefully.

I have read and I understand the following statement: All material supplied via a Digitised Thesis from Trinity College Library is protected by copyright and other intellectual property rights, and duplication or sale of all or part of any of a thesis is not permitted, except that material may be duplicated by you for your research use or for educational purposes in electronic or print form providing the copyright owners are acknowledged using the normal conventions. You must obtain permission for any other use. Electronic or print copies may not be offered, whether for sale or otherwise to anyone. This copy has been supplied on the understanding that it is copyright material and that no quotation from the thesis may be published without proper acknowledgement.

DERIVATION OF DOPAMINERGIC NEURONS FROM EMBRYONIC AND INDUCED PLURIPOTENT STEM CELLS

BY

EMMA WILLIAMS

A dissertation submitted to the University of Dublin in candidature for the degree of Doctor of Philosophy

School of Biochemistry and Immunology
& Trinity College Institute of Neuroscience,
Trinity College
Dublin

2011

TRINITY COLLEGE
19 JUL 2011
LIBRARY DUBLIN
THESIS
9118

DECLARATION

I declare that none of the work presented in this thesis has been submitted for any degree at this or at any other University. I declare this thesis is entirely my work. I agree that the library may lend or copy this thesis upon request.

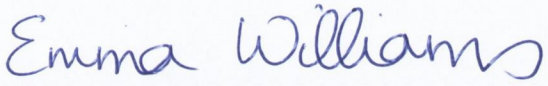

Emma Williams

ACKNOWLEDGEMENTS

I would sincerely like to thank my supervisor, Dr. Gavin Davey, who provided much encouragement, enthusiasm and optimism during the time I spent carrying out the work of this thesis. I would also like to express thanks to Prof. Keith Tipton for providing the use of his lab. I am indebted to Dr. Thorsten Lau, who made me feel very welcome when I spent time in Mannheim, taught me the essential techniques of this thesis and answered countless emails over the years. I would also like to acknowledge Prof. Patrick Schloss who allowed me to work in his lab while I was in Mannheim.

I cannot forget about all the people, past and present, that I have spent time with in lab one and helped to make it such a unique experience. The list grows the longer I am here and includes Stephen, Sonia, Laura, Jayne, Sean, Susan, Wenhao, Aldo, Darragh, Eloy, Rashmi, Aoife, Tania and Jeff. Without them I may not have survived the last four years.

I am also extremely grateful for my friends who I met in my very first week in Trinity eight years ago, you have provided much needed relief when experiments haven't worked and I needed to complain. Jim has also provided me with many laughs during the last four years and helped me see that there was light at the end of the tunnel.

I would also like to thank my family, who have supported me throughout all the years I've spent in college. I promise that I will now always be on time and get a real job! Sincere thanks must also go to my sister Sian, who has always provided me with support and guidance. Somehow you also managed to keep the house together, even with a newborn baby, while I was locked away in my room at my computer writing this thesis. And finally to Noah, whose arrival four weeks early made me realise if I could remain calm and level headed through that, anything was achievable. You have provided me with many smiles over the last 6 months.

Financial support from this work was provided by the Irish Research Council for Science, Engineering and Technology and is gratefully acknowledged.

SUMMARY

Dopamine (DA) neurons have several fundamental functions in the brain, dysfunction of which has been implicated in neurological and psychiatric disorders, including Parkinson's disease (PD) and schizophrenia. Embryonic stem cells (ESCs) and induced pluripotent stem cells (iPSCs) may provide an unlimited source of DA neurons for *in vitro* studies as they can be propagated indefinitely in culture in an undifferentiated state while retaining pluripotency. Interest has also focused on the use of DA neurons derived from these cells for regenerative medicine in PD. However, the potential of ESCs and iPSCs is greatly hindered by the heterogonous nature of cultures even after directed differentiation, with multiple cell types often of more than one germ layer being present. This may be partly or wholly overcome by expression of a marker, such as enhanced green fluorescent protein (EGFP), from a cell specific promoter, thus allowing both the selection of a particular cell type from a mixed cell population by fluorescent activated cell sorting (FACS) and differentiation to be followed in real time in live cells.

The dopamine transporter (DAT) is exclusively expressed in DA neurons in the brain and thus is a unique marker of these cells. Therefore, expression of EGFP under the control of the DAT promoter may label DA neurons, and the creation of such a stable mouse ESC line was a fundamental aim of this study. To this end, a vector was constructed to express EGFP from the mouse DAT promoter contained within a bacterial artificial chromosome (BAC). Transfection of this vector into ESCs and selection by antibiotic resistance generated 42 clones. Further analysis of these clones by polymerase chain reaction (PCR) of genomic DNA for the EGFP transgene identified 7 positive clones. However, following expansion and dopaminergic neuronal differentiation, no clones expressed detectable levels of EGFP protein even though DAT protein was observed.

Expression of EGFP from neural specific promoters, such as Sox1, in ESCs may allow sorting of neural precursors (NPs) during early neural differentiation by FACS. These cells may then be further amplified and differentiated *in vitro*. Such a Sox1-GFP reporter ESC line has previously been established and, while inconclusive, reports suggest that enriched populations of DA neurons can be obtained from this cell line. Therefore, the dopaminergic

differentiation potential of these cells was initially determined using a fast and efficient dopaminergic differentiation method (published by collaborators), which generates DA neurons from ESCs in a shorter time period than alternative differentiation procedures and thus is advantageous. This is achieved in a multi-stage procedure by the application of signalling molecules already at early stages of the differentiation process. Differentiated cultures were found to express the DA markers DAT, tyrosine hydroxylase (TH) and Nurr1, and the pre-synaptic protein synaptophysin. Sox1-GFP was first detected in cells during the neural proliferation stage of the differentiation procedure and was down-regulated, as expected, with terminal differentiation. NPs were effectively sorted based on Sox1-GFP expression and terminal differentiation generated a highly enriched neuronal population (65 $\pm$ 9.9% neurons/total cell population). These neurons also expressed the dopaminergic markers TH and DAT.

The generation of induced pluripotent stem cells (iPSCs) from somatic cells has opened remarkable avenues for basic research and regenerative medicine, and may offer unprecedented potential for studying both neurological and psychiatric disorders associated with DA neurons. However, for the promise of iPSCs to be realised fundamental questions need to be addressed about their pluripotency and lineage commitment, which can be assessed by direct comparison to ESCs. Thus the neural differentiation efficiency of a mouse iPSC clone was examined by formation of neural stem spheres (NSSs) in suspension culture. iPSC derived NSSs were found to be remarkably similar to those derived from ESCs from the same mouse strain based on morphological assessment, neuroectodermal and neuronal marker expression. The efficiency with which iPSCs differentiated to neurons was also analysed using a procedure in which differentiation was induced by culturing cells as monolayers in chemically defined medium. Analysis of neuronal populations after differentiation again revealed that iPSCs were remarkably similar to ESCs based on morphological analysis, Tuj1 colony number, Tuj1 colony size, neurite length and neuronal subtype marker expression, including those of the DA system.

The relevance of these results in the context of obtaining enriched DA neuronal populations from ESCs and iPSCs for further *in vitro* studies is discussed.

ABBREVIATIONS

AADC	Aromatic L-amino acid decarboxylase
AC	Adenylate cyclase
ADHD	Attention Deficit Hyperactivity Disorder
AFP	Alpha fetoprotein
ANOVA	Analysis of variance
ATP	Adenosine triphosphate
AP	Anterior-posterior
β-MeOH	Beta-mercaptoethanol
BAC	Bacterial artificial chromosome
bp	Base pair
BCA	Bicinchoninic acid
bFGF	Basic fibroblast growth factor
bGH	Bovine growth hormone gene
BMP4	Bone morphogenetic protein 4
BSA	Bovine serum albumin
cAMP	Cyclic adenosine monophosphate
cDNA	Complimentary DNA
CFU	Colony forming units
Chlor	Chloramphenicol
CMV	Cytomegalovirus
CNS	Central nervous system
DA	Dopamine
DARPP32	Dopamine and cAMP-regulated phosphoprotein, 32 kDa
DAT	Dopamine transporter
DMEM	Dulbecco's Modified Eagle Medium
DMSO	Dimethyl sulphoxide
DNA	Deoxyribonucleic acid
dNTP	Deoxyribonucleotide triphosphate
DV	Dorso-ventral
E	Embryonic day

EAAC1	Excitatory amino acid carrier 1
EB	Embryoid body
EGF	Epidermal growth factor
E.coli	*Escherichia coli*
EGFP	Enhanced green fluorescent protein
En	Engrailed
ER	Endoplasmic reticulum
ESC	Embryonic stem cell
F	Faraday
FACS	Fluorescent activated cell sorting
FBS	Foetal bovine serum
FD	Familial dysautomonia
FGF8	Fibroblast growth factor 8
g	Relative gravitational force
GABA	Gamma aminobutyric acid
GAD	Glutamic acid decarboxylase
GAPDH	Glyceraldehyde-3-phosphate dehydrogenase
GENSAT	Gene expression nervous system atlas
GFAP	Glial fibrillary acidic protein
GFI	Growth factor induced
GFP	Green fluorescent protein
GPe	External segment of the globus pallidus
GPi	Internal segment of the globus pallidus
HRP	Horse radish peroxidase
iPSC	Induced pluripotent stem cell
IRES	Internal ribosomal entry site
Kan	Kanamycin
kb	Kilobase
kDa	Kilodalton
KO-DMEM	Knock-out Dulbecco's Modified Eagle Medium
kV	kilovolt
l	Litre

L-AA	L-ascorbic acid
L-DOPA	L-dihydroxyphenylalanine
LB broth	Luria-Bertani broth
LIF	Leukemia inhibitory factor
LRRK2	Leucine-Rich Repeat Kinase 2
M	Molar
mA	Milliamp
mDA	Mesencephalic dopamine
MEF	Mouse embryonic fibroblast
MHR	Mid-/hindbrain region
min	Minute
NAT	Noradrenaline transporter
NEAA	Non-essential amino acids
Neo	Neomycin selection cassette
NeuN	Neuronal nuclei
Ngn2	Neurogenin 2
NP	Neural precursor
NSS	Neural stem sphere
OD_{600}	Optical density at 600 nm
ORF	Open reading frame
PBS	Phosphate buffered saline solution
PCR	Polymerase chain reaction
PDL	Poly-D-lysine
Pen/Strep	Penicillin/streptomycin
PFA	Paraformaldehyde
PFC	Prefrontal cortex
PGK	Phosphoglycerate kinase
PH	Phase contrast
PI	Propidium iodide
PKA	cAMP-dependent protein kinase
PLO	Poly-L-ornithine
PolyA	Polyadenylation signal

RNA	Ribonucleic acid
RNase A	Ribonuclease A
rpm	Revolutions per minute
RT	Room temperature
RT-PCR	Reverse transcriptase polymerase chain reaction
s	Second
SAP	Shrimp alkaline phosphatase
SDIA	Stromal cell derived inducing activity
SDS	Sodium lauryl sulphate
SEM	Standard error of the mean
SERT	Serotonin transporter
Shh	Sonic hedgehog
SMA	Spinal muscular atrophy
SNpc	Substantia nigra pars compacta
SNpr	Substantia nigra pars reticulata
SSEA1	Stage specific embryonic antigen 1
STN	Subthalamic nucleus
TAE	Tris-acetate EDTA solution
TBS	Tris buffered saline solution
TH	Tyrosine hydroxylase
U	Units of enzyme activity
UV	Ultraviolet
UTR	Untranslated region
V	Volts
VMAT2	Vesicular monoamine transporter 2
VTA	Ventral tegmental area
v/v	Volume per unit volume
w/v	Weight per unit volume

CONTENTS

Page number

Chapter 1 General introduction 1

1.1 Overview of dopamine system in the brain 2
1.2 Synthesis and metabolism of dopamine 2
1.3 Dopamine signalling 4
1.4 Dopaminergic cell groups in the brain 7
1.5 Mesencephalic dopaminergic pathways 9
1.5.1 Nigrostriatal pathway and movement 8
1.5.1.1 Parkinson's disease 11
1.5.2 Mesolimbic pathway and motivation 12
1.5.2.1 Addiction 14
1.5.3 Mesocortical pathway and cognition 15
1.5.3.1 Schizophrenia 15
1.5.3.2 Attention deficit hyperactivity disorder 17
1.6 Mesencephalic dopamine neuron development 19
1.6.1 Early neural development 19
1.6.2 Development of the isthmus 20
1.6.3 Induction of mesencephalic dopamine neurons 20
1.6.4 Specification of mesencephalic dopamine neurons 23
1.6.5 Further differentiation and maintenance of mesencephalic dopamine neurons 25
1.6.5.1 Nurr1 25
1.6.5.2 Lmx1b 26
1.6.5.3 Pitx3 26
1.6.5.4 Engrailed 1 and 2 27
1.7 Embryonic stem cells 28
1.7.1 Derivation of dopamine neurons from embryonic stem cells 29
1.7.2 Direction visualisation and selection of ESC derived dopamine neurons 31
1.7.2.1 Strategies to target EGFP to cell specific promoters 31

1.7.2.2 Strategies to enrich ESC derived dopamine neurons 32
1.8 Induced pluripotent stem cells 34
1.8.1 Generation of iPSCs 35
1.8.2 Application of iPSCs to neurodegenerative and psychiatric disorders 37
1.9 Aims of thesis 40

Chapter 2 General methods 41

2.1 Materials 42
2.2 Preparation of buffers and solutions 43
2.3 Pipetting 44
2.4 Mouse pluripotent stem cells 44
2.5 General cell culture equipment 44
2.6 General cell culture methods 44
2.6.1 Preparation of gelatine coated dishes 44
2.6.2 Preparation of feeder cells 45
2.6.3 Propagation of mouse pluripotent stem cells 45
2.6.4 Passaging of mouse pluripotent stem cells 46
2.6.5 Cell counting and cell viability assay 46
2.6.6 Freezing of cells 47
2.6.7 Preparation of plates for neural stem sphere attachment 47
2.7 Neuronal differentiation 48
2.7.1 Growth factor induced neuronal differentiation 50
2.7.1 Monolayer neuronal differentiation 51
2.8 Determination of protein concentration 52
2.9 SDS-PAGE and Western blotting 52
2.9.1 Preparation of samples 52
2.9.2 SDS-PAGE 53
2.9.3 Semi-dry transfer of proteins to PVDF membrane 54
2.9.4 Blocking and incubation with antibodies 54
2.9.5 Chemi-luminescent protein detection 55
2.9.6 Stripping of membranes for re-probing 55

2.9.7 Semi-quantitative densitometry 55
2.10 RNA extraction and reverse-transcription polymerase chain reaction 56
2.10.1 RNA extraction from cells 56
2.10.2 Reverse-transcriptase polymerase chain reaction 56
2.11 Polymerase chain reactions 57
2.12 Agarose gel electrophoresis 57
2.13 Immunocytochemistry 58
2.14 Tuj1 positive colony measurements 59
2.15 Statistical analysis 59

Chapter 3 Targeting EGFP to the DAT promoter and analysis of selected R1 ESC DAT-EGFP transgenic cell lines 60

3.1 Introduction 61
3.2 Methods 64
3.2.1 Overview of construction of DAT-EGFP vector 64
3.2.2 DNA vectors, bacterial strains and bacterial growth medium 67
3.2.3 DNA based cloning methods 68
3.2.3.1 Restriction endonuclease digestion 68
3.2.3.2 Blunting of DNA fragments 68
3.2.3.3 Dephosphorylation of linearised plasmid DNA 69
3.2.3.4 Ligation of DNA fragments 69
3.2.3.5 Polymerase chain reactions 69
3.2.4 Methods used to purify DNA 71
3.2.4.1 Purification of DNA fragments 71
3.2.4.1.1 QIAquick gel extraction 71
3.2.4.1.2 QIAquick PCR purification 72
3.2.4.2 Small scale purification of plasmid DNA 72
3.2.4.3 Large scale purification of plasmid DNA 73
3.2.4.4 Large scale purification of BAC DNA 74
3.2.5 Methods used to prepare and transform bacteria 75
3.2.5.1 Preparation of chemocompetent bacteria 75

3.2.5.2 Transformation of chemocompetent bacteria 76
3.2.5.3 Preparation of EL250 bacteria for recombineering 76
3.2.5.4 Transformation of EL250 bacteria 77
3.2.5.5 Preparation of electrocompetent bacteria 77
3.2.5.6 Transformation of electrocompetent bacteria 78
3.3.6 Methods used to transfect R1 ESCs and analyse antibiotic resistant clones 78
3.2.6.1 Determination of optimal G418 concentration to select stable clones 79
3.2.6.2 Transfection of R1 ESCs 79
3.2.6.2.1 Transient transfection of R1 ESCs and determination of transfection efficiency 79
3.2.6.2.2 Stable transfection of R1 ESCs 80
3.2.6.3 Picking of antibiotic resistant clones 82
3.2.6.4 Freezing of antibiotic resistant clones 82
3.2.6.5 Extraction of genomic DNA from antibiotic resistant clones 83
3.2.6.6 Expansion and neuronal differentiation of positive clones 83
3.4 Results 84
3.4.1 Construction of BAC-DAT vector 84
3.4.2 Analysis of antibiotic resistant clones after transfection and selection 86
3.4.3 Dopaminergic differentiation and analysis of R1 ESC DAT-EGFP transgenic cell lines 90
3.5 Discussion 99

Chapter 4 Derivation of dopaminergic neurons from Sox1-GFP embryonic stem cells 107

4.1 Introduction 108
4.2 Methods 111
4.2.1 Analysis of GFP expression during neuronal differentiation of Sox1-GFP ESCs 111
4.2.2 FACS based purification of Sox1-GFP neural precursors 112

4.2.3 Analysis of Sox1-GFP sorted samples after growth factor induced neuronal differentiation 112
4.3 Results 113
4.3.1 Comparison of neuronal populations derived from Sox1-GFP ESCs following growth factor induced and monolayer neuronal differentiation procedures 113
4.3.2. Comparison of neuronal populations derived from Sox1-GFP ESCs on day 10 and day 16 of the terminal differentiation stage of the growth factor induced neuronal differentiation procedure 124
4.3.3 Comparison of Sox1-GFP expression during growth factor induced and monolayer neuronal differentiation procedures 134
4.3.4 Isolation and analysis of Sox1-GFP expressing neural precursors at the neural proliferation stage of growth factor induced differentiation 145
4.3.5 Analysis of Sox1-GFP sorted samples following growth factor induced neuronal differentiation 148
4.4 Discussion 159

Chapter 5 Comparison of neural populations derived from embryonic and induced pluripotent stem cells 170

5.1 Introduction 171
5.2 Methods 172
5.2.1 Cell proliferation and population doubling time 172
5.2.2 Embryoid body and neural stem sphere assay 173
5.3 Results 174
5.3.1 Undifferentiated iPSCs express characteristic features of pluripotent stem cells and show no difference to ESCs 174
5.3.2 iPSCs form embryoid bodies in suspension culture and show overall similarities to ESC derived embryoid bodies 174
5.3.3 iPSCs form neural stem spheres in suspension culture with a similar efficiency as ESCs and express neuroectodermal and neuronal markers 183

5.3.4 iPSCs form neurons with a similar efficiency as ESCs following monolayer neuronal differentiation 187

5.4 Discussion 203

Chapter 6 General discussion 210

6.1 Discussion 211

6.2 Future work 219

Bibliography 222

Chapter 1

General Introduction

1.1 Overview of the dopamine system in the brain

Since the discovery of dopamine (DA) as a neurotransmitter by Carlsson some 50 years ago (Carlsson et al., 1957), research into this monoamine has increased considerably and today we are aware of its role in regulating several aspects of basic brain function (for review, see Girault and Greengard, 2004). Although DA neurons are rare (<1/100,000 brain neurons) they have a modulatory role in movement behaviour, cognition, motivation and reward, and the endocrine system (for review, see Girault and Greengard, 2004). Importantly, abnormalities in the DA signalling system are implicated in a myriad of neurological and psychiatric disorders, including schizophrenia, Attention Deficit Hyperactivity Disorder (ADHD), Parkinson's disease (PD) and drug abuse (for review, see Greengard, 2001). Therefore, investigating the function, and dysfunction, of DA neurons may provide insight into the underlying causes of these disorders. Embryonic stem cells (ESCs) and induced pluripotent stem cells (iPSCs) may represent an ideal source of cells to obtain DA neurons.

1.2 Synthesis and metabolism of dopamine

DA is classified as a catecholamine as it possesses a catechol nucleus (a 3,4-dihydroxylated benzene ring) and an ethylamine side chain (for review, see Rondou et al., 2010). This neurotransmitter is synthesised in dopaminergic neurons from the amino acid tyrosine in a two step enzymatic process (Fig. 1.1) (for review, see Rondou et al., 2010). The first, rate-limiting, reaction involves the hydroxylation of tyrosine to L-dihydroxyphenylalanine (L-DOPA) by the enzyme tyrosine hydroxylase (TH). L-DOPA is subsequently decarboxylated by aromatic L-amino acid decarboxylase (AADC) to form DA. In neurons possessing the enzyme dopamine β-hydroxylase, DA can be further transformed into noradrenaline.

After synthesis, DA is packaged into synaptic vesicles by the vesicular monoamine transporter 2 (VMAT2) in preparation for exocytosis (for review, see Parsons, 2000). VMAT2 has 12 transmembrane domains and transports DA using an electrochemical gradient generated by a vesicular ATP-dependent H^+ pump (for review, see Parsons, 2000).

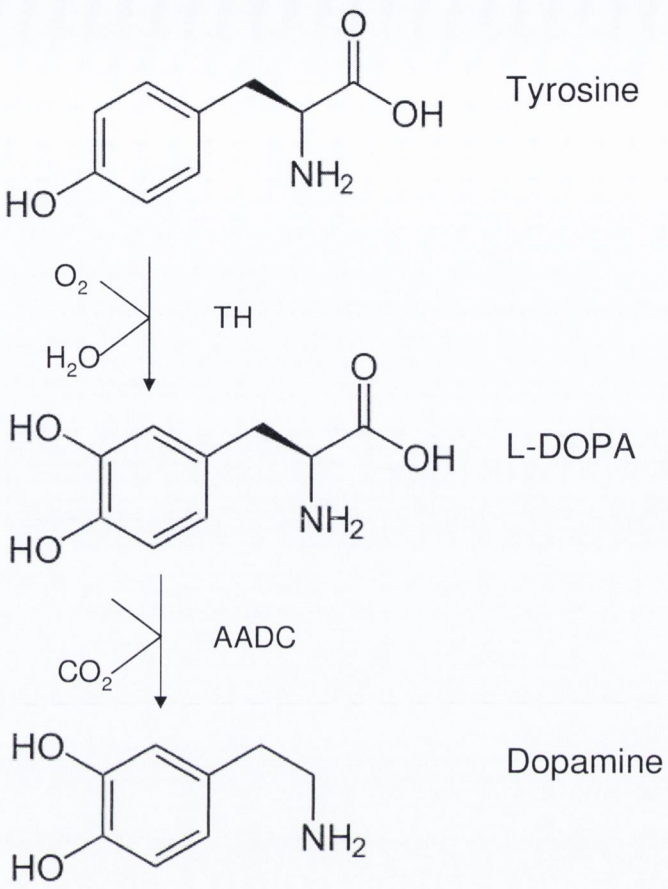

Figure 1.1: Biosynthesis of dopamine

Dopamine is synthesised from the amino acid tyrosine in a two step process. The first and rate-limiting step is catalysed by TH, using the cofactor tetrahydrobiopterin and generates L-DOPA. This is subsequently carboxylated by AADC to form dopamine. TH indicates tyrosine hydroxylase; L-DOPA, L-dihydroxyphenylalanine; AADC, aromatic L-amino acid decarboxylase. Adapted from Rondou et al. (2010).

Following signalling, the action of DA is terminated by re-uptake into DA neurons by the high affinity, cocaine sensitive dopamine transporter (DAT) (for review, see Torres et al., 2003). Transport of DA is accompanied by the co-transport of two Na^+ ions and one Cl^- ion (for review, see Torres et al., 2003). DAT is expressed exclusively in DA neurons and highest expression is observed in the ventral mesencephalic DA (mDA) cell group [substantia nigra pars compacta (SNpc) and ventral tegmental area (VTA)], where the protein is found on the dendritic plasma membrane (Augood et al., 1993; Ciliax et al., 1995; Hersch et al., 1997; Turiault et al., 2007). On DA nerve terminals, DAT is strongly expressed in the striatum and is essential for DA clearance (Ciliax et al., 1995; Jones et al., 1998; Moron et al., 2002). In this area, it is found on axons and the extrasynaptic regions of the axon terminal outside the active zone (Hersch et al., 1997). In the prefrontal cortex (PFC) DAT expression is low and DA uptake may be mediated by the noradrenaline transporter (NAT) in this area (Carboni et al., 1990; Moron et al., 2002).

After uptake by DAT, DA is metabolised or repackaged into vesicles by VMAT2 (for review, see Eisenhofer et al., 2004). Metabolism involves a two step process, with DA first being oxidatively deaminated by monoamine oxidase A to form the intermediate aldehyde 3, 4-dihydroxyphenylacetaldehyde and rapidly oxidised by aldehyde dehydrogenase to 3, 4-dihydroxyphenylacetic acid (for review, see Eisenhofer et al., 2004). In the PFC DA metabolism is thought to be mediated by catecol-O-methyl transferase, forming 3-methyoxytyramine (Karoum et al., 1994; Gogos et al., 1998; Tunbridge et al., 2004; Tunbridge et al., 2006).

1.3 Dopamine signalling

DA is classed as a slow-acting neurotransmitter, having a modulatory effect that is achieved over hundreds of milliseconds to minutes by binding to selective DA receptors (for reviews, see Greengard, 2001; Girault and Greengard, 2004). DA acts by controlling the efficacy of fast synaptic transmission by the neurotransmitters γ-aminobutyric acid (GABA) and glutamate (for review, see Greengard, 2001). The effect of DA is exerted in two ways, that is by binding to DA receptors located both pre- and postsynaptically (for review, see Greengard, 2001). At the presynaptic terminal DA regulates the

phosphorylation state of key proteins, thus modulating the efficacy of neurotransmitter release (namely, the amount of neurotransmitter released in response to an action potential) (for review, see Greengard, 2001). DA also regulates the phosphorylation state of neurotransmitter receptors present on the post-synaptic plasma membrane, thus modulating the responsivity of these receptors to released neurotransmitter (that is, the magnitude of electrophysiological response to a molecule of neurotransmitter) (for review, see Greengard, 2001).

DA receptors are metabotrophic G-protein coupled receptors, being composed of seven transmembrane domains (for reviews, see Girault and Greengard, 2004; Neve et al., 2004). Binding of DA to these receptors initiates an intracellular signalling cascades, mediated by activation of G-proteins, which modulate second messengers, protein kinases and protein phosphatases (for reviews, see Girault and Greengard, 2004; Neve et al., 2004). There are two major classes of DA receptors, the D1-like family, which is coupled to G proteins that activate adenylate cyclase (AC), and the D2-like family which is coupled to G proteins that inhibit AC (Fig. 1.2) (Kebabian et al., 1972; Stoof and Kebabian, 1981; for review, see Girault and Greengard, 2004). The D1-like family contains two subtypes, D1 and D5, while the D2-like family contains three subtypes, D2, D3 and D4 (for review, see Girault and Greengard, 2004). Stimulation of AC by the D1-like family results in elevation of cyclic adenosine monophosphate (cAMP) levels and subsequent activation of a cAMP-dependent protein kinase (PKA) (Kebabian et al., 1972). DARPP32 (dopamine and cAMP-regulated phosphoprotein, 32 kDa) is a key substrate of this enzyme (Hemmings et al., 1984b), with phosphorylation resulting in activation of this protein and subsequent inhibition of protein phosphatase 1 (Hemmings et al., 1984a). As this phosphatase controls the phosphorylation state of numerous physiological substrates, DA can modulate the activity of a large array of downstream physiological effectors (for reviews, see Greengard, 2001; Neve et al., 2004). In particular, DA mediated activation of PKA and DARPP23 has been shown to modulate the activity of the glutamatergic NMDA receptor (Snyder et al., 1998), the Na^+, K^+-dependent ATPase (Bertorello et al., 1990), Ca^{2+} channels (Surmeier et al., 1995), Na^+ channels (Surmeier et al., 1992) and gene expression (Fienberg et al., 1998).

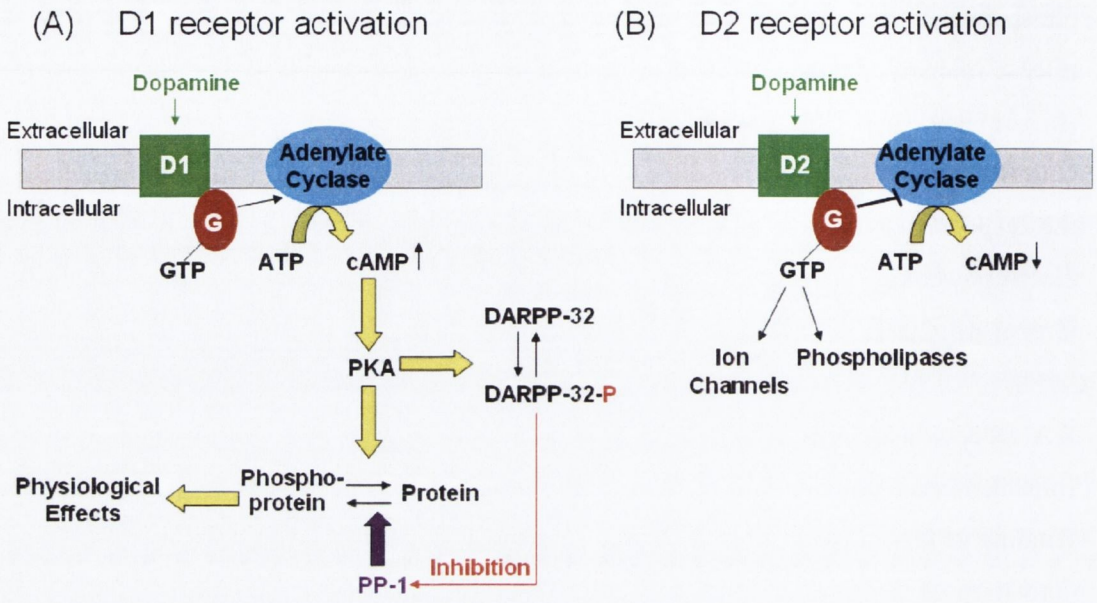

Figure 1.2: Dopamine receptor signalling

(A) Binding of dopamine to D1-like receptors results in activation of specific heterotrimeric G-proteins (G) that stimulate adenylate cyclase (AC). This leads to an elevation of cyclic adenosine monophosphate (cAMP) levels and subsequent activation of a cAMP-dependent protein kinase (PKA). DARPP32 (dopamine and cAMP-regulated phosphoprotein, 32 kDa) is a key substrate of this enzyme, with phosphorylation resulting in activation of this protein and subsequent inhibition of protein phosphatase 1 (PP1). As this phosphatase controls the phosphorylation state of numerous physiological substrates, dopamine can modulate the activity of a large array of downstream physiological effectors. (B) Binding of dopamine to D2-like receptors results in activation of specific heterotrimeric G-proteins that inhibit AC and a decrease in cAMP levels. These receptors also modulate phospholipases and ion channel conductance in the cell. ATP indicates adenosine triphosphate; GTP, guanosine triphosphate. Adapted from Girault and Greengard (2004).

In addition to inhibiting AC and reducing cAMP levels (Stoof and Kebabian, 1981), D2-like receptors also exert other effects in the cells (Fig. 1.2), including modulation of ion channel conductance (Lacey et al., 1987; Surmeier et al., 1992; Greif et al., 1995; Hernandez-Lopez et al., 2000), activation of phospholipase A_2 (Vial and Piomelli, 1995) and activation of phospholiase C (Hernandez-Lopez et al., 2000). Interestingly, D2-like receptors can also modulate the activity of DARPP32 independently of AC inhibition, with this being achieved by activating the calcium dependent protein phosphatase calcineurin, which subsequently dephosphorylates and inactivates DARPP32 (Nishi et al., 1997). The D2-like receptor family also function as autoreceptors, being located presynaptically on DA neurons and providing feedback that lowers extracellular DA levels (Mercuri et al., 1997; Khan et al., 1998; Benoit-Marand et al., 2001; Joseph et al., 2002).

1.4 Dopaminergic cell groups in the brain

The mammalian brain contains a number of distinct groups of DA neurons, designated A8-A17 depending on their structural position (Fig. 1.3) (for review, see Prakash and Wurst, 2006a). The largest of these groups is found in the ventral mesencephalon (A8-A10) (for review, see Prakash and Wurst, 2006a), with neurons projecting to different regions of the forebrain, forming the nigrostriatal, mesolimbic and mesocortical pathways (for review, see Greengard, 2001). These pathways modulate voluntary motor behaviour, motivation and cognitive function (for review, see Girault and Greengard, 2004). Degeneration or dysfunction in these pathways is associated with major neurological and psychiatric disorders, including PD, schizophrenia, ADHD and drug abuse (for review, see Greengard, 2001), and thus this cell group are of particular importance (for review, see Prakash and Wurst, 2006a) and will be discussed in detail below.

Another population of DA neurons is found in the diencephalon (hypothalamus/ventral thalamus) and comprises the A11-A15 groups (for review, see Prakash and Wurst, 2006a). The A11 group send major descending project to the autonomic areas of the lower brainstem and spinal cord (for review, see Prakash and Wurst, 2006a). The A12 and A14 groups project to the anterior pituitary and have endocrine functions, including inhibiting prolactin secretion and gene expression (for review, see Ben-Jonathan and Hnasko, 2001).

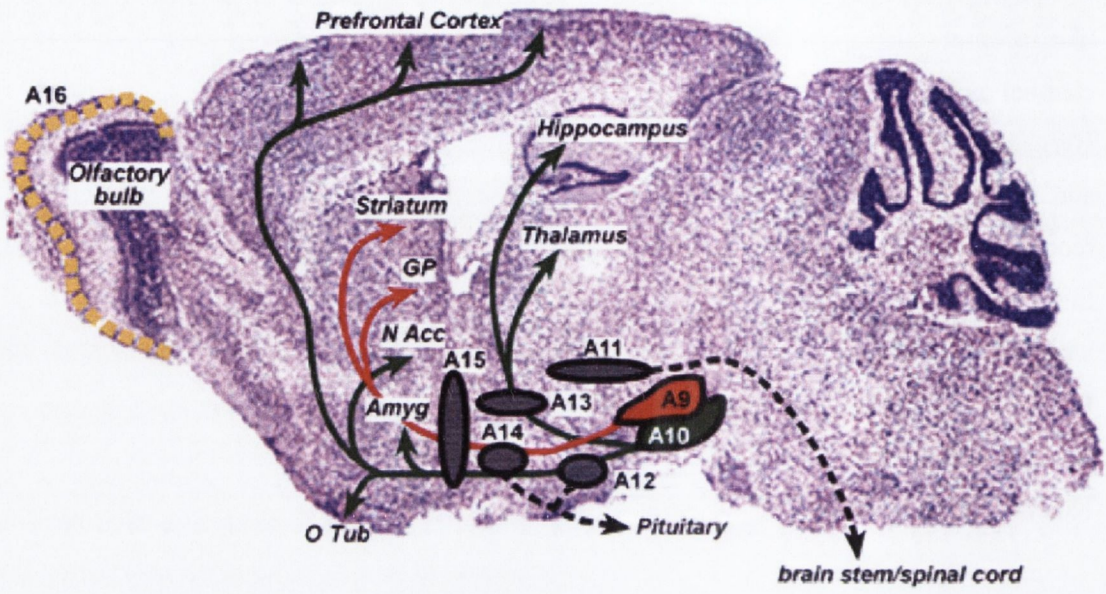

Fig. 1.3: Positions and axonal projections of DA cell groups in the adult rodent brain

The mesencephalic A9 (SNpc, red) group projects to the dorsal striatum (caudate nucleus and putamen) and the globus pallidus (GP) forming the nigrostriatal tract, while the A10 (VTA, green) group projects to the ventral striatum (nucleus accumbens, N Acc), amygdala (Amyg), olfactory tubercle (O Tub) and prefrontal cortex. Additional connections from the A10 (VTA) group are established with thalamic and hippocampal regions. The approximate location of the diencephalic A11-A15 groups of the hypothalamus/ventral thalamus (grey dotted fields) and their descending projections into the brain stem/spinal cord are indicated by dashed lines as they do not colocalise within the same section. Innervation of the anterior pituitary by the A12 (arcuate nucleus) and A14 (periventricular nucleus) groups is indicated by the dashed line and arrow. The telencephalic A16 group consists of interneurons within the olfactory bulb (yellow dashed line). The A8 (retrorubral field) and A17 (retina interneurons) DA groups as well as the local hypothalamic projections of the diencephalic groups have been omitted from the picture. Adapted from Prakash and Wurst (2006a).

Excess prolactin secretion (hyperprolactinemia) causes reproductive disturbance in men and women, and can result from loss of the inhibitory effect of DA on prolactin secreting cells (for review, see Ben-Jonathan and Hnasko, 2001). DA neurons in the A13 region project locally and to the amygdala (for review, see Prakash and Wurst, 2006a). The connectivity of the A15 group is unknown (for review, see Prakash and Wurst, 2006a). The telencephalic A16 and A17 DA cell groups function as local interneurons, and have roles in the olfactory (Davila et al., 2003) and visual (Witkovsky, 2004) systems, respectively.

1.5 Mesencephalic dopaminergic pathways

1.5.1 Nigrostriatal pathway and movement

DA neurons having their cell bodies in the SNpc that project to the dorsal striatum (caudate nucleus and putamen) form the nigrostriatal tract (for reviews, see Girault and Greengard, 2004; Prakash and Wurst, 2006a). Interestingly, the SNpc has undergone considerable expansion in man, in comparison to other species (Nelson et al., 1996). The dorsal striatum is a component of the basal ganglia, which are interconnected subcortical nuclei of the cerebrum and midbrain (for review, see Albin et al., 1989). The basal ganglia play a critical role in modulation of normal voluntary movement by forming a highly organised motor circuit with specific regions of the cerebral cortex and thalamus (for reviews, see Albin et al., 1989; DeLong and Wichmann, 2007). The dorsal striatum is the main input site of the basal ganglia, receiving projections from the cerebral cortex, thalamus and brainstem (Fig. 1.4) (for reviews, see Albin et al., 1989; DeLong and Wichmann, 2007). Striatal neurons project to the internal segment of the globus pallidus (GPi) and substantia nigra pars reticulata (SNpr), which provide the primary basal ganglia outputs to the thalamus and brainstem, and form the direct pathway of the basal ganglia (for review, see DeLong and Wichmann, 2007). Thalamic neurons in turn project to specific regions of the cerebral cortex, completing the motor circuit (for reviews, see Olanow, 2004; DeLong and Wichmann, 2007. The GPi and SNpr also receive projection from the subthalamic nucleus (STN), which constitutes the indirect pathway of the basal ganglia with the striatum and the external segment of the globus pallidus (GPe) (for review, see DeLong and Wichmann, 2007).

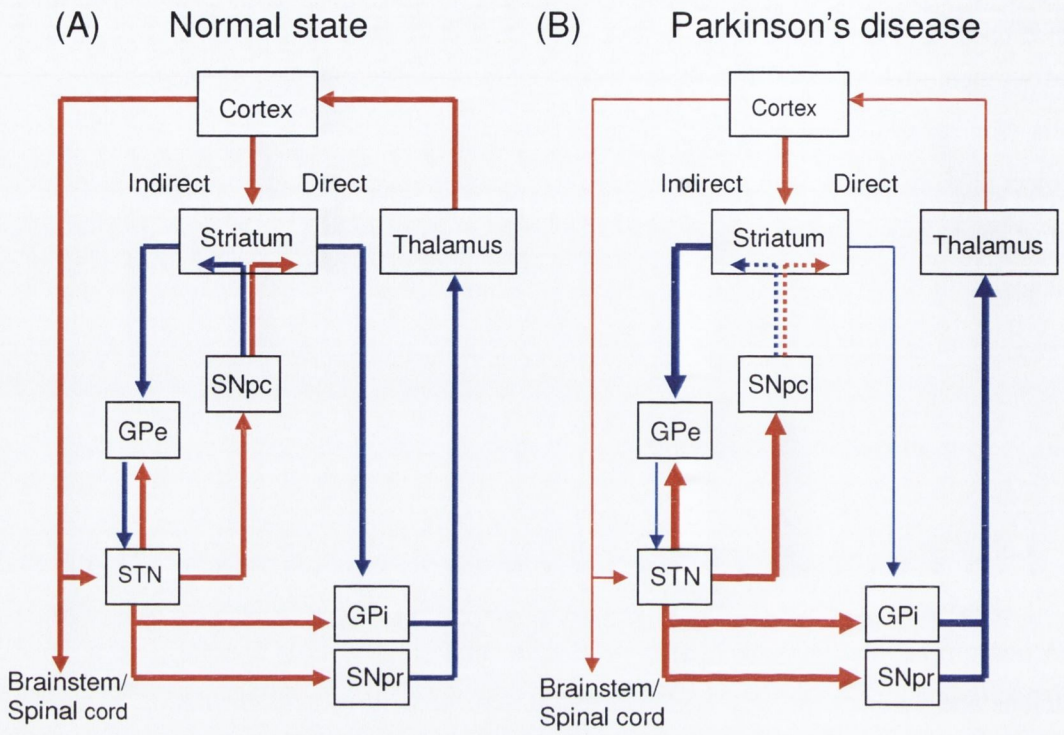

Figure 1.4: The basal ganglia-thalamocortical motor circuitry in the normal state and in Parkinson's disease

The dorsal striatum is the main input site of the basal ganglia, which in turn project to the main output region of the basal ganglia, the GPi and SNpr, by a direct and indirect pathway. Neurons in the direct and indirect pathways exert inhibitory and excitatory influences, respectively, on GPi/SNpr neurons and thus regulate their tonic inhibitory effect on the thalamocortical tract involved in the motor circuit. The balance between these pathways is mediated by DA projections from the SNpc. (A) In the normal state, DA increases activity of inhibitory neurons in the direct pathway and decreases excitatory influences in the indirect pathway, resulting in net activation of thalamocortical neurons. (B) In PD, depletion of DA projections from the SNpc leads to reduced activity in the direct pathway and increased activity in the indirect pathways, resulting in over-activation of GPi/STN neurons and excess inhibition of the thalamocortical projections, and the development of parkinsonian motor features. Red and blue arrows indicate excitatory and inhibitory connections, respectively. Thickness of arrows indicates activity level. SNpc indicates substantia nigra pars compacta; SNpr, substantia nigra pars reticulata; STN, subthalamic nucleus; GPe, external segment of globus pallidus; GPi, internal segment of globus pallidus. Adapted from Olanow (2004).

The connections between the dorsal striatum and output structures of the direct pathways are inhibitory, while those of the indirect pathway are both inhibitory, at the level of the striatum and GPe, and excitatory, at the STN (for review, see DeLong and Wichmann, 2007). Thus, neurons in the direct and indirect pathways exert inhibitory and excitatory influences, respectively, on GPi/SNpr neurons and therefore regulate their inhibitory activity on thalamocortical and brainstem neurons involved in the motor circuit (for review, see Olanow, 2004). The balance between the direct and indirect pathways is regulated by the differential actions of DA on striatal neurons, provided by nigral projections (for review, see DeLong and Wichmann, 2007). Release of DA in the striatum increases activity in the direct pathway (acting on D1 receptors in striatal neurons) and reduces activity in the indirect pathways (acting on D2 receptors in striatal neurons) (for review, see DeLong and Wichmann, 2007). Together these actions result in a net reduction in SNpr and GPi activity, thereby reducing inhibition of thalamocortical neurons and facilitating movements initiated in the cortex (for review, see DeLong and Wichmann, 2007).

1.5.1.1 Parkinson's disease

PD is characterised pathologically by preferential degeneration of DA neurons of the SNpc and a reduction in striatal dopamine (Ma et al., 1996). As discussed, DA is essential for regulation of the basal ganglia motor circuitry and modulation of movement, with absence of nigrostriatal projections resulting in the classical motor abnormalities observed with this disorder, including bradykinesia, resting tremor and rigidity (for review, see Olanow, 2004). The model of basal ganglia-thalamocortical circuitry predicts that DA depletion would result in an increase in the firing rate of GPi/SNpr neurons due to decreased activity in the direct pathways and increased activity in the indirect pathway, leading to excessive inhibition of thalamocortical projection neurons (Fig. 1.4) (for reviews, see Olanow, 2004; DeLong and Wichmann, 2007). This idea is supported by the finding that lesion of the STN that suppresses over-activity in both PD patients and experimental monkey models provide antiparkinsonian benefits (Bergman et al., 1990; Limousin et al., 1998; Grafton et al., 2006).

At present treatment of PD is largely based on DA replacement and no therapies have yet been developed to slow or halt disease progression (for reviews, see Olanow, 2004; Beal,

2010). In addition, the efficacy of symptomatic therapy typically wanes after 5 to 10 years (for reviews, see Olanow, 2004; Beal, 2010). A significant obstacle in the generation of more effective therapies is lack of insight into the underlying pathogenesis of idiopathic PD, which affects ~95% of patients (for review, see Olanow, 2004). This is due, in a large part, to lack of human nerve tissue and faithful disease models (for reviews, see Beal, 2010; Wichterle and Przedborski, 2010). Thus further knowledge of the disease process might be garnered by enhanced *in vitro* disease models, which may be provided by the use of ESCs and iPSCs (Martinat et al., 2004; Wichterle and Przedborski, 2010). ESC-derived DA neurons are also being actively investigated as a therapeutic cell source in the treatment of PD, with some success reported in animal models of the disease (Kim et al., 2002; Roy et al., 2006; Hedlund et al., 2008).

1.5.2 Mesolimbic pathway and motivation

DA neurons in the VTA (A10) which project to the to the medial components of the limbic system, including the ventral striatum (shell of nucleus accumbens), ventral pallidum, medial PFC, hippocampus and amygdale, form the mesolimbic tract (Figs 1.3, 1.5) (for review, see Pierce and Kumaresan, 2006). The limbic system is responsible for the influence of motivational, emotional, contextual and affective information on behaviour, with DA having a key modulatory role on this system and being particularly implicated in the processes of motivation and reward (for reviews, see Wise, 2004; Pierce and Kumaresan, 2006). Interestingly, recent evidence also suggests that DA signalling in the nigrostriatal tract may mediate reward (for review, see Wise, 2009). In particular, DA is required for mediating the reinforcement process, which is the strengthening or 'stamping-in' of stimulus associations and response habits that follows receipt of reward (for review, see Wise, 2004). Reinforcement is most often used in relation to instrumental learning, which is the learning and maintenance of habits that lead to reward (for review, see Wise, 2004). It has been demonstrated that rats do not learn to lever press for natural rewards, such as food, if training takes place in the absence of DA function (Wise and Schwartz, 1981), which has been separated from motor deficits (Franklin and McCoy, 1979).

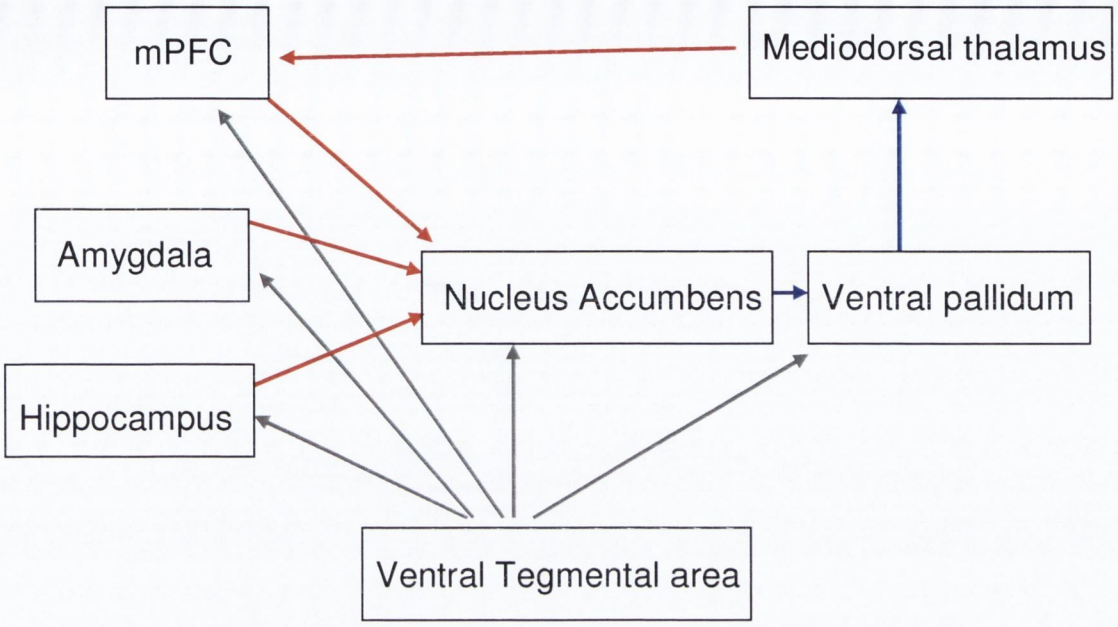

Figure 1.4: Circuitry of the limbic system

Limbic nuclei including the amygdala, hippocampus and medial prefrontal cortex (mPFC) send major glutamatergic connections to the nucleus accumbens. The nucleus accumbens sends major GABAergic projects to the ventral pallidum, which in turn projects to the mediodorsal thalamus. Glutamatergic projections from this area to the mPFC close the limbic circuit. Dopamine neurons of the VTA innervate the amygdala, hippocampus, mPFC, nucleus accumbens and ventral pallidum, with changes in dopamine transmission playing a critical role in modulating the flow of information through this circuitry. Red arrows indicate glutamatergic projections, blue arrows GABAergic projection and grey arrows dopaminergic projections. Adapted from Pierce and Kumaresan (2006).

Furthermore, a progressive decline in response occurs in the presence of DA blockers in well trained rats and is similar to the decline under conditions of non-reinforcement, highlighting the continued reinforcing property of DA (Fouriezos et al., 1978; Wise et al., 1978; Gerber et al., 1981; Wise, 2004). In addition, both natural rewards, such as food and sexual contact, and unsensed laboratory rewards, such as brain stimulation and intracranial drugs, can increase concentrations of extracellular DA in the nucleus accumbens in rats (Di Chiara and Imperato, 1988; Hernandez and Hoebel, 1988; Fiorino et al., 1993; Wenkstern et al., 1993; Pfaus et al., 1995; Pontieri et al., 1995). However, it should be noted that the reinforcing effects of some agents, such cholinergic agonists, opiates and $GABA_A$ antagonists, may be induced indirectly at the level of the VTA, such as by acting on other neuronal subtypes that modulate dopaminergic transmission (Devine and Wise, 1994; David et al., 1997; David et al., 2002; Ikemoto and Wise, 2002; Pierce and Kumaresan, 2006).

1.5.2.1 Addiction

Due to the central role of DA and the mesolimbic system in the reinforcing properties of rewards, it has been proposed that DA may be important in the habit- and addiction-forming properties of some drugs of abuse, with addiction being defined as a compulsive habit maintained despite harmful consequences (for reviews, see Wise, 2002; Wise 2004). However, while increased DA transmission seems both necessary and sufficient to promote psychostimulant reinforcement (Pettit et al., 1984; Gerrits and Van Ree, 1996), it may not be essential for the reinforcing effects of other substances not essential (for review, see Wise, 2004), such as opiates (Pettit et al., 1984; Gerrits and Van Ree, 1996) and ethanol (Ikemoto et al., 1997). While the neurobiological basis of addiction remains to be fully determined, two proposals have been postulated to explain compulsive behaviour (for review, see Wise, 2002). One states that initial 'recreational' drug use induces neuroadaptive changes in the addicted brain requiring the user to escalate drug intake to have the same effect, thus neuroadaptation explains the transition from recreational to compulsive drug use (for review, see Wise, 2002). Alternatively, it has been suggested that drug addiction results from neuroadaptive changes associated with learning of the drug-seeking behaviour, such that the drug reward is stamped in more strongly than natural

rewards (Hernandez and Hoebel, 1988; Wise, 2002). The role of DA in neuroadaptation may be important inasmuch as it is needed for initial drug reinforcement (Ikemoto et al., 1997; Wise, 2002; Wise, 2004).

1.5.3 Mesocortical tract and cognitive function

The mesocortical tract originates in the VTA (A10) and projects to the neocortex, particularly the PFC (for review, see Girault and Greengard, 2004). DA levels in the PFC are essential for modulating cognitive function (Brozoski et al., 1979; for reviews, see Goldman-Rakic et al., 2000; Tunbridge et al., 2006), with cognition being defined by the prominent cognitive psychologist Ulric Neisser (1967) as "all processes by which the sensory input is transformed, reduced, elaborated, stored, recovered and used.....cognition is involved in everything a human being might possibly do". In fact, research suggests that there is an inverted U-shaped relationship between DA activity and PFC cognitive function, with this being optimal at intermediate levels of DA and mediated by D1 and D2 receptors (Fig. 1.6) (for reviews, see Goldman-Rakic et al., 2000; Winterer and Weinberger, 2004; Tunbridge et al., 2006). In particular, D1 agonists and antagonists greatly impair normal working memory, with this being observed across species (Zahrt et al., 1997; Lidow et al., 2003; Vijayraghavan et al., 2007). In addition, both age (Mizoguchi et al., 2009) and stress (Mizoguchi et al., 2000) have been reported to negatively impact on working memory by a D1 receptor dependent manner. Thus, it has also been proposed that DA is crucial in the PFC to maintain the delicate balance between excitatory and inhibitory synaptic interactions by modulating the excitability of glutamatergic and GABA neurons in the PFC and consequently normal behaviour (for review, see Winterer and Weinberger, 2004).

1.5.3.1 Schizophrenia

Schizophrenia is a severe and chronic mental illness, associated with a prevalence of 0.5-1%, and associated with positive, negative and cognitive symptoms (for review, see Abi-Dargham and Laruelle, 2005). Positive symptoms include delusions and hallucinations, while negative symptoms include flattened affect and social isolation, and deficits of memory and attention are typical of cognitive symptoms.

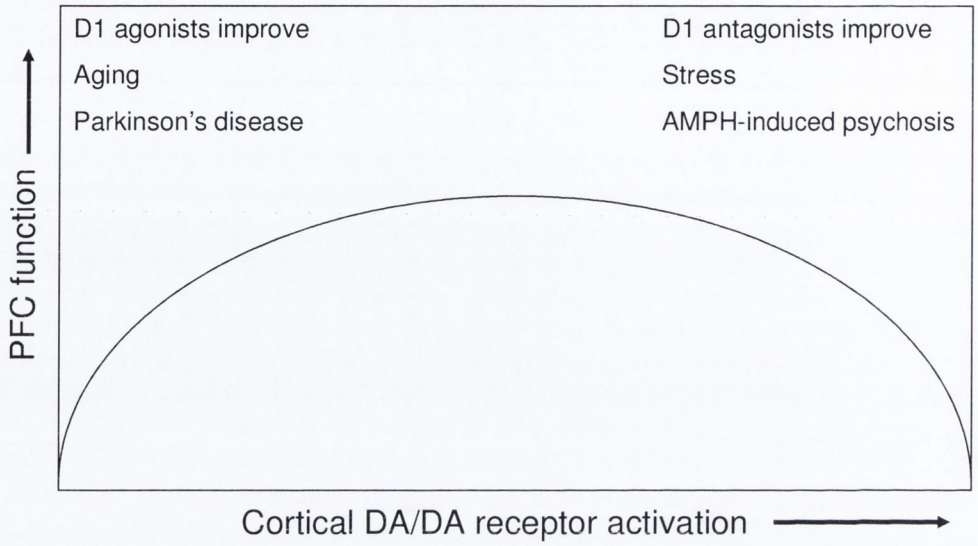

Figure 1.6: The inverted U-relationship between dopamine and prefrontal cortex function

Prefrontal cortex (PFC) function is optimal at intermediate dopamine (DA) levels, mediated particularly by D1 receptors. PFC function is impaired in states of dopaminergic hypofunction (e.g., in aged animals and patients with PD) and dopaminergic hyperfunction (e.g., in stressed animals and amphetamine (AMPH)-induced psychosis). Adapted from Goldman-Rakic et al. (2000) and Tunbridge et al. (2006).

The observation that antipsychotic drugs had anti-dopaminergic properties and DA mimicking drugs could induce psychotic episodes resembling the positive symptoms of schizophrenia resulted in the dopamine theory of schizophrenia, in which it was proposed that positive symptoms (psychosis) were the result of dopamine hyperactivity in the brain (Carlsson and Lindqvist, 1963; Seeman et al., 1976; Davis et al., 1991). However, this hypothesis was not convincingly confirmed (Brozoski et al., 1979; for reviews, see Weinberger, 1987; Davis et al., 1991) and thus a new model was postulated and suggested that decreased activity in the mesocortical pathway and increased activity in the mesolimbic pathway (nucleus accumbens), in particular the mesostriatal pathway, may cause the cognitive and negative, and positive symptoms of schizophrenia, respectively (for reviews, see Weinberger, 1987; Davis et al., 1991; Winterer and Weinberger, 2004).

This model proposes that in the normal state, the mesocortical projections to the PFC activate an inhibitory feedback loop to modulate the activity of the mesolimbic tract (Fig. 1.7) (for reviews, see Weinberger, 1987; Davis et al., 1991). However, in schizophrenia reduced activity in the inhibitory loop results in disinhibition and overactivation of the mesolimbic pathway (for reviews, see Weinberger, 1987; Davis et al., 1991; Winterer and Weinberger, 2004). Hence this raises the possibility that mesolimbic DA activity may be abnormal as a downstream effect of a primary prefrontal abnormality (for review, see Winterer and Weinberger, 2004). This model is supported by the finding that lesionings of the PFC or mesocortical pathway results in enhanced activity in the mesostriatal pathway, specifically in the nucleus accumbens (Pycock et al., 1980; Jaskiw et al., 1990). Support for increased activity in the mesostriatal tract has also been provided by numerous neuroimaging studies of schizophrenic patients (Abi-Dargham et al., 1998; Abi-Dargham et al., 2000; Abi-Dargham and Laruelle, 2005). Thus abnormality in DA signalling may be a prominent feature of this psychiatric disorder.

1.5.3.2 Attention deficit hyperactivity disorder

With a prevalence of 8-12% worldwide, ADHD is one of the most common childhood psychiatric disorders, with symptoms persisting into adolescence and adulthood in approximately 80% of suffers (Faraone et al., 2003).

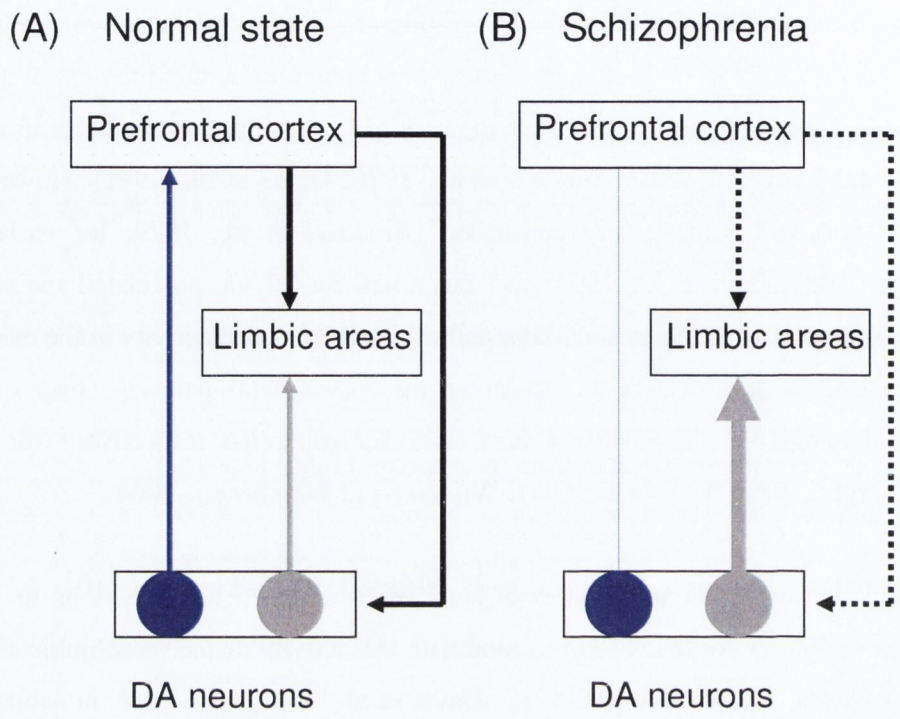

Figure 1.7: Dopamine model of schizophrenia

This model postulates that under the normal state (A) the dopamine (DA) neurons forming the mesocortical pathway (blue line) acts through an inhibitory feedback loop (black line) involving the prefrontal cortex to modulate the function of limbic areas and the dopamine mesolimbic pathway (grey line). A primary defect in schizophrenia (B) may be depressed activity in the mesocortical pathway and subsequent loss of inhibitory feedback from the prefrontal cortex (dashed black line) and hyperactivity of the mesolimbic pathway and limbic areas. Adapted from Weinberger (1987).

Although the neurobiological basis of this disorder has yet to be defined, there is a conveying role for dysfunction in the catecholamine system (for reviews, see Arnsten and Li, 2005; Biederman, 2005). For example, most medication used to treat ADHD facilitates catecholamine transmission (for review, see Arnsten and Li, 2005). Methylphenidate is an inhibitor of DAT and NAT and increases extracellular DA concentration in the PFC, striatum and nucleus accumbens, while increasing noradrenaline concentration in the PFC (Volkow et al., 1998; Volkow et al., 2001; Bymaster et al., 2002). In addition, it is widely recognised that ADHD has a strong familial and genetic component (Biederman, 2005; Faraone et al., 2005), with studies indicating an association between ADHD and genes related to the DA system such as *DAT* (Daly et al., 1999; Barr et al., 2001; Hawi et al., 2003). Furthermore, while the locus of brain dysfunction in ADHD has not been unequivocally identified, evidence suggests that, like schizophrenia, deficits in the PFC may exist (Ernst et al., 1998; Rubia et al., 1999; Hill et al., 2003; Arnsten and Li, 2005). As has been discussed, this area is essential for cognitive function and is highly connected to subcortical structures. Hence, it has been proposed that ADHD medication may have therapeutic effects by optimising catecholamine signalling in the PFC and thus modulating inhibitory influences on subcortical structures, alleviating symptoms of ADHD (for reviews, see Arnsten and Li, 2005; Biederman, 2005).

1.6 Mesencephalic dopamine neuron development

1.6.1 Early neural development

All neurons of the central nervous system (CNS) and most in the periphery, mediated by neural crest migration, are generated in a region-specific manner by a series of inductive events (for review, see Alavian et al., 2008). During gastrulation, a sheet of ectodermal cells begins to acquire neural properties and form the neural plate. Soon afterward, the neural plate starts to thicken, starts to roll up along its anterior-posterior (AP) axis, and closes eventually to form the neural tube, through a process called neurulation (for review, see Alavian et al., 2008). At this time, the embryonic neural tube begins to be patterned along its dorso-ventral (DV) axis by the floor plate (ventral) and the roof plate (dorsal), and along its AP axis by position-dependent organising centres, including the isthmus at the

junction of the mesencephalon and metencephalon (for review, see Prakash and Wurst, 2006b). These centres secrete signalling molecules which impose instructive information upon adjacent tissue, resulting in the appearance of new molecular boundaries (for reviews, see Prakash and Wurst, 2006b; Smits et al., 2006).

1.6.2 Development of the isthmus

The isthmus is a very important region which separates the fore- and midbrain from hindbrain anatomically and molecularly (for review, see Smits et al., 2006). It is established early during neural development by the opposing expression domains of two transcriptional repressors, *Otx2* in the presumptive fore- and midbrain (anterior neural tube), and *Gbx2* in the presumptive hindbrain and spinal cord (posterior neural tube) (Broccoli et al., 1999; Millet et al., 1999; Brodski et al., 2003). The effects of the isthmus can be mimicked by fibroblast growth factor 8 (FGF8)-containing beads and thus is considered to be the key signalling molecule of this centre (Crossley et al., 1996; Martinez et al., 1999), with patterning activity of its own along the AP axis of the neural tube (Ye et al., 1998). Wnt1 is another important signalling molecule secreted by the isthmus, and it has been demonstrated that FGF8 and Wnt1 cross-regulate each other (Crossley et al., 1996; Lee et al., 1997; Liu and Joyner, 2001; Chi et al., 2003). Expression of transcription factors belonging to homeodomain and paired-box families, such as Engrailed (En) 1 and 2, Pax2/5 and Lmx1b, is also initiated at or across the isthmus at roughly the same time as FGF8 and Wnt1, and prior to induction of mDA neurons (Urbanek et al., 1997; Adams et al., 2000; Liu and Joyner, 2001; Prakash et al., 2006; Prakash and Wurst, 2006b; Alavian et al., 2008). These factors participate in regional specification of midbrain tissue (for review, see Alavian et al., 2008).

1.6.3 Induction of mesencephalic dopamine neurons

After formation and positioning of the isthmus, signals from the floor plate and roof plate divide the mesencephalon into dorsal and ventral parts, with each region having its own specific developmental cascades (for review, see Smits et al., 2006). Essential in inducing the ventral mesencephalon is the glycoprotein sonic hedgehog (Shh), which is expressed

early during development in the floor plate and notochord and is the key signalling molecule conveying positional information along the DV axis (Hynes et al., 1995; Wang et al., 1995; for review, see Prakash and Wurst, 2006a). mDA progenitors first arise in the cephalic flexure at embryonic day (E) 9.5 in the mouse embryo in close vicinity to the floor plate and isthmus (Fig. 1.8) (Wallen et al., 1999; for review, see Prakash and Wurst, 2006a), with the position of the isthmus controlling the location and size of the dopaminergic population (Brodski et al., 2003). It has been demonstrated *in vitro* that cooperative signalling by Shh and FGF8 can induce mDA neurons at ectopic locations (Ye et al., 1998). Shh signalling is indispensable in this respect as mDA neurons are absent in *Shh* null mice and considerably reduced following conditional inactivation of the Shh receptor *Smoothened* at E9.0 (Blaess et al., 2006). Furthermore, ectopic expression of Shh and its downstream effector Gli-1 can induce mDA neurons in the dorsal mid-/hindbrain region (MHR), in areas where FGF8 and Wnt1 are normally expressed (Hynes et al., 1997). However, the necessity of FGF-signalling for mDA neuron development has been somewhat compromised by the finding that FGF receptor 1 ablation in the MHR, which is the prominent receptor in this area, had no effect on the mDA neuronal population, but instead reduced the most rostral serotonin neurons (Trokovic et al., 2003). Furthermore, FGF8-containing beads are unable to induce ectopic mDA neurons in *Wnt1* mutant forebrain cultures in contrast to wild-type tissue (Prakash et al., 2006). It has also recently been demonstrated that Wnt1 is required during early neural development for the *in vivo* generation of mDA neurons, and thus it has suggested that Shh (and FGF8) work in concert with this factor leading to the establishment of a mDA progenitor domain in the ventral mesencephalon which is competent to generate mDA precursors (Prakash et al., 2006).

In particular, it has been suggested that a Wnt1-regulated genetic network and a Shh-controlled genetic cascade may act in parallel or sequentially to establish this mDA domain (for review, see Prakash and Wurst, 2006b). Experimental data indicates that Wnt1 is engaged in a positive feedback loop with Otx2 within the ventral mesencephalon, such that secreted Wnt1 protein induces and/or maintains *Otx2* expression and vice verse (Prakash et al., 2006). Otx2 protein is in turn required for the repression of *Nkx2-2* within this domain of the neural tube and the development of rostral hindbrain 5-HT neurons (Prakash et al., 2006).

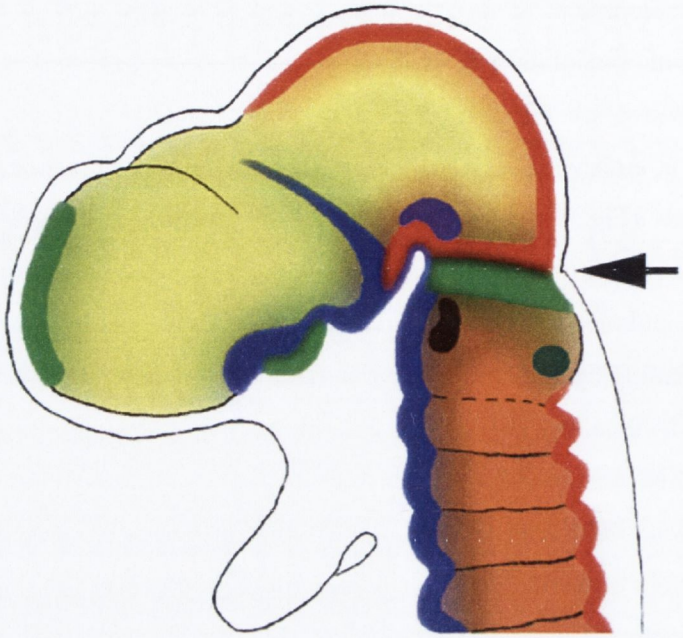

Fig. 1.8: Mesencephalic dopamine neurons develop close to two important signalling centres in the mouse embryo

Sagittal view of an E10.5 mouse embryo head; anterior is to the left. Sonic hedgehog (Shh, blue) is secreted from the floor plate of the spinal cord and hindbrain, and the floor plate of the midbrain and caudal forebrain, thus establishing a ventro-dorsal gradient that confers dorso-ventral positional information. The isthmus (black arrow) is established at the expression boundary of Otx2 (yellow) in the fore- and midbrain and Gbx2 (orange) in the hindbrain and spinal cord. Expression of the secreted factors fibroblast growth factor 8 (FGF8, green) and Wnt1 (red) is confined to the caudal border of the isthmus in the rostral hindbrain, ventral telencephalon and anterior neural ridge (FGF8), and the rostral border of the isthmus in the caudal midbrain, ventral midline (cephalic flexure) of the midbrain and dorsal midline of the hindbrain and spinal cord (Wnt1). Signals provided by the isthmus confer anterior-posterior positional information. The mDA precursors (purple) are induced within the cephalic flexure (ventral mesencephalon) by a combination of Shh, FGF8 and Wnt1 signals. Two additional neuronal populations develop close to the isthmus in the ventral hindbrain (serotonin neurons of the raphe nuclei, brown) or dorsal hindbrain (noradrenaline neurons of the Locus coeruleus, turquoise). Adapted from Prakash and Wurst (2006a).

Wnt1 and Lmx1 may also be involved in an auto-regulatory loop during mDA neuron development (Chung et al., 2009), with Shh and/or Wnt1 inducing expression of the homeodomain transcription factor *Lmx1a* in the ventral midbrain (Andersson et al., 2006b; Chung et al., 2009). Lmx1a activates the homeodomain transcription factor *Msx1*, which is a transcriptional repressor and targets the homeodomain transcription factor *Nkx6-1* (Andersson et al., 2006b; Chung et al., 2009). Nkx6-1 is broadly expressed in the ventral neural tube at early stages of development and repression of the most ventral *Nkx6-1* domain in the midbrain by Msx1 may therefore delimit the mDA progenitor domain from the more laterally located progenitors of motor neurons (Andersson et al., 2006b). Thus a *Wnt1*$^{+}$, *Otx2*$^{+}$, *Shh*$^{+}$, *Lmx1a*$^{+}$, *Msx1*$^{+}$ but *Nkx2-2*$^{-}$, *Nkx6-1*$^{-}$ domain may be established in the ventral mesencephalon from which mDA precursors develop (Fig. 1.9) (for review, see Prakash and Wurst, 2006b).

1.6.4 Specification of mesencephalic dopamine neurons

After the initial induction by Shh, Wnt1 and FGF8 in the ventral midbrain, the mDA precursor and postmitotic neurons go through several steps of specification (for review, see Alavian et al., 2008). However, current knowledge about the integrated mechanisms acting during early induction and specification of mDA cell fate is still rudimentary, with these signalling molecules possibly having a direct role in specification of mDA progenitors (for review, see Prakash and Wurst, 2006a). Nevertheless, evidence suggests that Lmx1a and Msx1 continue to be expressed, with Lmx1a and Wnt1 also in an auto-regulatory loop (Andersson et al., 2006b; Chung et al., 2009). Msx1 (Andersson et al., 2006b) and Oxt2 (Vernay et al., 2005) induce expression of the proneuronal transcription factor Neurogenin2 (*Ngn2*) in the ventral mDA precursors. Ngn2 appears to be required for the proper differentiation of mDA precursors by acquisition of generic neuronal properties, but not their terminal differentiation (Andersson et al., 2006a; Kele et al., 2006). Lmx1a also appears to induce expression of transcription factors required for proper differentiation of mDA precursors, including Nurr1 and Pitx3 (Chung et al., 2009; Friling et al., 2009).

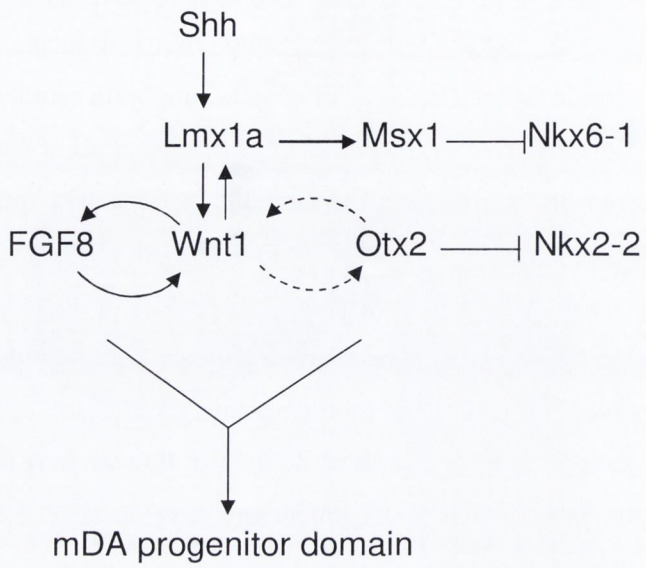

Fig. 1.9: Establishment of mesencephalic DA neuron progenitor domain during early stages of mouse neural development

Wnt1, Shh and Lmx1a expressed in the ventral mesencephalon positively control a genetic cascade including Otx2, required for repression of *Nkx2-2*, and *Msx1,* required for repression of *Nkx6-1.* This establishes a domain from which mDA precursors develop. Expression of *Lmx1a* in the ventral midbrain appears to require Shh. Wnt1 and Otx2 mutually induce and/or maintain their expression in the ventral midbrain, although neither factor is necessary for it (indicated by broken arrows). Wnt1 and FGF8 are also engaged in cross-regulation of their expression, but a strict requirement of FGF8 signalling for the development of mDA neurons *in vivo* is uncertain. Lmx1a and Wnt1 are also engaged in a auto-regulatory loop. Neither Lmx1a nor Wnt1 can induce DA neurons in the absence of Shh. Shh indicates sonic hedgehog; FGF8, fibroblast growth factor 8. Adapted from Prakash and Wurst (2006b) and Chung et al. (2009).

1.6.5 Further differentiation and maintenance of mesencephalic dopamine neurons

After initial specification, mDA precursor cells gradually become postmitotic and several transcription factors begin to be expressed which are essential for their neurotransmitter phenotype, survival and long term maintenance throughout life, including Nurr1, Pitx3, Lmx1b and En 1/2 (for review, see Alavian et al., 2008). It has been suggested that these genes may represent at least three independent molecular pathways (for review, see Alavian et al., 2008). *En1/2* and *Lmx1b* are widely expressed before induction of mDA neurons but their expression becomes relatively specific to postmitotic mDA neurons during later embryogenesis (Smidt et al., 2000; Simon et al., 2001; for review, see Alavian et al., 2008).

1.6.5.1 Nurr1

Nurr1 is an orphan nuclear receptor that is highly expressed during development in the CNS, including the ventral mesencephalon, and in the postnatal and adult brain, including in the mDA system (Zetterstrom et al., 1996; Zetterstrom et al., 1997). Analysis of *Nurr1*$^{-/-}$ mutant mice indicate that Nurr1 is not strictly required for the specification and initial birth of mDA precursors, but instead is involved in inducing the dopaminergic phenotype in these cells, and later for maintenance and survival, with lack of *Nurr1* expression resulting in selective death of mDA precursors during development (Zetterstrom et al., 1997; Castillo et al., 1998; Saucedo-Cardenas et al., 1998; Wallen et al., 1999; Smits et al., 2003; Kadkhodaei et al., 2009). Indeed, it has recently been demonstrated that targeted ablation of the *Nurr1* gene in late embryonic development results in a progressive decline of TH, DAT, VMAT2, AADC, Lmx1b and Pitx3 in the ventral mesencephalon, a reduction in striatal DA levels, and rapid cell loss in this area (Kadkhodaei et al., 2009). However, it should be noted that Nurr1 does not seem to be required for expression of *Pitx3, Lmx1b* and *AADC*, with evidence suggesting it induces, directly or indirectly, the expression of *TH*, *DAT* and *VMAT2* (Saucedo-Cardenas et al., 1998; Wallen et al., 1999; Sacchetti et al., 2001; Kim et al., 2003; Smits et al., 2003). Expression of the trophic factor receptor component, *Ret*, is also not detected in *Nurr1*$^{-/-}$ null mutant embryos from the earliest time point on (Zetterstrom et al., 1997; Wallen et al., 2001), which is of significance as Ret is required for long term survival of nigral DA neurons (Kramer et al., 2007). In fact, it has been observed

that inactivation of *Nurr1* in adulthood results in a progressive reduction in DA markers in the ventral mesencephalon and projection areas, and decrease in striatal DA levels (Kadkhodaei et al., 2009). Thus these results suggest that Nurr1 is essential for the proper differentiation and long term survival of mDA neurons.

1.6.5.2 Lmx1b

Lmx1b is a LIM homeodomain transcription factor and has been suggested to be important in the development of mDA neurons (Smidt et al., 2000; Prakash and Wurst, 2006a). Lmxb1 is expressed in ventral mesencephalon and caudal diencephalon of mid-gestational embryos, in the region where mDA neurons develop, and is later confined to the mDA progeny (Smidt et al., 2000). In the adult brain, it has a restricted expression pattern characterised by high expression in VTA and SNpc (Smidt et al., 2000). In wild-type animals, Lmbx1 is expressed prior to Nurr1, TH and Pitx3 and co-localises with Pitx3 in the ventral midbrain (Smidt et al., 2000). However, *Lmx1b*$^{-/-}$ null embryos fail to express Pitx3, while expression of TH and Nurr1 is intact (Smidt et al., 2000). Conversely, expression of Lmx1b and Pitx3 is maintained in *Nurr1*$^{-/-}$ null embryos and it has been proposed that at least two independent cascades may operate during mDA neuron development, one involving Lmx1b and Pitx3 and the other involving Nurr1 (Smidt et al., 2000). However, development of the midbrain appears to be generally disturbed in the *Lmx1b* knock-out (Smidt et al., 2000) and thus defects observed in the mDA neuronal population could therefore be a secondary consequence of disturbed midbrain patterning (for review, see Prakash and Wurst, 2006a).

1.6.5.3 Pitx3

Pitx3 is a paired-like homeodomain transcription factor that is exclusively transcribed in the CNS at the cephalic flexure of the neural tube during embryonic development (Smidt et al., 1997). Its expression continues throughout development and is restricted to mDA neurons in the adult brain (Smidt et al., 1997). Evidence suggests that Pitx3 is required for the proper differentiation of mDA neurons specifically in the SNpc, with *Pitx3*$^{-/-}$ null mice failing to develop these cells or their projections to the dorsal striatum and exhibiting some

motor deficits, while neurons in the VTA are relatively spared (Hwang et al., 2003; Nunes et al., 2003; van den Munckhof et al., 2003; Smidt et al., 2004; Maxwell et al., 2005). The selective loss of SNpc mDA neurons despite the expression of Pitx3 in the SNpc and VTA may be the result of differential transcriptional regulation of the *TH* gene (Maxwell et al., 2005). Pitx3 appears to be specifically required for the initiation and/or maintenance of *TH* transcription in the presumptive SNpc, while expression of this enzyme is induced prior to *Pitx3* in the presumptive VTA (Maxwell et al., 2005). Thus, Pitx3 may be required for proper terminal differentiation of mDA neurons that will form the SNpc, by activating the *TH* gene or other targets, ensuring cell survival (Prakash and Wurst, 2006a). However, cells of the prospective VTA are not dependent on Pitx3 for this component of terminal differentiation and thus are less affected by its absence (Maxwell et al., 2005). Recent evidence also suggests that, like Nurr1, *DAT* and *VMAT2*, may be downstream targets of Pitx3 (Hwang et al., 2009), with it now being proposed that Pitx3 and Nurr1 may, in fact, cooperatively promote terminal differentiation of mDA neurons (Martinat et al., 2006; Hwang et al., 2009; Jacobs et al., 2009).

1.6.5.4 Engrailed 1 and 2

Engrailed homeodomain transcription factors, En1 and En2, are expressed in early neural development (E8.0) in the anterior mouse neuroectoderm as patches which subsequently fuse to form a band of cells that will give rise to the isthmic organiser (Simon et al., 2001). After their initial expression in the mid/hindbrain, mDA neurons begin to express the two *En* genes between E11.5 and E14 and their expression continues in the postnatal and adult brain in the SNpc and VTA (Simon et al., 2001). Analysis of *En1/2*$^{-/-}$ null mice indicate that they have an essential role in survival and maintenance of mDA neuron (Simon et al., 2001). Interestingly it was observed that mDA neurons appeared similar to wild type mice in single homozygous mutants (*En1*$^{-/-}$ or *En2*$^{-/-}$) but were completely absent in double homozygotes (Simon et al., 2001). Furthermore, while mDA neurons were substantially diminished in *En1*$^{-/-}$/*En2*$^{+/-}$ mutants, mDA neurons in *En1*$^{+/-}$/*En2*$^{-/-}$ mutants were identical to wild type mice, thus acting in a gene dosage dependent manner (Simon et al., 2001). Notably, a cluster of TH positive neurons were generated in the ventral aspect of the cephalic flexure in the double homozygotes, although it was smaller than that observed in

wild type and heterozygous mice, providing direct evidence that these genes are not required for the induction of mDA neurons (Simon et al., 2001). However, these neurons disappeared in the double mutants over the next few days of development, suggesting they have maintenance and survival function (Simon et al., 2001). Further studies using *in vitro* embryonic ventral mesencephalic cultures have shown that the *En* genes are cell-autonomously required for the survival of mDA neurons and loss of *En* expression in these cells induces apoptosis (Alberi et al., 2004). Interestingly, analysis of mice heterozygous null for *En 1* and homozygous null for *En 2* ($En1^{+/-}/En2^{-/-}$) during the first 3 months of adulthood has revealed a progressive degeneration of DA neurons in the SNpc, suggesting that *En* gene expression may be required for long term survival of these this population of mDA neurons (Sgado et al., 2006).

1.7 Embryonic stem cells

As discussed, mDA neurons have several fundamental functions in the brain, dysfunction or degeneration of which are implicated in a myriad of psychiatric and neurological disorders (for review, see Greengard, 2001). In addition, while the development of these neurons has been intensively investigated, much remains to be elucidated (for review, see Prakash and Wurst, 2006a). As the brain is largely inaccessible, the analysis of DA neurons *in vitro* may provide further insight into the mechanisms controlling neuronal development, neuronal function and degeneration, and provide a system for drug discovery and toxicological screens (Martinat et al., 2004; Rolletschek et al., 2004). ESCs may provide an ideal source of DA neurons for such analysis as they can be propagated indefinitely in culture in an undifferentiated state while retaining pluripotency, and are easily accessible to genetic manipulation, allowing specific mutations to be readily analysed (Evans and Kaufman, 1981; Thomson et al., 1998; Lee et al., 2000; Martinat et al., 2004; Rolletschek et al., 2004; Wobus and Boheler, 2005). Furthermore, ESC derived DA neurons are being actively investigated as a therapeutic cell source in the treatment of PD as the use of ESCs circumvent problems associated with other transplantable tissues (Roy et al., 2006; Astradsson et al., 2008; Hedlund et al., 2008).

1.7.1 Derivation of dopamine neurons from embryonic stem cells

ESCs are pluripotent cells derived from the inner cell mass of the pre-implantation blastocyst-stage embryo and have been established from mouse (Evans and Kaufman, 1981; Martin, 1981), primate (Thomson et al., 1995) and human (Thomson et al., 1998) embryos. Protocols have been established to direct differentiation of these cells to neurons, including DA neurons, and are largely based on the *in vivo* neuronal development discussed above (Kawasaki et al., 2000; Lee et al., 2000; Kawasaki et al., 2002; Ying et al., 2003; Perrier et al., 2004; Parmar and Li, 2007; Sonntag et al., 2007; Cooper et al., 2010). Methods to differentiate mouse ESC to DA neurons largely fall into three categories (Kawasaki et al., 2000; Lee et al., 2000; Stavridis and Smith, 2003; Ying et al., 2003; Lau et al., 2006; Parmar and Li, 2007). One strategy involves co-culture of undifferentiated ESCs on monolayers of PA-6 bone marrow derived stromal cells, which have strong neural-inducing activity, and is based on what has been termed stromal-cell derived inducing activity (SDIA) (Kawasaki et al., 2000). 30% of neurons generated by this procedure express TH after 14 days of culturing and release DA following depolarisation (Kawasaki et al., 2000). Reports also suggest TH positive neurons also express markers typical of mDA neurons such as Pitx3 and Nurr1 (Kawasaki et al., 2000; Parmar and Li, 2007). While the molecular nature of the SDIA long remained elusive (Kawasaki et al., 2000), it now seems that factors present on the surface of stromal cells induce cell survival and overall neurogenesis, while secreted factors are primarily responsible for DA-inducing effects (Vazin et al., 2008).

The second approach involves a five-stage differentiation procedure in which *in vitro* differentiation recapitulates *in vivo* neuronal differentiation (Lee et al., 2000). Undifferentiated ESCs are first induced to form embryoid bodies (EBs) by growth in suspension culture (Lee et al., 2000), with EBs typically consisting of endodermal, ectodermal and mesodermal tissue and may reflect aspects of cell differentiation during early mammalian embryogenesis (Desbaillets et al., 2000). EBs are subsequently plated and neural precursors (NPs) are selected in defined medium (Lee et al., 2000). NPs then undergo expansion in the presence of the mitogen basic fibroblast growth factor (bFGF) (Murphy et al., 1990; Okabe et al., 1996) and signalling molecules Shh and FGF8 (Lee et

al., 2000), with terminal differentiation and maturation of neuronal cells completed by bFGF withdrawal and application of L-ascorbic acid (L-AA) (Lee et al., 2000). L-AA has been implicated in increasing DA neuron yield in primary CNS cultures (Kalir and Mytilineou, 1991; Yan et al., 2001). This procedure generates around 30% of TH positive neurons within 24 to 35 days of initiation of the differentiation method (Lee et al., 2000), with evidence suggesting that a proportion of these cells also expressing mDA markers such Nurr1 and Pitx3 (Kim et al., 2002; Friling et al., 2009). These neurons also released DA upon depolarisation and displayed electrophysiological properties of mature neurons (Lee et al., 2000). Lau et al. (2006) have developed a similar method, which allows the fast and efficient differentiation of ESCs to DA neurons within 14 days. In this protocol undifferentiated ESCs form neuronal stem spheres (NSSs) in suspension already in the presence of mitogens bFGF and epidermal growth factor (EGF), and L-AA (Lau et al., 2006). NSSs have been reported to contain a periphery of neural stem cells, a core of proliferating ESCs and an intermediate layer (Nakayama et al., 2004). EGF has previously been shown to induce the proliferation of embryonic NPs (Santa-Olalla and Covarrubias, 1995; Reynolds and Weiss, 1996). Plating of NSSs and culturing in the presence of EGF, FGF8, Shh and L-AA induces proliferation and patterning of NPs, with terminal neuronal differentiation being induced by withdrawal of growth factors but still culturing in the presence of L-AA (Lau et al., 2006). This protocol has been reported to generate 40% of DAT expressing cells (Lau et al., 2006).

Ying et al. (2003) have established a distinct method for inducing neuronal differentiation from ESCs, in which NPs are generated by plating ESCs in adherent monocultures in chemically defined medium. This procedure does not require the application of exogenous growth factors but instead depends upon autocrine FGF signalling (Ying et al., 2003). It has been reported that around 16% of neurons express TH after 14 days of differentiation, with this increasing to around 26% after application of bFGF, Shh and FGF8 (Ying et al., 2003; Parmar and Li, 2007). However, this method does not seem to typically support the generation of TH neurons co-expressing mDA neuronal markers, such as Pitx3 and Lmx1a (Parmar and Li, 2007; Friling et al., 2009).

1.7.2 Direct visualisation and selection of ESC derived dopamine neurons

An impediment in the use of ESC derived DA neurons for any application is that due to the developmental potency of ESCs it is not possible to synchronise the birth and development of cell populations to the extent seen in normal development, and consequently heterogeneous cell populations are typically generated after differentiation that contain cells at different stages of maturation and of more than one germ layer (for review, see Stavridis and Smith, 2003; Pruszak et al., 2007). Conversely, *in vitro* studies would greatly benefit from a large, homogenous cell population (for review, see Stavridis and Smith, 2003). The therapeutic potential of ESCs for regenerative medicine is also compromised by the heterogeneous nature of differentiated cell cultures (for review, see Stavridis and Smith, 2003; Pruszak et al., 2007). However, this obstacle may be partly or wholly overcome by introducing a reporter cassette, such as enhanced green fluorescent protein (EGFP), into a locus with restricted expression in the specific cell type, effectively labelling the cell of interest (for review, see Stavridis and Smith, 2003; Hedlund et al., 2008). This would not only allow the enrichment of a particular cell type from a mixed cell population by fluorescent cell sorting (FACS) but also enable differentiation to be followed *in vitro* in real time in live cells (Tomishima et al., 2007; Hedlund et al., 2008). This approach to label DA neurons derived from ESCs is of particular relevance as there are currently no good cell surface markers specific for the DA precursor population which allow for their specific selection (Cai et al., 2010).

1.7.2.1 Strategies to target EGFP to cell specific promoters

Targeting EGFP expression to a desired locus may be achieved in a number of ways, including site-specific targeting of EGFP into the endogenous gene of interest by homologous recombination, randomly integrating DNA containing a gene specific promoter or enhancer element adjacent to EGFP into the genome, and site-specific targeting of EGFP into the entire gene contained within a bacterial artificial chromosomes (BACs) and random integration into the genome (Hedlund et al., 2007; Tomishima et al., 2007; Hedlund et al., 2008). There are strengths and weaknesses in each strategy. Targeted insertion into the genome usually results in correct transgene expression but can be labour-

intensive and results in a cell line with only one copy of the gene of interest, as EGFP replaces the endogenous gene, which may disrupt normal cellular function (Spielewoy et al., 2001; Savelieva et al., 2002; Tomishima et al., 2007). Random integration of promoter-driven EGFP constructs requires mapping of the promoter structure (Tomishima et al., 2007). After mapping, recombinant DNA techniques must be used to create truncated promoters that typically are smaller than 20 kilobases (kb) due to the practical limitations of conventional cloning strategies (Tomishima et al., 2007). These smaller, randomly integrated transgenes are frequently dysregulated (Hedlund et al., 2007; Tomishima et al., 2007). Targeting EGFP into a gene within a BAC has several advantages over other strategies (Tomishima et al., 2007). As BACs can accommodate very long regions of genomic DNA (up to several hundred kb), high transgene fidelity is typically achieved, likely owing to the fact that all regulatory elements of the gene contained within the BAC are maintained and their large size insulates the integrated transgene from the effects of the surrounding chromatin structure (Zhang et al., 2004; Tomishima et al., 2007; Bian and Belmont, 2010). In addition, protocols have been established which allow BACs to be rapidly modified in *Escherichia coli (E.coli)* using a highly efficient phage-based homologous recombination system termed recombineering (Yu et al., 2000; Copeland et al., 2001; Lee et al., 2001). A disadvantage with the use of BACs is that due to their large size they are more difficult to handle than conventional sized plasmids.

1.7.2.2 Strategies to enrich ESC derived dopamine neurons

Two strategies may be implemented to enrich DA neurons from ESCs, including expression of EGFP from promoters specific to neural precursor (NPs), thus labelling cells at early stages of *in vitro* neuronal differentiation, and expression from promoter specific to post-mitotic DA neurons, hence labelling neurons at late stages of the differentiation process. In the case of neural specific promoters, sorting NPs may allow for further amplification and differentiation *in vitro* (Li et al., 1998) and may prevent large scale cell death which has been reported to occur following dissociation at later stages of neuronal differentiation (Yoshizaki et al., 2004). The early stages of the differentiation process could also be monitored in real time in live cells (Li et al., 1998). Nestin and Sox1 are both markers of NPs, being expressed at early stages of *in vivo* neural development and down-

regulated as development proceeds and cells become post-mitotic (Lendahl et al., 1990; Pevny et al., 1998; Wood and Episkopou, 1999). EGFP expressed from the nestin promoter in ESCs has been shown to be an effective way to purify NPs during *in vitro* differentiation, with a highly enriched neuronal and glial population generated after further differentiation (Andressen et al., 2001). No analysis was performed in this study to determine the specific neuronal subtypes present in differentiated cultures. Sox1-GFP is also an effective way to select ESC-derived NPs, with an enriched neuronal and dopaminergic population generated following further *in vitro* differentiation (Chung et al., 2006; Fukuda et al., 2006; Parmar and Li, 2007). However, the enrichment for DA neurons in these studies was highly variable, possibly due to the use of alternative differentiation procedures or time point of sorting.

Expressing EGFP from DA specific promoters may allow mature DA neurons to be enriched from other cell types by FACS, thus obtaining purified DA neurons which would otherwise be virtually impossible (Zhao et al., 2004; Hedlund et al., 2008). Labelling cells in this manner may also provide a model system to track the fate of *in vitro* generated DA neuron, thus enabling the identification of key determinants and regulatory genes governing this process (Zhao et al., 2004). To date EGFP has been targeted to the TH (Yoshizaki et al., 2004; Hedlund et al., 2007) and Pitx3 (Zhao et al., 2004; Hedlund et al., 2008) promoters in ESCs. Pitx3-EGFP reporter ESCs were found to be a good marker for DA neurons, with high over-lap detected between EGFP and TH expression (Zhao et al., 2004; Hedlund et al., 2008). However, the extent of co-expression appeared to be determined by the dopaminergic differentiation method used and TH positive cells were found in both studies that did not express EGFP, indicating that not all DA neurons were of a midbrain lineage (Zhao et al., 2004; Hedlund et al., 2008). Hedlung et al. (2008) also observed high over-lap of EGFP with midbrain specific transcription factors, such as Nurr1 and Lmx1, and that DA neurons could be effectively sorted to purity by FACS. However, differentiated Pitx3-EGFP DA neurons represented only 2-5% of all live cells in cultures after dissociation (Hedlund et al., 2008) and therefore may have limited potential for *in vitro* applications. Reports suggest that labelling ESC derived DA neurons by targeted expression of EGFP from the TH promoter may not be an effective way to enrich DA neurons, or at least was not the case in published studies using a TH promoter fragment

(Yoshizaki et al., 2004; Hedlund et al., 2007). While cells were detected in differentiated cultures which co-expressed EGFP and TH in both studies, a proportion of cells also expressed EGFP but not TH, and vice versa, and was correlated to the use of a promoter fragments or the expression of TH in other cell types during differentiation (Yoshizaki et al., 2004; Hedlund et al., 2007). Furthermore, Hedlund et al. (2007) also reported the presence of a mixed cell population containing markers of pluripotent stem cells and proliferative cells after transplantation of a FACS purified population into the rat brain. Selection of EGFP positive and stage-specific embryonic antigen 1 (SSEA1) negative cells resulted in the purification of only 1.4% of live cells in this study (Hedlund et al., 2007), with TH-EGFP ESCs representing 2.6% of live cells following neuronal differentiation in the study of Yoshizaki et al. (2004). These reports highlight the difficulties which can arise following the use of promoter fragments to drive transgene expression. Thus, targeting EGFP to a promoter which is more selectively expressed in DA neurons, such as DAT, and site-specific targeting to the endogenous gene contained within a BAC may overcome these problems.

1.8 Induced pluripotent stem cells

In 2006 a ground-breaking study published by Takahashia and Yamanaka (2006) reported that mouse embryonic and adult fibroblasts could be reprogrammed to cells resembling the morphology and growth properties of ESCs, and expressing ESC marker genes, by retroviral expression of four transcription factors, c-Myc, Sox2, Klf4 and Oct4. These cells were termed induced pluripotent stem cells (iPSCs). This discovery raised fundamental questions about the mechanisms by which transcription factors influence the epigenetic conformation and differentiation potential of cells during reprogramming and normal development (for review, see Stadtfeld and Hochedlinger, 2010). In addition, iPSCs offer unprecedented potential for disease research, drug screening, toxicology and regenerative medicine (for review, see Yamanaka, 2009). Soon after publication of this initial study, mouse iPSCs were generated that functionally and molecularly more closely resembled ESCs, including competency to generate germline chimeras (Maherali et al., 2007; Okita et al., 2007; Wernig et al., 2007) and more recently rare mouse iPSC lines have been generated that are capable of generating "all iPSC" live adult mice upon injection into

tetraploid blastocysts (Boland et al., 2009; Kang et al., 2009; Zhao et al., 2009; Stadtfeld et al., 2010a), suggesting that some iPSC clones have a developmental potency equivalent to ESCs (for review, see Stadtfeld and Hochedlinger, 2010). Importantly, iPSCs have also been derived from human fibroblasts (Takahashi et al., 2007; Yu et al., 2007; Park et al., 2008b) and other somatic cell populations, including neural cells (Eminli et al., 2008; Kim et al., 2008), melanocytes (Utikal et al., 2009) and stomach and liver cells (Aoi et al., 2008), thus underscoring the universality of induced pluripotency (for review, see Stadtfeld and Hochedlinger, 2010).

1.8.1 Generation of iPSCs

The first studies generating iPSCs used constitutively active retroviral vectors that stably integrated into the host cell genome to introduce c-Myc, Klf4, Oct4 and Sox2 (Takahashi and Yamanaka, 2006; Maherali et al., 2007; Okita et al., 2007; Wernig et al., 2007), and although typically silenced towards the end of reprogramming (Stadtfeld et al., 2008b), this process was often found to be incomplete, resulting in partially reprogrammed cell lines that continued to depend on the exogenous factor and failed to express the corresponding endogenous gene (Takahashi and Yamanaka, 2006). In addition, residual activity or reactivation of viral transgenes in iPSCs-derived somatic cells can interfere with their developmental potential (Takahashi and Yamanaka, 2006) and integration of viral transgenes often occurs within endogenous genes and can result in gene activation (for review, see Yamanaka, 2009). Thus alternative strategies have been developed to reprogram cells (for reviews, see Yamanaka, 2009; Stadtfeld and Hochedlinger, 2010). These include the use of inducible systems in which transgene expression is controlled by doxycycline, thus diminishing the risk of continued transgene expression and allowing the selection of fully reprogrammed cells, since cells that depend on exogenous factor expression readily stop proliferating upon doxycycline withdrawal (Brambrink et al., 2008; Stadtfeld et al., 2008a). Inducible polycistronic cassettes have also been generated in which all four reprogramming genes are expressed from one promoter, thus increasing efficiency and decreasing viral integration sites (Carey et al., 2009; Sommer et al., 2009). Mouse strains have also recently been developed harbouring a single copy of this polycistronic

cassette in a defined genomic position, thus allowing for the controlled induction of pluripotency in various somatic cells (Carey et al., 2010; Stadtfeld et al., 2010).

Alternative strategies have also been developed to derive iPSCs free of transgenic sequences, thus circumventing the potentially harmful effects of leaky transgene expression and insertional mutagenesis (for review, see Stadtfeld and Hochedlinger, 2010). Techniques to generate integration-free iPSCs can be divided into three categories (for review, see Stadtfeld and Hochedlinger, 2010). The first approach involves the use of vectors which do not integrate into the genome and reprogramming has been achieved with mouse cells using adenoviral vectors (Stadtfeld et al., 2008b) and plasmids (Okita et al., 2008), and human cells using adenoviral vectors (Zhou and Freed, 2009), the Epstein-Barr virus (Yu et al., 2009) and the Sendai virus (Fusaki et al., 2009). However, reprogramming efficiency with these non-integrating methods are several order of magnitude lower (~0.001%) than those achieved with integrating vectors (~0.1-1%), most likely because factor expression is not maintained for sufficient length of time to allow epigenetic remodelling (for review, see Stadtfeld and Hochedlinger, 2010). Thus, an alternative approach involves the use of integration-dependent gene delivery vectors which can subsequently be excised from the host genome after reprogramming has been completed (for review, see Stadtfeld and Hochedlinger, 2010). This has been achieved by incorporation of loxP sites into expression vector, which can subsequently be excised by transient expression of Cre recombinase, and has successfully been applied to polycistronic vectors (Chang et al., 2009; Soldner et al., 2009; Sommer et al., 2010). However, it remains to be determined if short vector sequences, which inevitably remain in the host genome after excision, affect cellular function (for review, see Stadtfeld and Hochedlinger, 2010). In addition, reprogramming of mouse and human cells has recently been achieved in the absence of viral or plasmid vectors, by application of purified reprogramming proteins (Kim et al., 2009; Zhou et al., 2009a), small molecules (Lin et al., 2009; Desponts and Ding, 2010; Li and Ding, 2010) and modified synthetic mRNA encoding reprogramming proteins (Warren et al., 2010). However, these approaches alone may also induce genetic or epigenetic abnormalities into the resultant iPSCs (for review, see Stadtfeld and Hochedlinger, 2010). Thus the generation of iPSCs still requires significant technical advancements (for review, see Yamanaka, 2009).

1.8.2 Application of iPSCs to neurodegenerative and psychiatric disorders

It has been suggested that while iPSC technology is still in its infancy and significant methodological improvements still need to be made, the potential application of these new pluripotent stem cells remains enormous (for review, see Yamanaka, 2009). In the short term it is anticipated that iPSCs will be used to create more effective disease models *in vitro* (for reviews, see Yamanaka, 2009; Stadtfeld and Hochedlinger, 2010), which is supported by the fact that multiple disease specific iPSCs have already been generated (Dimos et al., 2008; Park et al., 2008; Ebert et al., 2009; Lee et al., 2009; Soldner et al., 2009; Marchetto et al., 2010; Chiang et al., 2011; Nguyen et al., 2011). This may facilitate screening and identification of safer and more effective medication, therefore accelerating their translation to the clinic (for reviews, see Yamanaka, 2009; Stadtfeld and Hochedlinger, 2010). This is of significance as one of the main obstacle to drug discovery is lack of adequate disease models (for review, see Rubin, 2008). In the long term it has been proposed that iPSCs may be used in regenerative medicine, particularly in relation to autologous transplantation, potentially overcoming problems associated with ESCs (for review, see Yamanaka, 2009). Furthermore, it has been suggested that techniques which have been optimised with ESCs, such as directed differentiation and selection of specific cell types, may be translated to iPSCs (for review, see Stadtfeld and Hochedlinger, 2010).

The applications of iPSCs are of particular relevance to neurodegenerative and psychiatric disorders (for reviews, see Kim, 2010; Wichterle and Przedborski, 2010), subsets of which are caused by degeneration or dysfunction of the mDA system (for review, see Greengard, 2001). In both cases the underlying pathogenic mechanisms are largely unknown, due in part to limited access to human nerve cells, with cellular models of these disorders being extremely limited and rational treatments lacking in most cases (for reviews, see Kim, 2010; Wichterle and Przedborski, 2010). This is of particular importance in relation to neurodegenerative diseases, such as PD, with current medications having only a symptomatic effect and unable to halt or retard the degenerative process (for review, see Wichterle and Przedborski, 2010). Thus the derivation of disease specific iPSCs from individuals suffering from these neurodegenerative and psychiatric disorders and the directed differentiation of these cells to the particular neuronal subtype implicated in the

disease, such as DA neurons, may elucidate mechanisms of disease pathogenesis, allowing the creation of more faithful disease models which may facilitate the development of efficacious preventative or protective therapies (for reviews, see Yamanaka, 2009; Kim, 2010; Wichterle and Przedborski, 2010). In relation to the long term application of iPSCs, it has recently been shown that iPSC derived DA neurons survived transplantation and provided some behavioural recovery in animal models of PD, providing proof of principle for the use of these cells in regenerative medicine for PD (Wernig et al., 2008; Cai et al., 2010; Hargus et al., 2010).

To date, iPSCs have been generated from patients with a range of neurodegenerative and psychiatric disorders including PD, Huntington disease (HD), spinal muscular atrophy (SMA), amyotrophic lateral sclerosis (ALS), familial dysautonomia (FD), schizophrenia and Rett syndrome (Dimos et al., 2008; Park et al., 2008; Ebert et al., 2009; Lee et al., 2009; Soldner et al., 2009; Marchetto et al., 2010; Chiang et al., 2011; Nguyen et al., 2011). Importantly, these reprogrammed cells were capable of further differentiation to the specific neuronal type affected by the disease (Dimos et al., 2008; Ebert et al., 2009; Lee et al., 2009; Soldner et al., 2009; Cooper et al., 2010; Hargus et al., 2010; Marchetto et al., 2010; Nguyen et al., 2011). In particular, it was recently reported that PD iPSCs could be induced to differentiate to DA neurons expressing markers of the ventral mesencephalon, thus generating the specific dopaminergic subtype that degenerates in PD (Cooper et al., 2010). However, while neurons derived from SMA (Ebert et al., 2009) and FD (Lee et al., 2009) iPSCs recapitulated some of the hallmarks of these diseases, such as the decrease of survival motor neuron protein and nuclear localisation in SMA neurons (Ebert et al., 2009), these are developmental neuropathologies and thus far no disease-related phenotypes have been reported for late-onset sporadic diseases such as PD, suggesting that these phenotypes may only manifest themselves after challenging neural cells with stressors (Dimos et al., 2008; Soldner et al., 2009; Hargus et al., 2010; Wichterle and Przedborski, 2010). In fact, no disease specific markers of PD were detected 12 weeks after transplantation of DA neurons derived from sporadic PD iPSCs into the striatum of the rat brain, with the authors suggesting observation periods may need to be prolonged for up to 3 years to evaluate any PD-related changes (Hargus et al., 2010). It should also be noted that iPSCs generated from a patient suffering from a genetic form of PD (mutation in Leucine-Rich Repeat Kinase-2

(LRRK2) gene) could be differentiated to DA neurons and these neurons exhibited enhanced susceptibility to oxidative stress (Nguyen et al., 2011).

Clearly, for the promise of iPSCs to be realised, it is necessary to ask if and how effectively they may be differentiated to functional cells of various lineages (Hu et al., 2010). This question can be answered by direct comparison with ESCs, as iPSCs should, by definition, behave like ESCs in their self-renewal and lineage differentiation (Hu et al., 2010). Two studies recently published regarding the neural differentiation capacity of human iPSCs resulted in disparate conclusions (Hu et al., 2010; Boulting et al., 2011). While Hu et al. (2010) reported that human iPSCs followed the same temporal course during neural specification as human ESCs, iPSCs were found to exhibit lower and more variable neuroepithelial and neuronal differentiation efficiencies (Hu et al., 2010). However, Boulting et al (2011) reported that iPSCs gave rise to functional motor neurons with a range of efficiencies similar to that of ESCs. This study is of significance as more iPSC and ESC lines were compared (Boulting et al., 2011). Importantly, both studies suggested that the method used to generate iPSC clones did not negatively affect the neural differentiation propensity of these cells (Hu et al., 2010; Boulting et al., 2011). As human iPSCs and ESCs are derived from an outbred population, it may be of interest to analyse the neural differentiation efficiency of mouse iPSCs in comparison to genetically matched mouse ESCs.

1.9 Aims of thesis

1. DA neurons have many fundamental functions in the brain. ESCs may provide an unlimited source of these cells. To overcome the obstacle of heterogeneous cell populations post-differentiation, an objective was to label DA neurons with EGFP expressed from cell specific promoters. The purpose of this objective was to allow the direct visualisation of cells during the differentiation process and sorting of differentiated cells to obtain pure a DA neuron population. DAT is a unique marker of DA neurons in the brain. Thus mouse ESCs stably expressing EGFP from the DAT promoter would be extremely beneficial and the creation of such a cell line was an aim of this thesis.

2. Alternatively, EGFP may be expressed from neural specific promoters, such as Sox1, in ESCs to allow sorting of cells during early neural differentiation. NPs may be further amplified and differentiated to post-mitotic neurons *in vitro*. A Sox1-GFP reporter ESC line has previously been established and, while inconclusive, reports suggest that enriched populations of DA neurons may be obtained from this cell line. Therefore, the ability to purify NPs and obtain an enriched DA neuron population after further differentiation was investigated, with cells being directed to a DA fate using the previously untested fast and efficient dopaminergic differentiation procedure described by Lau et al. (2006).

3. iPSCs offer unprecedented potential for studying both neurological and psychiatric disorders associated with DA neurons. For the promise of iPSCs to be realised fundamental questions need to be addressed about their pluripotency and lineage commitment, and can be assessed by direct comparison to ESCs. Thus this aim was to assess the neural differentiation efficiency of a mouse iPSC clone compared to a mouse ESC line from the same genetic background.

Chapter 2

General Methods

2.1 Materials

NucleoBond PC 500 kit and NucleoBond BAC 100 were purchased from Macherey Nagel GmbH and Co. KG, Duren, Germany. Luria-Bertani (LB) broth, LB agar and SOB medium were supplied by Chromatrin Ltd., Dublin, Ireland. QIAquick PCR purification kit, QIAquick gel extraction kit, QIAprep spin miniprep kit and RNeasy Plus Micro Kit were from Qiagen Ltd., West Sussex, England. Knock-out Dulbecco's modified Eagle's medium (KO-DMEM), DMEM with GlutaMAX, DMEM/F-12, Neurobasal medium, foetal bovine serum (FBS), 100X N-2 supplement, 50X B-27 supplement, 200 mM L-glutamine, 100X non-essential amino acids (NEAA), 0.05% trypsin/EDTA solution, 100X penicillin (50 units/ml)/streptomycin (50 μg/ml) (pen/strep), SuperScript III First-Strand Synthesis System, goat anti-mouse and anti-rabbit Alexa 488 conjugated secondary antibodies, and goat anti-mouse, anti-rabbit and anti-rat Alexa 546 conjugated secondary antibodies (Molecular Probes) were from Invitrogen, California, USA. 1X phosphate buffered saline (PBS) was obtained from BioSera, East Sussex, UK. ESC qualified FBS was obtained from HyClone, Utah, USA. Restriction enzymes, shrimp alkaline phosphatase (SAP), T4 DNA polymerase, T4 DNA ligase with PEG and O'GeneRuler DNA ladder mix were purchased from Fermentas GmbH, St.Leon-Rot, Germany. High Fidelity PCR Enzyme Mix was obtained as kind gifts from Fermentas. Sodium selenite, putrescine dihydrochloride, progesterone, albumin from bovine serum (further purified Fraction V), sodium deoxycholate, kanamycin, chloramphenicol, gelatine from cold water fish skin, mitomycin C, bovine serum albumin (BSA), laminin, apo-transferrin, insulin solution, glucose, HEPES, ammonium persulfate, KOH, $CaCl_2$, $MnCl_2$, KCl, Tris, EDTA, glacial acetic acid, glycerol, agarose, ethanol, methanol, G418, triton X-100, β-merceptoethanol (β-MeOH), L-ascorbic acid (L-AA), propidium iodide (PI), bovine fibronectin, poly-D-lysine (PDL), poly-L-ornithine (PLO), protease inhibitor cocktail were obtained from Sigma Chemical Co., Poole, Dorset, England. DSF-Taq DNA polymerase and dNTP mixture were purchased from Bioron GmbH, Ludwigshafen, Germany. Mouse recombinant Shh, EGF, FGF8 and bFGF were obtained from R&D Systems Europe Ltd., Abingdon, United Kingdom. Ribonuclease A (RNase A) from bovine pancreas and cytidine were from Biochemika (Fluka), Seelze, Germany. Vectashield mounting medium with DAPI was from Vector Laboratories, Petersborough, England. Isopropanol was obtained from BDH

laboratory supplies, Poole, Dorset, England. ProtoGel (30%) was purchased from National Diagnostics, Atlanta, Georgia, USA. Bicinchoninic acid (BCA) protein assay kit was from Pierce, Rockford, Illinois, USA. Esgro (Leukemia inhibitory factor, LIF, $1x10^7$ units/ml), goat anti-rabbit and goat anti-mouse horse radish peroxidase (HRP) conjugated secondary antibodies, Immobilon-P PVDF, Immobilon Western Chemiluminescent HRP Substrate, Immobilon Blotting Filter Paper and the primary antibodies rabbit anti-green fluorescent protein (GFP), rabbit and rat anti-DAT, mouse and rabbit anti-TH, rabbit anti-glutamic acid decarboxylase (GAD), mouse anti-neuronal nuclei (NeuN) were from Millipore, Massachusetts, USA. Mouse anti-noradrenaline transporter (NAT) primary antibody was obtained from Mab technologies, Stone Mountain, Georgia, USA. Mouse anti-neuronal class III β-tubulin (Tuj1 clone) primary antibody was from Covance, Princeton, New Jersey, USA. Rabbit anti-synaptophysin primary antibody was from Synaptic Systems, Goettingen, Germany. Rabbit anti-excitatory amino acid carrier 1 (EAAC1) primary antibody was from Alpha Diagnostics, San Antonio, Texas, USA. Rabbit anti-glial fibrillary acidic protein (GFAP) primary antibody was from DAKO, Glostrup, Denmark. Mouse anti-serotonin transporter (SERT) primary antibody was from Advanced Targeting Systems, San Diego, California, USA. Mouse anti-stage specific embryonic antigen 1 (SSEA1) and rabbit anti-Nurr1 primary antibodies were purchased from Santa Cruz Biotechnology, California, USA. Mouse anti-glyceraldehyde-3-phosphate dehydrogenase (GAPDH) primary antibody was obtained from Ambion, Austin, USA. Oligonucleotides were purchased from Eurogentec, Seraing, Belguim. Sequencing was performed by GATC, Germany.

2.2 Preparation of buffers and solutions

Buffers and reagents were prepared using water deionised with a Direct-Q UV Millipore deioniser. Reagents were weighed on either a Mettler K7T model top balance, for weights greater than 5 g or a Mettler College Model analytical balance, for weights less than 5 g. The pH of solutions was measured using a Corning pH meter which was calibrated daily using standard pH buffers of pH 4, 7 and 10.

2.3 Pipetting

A set of Gilson automatic pipettes was used throughout experimental work to pipette volumes ranging from 0.2 µl-5 ml. Autoclaved pipette tips were used where applicable.

2.4 Mouse pluripotent stem cell lines

R1 mouse embryonic stem cells (ESCs) and mouse embryonic fibroblasts (MEFs) were received as a kind gift from Dr Thorsten Lau (Central Institute of Mental Health, Mannheim, Germany). 46C mouse ESCs (Sox-1-GFP knock-in ESCs) were obtained as a kind gift from Prof Austin Smith (Cambridge University, UK). V6.5 mouse ESCs and V6.5 mouse iPSCs were obtained as a kind gift from Dr Stephen Sullivan. iPSCs were derived from MEFs by retroviral transfection with c-Myc, Oct-4, Sox-2 and Klf-4.

2.5 General cell culture equipment

All cells were maintained in a Series 8000 DH CO_2 incubator. Conditions were set to a constant temperature of 37°C and 5% CO_2 with humidity. Cells were visualised daily with a Nikon Eclipse TS100 light microscope. Centrifugation steps were performed in a Heraeus Multifuge 3SR+ Centrifuge at 800 rpm for 5 min at room temperature (RT), unless otherwise stated. An Eppendorf 5415R bench top centrifuge was used for volumes <1.5 ml.

2.6 General cell culture methods

2.6.1 Preparation of gelatine coated dishes

0.1% (v/v) gelatine from cold water fish skin was prepared in water, sterilised by autoclaving and stored at 4°C. Cell culture dishes and plates were coated with gelatine solution to promote adhesion of ESCs. This was achieved by the addition of the required volume of gelatine solution (Table 2.1) to dishes/plates and incubation at RT for 30 min. The gelatine solution was subsequently removed and dishes/plates were dried by incubation for 1 hour at 37°C. Residual gelatine was removed prior to use by washing with 1X PBS.

Tissue culture dish/plate	Volume of 0.1% gelatine
10 cm dish	5 ml
T25 flask	3 ml
6-well plate	2 ml/well
24-well plate	0.5 ml/well
96-well plate	100 µl/well

Table 2.1: Volume of 0.1% (v/v) gelatine solution used to coat cell culture dishes and plates

2.6.2 Preparation of feeder cells

MEFs were used to make feeder cells, onto which R1 mouse ESCs were grown. Growth on feeder cells promotes health of ESCs and prevents differentiation. MEFs were cultured in DMEM with GlutaMAX containing 10% (v/v) FBS, 1X pen/strep and maintained in the incubator. Cells were routinely grown in 10 cm dishes until confluency was reached, at which point they were passaged at a 1:4 ratio. This was achieved by removing medium from cells, washing thrice with 5 ml of 1X PBS and adding 2 ml of pre-heated 0.05% trypsin/EDTA solution. Dishes were returned to the incubator for 5-10 min until cell detached. Trypsin was then inactivated with 6 ml of fresh medium and transferred to 4 new dishes containing 8 ml of medium. Dishes were rocked gently to ensure an even distribution. Cells were allowed to grow to confluency again and treated with 10 µg/ml mytomycin C for 2-2.5 hours at 37°C to inactivate the cell cycle. After this time, medium containing mytomycin C was removed, cells were washed 3 times with 5 ml 1X PBS and fresh medium was added. Cells were maintained in culture for 2-3 days to ensure the mytomycin C treatment was effective and cells were not damaged during the process, after which they were used as feeder layer for ESCs or frozen.

2.6.3 Propagation of mouse pluripotent stem cells

R1 ESCs were maintained on feeder layers. 46C ESCs, V6.5 ESCs and V6.5 iPSCs were feeder independent and maintained on gelatine coated dishes. A vial of cells was thawed

rapidly at 37°C until almost all ice crystals were dissolved. The vial was cleaned thoroughly with 70% (v/v) ethanol and the cells were transferred to 10 ml pre-warmed ESC medium (KO-DMEM supplemented with 15% (v/v) ESC qualified FBS, 1X NEAA, 1X pen/strep, 2 mM L-glutamine, 0.1 mM β-MeOH, 1000 units/ml LIF) in a Falcon tube. Cells were pelleted by centrifugation, resuspended in fresh pre-warmed ESC medium, and transferred to a 10 cm dish or T25 flask pre-coated with feeders or 0.1% (v/v) gelatine solution, as required. Dishes were rocked gently to ensure the cell suspension was evenly distributed and transferred to the incubator. Medium was changed daily and cells were typically passaged every second day.

2.6.4 Passaging of mouse pluripotent stem cells

Cells were routinely passaged when semi-confluency was reached. This was achieved by first removing medium from cells and washing thrice with 4 ml 1X PBS. Pre-heated 0.05% trypsin/EDTA solution (1 or 2 ml) was subsequently added to dishes/flasks and returned to the incubator for 5 min. After this time cells were observed microscopically to ensure detachment. Fresh medium (4 or 6 ml) was subsequently added to inactivate trypsin, the cell suspension was transferred to a Falcon tube and centrifuged. The cell pellet was resuspended in 4 ml of medium and 1 ml was transferred to new dishes or flasks pre-coated with feeders or 0.1% (v/v) gelatine solution, thus achieving a 1:4 split ratio. Fresh pre-heated medium was added, dishes were rocked gently to ensure an even distribution of cells, observed microscopically and returned to the incubator. Cells were passaged twice prior to use in experiments. Experiments with V6.5 ESCs and iPSCs were performed on cells of the same passage number, typically around passage number 24. Experiments with 46C ESCs and R1 ESCs were typically performed on cells of passage number 20-24.

2.6.5 Cell counting and cell viability assay

Cell counts and cell viability was routinely assessed with the Trypan blue exclusion assay. This assay is based on the principle that viable cells have intact cell walls and therefore exclude the dye (clear cytoplasm), whereas non-viable cells do not exclude the dye (blue cytoplasm). An aliquot of cell suspension (30 µl) was typically diluted 1:4 with Trypan

blue, vortexed and 10 µl placed on the counting chamber of a haemocytometer. The total number of cells and the number of unstained cells in four squares of the chamber were counted, allowing percentage viability and number of cells to be determined based on the following formulae:

$$\text{Number of cells/ml} = \frac{\text{Total number of cells counted}}{\text{Number of squares counted}} \times \text{dilution} \times 10^4$$

$$\% \text{ Viable cells} = \frac{\text{Number of unstained cells}}{\text{Total number of cells}} \times 100$$

2.6.6 Freezing of cells

Cells to be frozen were trypsinised and resuspended to a single cell suspension, a 30 µl aliquot was taken and a cell count was performed. The cell suspension was subsequently centrifuged and the cell pellet was resuspended in freezing medium (10% DMSO, 90% FBS) to obtain a density of around $2x10^6$ cells/ml (for plating in T25 flasks) or $4.5x10^6$ cells/ml (for plating in 10 cm dishes). One ml of the cell suspension was transferred to each labelled cryogenic vials and frozen slowly at -80°C in a Cryogenic freezing container. Vials were transferred to liquid nitrogen for long term storage the subsequent day. Feeder cells were frozen in a similar manner, with one dish being frozen per cryogenic vial.

2.6.7 Preparation of plates for neural stem sphere attachment

In order to determine the optimal conditions for attachment of neural stem spheres (NSSs), plates were coated with a range of substrate previously reported in the literature to enhance cell attachment and neuronal differentiation. Plates were coated as follows:

1. Gelatine/laminin: Plates were coated with gelatine as described above prior to the addition of 1 $\mu g/cm^2$ laminin solution for 3 hours at 37°C. Plates were washed with 1X PBS prior to the addition of cells.
2. PDL/laminin: Plates were coated with 10 $\mu g/cm^2$ PDL solution overnight at 37°C, washed thrice with 1X PBS and coated with laminin as described above.

3. PDL/fibronectin: Plates were coated with PDL as described above and subsequently coated with 0.1 $\mu g/cm^2$ bovine fibronectin for 3 hours at 37°C. Plates were washed with 1X PBS prior to use.
4. PLO/laminin: Plates were coated with 3.125 $\mu g/cm^2$ PLO solution (working concentration 15 µg/ml in H_2O) overnight at 37°C. Plates were subsequently washed thrice with H_2O and coated with laminin as described above. Plates were washed with 1X PBS prior to addition of cells.
5. PLO/fibronectin: Plates were coated with PLO first and then fibronectin as described above.
6. PLO/fibronectin/laminin: Plates were coated sequentially with PLO and fibronectin as described above, and laminin (1 $\mu g/cm^2$) for 1 hour at 37°C. Plates were washed with 1X PBS prior to the addition of cells

2.7 Neuronal differentiation

Neuronal differentiation was induced in pluripotent stem cells by two methods, including a multi-stage growth factor induced (GFI) protocol (Lau et al., 2006) and a monolayer (ML) procedure (Ying and Smith, 2003; Ying et al., 2003). An overview of each method is provided in Fig. 2.1. Details are provided in Table 2.2 of the differentiation method used with each cell line and the corresponding thesis chapter in which they are found.

Stem cell line	Differentiation protocol	Thesis chapter
R1 ESC	GFI	Chapter 3, 4
R1 ESC	ML	Chapter 4
46C ESC	GFI, ML	Chapter 4
V6.5 ESC	GFI, ML	Chapter 5
V6.5 iPSC	GFI, ML	Chapter 5

Table 2.2: Differentiation protocol used with each cell line and the corresponding thesis chapter in which they are found

ESC indicates embryonic stem cell; iPSC, induced pluripotent stem cell; GFI, growth factor induced differentiation; ML, monolayer differentiation.

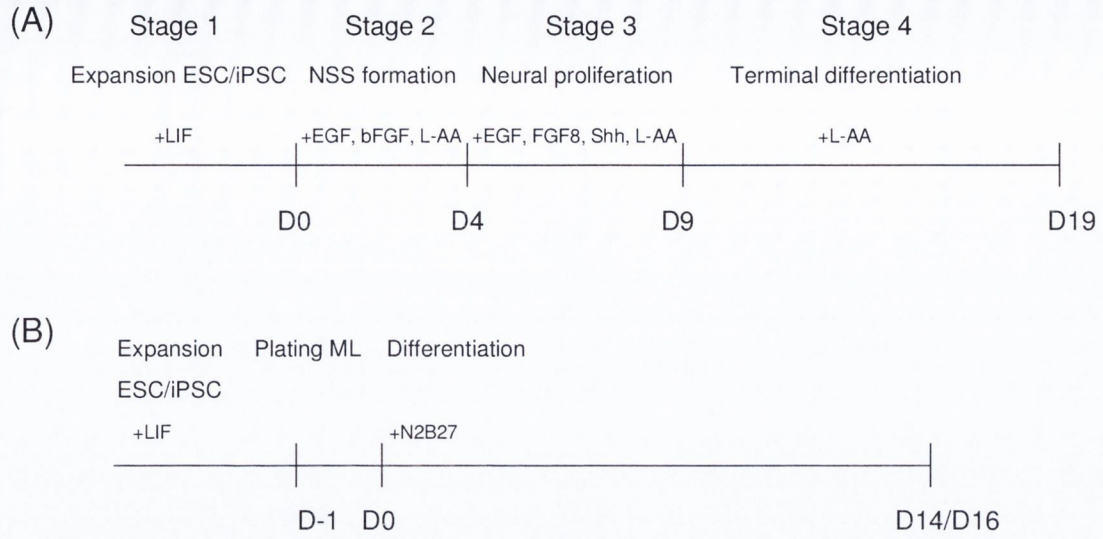

Fig. 2.1: Overview of neuronal differentiation methods

(A) Growth factor induced neuronal differentiation involved four stages, as indicated. (B) Monolayer neuronal differentiation was induced in N2B27 medium by plating cells as monolayers (ML), as indicated. Detailed descriptions for each protocol are provided in section 2.7. ESC indicates embryonic stem cells; iPSC, induced pluripotent stem cells; LIF, leukemia inhibitory factor; NSS, neural stem sphere; Shh, sonic hedgehog; EGF, epidermal growth factor; FGF8, fibroblast growth factor 8; bFGF, basic fibroblast growth factor; L-AA, L-ascorbic acid; D, day.

2.7.1 Growth factor induced neuronal differentiation

Cells were differentiated to dopamine (DA) neurons according to Lau et al. (2006), with modifications. This protocol involved culturing cells in four stages (Fig. 2.1) and typically generated DA neurons faster than alternative published reports (Lee et al., 2000; Rolletschek et al., 2001) by the application of growth factor at early stages of the differentiation process.

In the first stage (stage 1), undifferentiated pluripotent stem cells were expanded as described above in Section 2.6. When cells reached semi-confluency after being sub-cultured twice, they were induced to form NSSs by growth in suspension culture (stage 2). This was achieved by trypsinisation and resuspension in 10 ml NSS medium (KO-DMEM supplemented with 10% (v/v) ESC qualified FBS, 1X NEAA, 1X pen/strep, 2 mM L-glutamine with 20 ng/ml EGF, 20 ng/ml bFGF, 100 µM L-AA added freshly prior to use). LIF was removed at this stage to induce differentiation. 46C ESCs, V6.5 ESCs and V6.5 iPSCs were transferred to non-adhesive bacteriological dishes. R1 cells were successively transferred to three culture dish, for 20 min each time to separate ESCs from any remaining feeders prior to plating in non-adhesive dishes. Medium was changed after two days by allowing the spheres to settle to the bottom of a Falcon tube and resuspending the pellet in fresh pre-warmed medium.

NSSs were collected after 4 days by allowing the cell aggregates to drop to the bottom of a Falcon tube by gravity. 0.05% trypsin/EDTA (500 µl) was added and incubated at 37°C for 5 min in a water bath. Trypsin was inactivated with 2 ml proliferation medium (1:1 DMEM/F-12, 1X NEAA, 1X pen/strep, 2 mM L-glutamine, 1X N2 supplement, 1X B27 supplement, with 25 µg/ml insulin, 50 µg/ml apo-transferrin, 100 µM putrescine, 20 nM progesterone, 30 nM sodium selenite, 50 µg/ml BSA, 100 µM L-AA, 20 ng/ml EGF, 20 ng/ml FGF8, 25 ng/ml Shh added prior to use) supplemented with 10% FBS. Cells were filtered through a 40 µm cell strainer to obtain a single cell suspension and a cell count was performed. Cells were plated at a density of ~$8x10^4$ cells/cm^2 on substrate coated dishes. Proliferation medium supplemented with 10% FBS, to a final volume of 3 ml/well for a 6 well plate and 0.5 ml/well for a 24 well plate and the cells were incubated overnight. The

presence of FBS promotes adhesion of the cells. The medium was subsequently replaced with proliferation medium without serum to induce expansion of neural precursors (stage 3), and thereafter replaced every day.

After 5 days, proliferation medium was replaced with differentiation medium (1:1 DMEM/F-12, 1X NEAA, 1X pen/strep, 2 mM L-glutamine, 1X N2 supplement, 1X B27 supplement, with 100 µM L-AA added prior to use). The removal of growth factors induced terminal differentiation and maintenance of dopaminergic neurons, and encompassed stage 4 of the protocol. Differentiation medium was changed every second day and cells were typically harvested for analysis on day 10 of differentiation.

2.7.2 Monolayer neuronal differentiation

Undifferentiated pluripotent stem cells were also differentiated to neurons according to the protocol published by Ying et al (2003) and Ying and Smith (2003). In this procedure differentiation is induced by culturing cells as monolayers in chemically defined medium in the absence of LIF. It has been reported that autocrine signalling is required for neural conversion during this procedure (Ying et al., 2003). This method can also generate DA neurons without the application of extrinsic signalling molecules (Parmar and Li, 2007).

Briefly, when undifferentiated ESCs and iPSCs reached semi-confluency after being sub-cultured twice they were dissociated and plated at a density of $1.5x10^4$ cells/cm^2 on gelatine coated dishes in ESC medium. Medium was subsequently changed to N2B27 medium (1:1 mixture of Neurobasal medium with 1X B27 supplement and F12/DMEM with modified N2 supplement containing 25 µg/ml insulin, 100 µg/ml apo-transferrin, 100 µM putrescine, 20 nM progesterone, 30 nM sodium selenite and 50 µg/ml BSA, 1X NEAA, 1X pen/strep, 2 mM L-glutamine) and thereafter changed every second day (Fig. 2.1). Cells were analysed after 14 or 16 days of differentiation.

2.8 Determination of protein concentration

Protein concentration was determined using the detergent compatible BCA based assay from Pierce. This method combines the reduction of Cu^{2+} to Cu^{+} by protein in alkaline medium (biuret reaction) with the highly selective and sensitive colorimetric detection of the cuprous cation (Cu^{+}) using a unique reagent containing BCA. The reaction product of this assay is formed by the chelation of two molecules of BCA with one cuprous cation and exhibits a strong absorbance at 562 nm that is nearly linear with increasing protein concentration. A range of BSA concentrations (125-2000 µg/ml) were used to create a standard curve, from which total cellular protein was determined. A microplate procedure was used, in which 10 µl of each standard and sample was added in triplicate to a microplate followed by the addition of 200 µl of BCA reagent. The plate was subsequently mixed on a plate shaker and incubated for 30 min at 37°C. The absorbance was then measured at 562 nm using a SpectraMAX GeminiXS well plate reader and a standard curve was prepared.

2.9 SDS-PAGE and Western blotting

2.9.1 Preparation of samples

Cells were trypsinised at required time period, centrifuged and resuspended in 100 µl of ice-cold lysis buffer (150 mM NaCl, 1% (v/v) Triton X-100, 0.1% (w/v) SDS, 0.5% (w/v) sodium deoxycholate, 50 mM Tris, pH 8) containing freshly added protease inhibitor cocktail (1:1000 dilution). The cell solution was transferred to an ice-cold 1.5 ml microcentrifuge tube and shaken gently for 30 min at 4°C. Lysates were centrifuging at maximum speed (13,200 rpm) for 20 min at 4°C in a bench top centrifuge. The supernatant containing proteins was carefully transferred to a fresh labelled 1.5 ml microcentrifuge tube and stored at -80°C until required. Mouse brain lysate was used as a positive control to detect neuronal proteins. This was prepared by homogenising tissue in 4 ml modified RIPA buffer (1% (v/v) Triton X-100, 0.2% (w/v) SDS, 0.2% (w/v) sodium deoxycholate, 1 mM EDTA, 50 mM Tris, pH 7.4) with freshly added protease cocktail (1:1000 dilution). Homogenate was transferred to labelled 1.5 ml microcentrifuge tubes and tissue and cell

debris were removed by centrifugation in at maximum speed for 20 min at 4°C in a bench top centrifuge. The supernatant was subsequently removed, transferred to new 1.5 ml microcentrifuge tubes and centrifuged again. The cleared supernatants were transferred to new microcentrifuge tubes and stored at -80°C until required. Protein concentration was subsequently determined by the BCA assay (Section 2.8). Proteins (10-30 µg) were incubated with 1X Laemmli loading buffer (2% (w/v) SDS, 5% (v/v) β-MeOH, 10% (v/v) glycerol, 0.002% (w/v) bromophenol blue, 0.0625 mM Tris-HCl, pH 6.8) at 95°C for 5 min. Samples to be probed with NAT and EAAC1 antibodies were incubated with 1X loading buffer for 30 min at 37°C.

2.9.2 SDS-PAGE

Samples were typically run on 10% or 12% gels, with the composition of one 10% gel provided in Table 2.3. Glass plates were washed thoroughly with H_2O and ethanol, a spacer was placed along the length of one plate, plates were aligned and clamped. The resolving gel was added slowly, overlaid with ethanol and allowed to polymerise for 45 min-1 hour. Ethanol was carefully poured off, the gel surface was washed with H_2O and 5% stacking gel was added. A cleaned comb was placed in the stacking gel solution to create pockets for sample addition. Gels were run at 20 mA, typically for 1-2 hours in 1X running buffer (25 mM Tris, 0.192 M glycine, 0.1% (w/v) SDS). A pre-stained protein marker was electrophoresed with samples to determine the molecular weight of proteins.

5% Stacking gel, 4 ml	10% Resolving gel, 10 ml
2.7 ml H_2O	2.3 ml H_2O
0.67 ml 30% acrylamide mix	5.0 ml 30% acrylamide mix
0.5 ml 1.0 M Tris, pH 6.8	2.5 ml 1.5 M Tris, pH 8.8
0.04 ml 10% SDS	0.1 ml 10% SDS
0.04 ml 10% ammonium persulfate	0.1 ml 10% ammonium persulfate
0.004 ml TEMED	0.004 ml TEMED

Table 2.3: Composition of one 10% SDS polyacrylamide gel

2.9.3 Semi-dry transfer of proteins to PVDF membrane

When the migration front reached the bottom of the gel the power was switched off and the gel was incubated in 1X transfer buffer (24 mM Tris, 0.192 M glycine, 0.05% SDS, 10% MeOH) with agitation for 15 min. PVDF membrane was carefully cut to the same size as the gel, activated in 100% methanol for 1 min and placed in 1X transfer buffer for 5 min. Two pieces of BioRad thick filter paper were cut to the same size as the gel and saturated in 1X transfer buffer. A sandwich of filter paper/PVDF/gel/filter paper was arranged on the semi-dry apparatus, with air bubbles being carefully removed at each step. Proteins were transferred at 10 V for 1 hour. The transfer efficiency was typically analysed by incubating the PVDF membrane in Ponceau Red stain (0.1% (w/v) Poncaeu S, 5% (v/v) acetic acid) for 5 min. The membrane was subsequently washed in H_2O until protein bands were clearly visible. This was followed by complete destaining in 1X TBS-T (50 mM Tris, pH 7.4, 150 mM NaCl, 1% (v/v) Tween-20, pH 7.6) and re-activation of the membrane in 100% MeOH for 1 min. The membrane was then returned to 1X TBS-T until required.

2.9.4 Blocking and incubation with antibodies

The PVDF membrane was subsequently incubated in blocking buffer (5% (w/v) non-fat dry milk in 1X TBS-T) for 1 hour at RT to prevent non-specific background binding of the antibodies. After blocking, the membrane was washed 3 times for 5 min with 1X TBS-T. Rabbit anti-DAT (1:1000 dilution), mouse anti- neuronal class III β-tubulin (Tuj1 clone; 1:2000 dilution), rabbit anti-TH (1:1000 dilution), rabbit anti-GFP (1:500 dilution), rabbit anti-GAD (1:2000 dilution), rabbit anti-EAAC1 (1:500 dilution), rabbit anti-synaptophysin (1:2000 dilution), rabbit anti-GFAP (1:2000 dilution), mouse anti-NAT (1:2000 dilution), mouse anti-GAPDH (1:4000 dilution), rabbit anti-Nurr1 (1:1000 dilution), mouse anti-NeuN (1:1000 dilution) and mouse anti-SERT (1:2000 dilution) were diluted in 1X TBS-T and incubated for 1 hour at RT with agitation. After incubation, the membrane was washed once for 15 min and thrice for 5 min with 1X TBS-T at RT. The membrane was then incubated with goat anti-rabbit or goat anti-mouse HRP conjugated secondary antibodies (1:2000 dilution) diluted in 1X TBS-T for 1 hour at RT with agitation. The membrane was then washed with 1X TBS-T, once for 15 min and thrice for 5 min.

2.9.5 Chemi-luminescent protein detection

The chemi-luminescence reagent was prepared by mixing 500 µl HRP substrate luminal with 500 µl HRP substrate peroxidase. This was then added to the PVDF membrane and incubated with agitation for 2 min. Proteins were detected by exposure of the membrane to photographic films and processing in a developer or digitally using a FUJIFILM Intelligent Dark Box machine and Image Reader LAS-300 software.

2.9.6 Stripping of membranes for re-probing

When required, the membrane was stripped of antibody by incubation in stripping buffer (0.2 M glycine, 0.1% (w/v) SDS, 1% (v/v) Tween-20, pH 2.2) for 10 min twice, followed by washing in 1X PBS (137 mM NaCl, 2.7 mM KCl, 4.3 mM Na_2HPO_4, 1.47 mM KH_2PO_4, pH 7.4) for 10 min twice and 1X TBS-T for 5 min twice at RT. Blocking and probing were performed as described above.

2.9.7 Semi-quantitative densitometry

The relative amount of neuronal proteins in samples was quantified using the Gel Analyser Option of ImageJ. Briefly, digital images were opened in ImageJ and the rectangular selection tool was used to draw a rectangle around the first lane. This was subsequently selected and the remaining lanes were then highlighted. The lanes were plotted and a peak was generated for each lane. These were consecutively selected and the size of each peak was calculated, with the size being expressed as a percentage of the total size of all measured peaks. This was then repeated for GAPDH. The percentage values for each sample of neuronal protein were then divided by the values obtained for GAPDH, generating a value equivalent to relative intensity.

2.10 RNA extraction and reverse-transcription polymerase chain reaction

2.10.1 RNA extraction from cells

Total ribonucleic acid (RNA) was extracted from cells using the RNeasy Plus Micro Kit from Qiagen. This kit allows the purification of high-quality RNA molecules longer than 200 nucleotides from a small numbers of cells, with the removal of genomic deoxyribonucleic acid (DNA). Briefly, cells were harvested and spun down in RNase-free tubes. The supernatant was carefully removed and 350 µl of Buffer RLT Plus added. Samples were pippetted to mix and passed through a blunt 20 gauge needle fitted with an RNase free syringe at least 5 times. The homogenised lysates were transferred to gDNA eliminator spin columns placed in 2 ml collection tubes to remove genomic DNA and centrifuged at full speed in a bench top centrifuge for 2 min at RT. Columns were subsequently discarded, 350 µl of 70% (v/v) ethanol was added and mixed by pipetting. Samples was transferred to RNeasy MinElute spin columns in 2 ml collection tubes and centrifuged for 15 sec at maximum speed. The flow through was discarded, 700 µl Buffer RW1 was added to spin columns and centrifuged at maximum speed for 15 sec. The flow through was again discarded, 500 µl Buffer RPE was added and centrifuged at maximum speed for 15 sec. The flow through was again discarded, 500 µl of 80% (v/v) ethanol was added to the spin column and centrifuged for 2 min at full speed. Spin columns were placed in new 2 ml collection tubes and centrifuged for 5 min. Spin columns were then placed in new 1.5 ml collection tubes, 14 µl of RNase free H_2O was added and centrifuged for 1 min. The concentration of RNA was determined with an eppendorf BioPhotometer Plus spectrophotometer and used for complementary DNA (cDNA) synthesis.

2.10.2 Reverse-transcriptase polymerase chain reaction

cDNA was synthesised using the SuperScript III First-Strand Synthesis System from Invitrogen. Briefly, 1 µg of RNA was mixed with 1 µl of 50 ng/µl random hexamers, 1 µl of 10 mM dNTP mix and DEPC H_2O was added to a final volume of 10 µl. The mixture was incubated at 65°C for 5 min and placed on ice for at least 1 min. During incubation the cDNA Synthesis Mix was prepared on ice and contained 10X RT buffer (2 µl/reaction), 25

mM $MgCl_2$ (4 µl/reaction), 0.1 M DTT (2 µl/reaction), RNaseOUT (1 µl/reaction), SuperScriptIII RT (1 µl/reaction). 10 µl of cDNA Synthesis Mix was added to each RNA/primer mix, mixed gently and incubated for 10 min at 25°C and 50 min at 50°C. The reaction was terminated by incubation at 85°C for 5 min and chilled on ice. The mixture was subsequently collected by brief centrifugation and RNA was digested by incubation with 1 µl RNase H for 20 min at 37°C. cDNA (1 µl) was then amplified using the following primers: GAPDH: 5'-GACCACAGTCCATGCCATCACT-3', 5'-TCCACCACCCTGTTG CTGTAG-3', 454 bp (Fukuda et al., 2006); Nestin, 5'-GGAGTGTCGCTTAGAGGTGC-3', 5'-TCCAGAAAGC CAAGAGAAGC-3', 327 bp (Lee et al., 2000) ; Oct4, 5'-GGCGTT CTCTTTGGAAAGGTGTTC-3', 5'-CTCGAACCACATCCTTCTCT-3', 312 bp (Ying et al., 2003); Nanog, 5'-AGGGTCTGCTACTGAGATGCTCTG-3', 5'-CAACCACTGGTT TTTCTGCCACCG-3', 363 bp (Chung et al., 2006); alpha-fetoprotein (AFP), 5'-GCCACC GAGGAGGAAGTG-3', 5'-AGTCTTCTTGCGTGCCAGC-3', 262 bp; bone morphogenic protein 4 (BMP-4), 5-TA GCAAGAGTGCCGTCATTCC-3', 5'-CCAGTCTCGTGCCAGT AGTCG-3', 398 bp (Ying et al., 2003); Sox-1, 5'-CCTCGGATCTCTGGTCAAGT-3', 5'-TACAGAGCCGGCAGTCATAC-3', 593 bp (Ying et al., 2003). All primers spanned at least one intron of genomic sequence. PCRs were carried out as described in Section 2.11.

2.11 Polymerase chain reactions

PCRs were performed with 0.2 mM of each dNTP, 1 x reaction buffer, 0.5 µM each of forward and reverse primers, 1 µl of template DNA (100-500 ng) or cDNA and 0.625 U Taq polymerase, to a final volume of 25 µl. Samples were amplified in a Peqlab Primus 96 Thermocycler under the following conditions: denaturation step at 95°C, 2 min; denaturation step at 95°C, 30 sec, annealing step at 55°C, 30 sec, amplification step at 72°C, 1 min, for 25-30 cycles; and final amplification step at 72°C, 5 min. Reactions with Sox-1 primers were performed at an annealing temperature of 58°C and with 5% (v/v) DMSO.

2.12 Agarose gel electrophoresis

Agarose gel electrophoresis was used to resolve DNA fragments after PCR. Typically 1% (w/v) or 1.5% (w/v) agarose gels were used, depending on the size of the fragments to be

visualised. This was prepared by dissolving agarose in 1X TAE buffer (40 mM Tris-acetate, 1 mM EDTA), with the addition of 1 μg/ml ethidium bromide to visualise DNA. Samples were mixed with 6X loading dye and loaded onto into pockets of the gel. A DNA ladder mix (10 μl) ranging from 0.1 to 10 kb was also loaded to determine the size of samples. The gel was run in a Jencon electrophoresis chamber in 1X TAE buffer at 70 V for 1-2 hours and visualised in a UV chamber with short-wave UV light (320 nm).

2.13 Immunocytochemistry

Cells were washed twice with 1X PBS (37°C) and fixed with pre-warmed 4% (w/v) paraformaldehyde (PFA) solution in 1X PBS containing 4% (w/v) sucrose, 5 mM $MgCl_2$, 10 mM EGTA, pH 7.4 for 15 min. PFA was dissolved with 10 N NaOH and the pH was adjusted with 6 N HCl. PFA was subsequently removed, cells were washed twice in ice-cold PBS and permeabilised with 0.1% (v/v) Triton X-100 in 1X PBS for 10 min. Samples were washed three times with 1X PBS, 5 min per wash, and incubated with blocking buffer (0.1% (v/v) Triton X-100, 1% (w/v) BSA in 1X PBS) for 30 min. Primary and secondary antibodies were diluted in blocking buffer and sequentially applied to samples for one hour each at RT. Alternatively primary antibody was applied overnight at 4°C. Incubation with secondary antibodies was performed in the dark. Cells were washed thrice with 1X PBS, 5 min per wash, after each antibody incubation step. Samples were mounted with Vectashield mounting medium containing DAPI to counter-stain nuclei and stored in the dark at 4°C until analysed by microscopy. Negative controls were included, in which primary antibodies were omitted. The following primary antibodies were used: mouse anti-SSEA1 (1:50 dilution), rabbit anti-GFP (1:200 dilution), rabbit anti-DAT (1:200 dilution), rat anti-DAT (1:200 dilution), rabbit anti-GFAP (1:200 dilution), rabbit anti-TH (1:200 dilution) and mouse anti- neuronal class III β-tubulin (Tuj1 clone; 1:500 dilution). Goat anti-mouse, goat anti-rabbit and goat anti-rat secondary antibodies were conjugated to Alexa 488 and Alexa 546 (1:1000 dilution). Images were collected using an Olympus FV1000 laser scanning confocal microscope set to UPlanSAPO 40 x oil objective or Olympus IX81-long focal length fluorescent microscope set to 4 x, 10 x or 40 x objective as indicated. Images were processed with ImageJ analysis software.

2.14 Tuj1 positive colony measurements

The average number of neuronal class III β-tubulin (Tuj1 clone) positive colonies per well was determined by taking 10 randomly selected images per well of a 24-well plate. The average diameter of Tuj1 colonies was calculated from 10 randomly selected Tuj1 positive colonies per well, with the diameter of the colony at its centre and along the shorter axis being measured using ImageJ analysis software. The average length of Tuj1 positive neurites for each Tuj1 positive colony was determined by measuring the length of 10 randomly selected neurites per colony for 5 colonies per well using the NeuronJ application of ImageJ. This was achieved by manually tracing along each neurite from the colony to its tip. All images were acquired using an Olympus IX81-long focal length fluorescent microscope set to 4 x or 10 x objective. Experiments were performed in triplicate and repeated with three independent cell preparations, unless otherwise stated.

2.15 Statistical analysis

Data are presented as mean + standard error of the mean (SEM). Student's unpaired two-tailed t-test was used to determine significance of data. Values of $p<0.05$ were taken as significant. Statistical analysis was performed with SPSS software.

Chapter 3

Targeting EGFP to the DAT promoter and analysis of selected R1 ESC DAT-EGFP transgenic cell lines

3.1 Introduction

DA neurons have several fundamental functions in the brain, dysfunction of which are implicated in multiple disease states, including PD and schizophrenia (for review, see Greengard, 2001). ESCs can be propagated indefinitely in culture in an undifferentiated state while retaining pluripotency (Evans and Kaufman, 1981) and therefore may provide an unlimited source of DA neurons for *in vitro* studies. Intense interest has also focused on the ability to use ESC derived DA neurons for regenerative medicine in PD (for review, see Astradsson et al., 2008). However, the potential use of ESC is greatly hindered by the heterogonous nature of cultures even after directed differentiation (for review, see Stavridis and Smith, 2003; Pruszak et al., 2007). This may be overcome by expression of EGFP from a cell specific promoter, thus allowing the selection of a particular cell type from a mixed cell population by FACS, enabling the study of a pure cell population which would otherwise be virtually impossible (Chung et al., 2006; Hedlund et al., 2008; Placantonakis et al., 2009). Furthermore, it would also allow differentiation to be followed in real time in live cells, greatly enhancing our ability to study gene regulation and lineage choice during development (Tomishima et al., 2007). Therefore, expression of EGFP from a DA specific promoter would not only allow the genesis of DA neurons to be analysed *in vitro* during neural induction but also the selection of DA neurons by FACS. This homogenous cell population could subsequently be used for many functions, including *in vitro* disease modelling.

Two key markers of the DA system are the biosynthesis enzyme TH and transporter DAT. While TH is the rate limiting step in the synthesis of DA, this neurotransmitter is the precursor of noradrenaline and adrenaline and therefore is also a marker of noradrenergic and adrenergic neurons. In addition, expression of EGFP from a fragment of the TH promoter thought to be sufficient to drive TH expression resulted in a mixed cell population containing markers of pluripotent stem cells and proliferative cells ten weeks after sorting and transplantation into the rat brain (Hedlund et al., 2007). DAT is expressed exclusively in DA neurons in the brain (Augood et al., 1993; Turiault et al., 2007) and is also a key regulator of the dopaminergic system (Jones et al., 1998), being located on pre-synaptic DA neurons and functioning to transport this neurotransmitter from the synaptic cleft after

exocytosis (for review, see Torres et al., 2003). Previous studies have identified the DAT promoter as an effective system for driving transgene expression in mice in a DA specific manner (Zhuang et al., 2005; Backman et al., 2006; Ekstrand et al., 2007; Turiault et al., 2007; Lu et al., 2009). At the time of performing these studies no reports had been published of ESCs expressing EGFP from the DAT promoter. Therefore, the creation of such a cell line was a primary aim of this thesis.

Analysis of the human DAT gene suggests the 5' untranslated region (UTR) has a role in regulating its transcription (Donovan et al., 1995; Sacchetti et al., 1999; Bannon et al., 2001). Sequence conservation is found between non-coding region of the mouse and human DAT genes (Donovan et al., 1995) and therefore a strategy was developed to clone EGFP into exon 2 of the DAT gene at the level of the start codon so as to preserve any possible non-coding regulatory regions. It has also been observed that DAT heterozygous mice display subtle behavioural and biochemical abnormalities (Spielewoy et al., 2000; Spielewoy et al., 2001; Savelieva et al., 2002; Hall et al., 2003). Therefore, due to these considerations, EGFP expression was targeted to the DAT promoter contained within a bacterial artificial chromosome (BAC), as published reports suggest that this is an effective way to drive gene expression in transgenic mice (Turiault et al., 2007; Lu et al., 2009; GENSAT). GENSAT (Gene Expression Nervous System Atlas) is a publicly available gene expression atlas of the developing and adult central nervous system in the mouse. The project also generates transgenic BAC-EGFP reporter mouse lines.

One of the key advantages of using BAC vectors is that due to their large size they can accommodate very long regions of genomic DNA and therefore high transgene fidelity can be achieved (Tomishima et al., 2007). It is thought that this is owing to the fact that all regulatory elements of the gene contained within the BAC are maintained and that their large size insulates the integrated transgene from the effects of the surrounding chromatin structure (Tomishima et al., 2007). Another key advantage is that protocols have been established which allow BACs to be rapidly modified in bacterial cells (Yu et al., 2000; Lee et al., 2001). These are based on a highly efficient prophage-mediated homologous recombination system in *Escherichia coli* (*E.coli*) termed recombineering (Copeland et al., 2001). In the most effective of these methods, bacterial cells contain a defective λ prophage

integrated into the *E.coli* genome (Yu et al., 2000; Lee et al., 2001). Only two phage proteins are required for recombination, Exo and Beta, encoded by *Red* genes *exo* and *bet*, respectively (Liu et al., 2003). Exo is a 5'-3' exonucleases that acts on 5' ends of linear double stranded DNA (dsDNA) to produce 3' single stranded DNA (ssDNA) overhangs, while Beta is an annealing protein that binds to these ssDNA overhangs and promotes annealing to complementary sequences on target DNA (Liu et al., 2003). Expression of these proteins is typically accompanied by that of λ-encoded Gam protein which prevents degradation of linear DNA (Yu et al., 2000). Expression of the prophage genes is controlled by the pL promoter, which is itself under the control of the temperature-sensitive λ repressor *cI857* (Yu et al., 2000; Lee et al., 2001; Liu et al., 2003). At temperatures below 32°C, expression of *exo*, *bet* and *gam* is undetectable (Yu et al., 2000; Liu et al., 2003). However, increasing culturing temperature to 42°C for a short period of time (15 min) results in de-repression of the pL promoter, expression of the *Red* genes and induction of recombination (Yu et al., 2000; Lee et al., 2001; Liu et al., 2003). This process is so efficient that the gene of interest to be recombined need only be flanked by short sequences of homology, typically 40-50 bp, allowing fragments to be generated by PCR (Lee et al., 2001).

BACs have, in fact, recently been shown to be an effective way to express EGFP from multiple neural specific promoters in mouse and human ESCs (Tomishima et al., 2007; Placantonakis et al., 2009). In both cell types, EGFP was successfully monitored in real time in live cells during the process of neural induction and motor neurons derived from human ESCs were enriched from a mixed cell population and subsequently differentiated and analysed (Tomishima et al., 2007; Placantonakis et al., 2009). Therefore, it was hypothesised that expression of EGFP from the DAT promoter in mouse ESCs would not only be of great value but also readily achievable using a BAC carrying the DAT gene. Therefore, this chapter details the insertion of EGFP into the DAT gene contained with a BAC by recombineering, transfection of mouse R1 ESCs with this construct and selection of antibiotic resistant clones, expansion and analysis of these resistant clones by PCR of genomic DNA, *in vitro* dopaminergic neuronal differentiation (Lau et al., 2006) of positive clones, and analysis of the level of EGFP and DAT protein by Western blotting and the

cellular distribution of EGFP and DAT by immunocytochemistry in these differentiated cells.

3.2 Methods

3.2.1 Overview of construction of DAT-EGFP vector

A BAC clone (RP23-150M11) was obtained that encompassed a large segment of mouse chromosome 13 (~217.5 kb) including the DAT gene, with ~22.8 kilobases (kb) of genomic DNA upstream and ~152.7 kb downstream of the gene (referred to as BAC-DAT; Fig. 3.1). A recombination fragment EGFP-polyA-PGK-Em7-Neo-polyA (referred to as EGFP targeting cassette) was recombined into the DAT gene to direct expression of EGFP from the DAT promoter (Fig. 3.1). The EGFP targeting cassette was composed of the open reading frame (ORF) of EGFP followed by a polyadenylation (polyA) signal and neomycin selection cassette (neo) with polyA signal (Fig. 3.1).

The cloning strategy used to construct this vector consisted of the following steps:

1. EGFP-polyA was digested from IRES-EGFP-PolyA plasmid and inserted into linearised plasmid pL451 by ligation. After selection and screening this formed pL451-EGFP.
2. pL451-EGFP was used as template to amplify the EGFP targeting cassette with primers that contained two parts, a 5' end homologous to exon 2 of the DAT gene and a 3' end that primes the plasmid DNA, thus enabling recombination into the DAT gene (Fig. 3.2).
3. The EGFP targeting cassette was electroporated into recombineering competent bacteria containing the BAC-DAT vector and clones positive for recombination were selected by antibiotic resistance and whole cell PCR. This generated vector BAC-DAT-EGFP-Neo (referred to as DAT-EGFP).

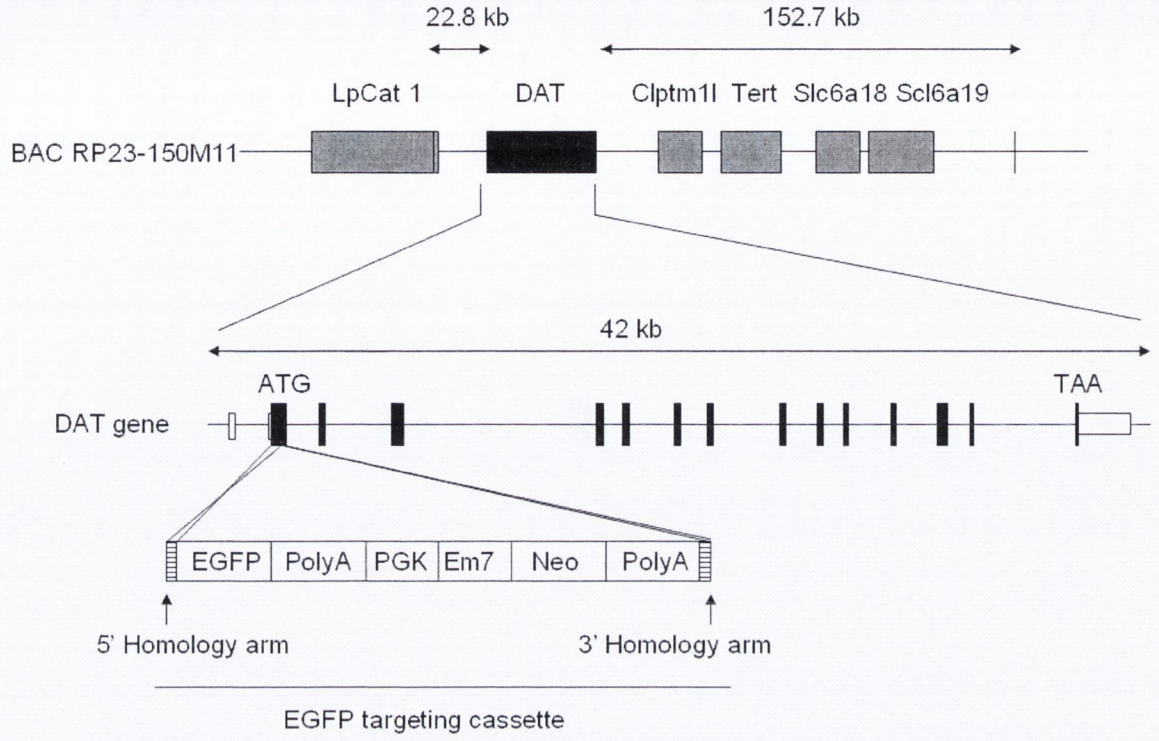

Figure 3.1: Schematic representation of the DAT-EGFP construct and its structure.

The position of the DAT gene in BAC clone RP23-150M11 is indicated, along with the other putative genes contained with the BAC. The intron/exon structure of the DAT gene is shown. The gene has 14 coding exons (black squares) and one non-coding exon (exon 1, white square). Recombination targeted the second exon, with the start codon (ATG) of DAT being replaced with the start codon of EGFP. The EGFP targeting cassette (EGFP-PolyA-PGK-Em7-Neo-PolyA) consisted of the EGFP open reading frame followed by a polyA signal and the neomycin selection cassette with a polyA signal. The neomycin gene was expressed from the PGK promoter in eukaryotic cells and the Em7 promoter in prokaryotic cells and therefore was independent of the DAT promoter. EGFP indicates enhanced green fluorescent protein; DAT, dopamine transporter; Neo, neomycin selection cassette; PolyA, polyadenylation signal; PGK, phosphoglycerate kinase promoter. Adapted from Turiault et al. (2007).

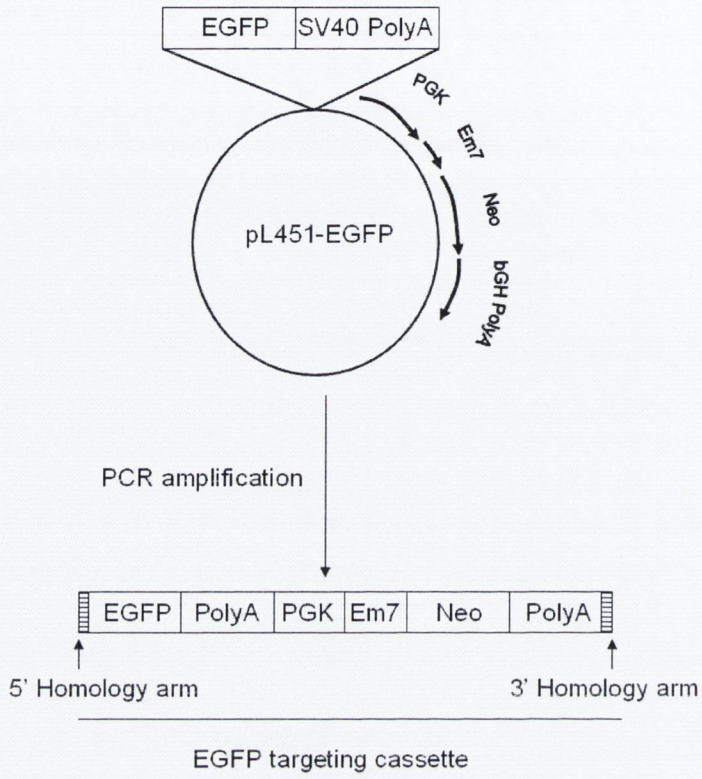

Figure 3.2: Construction and schematic representation of EGFP targeting cassette

The open-reading frame of EGFP with the SV40 polyA signal was ligated into pL451 just preceding the PGK promoter. This generated the plasmid pL451-EGFP. The EGFP targeting cassette (EGFP-PolyA-PGK-Em7-Neo-PolyA) was subsequently amplified from this plasmid by PCR with primers containing two parts, a 5' end homologous to exon 2 of the DAT gene and a 3' end that primes the plasmid DNA This created the targeting cassette with homology arms and allowed recombination into the DAT gene. The neomycin gene was followed by a polyA signal from bovine growth hormone (bGH) gene and was expressed from the PGK promoter in eukaryotic cells and the Em7 promoter in prokaryotic cells. EGFP indicates enhanced green fluorescent protein; DAT, dopamine transporter; Neo, neomycin selection cassette; PolyA, polyadenylation signal; PGK, phosphoglycerate kinase promoter; PCR, polymerase chain reaction.

3.2.2 DNA vectors, bacterial strains and bacterial growth medium

The BAC vector pBACe3.6 containing segment of mouse chromosome 13 (clone RP23-150M11) was obtained in the *E.coli* strain EL250 from Dr Thorsten Lau (Central Institute of Mental Health, Mannheim). pL451 was obtained as from Katrin Bartels (Central Institute of Mental Health, Mannheim). IRES-EGFP-PolyA plasmid was obtained from Dr Kai Schonig (Central Institute of Mental Health, Mannheim). One Shot TOP10 competent *E.coli* cells were obtained from Dr Tania O'Connor (Trinity College Dublin, Dublin).

Luria-Bertani (LB) broth and LB agar were used to grow bacterial strains. SOB was used to prepare chemocompetent cells. SOC was used as recovery medium following transformation of bacteria. These were prepared as described below in Table 3.1. After preparation the solutions were autoclaved, allowed to cool to RT and stored until use. LB agar was melted prior to use and antibiotics were added when the temperature of the agar reached 52°C. Antibiotics were prepared as described in Table 3.2 and stored at -20°C.

Growth medium	Preparation
LB broth, pH 7	10 g tryptone, 5 g yeast extract, 5 g NaCl dissolved in 1 L of H_2O
LB agar, pH 7	5 g yeast extract, 5 g NaCl, 15 g bacteriological agar, 10 g tryptone dissolved in 1 L of H_2O
SOB, pH 7	20 g tryptone, 5 g yeast extract, 5 g $MgSO_4$, 5 g NaCl, 0.186 g KCl dissolved in 1 L of H_2O
SOC	SOB+10 mM sterile glucose immediately prior to use

Table 3.1: Composition of bacterial growth media

Antibiotic	Stock concentration (w/v)	Working concentration (w/v)	
		Plasmid	BAC
Kanamycin (Kan)	50 mg/ml in H_2O, sterile filtered	50 µg/ml	25 µg/ml
Chloramphenicol (Chlor)	34 mg/ml in EtOH	NA	12.5 µg/ml

Table 3.2: Composition and concentration of antibiotics used with plasmid and BAC containing bacteria. NA indicates not applicable.

3.2.3 DNA based cloning methods

A number of DNA based cloning methods were used to construct the DAT-EGFP vector and are described in the following sections.

3.2.3.1 Restriction endonuclease digestion

Restriction endonucleases (10 units (U)/µl) were supplied in storage buffer containing 50% glycerol, with corresponding 10X reaction buffer. Digestion reactions were typically performed for 1-3 hours at 37°C. To prepare DNA for subsequent cloning, 10-30 U of enzyme, 1X reaction buffer and 1-3 µg DNA was prepared to a final volume of 50 µl with MilliQ H_2O. When multiple plasmids were digested with the same restriction enzyme, a mastermix was typically prepared with 2-5 U of restriction enzyme per reaction. This was subsequently mixed with 500 ng of DNA and made to a final volume of 20 µl with MilliQ H_2O. Double digests containing two different restriction enzymes were carried out in the same 1X reaction buffer if this was compatible with enzyme activity. If this was not the case, reactions were carried out separately in the recommended buffers, with DNA purification being performed between digestions.

3.2.3.2 Blunting of DNA fragments

T4 DNA polymerase was supplied with 5X reaction buffer. This enzyme is a template dependent mesophilic enzyme that catalyses 5' to 3' synthesis from single stranded DNA molecules, thereby creating blunted DNA ends. It is used when it is required to ligate DNA fragments that do not have compatible ends. This is the case when, for example, plasmid DNA and insert DNA have been digested with different restriction enzymes. Reactions were typically carried out with 2.5 U (0.5 µl) of polymerase, 1X reaction buffer, 0.1 mM dNTPs and digested DNA. The final volume was made up to 20 or 30 µl with MilliQ H_2O and incubated at room temperature for 5 min. The reaction was subsequently terminated by heating to 75°C for 10 min.

3.2.3.3 Dephosphorylation of linearised plasmid DNA

Linearised plasmid DNA was treated with shrimp alkaline phosphatase (SAP) in order to dephosphorylate the vector. The enzyme catalyses the release of 5'-phosphate groups from DNA, thus ensuring that the linearised vector does not re-ligate when 5' and 3' ends are compatible. The enzyme was supplied with 10X reaction buffer. Dephosphorylation reaction typically consisted of 2 µg of plasmid DNA, 1X reaction buffer, SAP (1 U/1 picomole DNA 5'-termini, 1 U/µl) to a final volume of 50 µl with MilliQ H_2O. The reaction was incubated at 37°C for 30 min. This was followed by inactivation at 65°C for 20 min. DNA was purified using QIAquick PCR purification kit and DNA concentration was determined spectrophotometrically.

3.2.3.4 Ligation of DNA fragments

Ligation reactions were catalysed with T4 DNA ligase. This enzyme catalyses the formation of a phosphodiester bond between 5'-phosphate and 3'-hydroxyl termini in double stranded DNA and requires ATP as a cofactor. Ligation reactions consisted of linearised plasmid DNA, insert DNA, 2 µl PEG, 1X reaction buffer (2 µl), 1 µl ligase (5 U/µl) to a final volume of 20 µl with MilliQ H_2O, and were incubated overnight at 16°C.

3.2.3.5 Polymerase chain reactions

The EGFP targeting cassette was amplified from pL451-EGFP using High Fidelity PCR Enzyme Mix with forward primer GFPHA_F100 and reverse primer NeoHA_R100 (Table 3.3). The forward primer contained 42 nucleotides homologous to the 5' region of exon 2 of the DAT gene and 28 nucleotides homologous to EGFP in the template DNA. The reverse primer contained 42 nucleotides homologous to the 3' region of exon 2 of the DAT gene and 28 nucleotides homologous to polyA sequence of neo in template DNA. The start codon of the DAT gene is located in exon 2 and the forward primer was designed to replace this with the start codon of EGFP. Samples were amplified under the following conditions: denaturation step at 95°C, 2 min; denaturation step at 95°C, 30 sec, annealing step at 66°C,

30 sec, amplification step at 68°C, 3.5 min, for 30 cycles; and final amplification step at 68°C, 10 min. The final product was 3.2 kb.

Whole cell PCR was performed on colonies following electroporation of bacteria with the EGFP targeting cassette using forward primer DATintron1_F and reverse primer GFPHA_R (Table 3.3), with an annealing temperature of 55°C and standard PCR conditions (Section 2.11). PCR of genomic DNA (1 µl) was performed on antibiotic resistant R1 ESC clones transfected with DAT-EGFP using primers DATintron1_F and EGFP_R1 (Table 3.3), with annealing temperature of 55°C and standard PCR conditions (Section 2.12). In both instances, the forward primer was complimentary to intron 1 of the BAC-DAT vector and the reverse primer was complimentary to inserted DNA. All PCR products were resolved by agarose cell electrophoresis (Section 2.12). DAT-EGFP vector was sequenced prior to transfection with primers NeoCassette_Forward1, NeoCassette_Forward2, EGFP_ Forward and DATintron1_Forward (Table 3.3)

Primer name	Primer sequence
GFPHS_F100	5'-CGAAGAAGAAGGAAACAGACTTCCTCGGGCTCCCGTCT ACCCATGGTGAGCAAGGGCGAGGAGCTGTTCA-3'
NeoHS_R100	5'-GGAGGCCAGGCCACACTCACCTCCACCATTTTTGTAGC ACAGGTCTAGAACTAGTGGATCCACCTAATAAC-3'
DATintron1_F	5'-GTCTCTGTGTTCAACCCAAG-3'
GFPHA_R	5'-AGAAGATATCCGATGCCCTT-3'
EGFP_R1	5'-ACTTGTACAGCTCGTCCAT-3'
DATintron1_Forward	5'-GTCTCTGTGTTCAACCCAAG-3'
EGFP_Forward	5'-GCAAAGACCCCAACGAGAAG-3'
NeoCassette_Forward1	5'-GTTCTCCTCTTCCTCATCTCC-3'
NeoCassette_Forward2	5'-TCTCTAGAGCTCGCTGATCA-3'

Table 3.3: Sequence of PCR primers used in this chapter

3.2.4 Methods used to purify DNA

DNA fragments were purified from reaction mixtures, and intact plasmids and BACs were isolated after overnight amplification in bacteria, as described in the succeeding sections.

3.2.4.1 Purification of DNA fragments

3.2.4.1.1 QIAquick gel extraction

QIAquick gel extraction kit from Qiagen was typically used to extract and purify DNA fragments after restriction digestions that had been resolved on a 1% agarose gel with 5 mM cytidine (section 2.12). Gels were visualised with long-wave UV light (360 nm). High grade 100% EtOH was added to Buffer PE (concentrate) prior to use, as instructed in the manual. All centrifugation steps were performed in a bench top centrifuge at RT and maximum speed (13,200 rpm) for 1 min. The desired agarose band corresponding to the fragment of interest was excised from the agarose gel using a clean, sharp scalpel and collected in a pre-weighed 1.5 ml microcentrifuge tube. The tube was re-weighed and the final weight of the band was determined. Buffer QC was subsequently added to the gel slice, with a 3:1 ratio of buffer volume to gel weight being used to determine required volume. The gel was dissolved in the buffer by heating at 50°C with regular vortexing. If the colour of the ensuing solution was not yellow, 10 µl of NaOAc (3M, pH 5) was added, as DNA only adsorbs to the column when the pH is less than 7.5. One gel volume of room temperature isopropanaol was added and vortexed, aiding recovery of DNA. The solution was then loaded onto QIAquick column and centrifuged. The flow-through was re-applied to the column and centrifuged. This step was again repeated and the flow-through was then discarded. The column was loaded with 0.5 ml Buffer QC, centrifuged and the flow-through discarded. The column was then washed with 0.75 ml of Buffer PE and centrifuged. The flow-through was discarded and the column was centrifuged empty to ensure the removal of any residual ethanol. The column was placed into a clean labelled 1.5 ml microcentrifuge tube and bound DNA was eluted by applying 32 µl of elution buffer (10mM Tris-Cl, pH 8.5) pre-warmed to 65°C directly onto the centre of the membrane. The

column was allowed to stand for 1 min prior to centrifugation to allow maximum recovery of DNA. DNA yield was determined spectrophotometrically at 260 nm and stored at -20°C.

3.2.4.1.2 QIAquick PCR purification

QIAquick PCR purification kit from Qiagen was typically used to purify DNA from PCR mixtures and linearised plasmids from restriction digest mixtures. High grade 100% ethanol was added to Buffer PE (concentrate) prior to use as instructed in manual. All centrifugation steps were performed at RT in a bench top centrifuge for 1 min at maximum speed (13,200 rpm). Buffer PBI was added to samples in a 5:1 volume ratio and vortexed. If the ensuing solution was not yellow, 10 µl of 3M NaOAc, pH 5 was added and vortexed. This ensures that the pH is suitable for DNA adsorption onto the QIAquick column. To bind DNA, the sample was loaded onto a QIAquick column and centrifuged. The flow-through was discarded and 0.75 ml PE Buffer was added to wash the column. The flow-through was again discarded and the column was centrifuged to empty ensure all residual ethanol was removed. The column was transferred to a clean labelled 1.5 ml microcentrifuge tube. DNA was eluted by applying 32 µl of elution buffer pre-warmed to 65°C directly onto the centre of the membrane. The column was allowed to stand for 1 min prior to centrifugation. DNA yield was determined spectrophotometrically at 260 nm and stored at -20°C.

3.2.4.2 Small scale purification of plasmid DNA

Small amounts of pure plasmid DNA were prepared using QIAprep Spin Miniprep Kit from Qiagen. This kit is optimised for the purification of plasmids less than 10 kb. Prior to use, RNase A and LyseBlue reagent were added to Buffer P1, and this was subsequently refrigerated. High grade 100% ethanol was added to Buffer PE (concentrate) as instructed in manual. All centrifugation steps were performed at maximum speed (13,200 rpm) for 1 min at RT in a bench top centrifuge, unless otherwise stated.

Single clones from LB agar plates were used to inoculate 5 ml of LB broth with appropriate antibiotics and grown overnight at 37°C with shaking. The cells were pelleted by

centrifugation (2000 g, 15 min, 4°C). The supernatant was immediately removed and the cells were resuspended in 250 µl Buffer P1 and transferred to a clean labelled 1.5 ml microcentrifuge tube. Cells were subsequently lysed by the addition of 250 µl Buffer P2. The cell suspension turned blue and the tube was inverted 4-6 times until a homogenously coloured sample was formed. The lysis reaction was stopped by addition of 350 µl Buffer P3. The tube was mixed immediately and thoroughly by inverting 4-6 times until all traces of colour was gone and the suspension was colourless. The sample was centrifuged (13,200 rpm, 10 min, RT) and the clear supernatant was carefully decanted from the tube and applied to a QIAprep spin column. The column was centrifuged to bind DNA, washed by loading once with 0.5 ml PB buffer and centrifuging and once with 0.75 ml PE buffer and centrifuged. The flow-through was discarded after each washing step. The column was centrifuged empty after PE buffer to ensure all residual ethanol had been removed. The column was transferred to a clean labelled 1.5 ml microcentrifuge tube and DNA was eluted by applying 50 µl of elution buffer pre-warmed to 65°C directly onto the centre of the membrane. The column was allowed to stand for 1 min prior to centrifugation to ensure maximum DNA recovery. DNA yield was determined spectrophotometrically at 260 nm and stored at -20°C.

3.2.4.3 Large scale purification of plasmid DNA

Large amounts of ultra-pure plasmid were prepared using NucleoBond AX 500 columns with supplied buffers. A single colony from a LB agar plate was used to inoculate 500 ml LB broth containing appropriate antibiotics. This was shaken overnight at 37°C. The culture was subsequently transferred to a 500 ml centrifuge tube and the cells were pelleted by centrifugation (2000 g, 20 min, 4°C). The supernatant was removed and the pellet was resuspended in 12 ml S1 buffer containing freshly added RNase A (100 µg/ml). The cell suspension was transferred to a 50 ml centrifuge tube and the cells were lysed with 12 ml S2 buffer. The tube was carefully inverted 8-10 times and the mixture was incubated for 3 min at RT. The lysis reaction was stopped with 12 ml ice-cold S3 neutralisation buffer. The cell suspension was inverted 8-10 times and placed on ice for 5 min. The bacterial lysate was cleared by centrifugation (12000 g, 45 min, 4°C). The supernatant was then loaded onto wet filter paper and the flow-through was collected. The filter paper was moistened

with 6 ml N2 buffer prior to use. The cleared lysate was loaded onto a NucleoBond AX500 column that had been pre-equilibrated with 6 ml N2 buffer and allowed to empty by gravitational flow. The flow-through was discarded. The column was subsequently washed with 32 ml of N3 buffer and the flow-though was discarded. The DNA was eluted with 15 ml of N5 buffer at 55°C. The DNA was subsequently precipitated with 11 ml of RT isopropanol and centrifuged (15000 g, 45 min, 4°C). The supernatant was then carefully removed and 5 ml of 70% EtOH was added. The DNA was pelleted by centrifugation (15000 g, 10 min, RT). The ethanol was removed and the pellet was allowed to air dry for ~15 min at RT. The dried pellet was re-dissolved in 200 µl of elution buffer pre-warmed to 65°C and DNA yield was determined spectrophotometrically.

3.2.4.4 Large scale purification of BAC DNA

Large amounts of ultra-pure BAC were prepared using NucleoBond BAC 100 kit, which has been adapted for the low copy number and large size of BAC DNA. A starter culture (5 ml) was inoculated with a single colony picked from a freshly streaked agar plate of BAC-DAT-EGFP-Neo and grown with agitation at 28°C or 37°C depending on the bacterial strain for ~8 hours at ~300 rpm in LB broth/kan/chlor. An overnight culture was subsequently prepared by diluting the starter culture 1/1000 into 400 ml of LB broth/kan/chlor and grown overnight with shaking at 28°C or 37°C. The overnight culture was transferred to a 500 ml centrifuge tube and the cells were pelleted by centrifugation (2000 g, 20 min, 4°C). The supernatant was removed and the pellet was resuspended in 24 ml S1 buffer containing freshly added RNase A (100 µg/ml). The cell suspension was transferred to a 50 ml centrifuge tube and the cells were lysed with 24 ml S2 buffer. The tube was carefully inverted 20 times and the mixture was incubated for 3 min at room temperature. The lysis reaction was stopped with 24 ml ice-cold S3 neutralisation buffer. The cell suspension was inverted 20 times and placed on ice for 5 min. The bacterial lysate was loaded onto filter paper moistened with 6 ml N2 buffer and the flow-through was collected. The cleared lysate was loaded onto a NucleoBond column that had been pre-equilibrated with 6 ml N2 buffer and allowed to empty by gravitational flow. The flow-through was discarded. The column was subsequently washed with 36 ml of N3 buffer and the flow-though was discarded. The DNA was eluted with 15 ml of N5 buffer pre-warmed

to 55°C. The DNA was subsequently precipitated with 11 ml of RT isopropanol and centrifuged (15000 g, 45 min, 4°C). The supernatant was then carefully removed and 5 ml of 70% EtOH was added. The DNA was pelleted by centrifugation (15000 g, 10 min, RT). The ethanol was removed and the pellet was allowed to air dry for ~15 min at RT. The dried pellet was re-dissolved in 200 µl of 65°C elution buffer and DNA yield was determined spectrophotometrically.

3.2.5 Methods used to prepare and transform competent bacteria

The methods used to prepare and transform chemocompetent, electrocompetent and recombineering competent bacteria are described in the ensuing sections. The choice of transformation method used depended on the requirement of the experiment, as indicated.

3.2.5.1 Preparation of chemocompetent bacteria

Chemocompetent cells were prepared according to Inoue et al. (1990). Briefly, One Shot Top10 cells were grown overnight at 37°C in 5 ml of LB broth with shaking. The inoculum was diluted into 250 ml of SOB and incubated at 25-30°C with shaking (160 rpm) until the optical density at 600 nm (OD_{600}) reached 0.4-0.5. The cells were subsequently chilled on ice for 15 min and centrifuged (2000 x g, 10 min, 4°C) to pellet bacteria. The supernatant was immediately removed and the cell pellet was gently resuspended in 40 ml of sterile TB buffer (10 mM HEPES, 15 mM $CaCl_2$, 55 mM MnCl, 250 mM KCl, pH 6.7 with KOH) and incubated on ice for 10 min. The cells were again centrifuged (2000 g, 10 min, 4°C). The supernatant was immediately removed and the cells were resuspended in 10 ml TB-DMSO solution (10 mM HEPES, 15 mM $CaCl_2$, 55 mM MnCl, 250 mM KCl, pH 6.7 with KOH, 7% DMSO). The cell solution was incubated on ice for 10 min and 50 µl was transferred to sterile cryogenic vials. The cells were shock freezed in liquid nitrogen and stored at -80°C. Before use in experiments, the transformation efficiency of the cells was determined by performing control transformation with plasmid DNA and calculating the colony forming units (CFU)/µg DNA. Only bacterial preparations that generated high transformation efficiencies were used.

3.2.5.2 Transformation of chemocompetent bacteria

A vial of chemocompetent cells was thawed on ice and 50 µl was aliquoted into sterile 1.5 ml microcentrifuge tubes. Ligation mixture (1-5 µl) or pure plasmid (1-10 ng) was added to the tube and incubated on ice for 30 min. The cells were subsequently heat shocked at 42°C for 30 sec and placed on ice. Cells were gently mixed with 250 µl SOC and shaken at 37°C for one hour. Varying volumes were then spread on LB agar plates with appropriate antibiotics and grown overnight at 37°C.

3.2.5.3 Preparation of EL250 bacteria for recombineering

EL250 bacterial cells containing BAC clone RP23-150M11 were recombineering competent as they contained the defective λ prophage integrated into the *E.coli* genome, allowing recombination to occur at culturing temperatures above 42°C (Yu et al., 2000; Lee et al., 2001). Cells were prepared for recombineering according to Liu et al. (2003), with slight modifications. Briefly, bacteria were scraped from a glycerol stock and shaken in 1 ml SOC without selection for 1 hour at 28°C before spreading on LB/chlor agar plates. Plates were grown overnight at 28°C and a single clone was subsequently used to inoculate 5 ml LB/chlor broth and grown overnight at 28°C. The following day a 1:50 dilution was performed by adding 400 µl of overnight culture to 20 ml of LB/chlor broth and shaken (180 rpm) in 50 ml Falcon tube until the OD_{600} reached 0.6-0.8. The culture was transferred to two 50 ml Falcon tubes (10 ml each), with one remaining at 28°C (uninduced control) and one being shaken at 42°C in a water bath for 15 min to induce genes for recombination. Immediately after induction, both tubes were rapidly placed in ice-water slurry, shaken gently to reduce the temperature as quickly as possible and placed on ice for 10 min. Bacteria were pelleted by centrifugation (5000 rpm, 5 min, 0°C). The supernatant was rapidly removed, the tubes were briefly inverted on paper towel and resuspended in 1 ml sterile ice-cold MilliQ H_2O by shaking tube gently in ice-water slurry. The cell suspension was transferred to a chilled 1.5 ml microcentrifuge tube and spun at maximum speed (13,200 rpm) in bench top centrifuge for 30 sec at 4°C. This process was repeated an additional two times. Finally, all supernatant was removed and cells were resuspended in

100 µl ice-cold MilliQ H_2O, providing enough cells for two electroporation procedures (~$8x10^6$ cells per reaction) (Yu et al., 2000).

3.2.5.4 Electroporation of EL250 bacteria

The EGFP targeting cassette was prepared for recombineering by PCR, template (plasmid) DNA was destroyed by treatment with DpnI (Yu et al., 2000), and the recombination fragment was purified by gel extraction. Electrophoresis was performed at a low voltage (20 V) overnight to ensure all plasmid DNA was removed. Purified DNA (25 ng, 50 ng) was added to 50 µl of induced EL250 cells on ice. The microcentrifuge tubes were tapped gently to mix and transferred to chilled 0.2 cm electroporation cuvettes. The outside of the curette was dried with paper towel and placed in the Bio-Rad electroporation machine. An electrical pulse was initiated (2.5 kV, 25 µF, 200 ohms) and 1 ml of SOC was immediately added to the cells. This was repeated until all samples (DNA with induced cells, DNA with uninduced control cells, 2 µl H_2O with induced cells) had been electroporated. The samples were transferred to labelled 1.5 ml microcentrifuge tubes and gently shaken at 28°C for two hour. Recombined mutants were selected by growth on LB/kan/chlor agar plates for 18-24 hours at 28°C until colonies were apparent. While resistant mutants colonies were sometimes observed on control plates, they were always far more numerous on plates with induced bacteria and DNA.

3.2.5.5 Preparation of electrocompetent bacteria

Electrocompetent cells were prepared according to Morrison (2001). Briefly, One Shot Top10 cells were grown overnight at 37°C in 5 ml of LB broth with shaking (250 rpm). The inoculum was added to 500 ml LB broth and incubated at 37°C with shaking (250 rpm) until the OD_{600} reached 0.5-1. The culture was chilled on ice for 15 min and centrifuged (2000 x g, 10 min, 4°C) to pellet bacteria. The supernatant was immediately removed and the pellet was gently resuspended in 500 ml ice-cold sterile H_2O and centrifuged (2000 x g, 15 min, 4°C). This washing process was repeated with 250 ml ice-cold sterile H_2O, followed by centrifugation (2000 x g, 15 min, 4°C) and removal of supernatant. The pellet was resuspended in 10 ml of ice-cold 15% (v/v) glyercol and centrifuged (1500 x g, 15

min, 4°C). The supernatant was decanted and the pellet was transferred to a 1.5 ml microcentrifuge tube. This was centrifuged in a bench top centrifuge (13,000 rpm, 5 min, 4°C) and the pellet was resuspended in 1.5 ml of ice-cold 15% (v/v) glyercol solution. The bacterial cells were distributed into sterile cryogenic vials (50 µl), shock freezed in liquid nitrogen and stored at -80°C. Before use in experiments, the transformation efficiency of the cells was determined by performing control transformation with plasmid DNA and calculating the CFU/µg DNA. Only bacterial preparations that generated high efficiency were used.

3.2.5.6 Transformation of electrocompetent bacteria

Following identification of DAT-EGFP positive clones, BAC DNA was purified from EL250 cells and electroporated into non-recombination electrocompetent bacterial cells for large scale amplification and purification of DNA. A vial of electrocompetent bacterial cells was thawed on ice. Freshly prepared ice-cold BAC DNA (500 ng) was added to the cells. The cell suspension was transferred to an ice-cold 0.2 cm electroporation cuvette and incubated on ice for 10 min. The outside of the cuvette was dried thoroughly and placed in the Bio-Rad electroporation machine. An electrical pulse was initiated (2.5 kV, 25 µF, 200 ohms) and 1 ml of SOC was immediately added to the cells. The samples were transferred to labelled 1.5 ml microcentrifuge tubes and gently shaken at 37°C for one hour. Varying volumes were spread on LB agar/kan/chlor plates and incubated overnight at 37°C. BAC DNA was subsequently purified as described in Section 3.2.4.4 and the location and sequence of the targeted DNA was verified by sequencing using the primers in Table 3.3 prior to use.

3.2.6 Methods used to transfect R1 ESCs and analyse antibiotic resistant clones

Undifferentiated R1 ESCs were transfected with the DAT-EGFP vector and selected by antibiotic resistance. Surviving clones were subsequently analysed for insertion of the BAC vector into the genome and those that were positive were expanded and differentiated to DA neurons and analysed for EGFP expression. The steps taken during this procedure are detailed in the following sections.

3.2.6.1 Determination of optimal G418 concentration to select stable clones

Expression of the neo selection cassette from the PGK promoter in DAT-EGFP allowed selection of transfected clones by resistance to G418. In order to determine the optimal concentration of G418 required to kill non-transfected cells, $2x10^6$ R1 ESCs, cultured according to Section 2.7, were separated from feeder cells, plated on gelatine coated dishes and treated with 0, 200 µg/ml, 300 µg/ml, 400 µg/ml , 500 µg/ml, 600 µg/ml G418 for 7 days. G418 stock solution (100 mg/ml) was prepared by dissolving 1 g of G418 in 9.8 ml PBS, followed by the addition of 180 µl 10 N NaOH. The solution was sterile filtered and stored, protected from light, at 4°C. Culture medium and G418 were changed daily. Cell death was observed microscopically every day. The lowest concentration which resulted in cell death within 7 days was 200 µg/ml and was selected for additional experiments.

3.2.6.2 Transfection of R1 ESCs

Mouse R1 ESCs were transfected by nucleofection developed by Amaxa. In this technique, cells are exposed to a unique combination of cell-type specific solutions and electrical parameters in a Nucleofector device. Mouse ESCs nucleofector kit was used for all transfection procedures. Prior to nucleofection, 0.5 ml Supplement was added to 2.25 ml Mouse ESC Nucleofector Solution, mixed gently and stored at 4°C. This was heated to room temperature prior to use. Transient transfections were initially performed with the plasmid pmaxGFP contained in the kit, which expresses maxGFP from a CMV promoter. Only exponentially growing culture with cells in well-formed colonies were used for transfection procedures.

3.2.6.2.1 Transient transfection of R1 ESCs and determination of transfection efficiency

Four programs, A-013, A-023, A-024, A-030, are recommended for transfection of mouse ESCs with plasmid DNA, with no program recommended for BAC DNA, and therefore transient transfections were initially performed to determine the program resulting in the highest transfection efficiency with R1 ESCs. Cells were cultured according to Section 2.6.

Nucleofection is most efficient in the absence of feeder cells and therefore ESCs were separated from feeders by successive plating on cell culture dishes three times for 20 min each. Non-adherent cells were collect and a cell count was performed to determine the cell number. Two million cells were added to four tubes and centrifuged (200 g, 5 min, RT). Cell pellets were then washed with 5 ml PBS and centrifuged again (200 g, 5 min, RT). Parallel to these centrifugation steps, four tubes were prepared containing 2 µg pmaxGFP in 10 µl of pre-warmed supplemented Mouse ESC Nucleofection Solution. Culture medium (10 ml) was added to four gelatine coated 10 cm dishes and pre-incubated in a humidified 37°C/5% CO_2 incubator. Cell pellets were sequentially resuspended in 90 µl supplemented Mouse ESC Nucleofection Solution, mixed with 10 µl of DNA solution by pipetting up and down and transferred to a cuvette. This was placed in the cuvette holder, the required program was selected and the cells were nucleofected. Pre-heated medium (500 µl) was then added to the cuvette and the cells were transferred to pre-incubated medium. This procedure was repeated for all samples. Two million untransfected cells were also plated as above as control cells. EGFP expression was monitored 24 and 48 hours after transfection by fluorescent microscopy. Transfected cells were analysed by FACS after 48 hours to determine which program resulted in the highest percentage of GFP expressing cells. High cell death was observed after transfection with program A-030 and therefore the cells were not analysed. Cells were harvested for FACS by trypsinisation, resuspension in 500 µl PBS containing 2% FBS and filtration through a 50 µm cell strainer. Cells were first gated by forward and side scatter to remove cell debris and doublets and subsequently by forward scatter and GFP fluorescence. An untransfected cell sample was used to set gates for fluorescence, with 20,000 cells being analysed for each sample. A Dako CyAn ADP machine was used and data were processed using FlowJo software. Program A-023 resulted in 66.7% GFP expressing cells and resulted in the highest transfection efficiency (Figure 3.3). It was used for all subsequent transfections.

3.2.6.2.2 Stable transfection of R1 ESCs

ESCs were transfected as described above. Two reactions were prepared, containing $2x10^6$ cells with or without (control) 10 µg DAT-EGFP and transfected with program A-023. Inspection of cells the following day by light microscopy verified high cell survival.

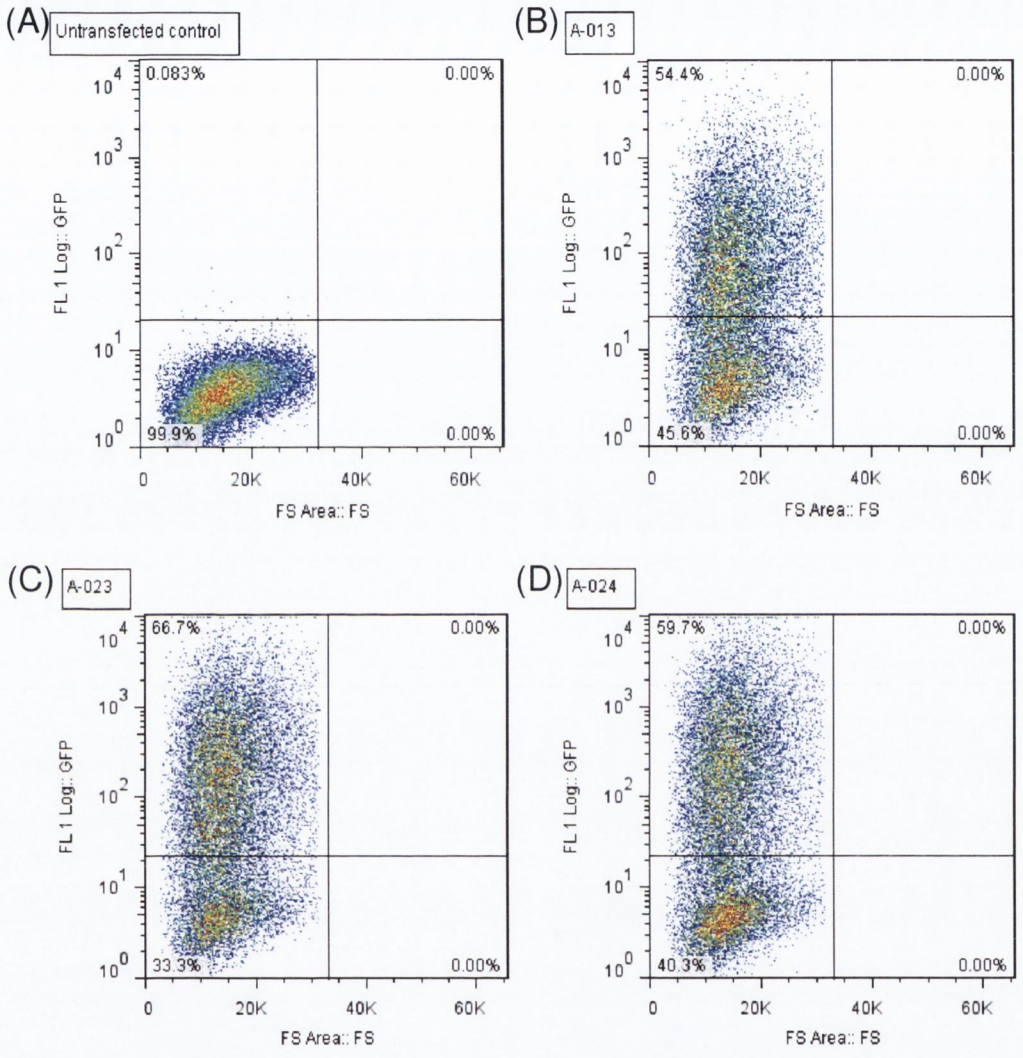

Figure 3.3: Program A-023 results in the highest transfection efficiency of R1 ESCs

Two million undifferentiated R1 ESCs were transfected with 2 µg pmaxGFP plasmid by nucleofection using the recommended programs and analysed 48 hours later by FACS to determine which resulted in the greatest number of GFP fluorescent cells. Flow cytometry profiles for program A-013 (B), A-023 (C) and A-024 (D) are provided, with untransfected control cells (A) included to identify GFP fluorescent cells, which are observed in the top left quadrant. Non-fluorescent cells are observed in the bottom left quadrant.

Cells were allowed to recover for 48 hours in non-selective medium and subsequently treated with selective medium containing 200 µg/ml G418. Two million untransfected control cells were also treated with G418 in a similar manner to determine toxicity of the medium. Selective medium was changed daily. After 10 days of selection, surviving colonies were expanded in non-selective medium for one day, followed by mechanical picking.

3.2.6.3 Picking of antibiotic resistant clones

After selection, 42 round undifferentiated colonies were picked, as described by Tompers and Labosky (2004). Ideal colonies were initially identified microscopically and the bottoms of the culture dishes were marked. Medium was subsequently removed from dishes and cells were washed twice with 5 ml PBS, followed by the addition of 5 ml PBS. Colonies were picked from the dishes with a micropipette set to 10 µl and transferred to a well of a gelatine coated 96-well plate. Following picking, colonies were trypsinised with 50 µl 0.05% trypsin/EDTA solution and incubated at 37°C for 5 min. Trypsinisation was stopped by the addition of 150 µl non-selective medium and the cell suspension was aspirated to obtain a single cell suspension. Colonies were allowed to grow until they became semi-confluent, at which time they were split (1:2) to two gelatine coated 96-well plates. This was achieved by washing each well thrice with PBS, treating with 50 µl 0.05% trypsin/EDTA solution for 5 min at 37°C, inactivation with 200 µl medium and transferring 125 µl to two wells. An additional 75 µl of medium was subsequently added to bring the final volume to 200 µl per well. This was repeated so as to obtain 4 dishes, 3 of which were frozen and one was maintained in culture to perform PCR of genomic DNA to determine if clones contained inserted DNA.

3.2.6.4 Freezing of antibiotic resistant clones

Medium was removed from each well of the 96-well plate and washed twice with 100 µl PBS. 0.05% trypsin/EDTA solution (50 µl) was subsequently added to each well and incubated at 37°C for 5 min. Ice cold freezing medium (50 µl, 20% DMSO, 60% FBS, 20% ESC medium) was added to each well and cells were aspirated gently to obtain a single cell

suspension. Each well was carefully layered with 100 µl sterile mineral oil to prevent evaporation during freezing. Plates were wrapped with parafilm and placed in a well-insulated Styrofoam box in -80°C freezer.

3.2.6.5 Extraction of genomic DNA from antibiotic resistant clones

Cells were allowed to grow until wells became confluent. Medium was subsequently removed and wells were washed twice with 100 µl PBS. Cells were then lysed by the addition of 50 µl lysis buffer (100 mM NaCl, 50 mM Tris-HCl, pH 7.5, 10 mM EDTA, 0.5% SDS, freshly added 1 mg/ml proteinase K) to each well. Plates were wrapped with parafilm and incubated overnight at 55°C in humid conditions. The following morning plates were centrifuged (1000 rpm, 10 min) to collect any moisture and DNA was extracted from lysed cells by the addition of 50 µl isopropanol to each well. Plates were incubated for 1 hour with gentle rotation to precipitate DNA. Plates were subsequently centrifuged (1000 rpm, 10 min) to attach DNA firmly to the bottom of each well and liquid in each well was carefully removed. Wells were washed thrice with 100 µl ice-cold 70% ethanol. DNA was allowed to air dry for 30 min and dissolved in 50 µl elution buffer. DNA was dissolved overnight at 4°C with gentle shaking. PCR was performed the following morning as described in sections 2.12 and 3.2.2.5.

3.2.6.6 Expansion and neuronal differentiation of positive clones

Once positive clones were identified by PCR, individual colonies were thawed and expanded. Frozen 96-well plates were thawed by incubation at 37°C/5% for 10-15 min in the morning. The lower layer of cells (100 µl) was transferred to individual wells of gelatine coated 96-well plate, with care being taken to avoid pipetting the layer of mineral oil. Fresh ESC medium (100 µl) was subsequently added to each well and the cells were allowed to recover. In the afternoon, after cells had settled and attached to the dish, the medium was removed, each well was washed thrice with PBS and 200 µl of fresh medium was added. When cells became ~70% confluent they were split between two 96-well plates as described above. When cells reached ~70% confluency again they were each expanded to a well of 24-well plate containing feeder cells. When cells in this plate became confluent

they were subsequently transferred to a 6-well plate containing feeder cells. Finally, cells were transferred to 10 cm dishes containing feeder cells and expanded to freeze down several vials of cells for each clone. Cells were subsequently differentiated to dopaminergic neurons by the growth factor induced (GFI) differentiation procedure (Lau et al., 2006) described in section 2.7.1. Briefly, when undifferentiated cells reached the required density they were transferred to non-bacteriological dishes to form neural stem spheres (NSSs) in suspension culture, with medium containing EGF, bFGF and L-AA (stage 2 of differentiation procedure). NSSs were collected after 4 days, dissociated and plated in neural proliferation medium containing EGF, Shh, FGF8 and L-AA (stage 3). After 5 days, differentiation was induced by replacing proliferation medium with differentiation medium in the absence of growth factors (stage 4). Samples were analysed on day 10 of differentiation for EGFP and DAT expression by immunocytochemistry and Western blotting (sections 2.9, 2.13).

3.4 Results

3.4.1 Construction of DAT-EGFP vector

EGFP-polyA was cloned into linearised pL451 by overnight ligation. Following transformation and overnight culturing, plasmid DNA was purified from 12 clones, digested with EcoRI and resolved by agarose gel electrophoresis (Fig. 3.4A). Four clones (Clone 2, 3, 5, 7) generated a fragment of 6.4 kb and verified the presence of EGFP-polyA. A second fragment predicated at 0.28 kb following digestion by EcoR1 was not visually detected in these clones. The remaining clones contained linearised plasmid DNA (4.8 kb). Plasmid DNA from the four positive clones was further digested with BamHI/EcoRI to investigate if the DNA fragment was correctly oriented in pL451 (Fig. 3.4B). This was necessary as the linearised plasmid and EGFP-polyA were blunted prior to ligation (as they had incompatible ends after digestion with different restriction enzymes) and therefore the DNA fragment could insert in the incorrect orientation. However, all clones yielded two products of the correct size (2.9, 3.7 kb) and created plasmids pL451-EGFP-2, -3, -5 and -7.

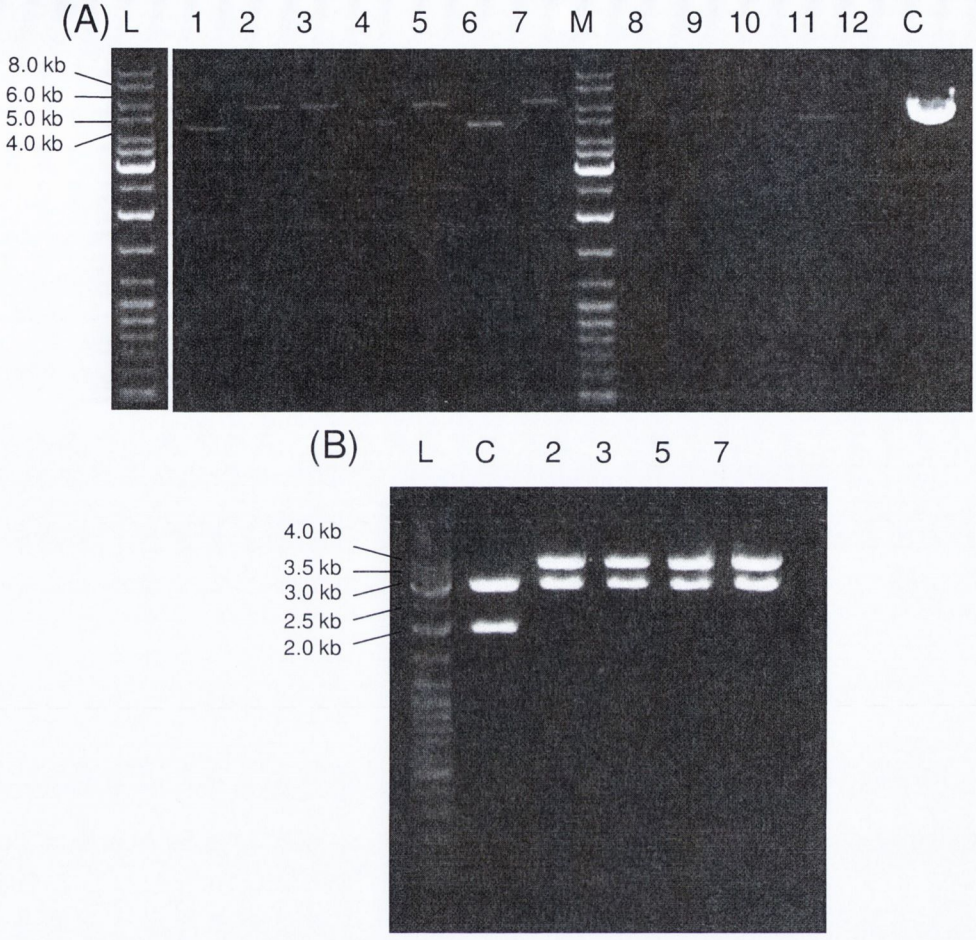

Figure 3.4: Four clones tested positive for the insertion of EGFP-polyA into pL451

(A) Control digestion with EcoRI was performed on plasmid DNA isolated from 12 selected colonies after transformation with pL451 and EGFP-polyA ligation reaction (Clones 1-12). Positive clones yielded bands 0.28 and 6.4 kb. Control pL451 plasmid digest (C) yielded one band of 4.8 kb. (B) Control digest of four positive clones carrying EGFP-polyA cassette was performed with BamHI/EcoRI (Clone 2, 3, 5, 7). Correctly oriented insert DNA was cut twice and yielded bands 2.9 and 3.7 kb. Control pL451 plasmid digest was cut twice and yielded bands 1.8 and 2.9 kb (C). In both images L indicates ladder and contained bands corresponding to the following sizes (kb): 10, 8, 6, 5, 4, 3.5, 3, 2.5, 2, 1.5, 1, 0.9, 0.8, 0.7, 0.6, 0.5, 0.4, 0.3, 0.2, 0.1.

The EGFP targeting cassette was amplified from pL451-EGFP-2 using primers that created homology arms for recombination into BAC-DAT (Sections 3.2.1, 3.2.3.5). Resolution of PCR product by agarose gel electrophoresis demonstrated product of the predicted size (3.2 kb) had been amplified (Fig. 3.5A). The PCR product was subsequently digested with NheI and yielded two fragments of the correct size (1.3, 1.9 kb), verifying the correct sequence had been amplified (Fig. 3.5B). This created the EGFP targeting cassette.

The EGFP targeting cassette was subsequently electroporated into EL250 recombineering competent bacteria containing BAC-DAT which had been induced to express prophage proteins. Two control transformations were included. In one control induced bacteria were electroporated with H_2O to assess the number of clones that were spontaneously resistant to kan/chlor selection. In the other control uninduced bacteria were electroporated with the targeting cassette. The presence of colonies after kan/chlor selection may indicate that the targeting cassette was not completely purified from the template (pL451-EGFP) prior to electroporation. Following overnight incubation and selection on LB agar/kan/chlor plates, few colonies were present on control plates whereas numerous colonies were detected with the positive transformation. Whole cell PCR was then performed on 13 colonies (Clone 1-13) from the positive sample and one colony from non-induced bacteria plus DNA as control. Resolution of PCR products by agarose gel electrophoresis identified one colony that amplified the correct sized product (clone 8, 580 bp) and generated vector DAT-EGFP (Fig. 3.6). No PCR product was detected in non-induced sample.

3.4.2 Analysis of antibiotic resistant clones after transfection and selection

Following transfection of DAT-EGFP into R1 ESCs and selection by G418 resistance, 42 colonies were picked and genomic DNA was isolated from these clones. PCR was subsequently performed using this genomic DNA as template and primers specific to the vector DNA. Seven clones generated PCR products of the correct size (850 bp; Fig. 3.7). Although the band intensities of these PCR products varied across samples all were considered as indicative of vector insertion and generated positive clones 1, 2, 16, 18, 23, 37 and 42. A positive control reaction using DAT-EGFP vector was included and amplified the correct sized PCR product as expected.

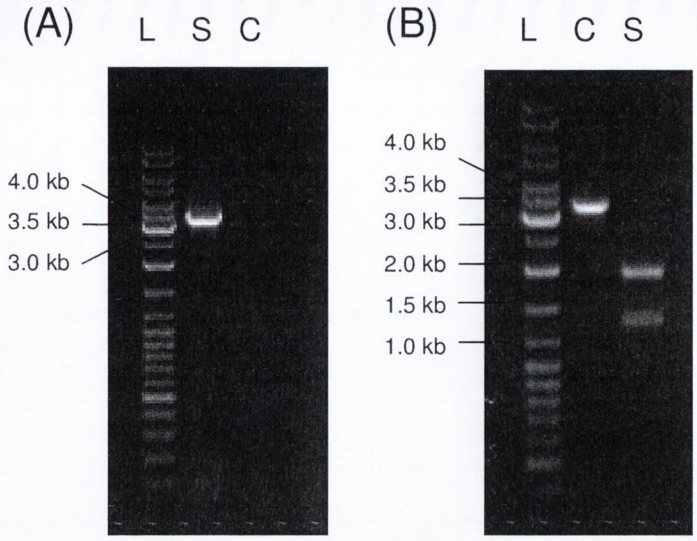

Figure 3.5: Amplification and digestion of EGFP targeting cassette

(A) EGFP targeting cassette was amplified from pL451-EGFP-2 and generated product of the predicted size (S; 3.2 kb). Negative control was included containing no DNA and no PCR product was detected (C). (B) PCR product was digested with NheI and gel electrophoresis of digest reaction detected band of the predicted size (1.3, 1.9 kb), verifying the correct sequence had been amplified (S). Undigested EGFP targeting cassette was run as control (C). In both images L indicates ladder and contained bands corresponding to the following sizes (kb): 10, 8, 6, 5, 4, 3.5, 3, 2.5, 2, 1.5, 1, 0.9, 0.8, 0.7, 0.6, 0.5, 0.4, 0.3, 0.2, 0.1.

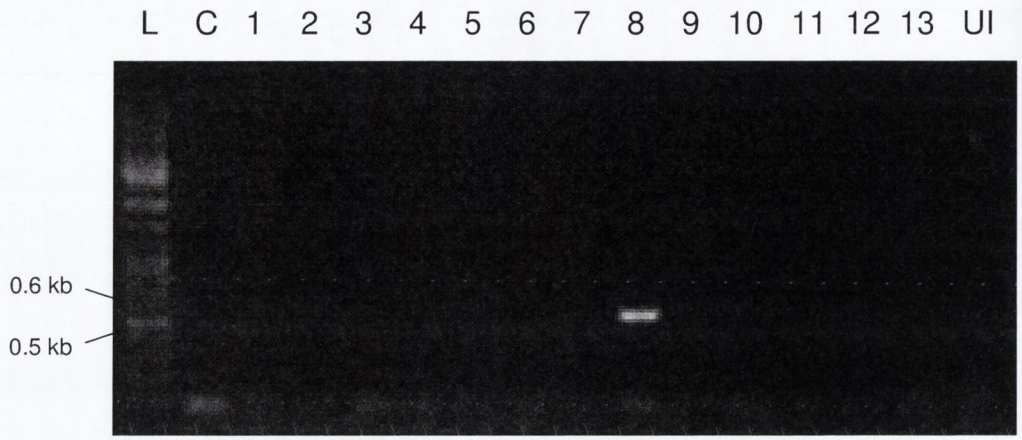

Figure 3.6: One BAC-DAT clone tested positive for recombination of EGFP targeting cassette

Whole cell PCR was performed on 13 clones from induced bacteria (Clones 1-13) and one clone from non-induced bacteria (UI) following recombination of EGFP targeting cassette into BAC-DAT. Positive clones yielded band of 580 bp. No PCR product was detected in non-induced sample. Negative control was included containing no template DNA (C). L indicates marker and contained bands corresponding to the following sizes (kb): 10, 8, 6, 5, 4, 3.5, 3, 2.5, 2, 1.5, 1, 0.9, 0.8, 0.7, 0.6, 0.5, 0.4, 0.3, 0.2, 0.1.

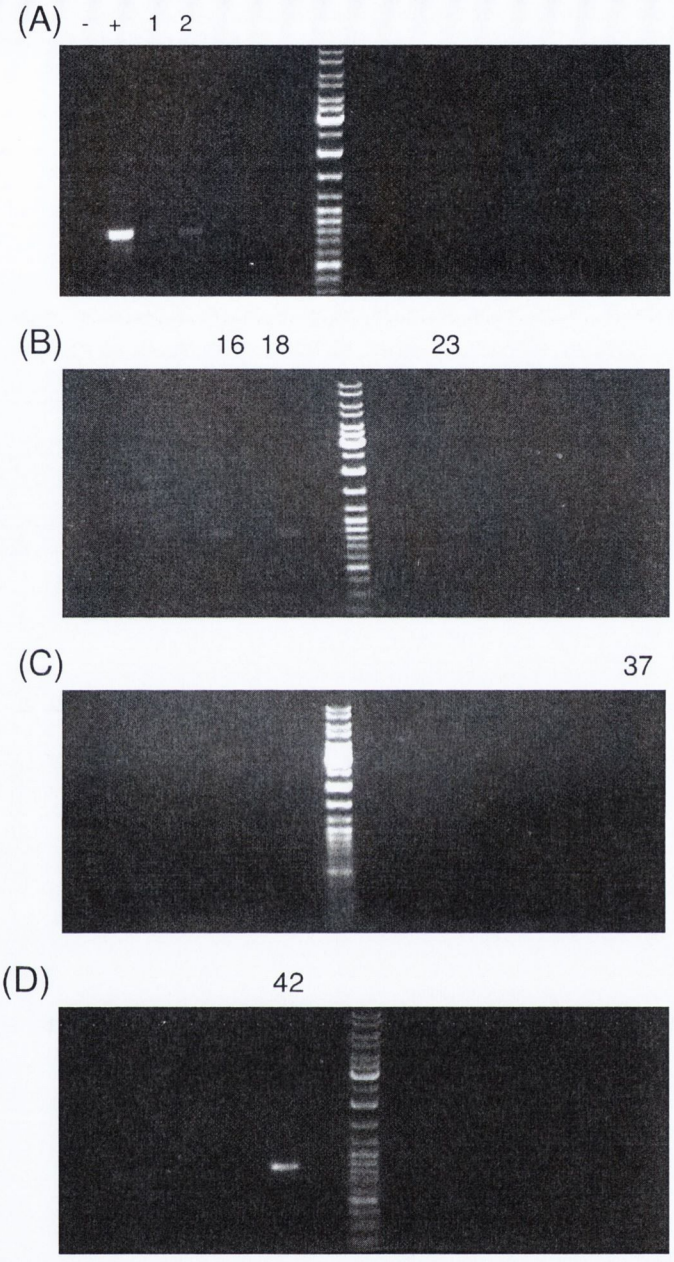

Figure 3.7: Seven R1 ESC clones tested positive for the integration of DAT-EGFP after selection with G418 by PCR of genomic DNA

PCR was performed using genomic DNA isolated from 42 clones resistant to G418 as template (A, B, C, D). Positive clones yielded band of 850 bp. Negative control (-) reaction contained no DNA and did not amplify PCR product. Positive control (+) reaction contained DAT-EGFP as template and amplified 850 bp product. In all gels L indicates marker and contained bands corresponding to the following sizes (kb): 10, 8, 6, 5, 4, 3.5, 3, 2.5, 2, 1.5, 1, 0.9, 0.8, 0.7, 0.6, 0.5, 0.4, 0.3, 0.2, 0.1.

No PCR product was detected in negative control in the absence of DNA. Expansion of these positive clones created seven transgenic cell lines named R1 ESC DAT-EGFP-1, -2, -16, -18, -23, -37 and -42. One clone (Clone 10) which did not amplify PCR product was included as a control (transgenic line R1 ESC DAT-EGFP-10) to investigate the specificity of the genomic screen.

3.4.3 Dopaminergic differentiation and analysis of R1 ESC DAT-EGFP transgenic cell lines

These transgenic cell lines were then subjected to *in vitro* GFI dopaminergic neuronal differentiation (section 2.7.1) to analyse EGFP expression. EGFP fluorescence was monitored daily during the process of terminal differentiation (stage 4 of differentiation procedure) in each transgenic cell line (1, 2, 10, 16, 18, 23, 37, 42) by fluorescent microscopy of live cells (Fig. 3.8). However, no EGFP was detected at any time point in any cell line, with representative images on day 10 of stage 4 provided in Fig. 3.8. Cells exhibiting a neuronal morphology were apparent at this stage of the differentiation process.

To further assess EGFP and DAT expression in clones, Western blotting was performed on protein extracts from day 10 of terminal differentiation for each cell line (Fig. 3.9). It had previously been determined that DAT can be detected already by day 5 of this stage in wild-type cells, with neuronal processes clearly being visualised and co-express of DAT and the neuronal marker Tuj1 observed (Fig. 3.10). Therefore it was predicted that EGFP would have had sufficient time to fold and accumulate by day 10. While DAT was observed in each differentiated population, no EGFP was detected (Fig. 3.9). A positive control sample was also analysed using protein extracted from HeLa cells which constitutively expressed EGFP from the CMV promoter to detect the GFP band.

EGFP expression was also analysed at the cellular level by immunocytochemistry at day 10 of terminal differentiation to identify if even a subset of differentiated cells were positive for this protein, with the level of EGFP protein possibly below the level of detection by Western blotting. However, no EGFP expression was observed in any transgenic cell lines, as determined by endogenous EGFP expression and using an anti-GFP antibody (Fig. 3.11).

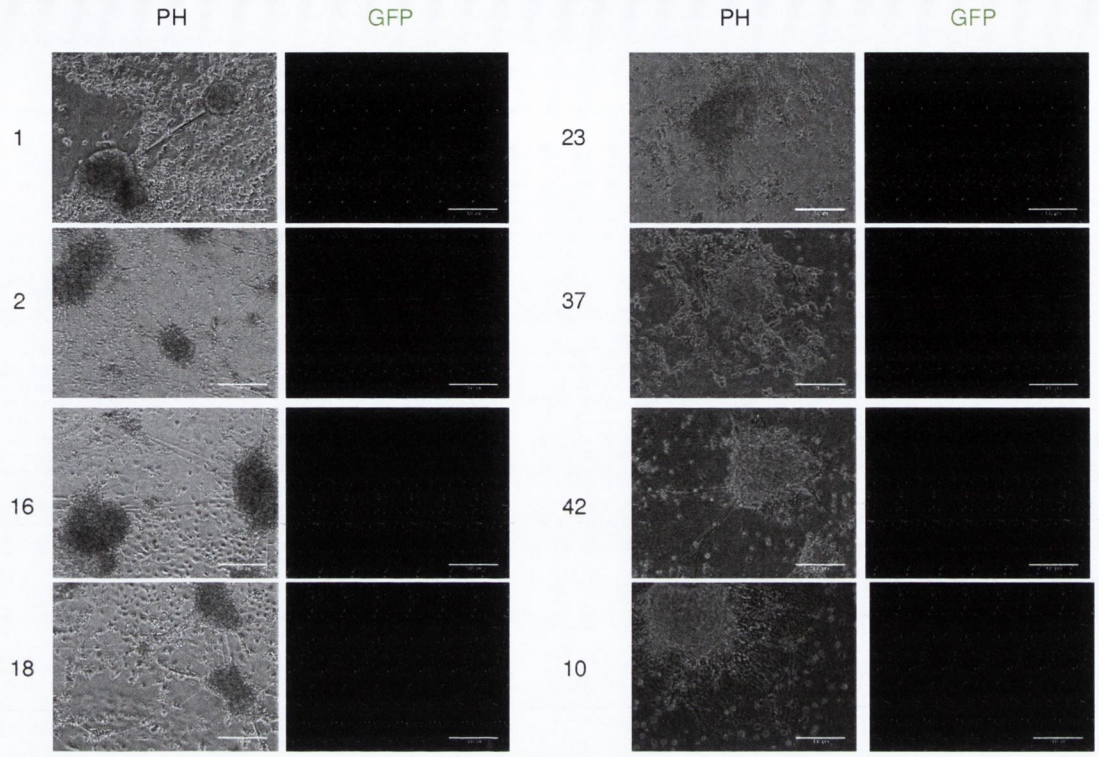

Figure 3.8: EGFP fluorescence is not detected in live R1 ESC DAT-EGFP transgenic cell lines at day 10 of terminal neuronal differentiation

EGFP fluorescence was analysed in seven positive transgenic cell lines (1, 2, 16, 18, 23, 37, 42 in image) and one negative cell line (10 in image) on each day of terminal differentiation (stage 4) during the growth factor induced dopaminergic neuronal differentiation procedure using an Olympus IX81-long focal length fluorescent microscopy with phase contrast and GFP filters. Images were captured at 10 x objective with an F-View II digital camera. Representative images are presented for clones on day 10 of terminal differentiation. PH indicates phase contrast; EGFP, enhanced green fluorescent protein. Scale bar: 100 μm.

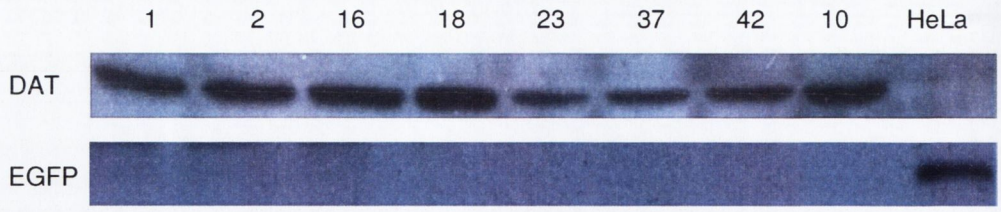

Figure 3.9: R1 ESC DAT-EGFP transgenic cell lines express DAT protein but not EGFP protein on day 10 of terminal neuronal differentiation

Protein was extracted from seven R1 ESC DAT-EGFP positive cell lines (1, 2, 16, 18, 23, 37, 42) and one negative cell line (10) on day 10 of terminal differentiation of the growth factor induced dopaminergic neuronal differentiation procedure and 10 µg of each sample was run on a 12% SDS-PAGE gel. Membranes were probed for DAT and EGFP expression using anti-DAT and anti-GFP antibodies, as indicated. HeLa cells (HeLa) constitutively expressing EGFP from CMV promoter was run as a positive control. DAT indicates dopamine transporter, ~55 kDa; EGFP, enhanced green fluorescent protein, ~28 kDa.

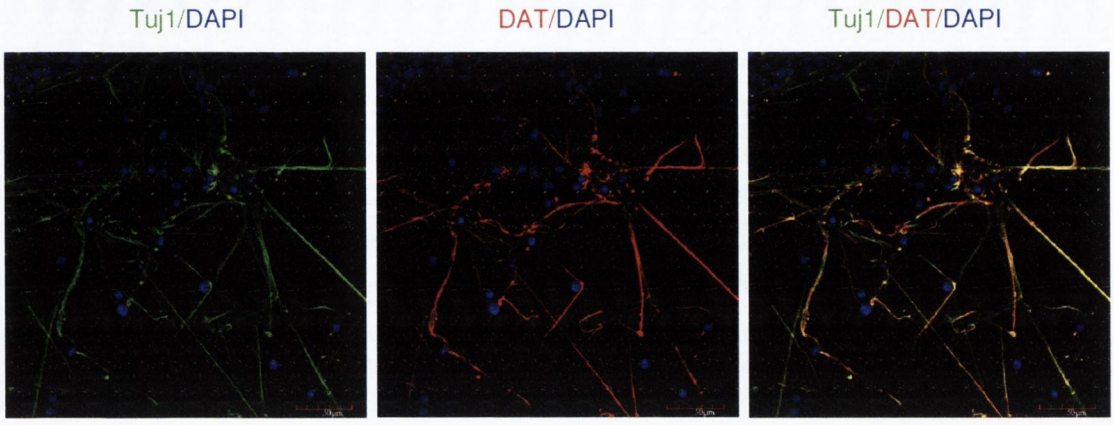

Figure 3.10: DAT expressing neurons are already detected on day five of terminal neuronal differentiation

R1 ESCs were fixed and stained for Tuj1 (green) and DAT (red) expression on day 5 of terminal differentiation of the growth factor induced dopaminergic neuronal differentiation procedure. Cells expressing Tuj1 and DAT appear yellow. Nuclei were counterstained with DAPI (blue). Samples were analysed using an Olympus FV1000 laser scanning confocal microscope at 40 x objective. DAT indicates dopamine transporter. Scale bar: 50 µm.

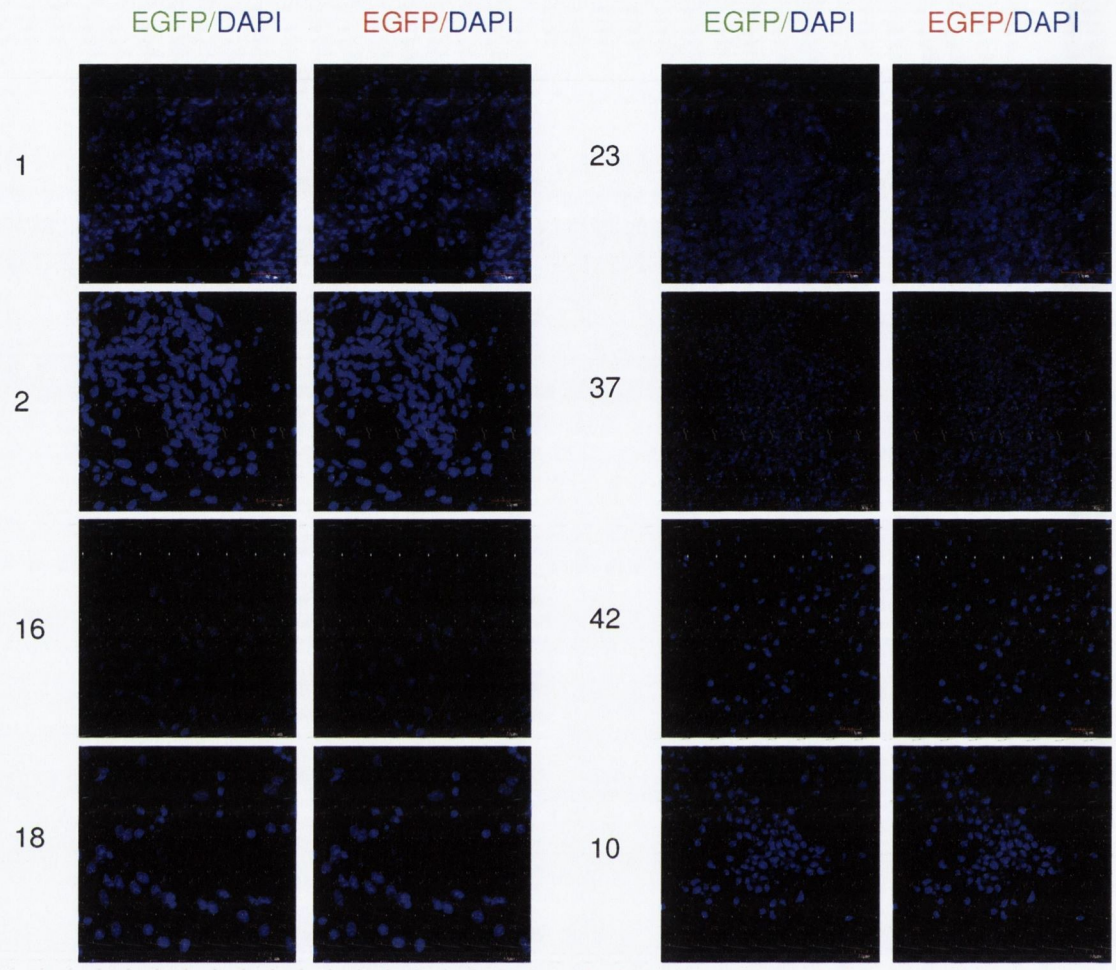

Figure 3.11: R1 ESC DAT-EGFP transgenic cell lines do not express EGFP at the cellular level on day 10 of terminal neuronal differentiation

Cells from DAT-EGFP positive cell lines (1, 2, 16, 18, 23, 37, 42) and one negative cell line (10) were fixed and stained for EGFP expression with an anti-GFP antibody (red) on day 10 of terminal differentiation of the growth factor induced dopaminergic neuronal differentiation procedure. Nuclei were counter-stained with DAPI (blue). Shown are representative images for each clone. No endogenous EGFP fluorescence was detected in any clones (green). No EGFP was detected with anti-GFP antibody in any clones. Samples were analysed using an Olympus FV1000 laser scanning confocal microscope at 40 x objective. EGFP indicates enhanced green fluorescent protein. Scale bar: 50 µm.

All cell lines were also stained for co-expression of DAT and EGFP (using an anti-GFP antibody) to examine the cellular expression of DAT (Fig. 3.12). The results from this series of stains corroborated the findings from Western blotting, with all differentiated samples expressing DAT but no EGFP was observed. Neuronal processes were typically stained in these cell lines, with staining similar to that observed in wild-type cells (Fig. 3.14). To further assess the neuronal phenotype of these differentiated cells, samples from each representative transgenic line were probed for co-expression of the general neuronal marker Tuj1 and EGFP (Fig. 3.13). All samples were found to express Tuj1 and no sample expressed EGFP. The detection of neuronal proteins by immunocytochemistry at this time point of terminal differentiation is in agreement with wild-type R1 ESCs differentiated by this procedure, in which DAT, TH and Tuj1 are typically observed (Fig. 3.14). In each case, neuronal processes are visualised. Therefore, by the methods used here to assess EGFP expression by R1 ESC DAT-EGFP transgenic cell lines it was determined that no cell line expressed detectable levels of EGFP protein, although the dopaminergic genotype of the ESC-derived neurons was proven by DAT expression.

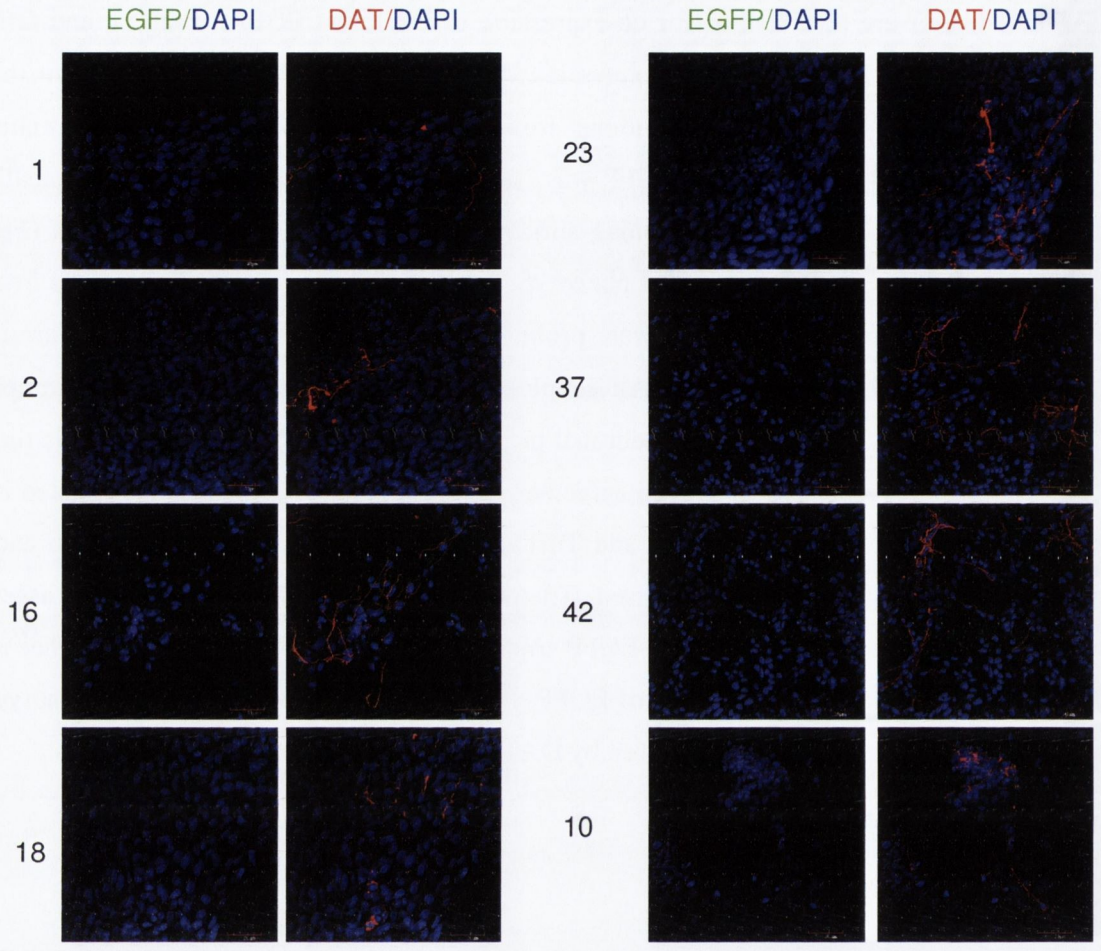

Figure 3.12: R1 ESC DAT-EGFP transgenic cell lines express DAT but not EGFP and have a typical neuronal morphology on day 10 of terminal neuronal differentiation

Cells from seven R1 ESC DAT-EGFP positive cell lines (1, 2, 16, 18, 23, 37, 42) and one negative cell line (10) were fixed and stained for EGFP and DAT expression with anti-GFP (green) and anti-DAT (red) antibodies on day 10 of terminal differentiation of the growth factor induced dopaminergic neuronal differentiation procedure. Nuclei were counter-stained with DAPI (blue). Shown are representative images for each clone. All clones expressed DAT and had a typical neuronal morphology. No clones expressed EGFP. Samples were analysed using an Olympus FV1000 laser scanning confocal microscope at 40 x objective. DAT indicates dopamine transporter; EGFP, enhanced green fluorescent protein. Scale bar: 50 µm.

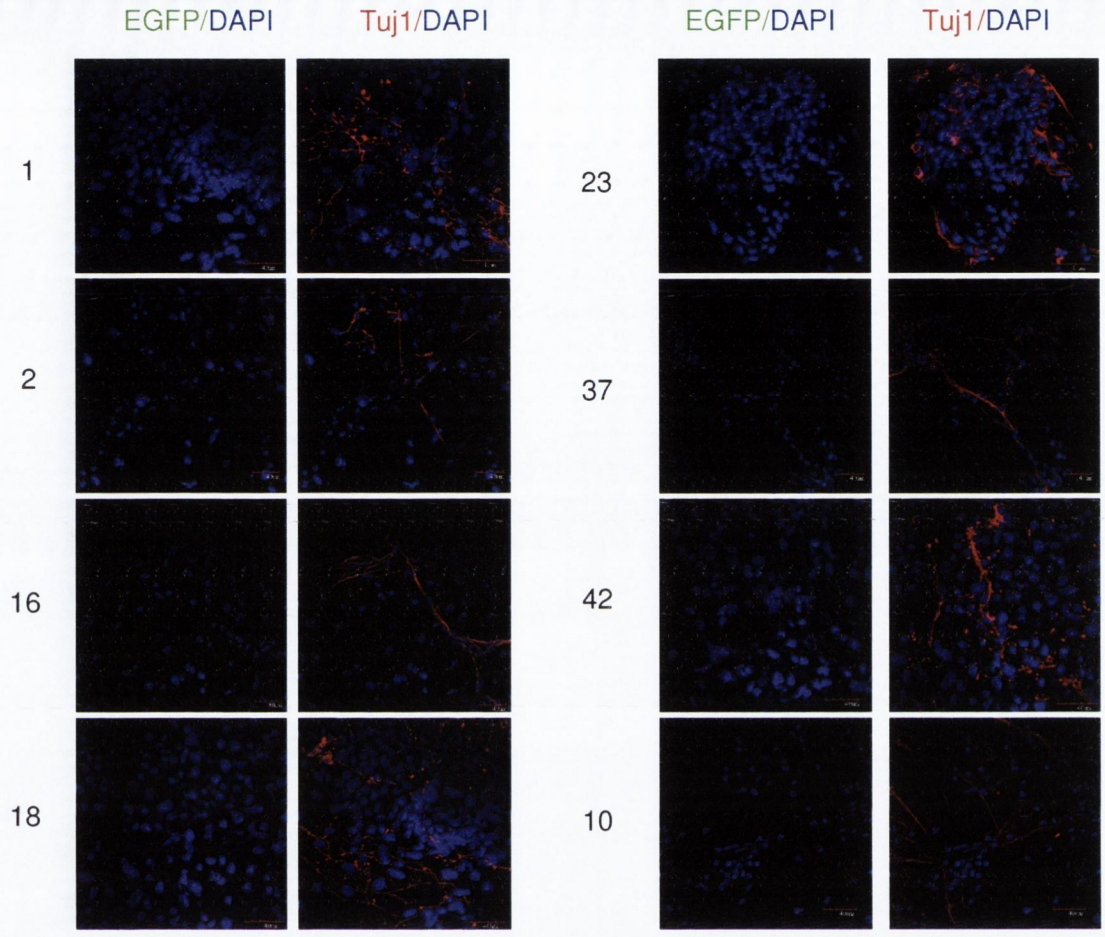

Figure 3.13: R1 ESC DAT-EGFP transgenic cell lines express the neuronal marker Tuj1 but not EGFP on day 10 of terminal neuronal differentiation

Cells from seven R1 ESC DAT-EGFP positive cell lines (1, 2, 16, 18, 23, 37, 42) and one negative cell line (10) were fixed and stained for EGFP and Tuj1 expression with anti-GFP (green) and anti-Tuj1 (red) antibodies on day 10 of terminal differentiation of the growth factor induced dopaminergic neuronal differentiation procedure. Nuclei were counter-stained with DAPI (blue). All clones expressed Tuj1 and had a typical neuronal morphology. No clones expressed EGFP. Samples were analysed using an Olympus FV1000 laser scanning confocal microscope at 40 x objective. EGFP indicates enhanced green fluorescent protein. Scale bar: 40 µm.

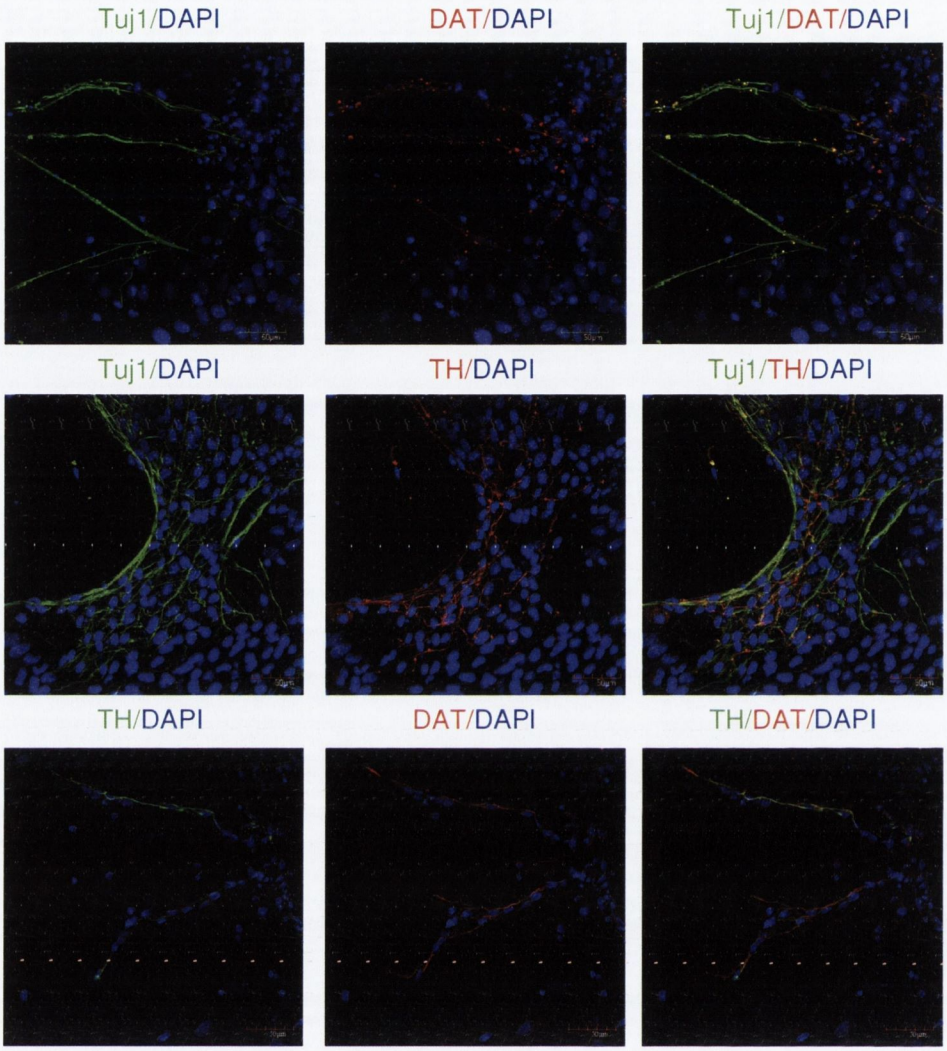

Figure 3.14: R1 ESCs co-express the neuronal marker Tuj1 and dopaminergic markers DAT and TH on day 10 of terminal differentiation

R1 ESCs were fixed and stained for Tuj1 (green), DAT (red) and TH (red/green) expression, as indicated, on day 10 of terminal differentiation of the growth factor induced dopaminergic neuronal differentiation procedure. Nuclei were counterstained with DAPI (blue). Samples were analysed using an Olympus FV1000 laser scanning confocal microscope at 40 x objective. DAT indicates dopamine transporter; TH, tyrosine hydroxylase. Scale bar: 50 µm.

3.5 Discussion

In order to achieve the aim of expressing EGFP from the DAT promoter in ESCs, the vector DAT-EGFP was first constructed in bacterial cells (Fig. 3.1). Generation of this vector involved a number of steps, including standard cloning techniques and recombineering (Figs 3.1, 3.2). EGFP-polyA was first digested from IRES-EGFP-polyA plasmid and ligated into the plasmid pL451. Following transformation and selection, plasmid DNA was isolated from 12 clones and subjected to digestion with EcoRI. Four clones were identified that yielded products of the predicted size to indicate the ligation reaction was successful (Fig. 3.4A). All remaining clones contained plasmid DNA. This may suggest that plasmid DNA was not successfully linearised, thus allowing cells to express the kan resistance gene and survive the selection process, or that the linearised plasmid was not adequately dephosphorylated with SAP, thus allowing the linearised plasmid to re-ligate and confer resistance to kan. Subsequent digestion of plasmid DNA from the four positive clones indicated that they all had inserted the DNA fragment in the correct orientation and generated plasmid pL451-EGFP (Fig. 3.4B). This completed the first step in the construction of DAT-EGFP

The EGFP targeting cassette was subsequently amplified from pL451-EGFP by long range PCR, using primers that contained a 5' end homologous to flanking regions of the exon 2 of the *DAT* gene and a 3' end that primed the plasmid DNA for replication (Fig. 3.5). After purification, this recombination fragment was electroporated into EL250 bacteria containing the BAC-DAT vector, which had been induced to express the prophage genes needed for recombination by culturing at 42°C, and numerous mutant clones survived following selection by chlor/kan resistance. This is in agreement with previous reports suggesting that high recombination efficiency can be obtained using homology sequences between 40 and 50 bp (Yu et al., 2000; Lee et al., 2001). Two control transformations were also performed to assess the efficiency of the recombination procedure. One control contained induced bacteria with H_2O and the other contained uninduced bacteria with the targeting cassette. A small number of colonies were detected with both control transformations. The presence of colonies with induced bacteria in the absence of targeting cassette might suggest that some colonies are spontaneously resistant (Yu et al., 2000) to

kan. The presence of colonies with uninduced bacteria may indicate the targeting cassette was not completely purified from the template (pL451-EGFP) after gel electrophoresis, thus allowing survival under selective conditions.

Whole cell PCR was subsequently performed on selected colonies from induced bateria plus targeting cassette and identified one positive colony that amplified the correct sized product (Fig. 3.6). While this is lower than expected (Lee et al., 2001) the presence of colonies on control plates may indicate spontaneous resistance or residual plasmid DNA, as discussed above. However, as no PCR product was amplified from an uninduced bacterial colony (Fig. 3.6) it verified the specificity of the recombination system as template DNA can not recombine into the BAC-DAT vector in the absence of prophage proteins. It has also previously been proposed that short regions of homology, as used to recombine target DNA in this study, might have similar sequences in other regions of the BAC (Liu et al., 2003) and thus colonies may be generated that are antibiotic resistant due to recombination into other areas of the BAC vector but that would not amplify the correct PCR product due to the specificity of primers used here for the DAT gene and EGFP. Higher recombination efficiency may have been achieved using longer homology arms (Liu et al., 2003). However, sequencing of the purified DAT-EGFP vector verified the correct integration and sequence of the targeting cassette and thus was used for transfections.

Following nucleofection of purified DAT-EGFP into R1 ESCs and selection by G418 resistance, 42 clones survived and were picked for further analysis (Fig. 3.7). While this figure is lower than that reported in a previous study of mouse ESCs transfected with BAC DNA (115, 123, 281 resistant clones obtained using BAC vectors Dll1-GFP, GFAP-GFP and Hes5-GFP, respectively), the experimental procedure differed from that in the present study (Tomishima et al., 2007). In particular, Tomishima et al. (2007) electroporated 100 µg of BAC DNA into $5.6x10^6$ ESCs. In the present study 10 µg of DNA was nucleofected into $2x10^6$ ESCs. While it is difficult to compare ESCs across different species, nucleofection of $5x10^6$ human ESCs with the 5 µg of the same BAC vectors used by Tomishima et al. (2007) generated far fewer clones (15 with Hes5-GFP, 23 with Dll1-GFP, 28 with HB9-GFP) (Placantonakis et al., 2009). No other studies have been identified thus far using nucleofection to introduce BAC DNA into mouse ESCs.

Further analysis of resistant clones by PCR of genomic DNA using primers selective for inserted DNA identified 7 positive clones (~17% positive clones/analysed clones; Fig. 3.7), suggesting that only a fraction of clones may have been transfected with intact BAC DNA (Placantonakis et al., 2009). This is somewhat lower than previously reported for human ESCs transfected with BAC DNA, in which ~33% (9 positive clones/27 analysed clones) of antibiotic resistant clones expressed detectable levels of the *GFP* transgene, as determined by quantitative PCR of genomic DNA (Placantonakis et al., 2009). In the present study, as in the case using quantitative PCR (Placantonakis et al., 2009), variable levels of transgene were amplified by different clones and all clones were assumed to be positive for inserted DNA. It should be noted, however, that the level of PCR product generated by the positive control (DAT-EGFP vector) is not comparable to that of the genomic DNA samples as, presumably, amplification using purified vector DNA as template will be more efficient than that using genomic DNA preparations.

Expansions of these positive clones created seven R1 ESC DAT-EGFP transgenic lines. Each cell line was then subjected to GFI dopaminergic neuronal differentiation using the protocol established by Lau et al. (2006) and described in section 2.7.1. Terminal neuronal differentiation of neural precursors is induced by withdrawal of growth factors in this method and cells are typically analysed at day 10 of differentiation for marker expression. EGFP fluorescence was monitored daily during the process of differentiation for each cell line. However, no EGFP fluorescence was detected in live cells during this period, with representative images for each cell line at day 10 of terminal neuronal differentiation provided in Fig. 3.8. As DAT protein can already be detected at day 5 of terminal differentiation in wild-type cells (Fig. 3.9) and is maintained until at least day 10 of this stage (Fig. 3.14), it was expected that EGFP would have had sufficient time to fold and accumulate during this period to allow fluorescence to be detected. The analysis of EGFP in live cells would have benefited from the inclusion of a positive control sample, such as by the analysis of fixed cells stained with an Alexa-488 secondary antibody, to ensure that the fluorescent microscope being used was successfully detecting EGFP fluorescence.

Samples representative of each transgenic cell line were then processed on day 10 of terminal differentiation of the GFI differentiation to assess the level of EGFP and DAT

protein by Western blotting (Fig. 3.9). DAT protein was detected in all samples by this method but EGFP protein was not observed (Fig 3.9). Cellular protein extracted from HeLa cells expressing EGFP under control of the CMV promoter was used as a positive control in these blots to ensure the EGFP band for each clone was approximately the same size as in the control and to determine if the anti-GFP antibody was successfully detecting the protein. Even though the same amount of protein was loaded for each sample and the positive control, the level of EGFP between the samples and control are not comparable as EGFP expressed from a CMV promoter likely does not correlate with that expressed from a cell specific, developmentally regulated promoter such as DAT.

The cellular localisation of EGFP was also examined by immunocytochemistry in samples from each transgenic cell line at day 10 of terminal differentiation (Fig 3.11-3.13). The rational for this set of experiments was that only a small subset of cells may have expressed EGFP, being below the level detected by Western blotting. However, while DAT was detected by every sample, no EGFP was observed (Figs 3.11, 3.12). This set of experiments would have been improved by the inclusion of a positive control, such as undifferentiated R1 ESCs transiently transfected with the pmaxGFP plasmid, to ensure that the anti-GFP antibody and the confocal microscope was successfully detecting EGFP protein under the experimental conditions used. The anti-DAT antibody had previously been determined to effectively detect this protein in differentiated cells at this time point (Fig. 3.14). These cells also had a typically neuronal morphology and stained positive for the general neuronal marker Tuj1 (Fig. 3.13). In the study of Tomishima et al. (2007) discussed above, the authors reported that that around 40% (10 expressing clones/24 total clones) of drug resistant clones expressed GFP from two neural specific promoters after *in vitro* neural differentiation, thus providing evidence that GFP can be successfully expressed from promoters contained within BACs in mouse ESCs. Interestingly, in the study of Placantonakis et al. (2009) discussed above, only one of the 9 positive clones, determined by quantitative PCR of genomic DNA, expressed GFP following neuronal differentiation and surprisingly only low levels of the *GFP* transgene were detected in this clone following analysis of genomic DNA. Thus this suggests that the use of large DNA vectors containing all the presumptive regulatory regions of a gene is not always sufficient to drive transgene expression from developmentally regulated promoters.

As there was a complete lack of EGFP protein in all clones examined it is possible that an inherent problem existed with the vector such that no mRNA was transcribed. However, steps were taken during its design and construction to preserve regulatory elements which may control gene transcription from the DAT promoter. For example, as mentioned previously, it is thought that the 5' UTR of the DAT gene has a key role in regulating its transcription (Donovan et al., 1995; Sacchetti et al., 1999; Bannon et al., 2001) and therefore DAT-EGFP was designed in such a way to conserve these regions. In addition, cloning into exon 2 of the *DAT* gene contained within BACs has been shown to be an effective way to drive gene expression in transgenic mice (Turiault et al., 2007; Lu et al., 2009; GENSAT). In fact, Turiault et al. (2007) inserted their gene of interest in a similar manner as in this study, at the start codon of the DAT gene. However, in the present report the entire coding region of exon 2 was removed and although unlikely to have interfered with expression of EGFP, as a fusion mRNA composed of the 5' UTR of DAT, the ORF of EGFP and exogenous polyA signal, would have been transcribed in all cases, it cannot be discounted.

In addition, it is generally thought that expression of transgenes from large BAC DNA vectors (~217.5 kb in this case) insulates the integrated transgene from the effects of the surrounding chromatin structure and therefore transgene silencing (Zhang et al., 2004; Tomishima et al., 2007), which is of importance in this study as the BAC DNA integrated randomly into the genome. This assumption is supported by the finding that insertion of genes in multiple locations in a BAC vector resulted in position-independent transgene expression following transfection into mammalian cell lines, with BACs adopting large-scale chromatin conformations independent of their chromosome integration site, including insertion within centromeric heterochromatin (Bian and Belmont, 2010). Thus this would suggest that the transgene may have been transcribed from the DAT promoter and it is possible that the DAT promoter itself is not sufficient to drive *GFP* expression at an adequate level to detect EGFP protein. This is supported by the results of a recent study in which EGFP expression was faint after multi-stage dopaminergic differentiation of an ESC line with EGFP knocked into the DAT gene and not bright enough to select DA neurons by FACS (Zhou et al., 2009b). In addition, it has also been reported that BAC DNA only

displayed one integration site in the genome following transfection into human ESCs, which was independent of the endogenous locus, indicating that integration did not occur by homologous recombination (Placantonakis et al., 2009). It has also been reported that a positive correlation exists between transgene copy number and fluorescence following transfection of BAC into mammalian cell lines (Bian and Belmont, 2010). Thus as the approach taken here to target EGFP to the DAT promoter contained within a BAC had not previously been attempted, it is possible that multiple fluorescent tags may need to be expressed from this promoter to allow EGFP protein to be detected following differentiation of ESCs to DA neurons.

Alternatively, it is possible that a difference between promoter activity and mRNA or protein stability resulted in lack of transgene expression (Tomishima et al., 2007) in these transgenic cell lines, implying that a problem existed at the post-transcriptional level, which may be supported by detection of DAT protein in all cell lines following differentiation (Figs 3.9, 3.12). This would have been clarified by analysis of mRNA from differentiated samples with EGFP specific promoter, to determine if transgene transcripts were present in differentiated cells. This was not performed as the desired application of these transgenic cell lines was visualisation of cells during dopaminergic differentiation and prospective sorting of post-mitotic neurons, and thus if levels were below that of detection they would not have been usable.

mRNA stability is highly regulated and thought to involve the 3' UTR of the mRNA molecule (for review, see Guhaniyogi and Brewer, 2001). As the transgene mRNA fusion did not contain this region, it is possible that this may have resulted in its instability and degradation. However, as the polyA tail has been reported to play a role in nuclear mRNA processing, export of the mRNA molecule to the cytoplasm, translation and cytoplasmic mRNA stability (for review, see Guhaniyogi and Brewer, 2001), and was included in the EGFP targeting cassette, it may be expected to afford some level of stability and prevent its decay. In addition, the 5' UTR facilitates translation (for review, see Pickering and Willis, 2005) and may also confer stability to the mRNA molecule (for review, see Guhaniyogi and Brewer, 2001), and as the 5' UTR of DAT is a part of the transgene mRNA fusion it may have assisted is these processes. This may be supported by the fact that previous

studies have successfully expressed transgenes from the DAT promoter contained with BACs using similar methodology as the present study (Turiault et al., 2007; Lu et al., 2009; GENSAT).

As DAT is a multi-spanning transmembrane protein (for review, see Torres et al., 2003) it is targeted to the endoplasmic reticulum (ER) during translation by a signal sequence contained within the nascent protein (for review, see Lecomte et al., 2003). As the transcribed transgene does not include any of the coding sequence of DAT, translation presumably occurs in the cytoplasm without targeting to the ER. Therefore, it would seem unlikely that lack of EGFP protein in differentiated transgenic cell lines is related to ER associated degradation (for review, see Vembar and Brodsky, 2008) and, as discussed above, may be supported by the detection of transgenes expressed from the DAT promoter in previous studies (Turiault et al., 2007; Lu et al., 2009; GENSAT).

Prior to the formation of the chromophore responsible for GFP fluorescence, the translated polypeptide chain must fold to its near-native β-barrel structure (for review, see Ormo et al., 1996; Reid and Flynn, 1997; Craggs, 2009). Under physiological conditions, protein misfolding and aggregation of GFP has been reported to occur (for review, see Tsien, 1998; Fukuda et al., 2000), with the chromophore thus not developing and green fluorescence not observed (Tsien, 1998; Fukuda et al., 2000; Craggs, 2009). Misfolded and damaged polypeptides are typically targeted for degradation by the proteasome (for review, see Goldberg, 2003), and hence may contribute to lack of EGFP fluorescence in these differentiated cells. Thus it is possible, at least to some degree, that even though EGFP is a widely used fluorescent marker and a similar approach was used in this study as those previously published to express the transgene from the DAT promoter, EGFP mRNA or protein instability and degradation occurred in transgenic cell lines and resulted in absence of detectable EGFP protein after neuronal differentiation. However, it should be noted, that protein or mRNA instability may have been more likely to result in mosaic EGFP expression (Alami et al., 2000; Tomishima et al., 2007) rather than a total lack of EGFP as observed here.

This study and those reported previously targeting EGFP to the Pitx3, TH and DAT promoters (Yoshizaki et al., 2004; Zhao et al., 2004; Hedlund et al., 2007; Hedlund et al., 2008; Zhou et al., 2009b) highlight the complexity of using genetic reporters to label ESC derived DA neurons. Although it can be speculated that absence of EGFP in this system may be due to insufficiency at the level of the DAT promoter, and/or mRNA or protein instability and degradation, it is impossible to formulate a conclusive answer without further examination of transgenic cell lines. However, due to time restrictions, alternative studies were performed to obtain enriched DA neurons from ESCs.

Chapter 4

Derivation of dopaminergic neurons from Sox1-GFP embryonic stem cells

4.1 Introduction

DA neurons are of particular interest as they have a fundamental role in many body functions and processes, dysfunction or degeneration of which have been implicated in psychiatric and neurological disorders (for review, see Greengard, 2001). ESCs may provide an unlimited source of DA neurons as they can be propagated indefinitely in culture in an undifferentiated state while retaining pluripotency (Thomson et al., 1998; Amit et al., 2000). Unfortunately, the analysis of ESC-derived DA neurons is greatly impeded by the heterogeneous nature of ESC cultures even after directed differentiation, with the population of cells being composed of multiple cell types often of more than one germ layer (for review, see Stavridis and Smith, 2003; Pruszak et al., 2007). This obstacle may be partly or wholly overcome by introducing reporter cassettes, such as EGFP, into a locus with restricted expression in the desired cell type, effectively labelling the cell of interest (for review, see Stavridis and Smith, 2003).

The results of the preceding chapter and those from previous published reports discussed thus far (Yoshizaki et al., 2004; Zhao et al., 2004; Hedlund et al., 2007; Hedlund et al., 2008; Zhou et al., 2009b) highlight the difficulties associated with labelling mature DA neurons with the aim of generating enriched dopaminergic neuronal populations. For example, expression of EGFP from a fragment of the TH promoter thought to be sufficient to drive transgene expression resulted in a mixed cell population after FAC sorting, containing both pluripotent stem cells and proliferative cells after transplantation into the rat brain (Hedlund et al., 2007). Selection of EGFP positive and SSEA1 negative cells in this report resulted in the purification of only 1.4% of live cells (Hedlund et al., 2007), with TH-EGFP ESCs representing 2.6% of live cells following differentiation in another study (Yoshizaki et al., 2004). Furthermore, high cell death has typically been observed following dissociation and sorting of mature DA neurons at later stages of the differentiation process (Yoshizaki et al., 2004; Hedlund et al., 2008). Thus purification of labelled neural precursors (NPs) with the aim of obtaining enriched DA neurons from ESCs may be an attractive alternative as these cells have the potential for further *in vitro* amplification and differentiation after selection (Li et al., 1998).

Two markers of NPs are nestin and Sox1. Nestin is a type VI intermediate filament protein expressed in neural stem cells and is downregulated as differentiation proceeds (Lendahl et al., 1990). EGFP expressed from the nestin promoter has been shown to be an effective way to select NPs, with a highly purified neuronal and glial population generated after neural differentiation (Andressen et al., 2001). The dopaminergic differentiation potential of these cells was not investigated in this study (Andressen et al., 2001). However, nestin is now recognised as a marker of multi-lineage progenitor cells, being detected in cells of mesodermal, ectodermal and neuroectodermal fate (for review, see Wiese et al., 2004). In addition, as only a fragment of the nestin promoter was used to drive transgene expression in the report by Andressen et al. (2001) and due to the aberrant expression pattern often seen with this type of expression system, such as that observed in the study of Hedlund et al.(2007) using a fragment of the TH promoter, it is possible that this system may encounter difficulties.

Sox1 is a Sry-related high mobility group-box transcription factor and the earliest known specific marker of the neuroectoderm in the mouse embryo (Wood and Episkopou, 1999). It is first expressed in the neural plate and subsequently maintained in neuroepithelial cells throughout the entire neuroaxis, but is downregulated during neuronal and glial differentiation (Pevny et al., 1998; Ying et al., 2003). In addition, a Sox1-GFP ESC reporter line (named 46C ESC line) has previously been generated by a knock-in approach to replace the ORF of the endogenous *Sox1* gene with the coding sequence for GFP (Ying et al., 2003). The fidelity of the Sox1-GFP reporter has been demonstrated *in vivo* and *in vitro* (Aubert et al., 2003; Ying et al., 2003). In addition, heterozygous Sox1-GFP mice are viable and healthy with no apparent phenotype (Aubert et al., 2003). Thus this 46C ESC reporter line may represent an ideal system for purifying NPs, which can be further differentiated to post-mitotic dopaminergic neurons and provide a novel system to investigate the function and regulation of these cells.

Previous reports which have investigated the ability to sort NPs based on Sox1-GFP expression and obtain an enriched dopaminergic population from these cells following further *in vitro* differentiation have resulted in conflicting results (Chung et al., 2006; Fukuda et al., 2006; Parmar and Li, 2007), possibly due to the use of different *in vitro*

differentiation procedures. While Chung et al. (2006) obtained an enriched neuronal population (Tuj1+ cells) following differentiation of NPs using the multi-stage method of Lee et al. (2000), a low proportion of these neurons co-expressed TH (~6%) (Chung et al., 2006). However, Fukuda et al. (2006) reported around 22% of neurons were TH+ following sorting of NPs and differentiation on PA6 stromal cells (Kawasaki et al., 2000). This study highlights the dopaminergic differentiation potential of these Sox1-GFP ESCs and the possibility of generating enriched DA neurons. However, the presence of stromal cells after differentiation likely impedes *in vitro* studies of DA neurons due to the undefined effects of these cells. The neuronal differentiation potential of this 46C ESC line was initially reported by Ying and Smith (2003) and Ying et al. (2003) using a monolayer culture system. Further studies have identified that TH+ neurons can be generated at a frequency of 16%, with this increasing to around 26% by the addition of Shh and FGF8 (Parmar and Li, 2007). In addition, sorting of these cells based on GFP expression resulted in 14% of neurons expressing TH (Parmar and Li, 2007). This study did not report purity of sorted cells (i.e. the percentage of neurons) after differentiation.

Lau et al. (2006) have recently published a fast and efficient differentiation method (referred to in previous sections as growth factor induced (GFI) neuronal differentiation) which generates DA neurons from ESCs in a shorter time period than alternative differentiation procedures (Lee et al., 2000; Rolletschek et al., 2001) and thus is advantageous. This is achieved in a multi-stage procedure by the application of signalling molecules at early stages of the differentiation process, and has been described in section 2.7.1 (Fig. 2.1). In particular, culturing of undifferentiated ESCs in suspension induces the formation of neural stem spheres (NSSs), with L-AA and the mitogens EGF and bFGF already applied at this stage (stage 2). Subsequent dissociation of these colonies and culturing in serum free medium with L-AA, EGFP and the DA inducing morphogens Shh and FGF8 induces the proliferation and patterning of NPs (stage 3), with terminal differentiation being induced by withdrawal of these growth factors (stage 4). Thus sorting of NPs based on GFP expression using the Sox1-GFP reporter ESC line and differentiation by this method may represent an efficient way to generate highly enriched dopaminergic neurons for further *in vitro* studies. Therefore, the overall aim of this study was to investigate if an enriched population of DA neurons could be generated following sorting

of Sox1-GFP NPs, re-plating and further differentiation by the GFI neuronal differentiation method.

In order to achieve this aim a number of investigations were initially performed. As the discussed studies demonstrate, variation exists in the neuronal and dopaminergic differentiation potential of the same cell line under different methods. Thus to initially evaluate the neuronal and dopaminergic differentiation potential of the GFI method with 46C Sox1-GFP ESCs, the neuronal population generated from these cells following this procedure was compared to that obtained by monolayer (ML) differentiation. As discussed these 46C ESCs were initially characterised by this method and can effectively generate DA neurons by this procedure (Ying et al., 2003; Parmar and Li, 2007). The ML differentiation method is described in section 2.7.2 (Fig. 2.1). Furthermore, as the GFI differentiation protocol is abbreviated in comparison to other published reports regarding DA differentiation (Lee et al., 2000; Rolletschek et al., 2001), it was of interest to analyse if a more mature neuronal phenotype could be obtained following extended terminal differentiation. The appearance of Sox1-GFP NPs was monitored by fluorescent microscopy and FACS to determine the optimal time point for sorting cells, and again was compared with cells differentiated by the ML procedure as control. Using this information, NPs were sorted and further differentiated to assess purity of cultures and propensity to form DA neurons.

4.2 Methods

4.2.1 Analysis of GFP expression during neuronal differentiation of Sox1-GFP ESCs

Sox1-GFP expression by this cell line was observed at each day of differentiation using both ML and GFI differentiation procedures by live imaging of GFP in cells and FACS to determine the optimal time point to sort cells. Cells were differentiated as described in Section 2.7 and analysed using an Olympus IX81-long focal length fluorescent microscope with 10 x objective. Phase contrast and GFP fluorescent images were obtained using an F-View II digital camera. For FACS analysis, R1 and 46C Sox1-GFP ESCs at the same stage

of differentiation were collected by trypsinisation, centrifuged and resuspended in 500 µl of ice-cold 2% FBS/1X PBS. The cells were triturated and passed through a 50 µm cell strainer to obtain a single cell suspension. Propidium iodide (PI; 1 µg/ml) was then added to determine cell viability and the samples were immediately analysed using a Dako CyAn ADP flow cytometer. GFP and PI were excited using 488 nm laser and analysed using 530/40 nm laser and 613/20 nm laser, respectively. Samples were first gated by forward-side scatter and then by within this population by GFP and PI. Non-GFP expressing R1 cells at the same stage of differentiation were used as negative control for background fluorescence. Data were analysed using FlowJo software.

4.2.2 FACS based purification of Sox1-GFP neural precursors

NPs were sorted at day 5 of the neural proliferation stage (stage 3) of the GFI differentiation procedure (section 2.7.1; Fig. 2.1). This day was selected as robust GFP expression was visualised at this time point but neurites were not yet present. Cells were prepared as described above and resuspended in ice-cold 4% FBS/1X PBS. Positive and negative populations were sorted using Dako MoFlo Cell Sorter into sterile 15 ml Falcon tubes containing complete differentiation medium (section 2.7.1). Cells were first gated by forward-side scatter and within this population by GFP expression. Non-GFP expressing R1 cells at the same stage of differentiation were used as negative control for background fluorescence. At this stage cells were either used for RNA extraction for RT-PCR (section 2.10) or re-plated onto poly-D-lysine (PDL)/laminin coated dishes (section 2.6.7) in differentiation medium at a density of $8x10^4$ cells/cm^2 in 24-well plates.

4.2.3 Analysis of Sox1-GFP sorted samples after growth factor induced neuronal differentiation

The average number of neurons in the Sox1-GFP+ and Sox1-GFP- population was determined at day 10 of terminal differentiation (stage 4) of the GFI neuronal differentiation procedure. This was achieved by staining cells with an anti-neuronal class III β-tubulin (Tuj1 clone) antibody and counterstaining nuclei with DAPI (section 2.13) and taking 10 randomly selected images per well using GFP and DAPI filters. Images were

acquired using an Olympus IX81-long focal length fluorescent microscope set to 10 x objective with an F-View II digital camera. Images were processed in ImageJ, with the number of DAPI+ nuclei first being counted followed by Tuj1+ cells.

4.3 Results

4.3.1 Comparison of neuronal populations derived from Sox1-GFP ESCs following growth factor induced and monolayer differentiation procedures

As 46C Sox1-GFP ESCs had not previously undergone neural induction using the GFI method, NSSs derived from these cells were dissociated following suspension culture and plated at two densities, $5x10^4$ cells/cm^2 (Fig. 4.1A) and $1x10^5$ cells/cm^2 (Fig. 4.1B) on a range of commonly used substrates to identify which resulted in the best attachment and supported neuronal differentiation. Cells attached well at both densities to all substrates tested when observed one day after plating (Fig. 4.1). Analysis of cells at day 10 of differentiation revealed the appearance of small round colonies which stained positive for the neuronal marker Tuj1 (Fig. 4.1). Numerous single cells were also present that did not stain with Tuj1. Neurites extending from Tuj1 colonies were most apparent at lower densities. In addition, by gross morphological analysis all substrates were equivalent in supporting neuronal proliferation and differentiation.

As 46C Sox1-GFP ESCs have typically been induced to undergo neuronal differentiation by ML culture conditions (Ying and Smith, 2003; Ying et al., 2003), a simple comparative study was performed to assess the neuronal population derived from these cells following differentiation by GFI and ML procedures. In particular, analysis was performed on day 10 of terminal differentiation (stage 4) of the GFI differentiation procedure and day 14 of the ML differentiation procedure (Fig. 2.1). Tuj1 positive colonies of different sizes with extensive neurites were present after differentiation by both protocols (Fig. 4.2). These colonies were more abundant following GFI differentiation (GFI, 23.56 $\pm$ 0.4 colonies; ML, 14.56 $\pm$ 0.78 colonies; $p<0.01$; Fig. 4.3). However, the diameter of colonies obtained following ML differentiation were significantly larger than those derived from GFI differentiation (GFI, 188.93 $\pm$ 11.11 µm; ML, 290.54 $\pm$ 12.57 µm; $p<0.01$; Fig. 4.4).

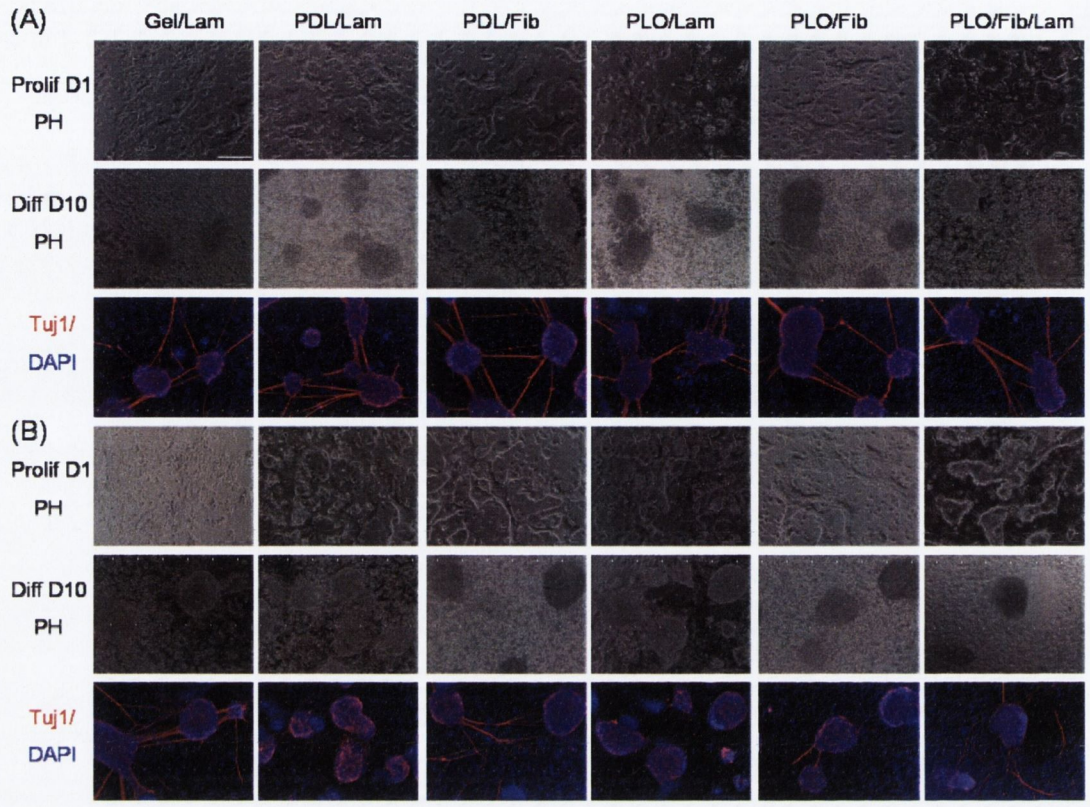

Figure 4.1: Neural stem spheres derived from Sox1-GFP ESCs attach to a range of extracellular matrices and differentiate to neurons by the growth factor induced neuronal differentiation procedure

Following 4 days of suspension culture, NSSs were dissociated and plated in proliferation medium containing growth factors at $5x10^4$ cells/cm^2 (A) and $1x10^5$ cells/cm^2 (B) on poly-L-ornithine/fibronectin/laminin (PLO/Fib/Lam), gelatine/laminin (Gel/Lam), poly-D-lysine/laminin (PDL/Lam), poly-D-lysine/fibronectin (PDL/Fib), poly-L-ornithine/ laminin (PLO/Lam) and poly-L-ornithine/fibronectin (PLO/Fib), as indicated. Cell attachment was assessed one day later, as observed in phase contrast images at day 1 of neural proliferation (Prolif D1 PH). Terminal differentiation was induced five days later by withdrawal of growth factors from proliferation medium. Ten days later, samples were fixed and stained for Tuj1 (red) and nuclei were counterstained with DAPI (blue), with phase contrast images also obtained at this time point (Diff D10 PH). Samples were analysed using an Olympus IX81-long focal length fluorescent microscopy using phase contrast, DAPI and Cy3 filters. Images were obtained at 10 x objective with an F-View II digital camera. Scale bar: 100 µm.

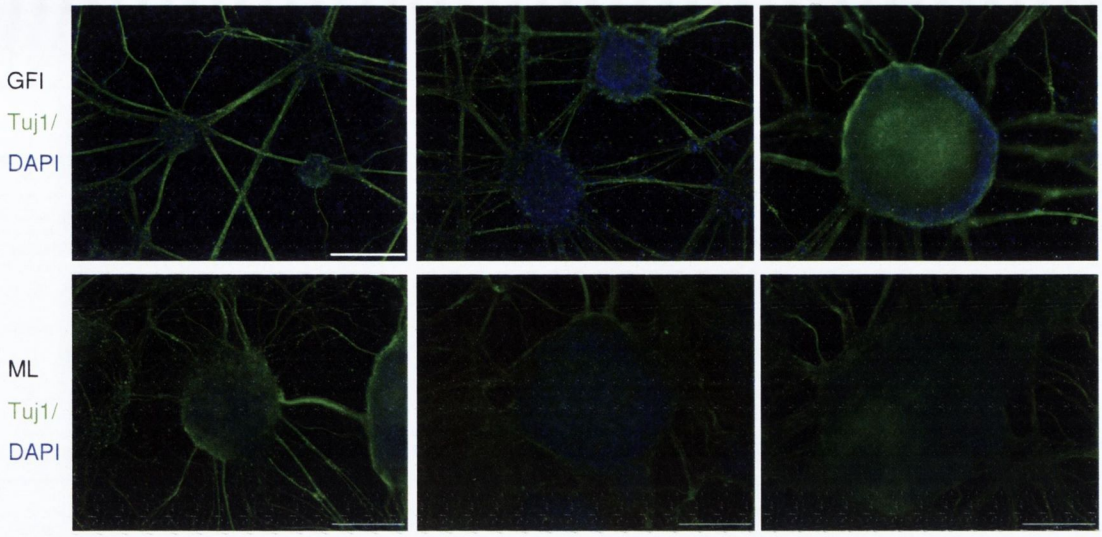

Figure 4.2: Tuj1 positive colonies of different sizes with neurite extensions are derived from Sox1-GFP ESCs following growth factor induced (GFI) and monolayer (ML) differentiation procedures

Sox1-GFP ESCs were fixed and stained for Tuj1 expression (green) on day 10 of terminal differentiation of the GFI differentiation procedure (GFI) and day 14 of the ML differentiation protocol (ML). Nuclei were counterstained with DAPI (blue). The GFI and ML rows illustrate three different sized Tuj1 positive colonies from a single GFI or ML differentiation procedure, respectively. Samples were analysed using an Olympus IX81-long focal length fluorescent microscopy using DAPI and GFP filters and images were captured at 10 x objective with an F-View II digital camera. Scale bar: 200 µm.

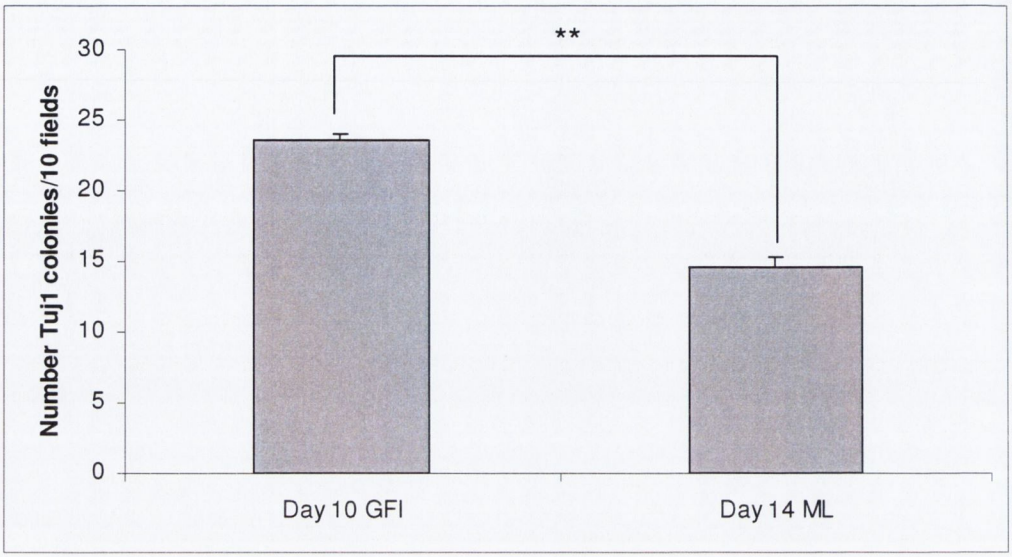

Figure 4.3: Tuj1 positive colonies derived from Sox1-GFP ESCs are more abundant following growth factor induced (GFI) neuronal differentiation than following monolayer (ML) neuronal differentiation

Sox1-GFP ESCs were fixed and stained for Tuj1 expression on day 10 of terminal differentiation of the GFI differentiation protocol (Day 10 GFI) and day 14 of the ML differentiation protocol (Day 14 ML). Ten randomly selected images were taken per well and the number of Tuj1 positive colonies was counted. Data shown represent the mean + SEM of experiments performed in triplicates on three independent cell populations. **$p<0.01$; Student's two-tailed t-test.

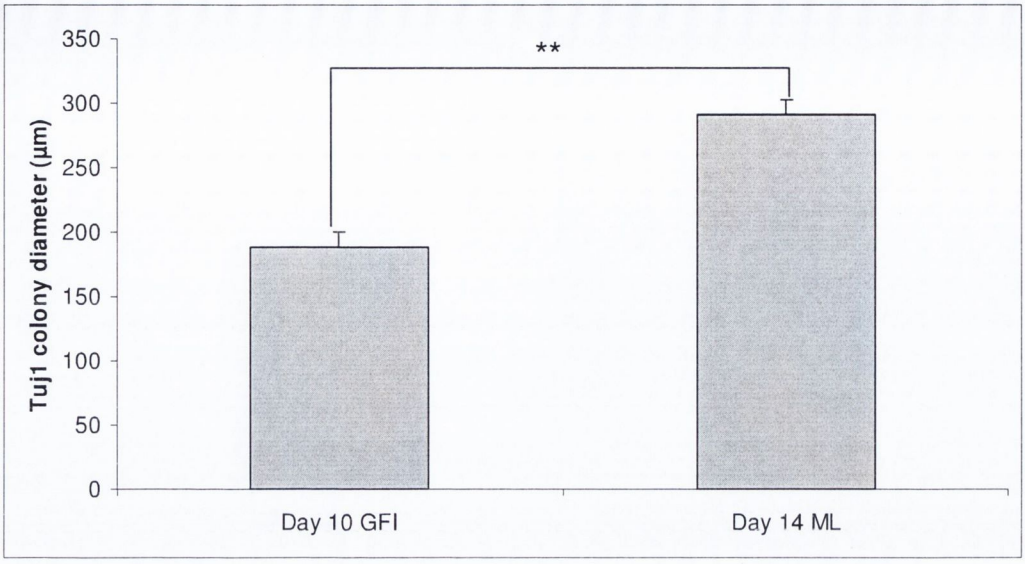

Figure 4.4: The diameter of Tuj1 positive colonies derived from Sox1-GFP ESCs are smaller following growth factor induced (GFI) neuronal differentiation than following monolayer (ML) neuronal differentiation

Sox1-GFP ESCs were fixed and stained for Tuj1 expression on day 10 of terminal differentiation of the GFI differentiation procedure (Day 10 GFI) and day 14 of the ML differentiation procedure (Day 14 ML). Ten randomly selected images were taken of Tuj1 positive colonies per well and the diameters were measured in ImageJ. Data shown represent the mean + SEM of experiments performed in triplicates on three independent cell populations. **$p<0.01$; Student's two-tailed t-test.

Furthermore, Tuj1 positive colonies derived from Sox1-GFP ESCs extended longer neurites following GFI neuronal differentiation than following ML neuronal differentiation (GFI, 510.62 ± 35.23 μm; ML, 402.31 ± 10.26 μm; $p<0.05$; Fig. 4.5).

Western blotting was performed to compare the neuronal subtypes derived from Sox1-GFP ESCs following differentiation by both methods in three independent cultures. The analysis was carried out in this manner as opposed to immunocytochemistry of cells as differentiation by these protocols typically resulted in the formation of three-dimensional clusters, as observed in Fig. 4.2, rendering numerical analysis of different neuronal subtypes difficult, as mentioned previously (Lorincz, 2006; Hedlund et al., 2008). Analysis of cellular proteins after differentiation identified the presence of Tuj1 in all samples following neuronal differentiation by both methods (Fig. 4.6). While expression of the pre-synaptic neuronal marker synaptophysin was low, it was almost exclusively found after GFI differentiation (Fig. 4.6). Expression of the astrocyte specific intermediate filament GFAP was completely absent in ML cultures and was detected at low levels in two of the GFI samples (Fig. 4.6).

Protein markers for the GABAergic (GAD), dopaminergic (Nurr1, DAT, TH) and serotonergic (SERT) neuronal subtypes were present following differentiation by both procedures (Fig. 4.7). None of the samples examined detected the glutamatergic marker EAAC1 or the noradrenergic marker NAT (Fig. 4.7). GAD levels were inconsistent across cultures, with higher variability observed after ML differentiation and the protein being almost undetectable in two of these cultures (Fig. 4.7). SERT expression was also quite changeable, with more variability observed in GFI cultures (Fig. 4.7). The SERT antibody recognised only one band in mouse brain lysate but two bands in cell culture samples (Fig. 4.7). As this antibody was highly specific, both bands are considered to be SERT protein. As discussed previously, Nurr1 is a transcription factor required for the induction of the mDA phenotype (Zetterstrom et al., 1997; Castillo et al., 1998; Saucedo-Cardenas et al., 1998; Wallen et al., 1999). Expression of DAT and Nurr1 was relatively constant across cultures for both differentiation methods (Fig. 4.7). By semi-quantitative analysis of blots, the levels of both of these proteins were higher after GFI differentiation ($p<0.05$ for both; Figs 4.8, 4.9).

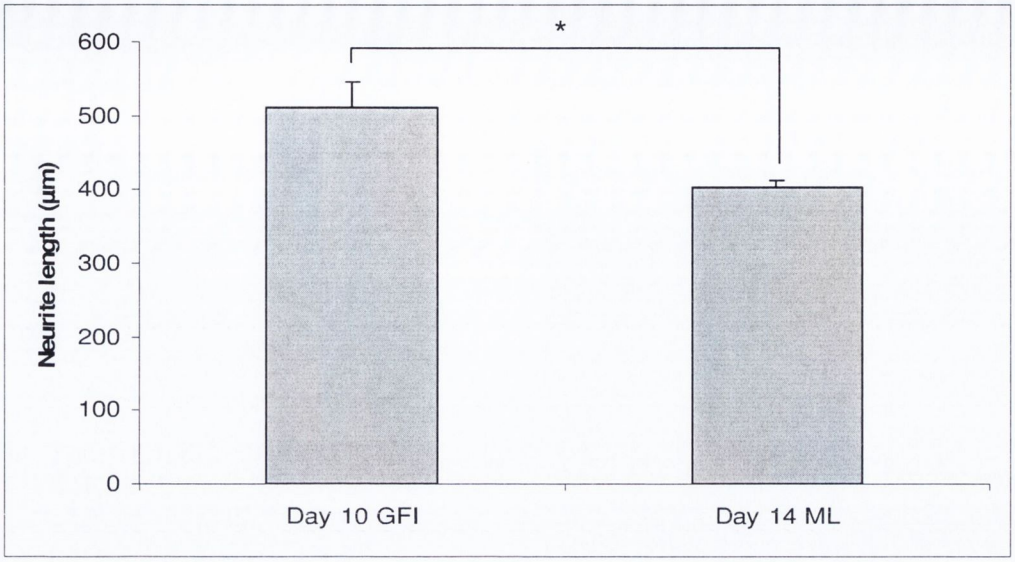

Figure 4.5: Tuj1 positive colonies derived from Sox1-GFP ESCs extend longer neurites following growth factor induced (GFI) neuronal differentiation than following monolayer (ML) neuronal differentiation

Sox1-GFP ESCs were fixed and stained for Tuj1 expression on day 10 of terminal differentiation of the GFI differentiation procedure (Day 10 GFI) and day 14 of the ML differentiation procedure (Day 14 ML). Five Tuj1 positive colonies were randomly selected per well and the length of 10 randomly selected neurites per colony was measured using the NeuronJ application of ImageJ. Data shown represent the mean neurite length + SEM of experiments performed in triplicates on three independent cell populations. *$p<0.05$; Student's two-tailed t-test.

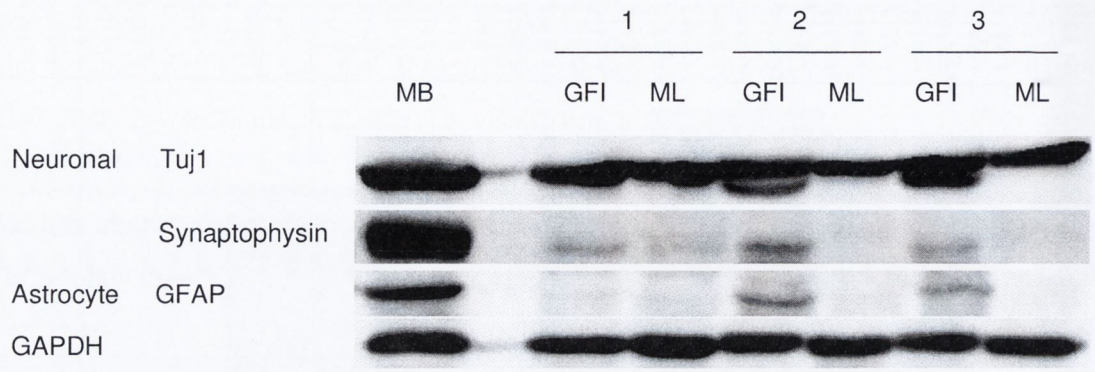

Figure 4.6: Cell populations consistently express the neuronal protein Tuj1 but expression of pre-synaptic protein synaptophysin and astrocytic protein GFAP is variable after neuronal differentiation of Sox1-GFP ESCs by growth factor induced (GFI) and monolayer (ML) protocols

Protein was extracted from Sox1-GFP ESCs on day 10 of terminal differentiation of the GFI differentiation protocol (GFI) and day 14 of the ML differentiation protocol (ML) and 20 µg (GFAP, Tuj1) or 30 µg (synaptophysin) was run on 10% SDS-PAGE gels. Mouse brain lysate (MB) was run as positive control to identify the presence of neuronal proteins. Membranes were probed with antibodies as indicated in the figure. GAPDH was analysed to verify equal loading and a representative blot is shown. GFI indicates growth factor induced neuronal differentiation; ML, monolayer neuronal differentiation; 1-3, three independent differentiation procedures; GFAP, glial fibrillary acidic protein, 50 kDa; GAPDH, glyceraldehyde-3-phosphate dehydrogenase, 36 kDa; synaptophysin, 38 kDa; Tuj1, 50 kDa.

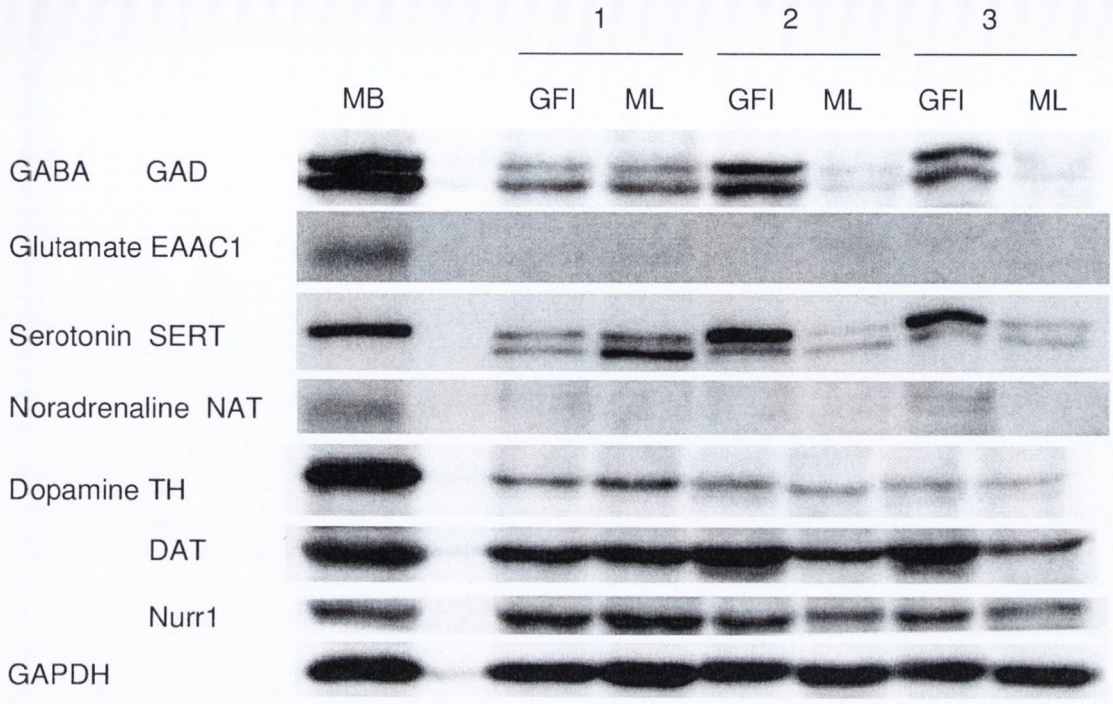

Figure 4.7: Sox1-GFP ESCs express dopaminergic, GABAergic and serotonergic neuronal markers after neuronal differentiation by growth factor induced (GFI) and monolayer (ML) protocols

Protein was extracted from Sox1-GFP ESCs on day 10 of terminal differentiation of the GFI differentiation protocol (GFI) and day 14 of the ML differentiation protocol (ML), as indicated, and 20 µg or 30 µg (Nurr1) was run on 10% SDS-PAGE gels. Mouse brain lysate (MB) was run as positive control to identify the presence of neuronal proteins. Membranes were probed with antibodies against each neuronal subtype as indicated. GAPDH was analysed to verify equal loading and a representative blot is shown. 1-3 indicates three independent differentiation procedures; TH, tyrosine hydroxylase, ~66 kDa; DAT, dopamine transporter, ~55 kDa; GAD, glutamic acid decarboxylase, 65 and 67 kDa; NAT, noradrenergic transporter, ~80 kDa; GAPDH, glyceraldehyde-3-phosphate dehydrogenase, 36 kDa; EAAC1, excitatory amino acid carrier 1, ~69 kDa; SERT, serotonin transporter, ~100 kDa; Nurr1, 66 kDa.

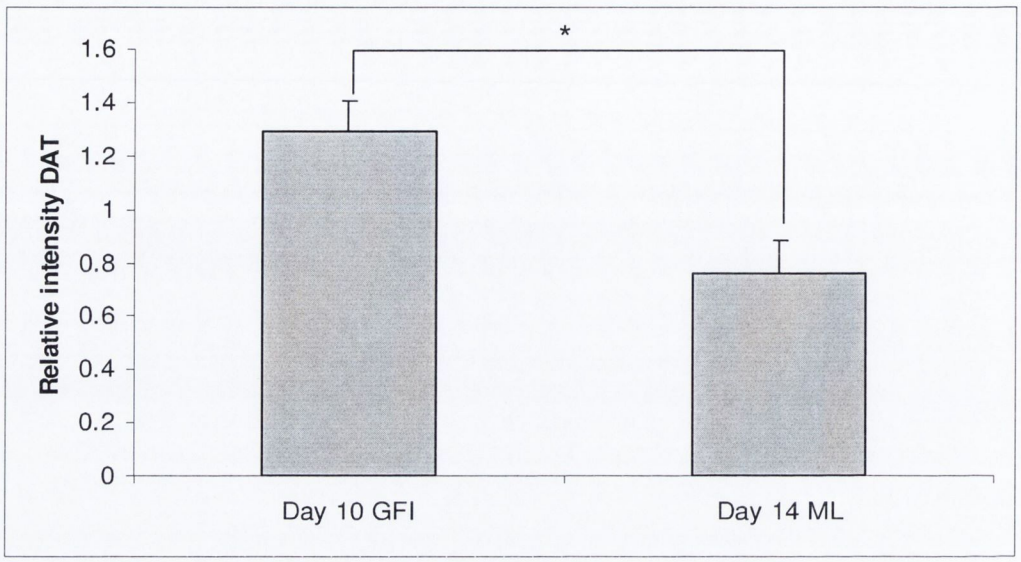

Figure 4.8: Levels of DAT protein in Sox1-GFP ESC derived neurons are higher following growth factor induced (GFI) neuronal differentiation than following monolayer (ML) neuronal differentiation

The DAT and GAPDH blots from Fig. 4.7 were processed in ImageJ to calculate the amount of DAT protein in each sample on day 10 of terminal differentiation of the GFI differentiation protocol (Day 10 GFI) and day 14 of the ML differentiation protocol (Day 14 ML) relative to the amount of GAPDH protein, and are expressed as the relative intensity of DAT. Data shown represent the mean + SEM of experiments performed in triplicates on three independent cell populations. *$p<0.05$; Student's two-tailed t-test. DAT indicates dopamine transporter.

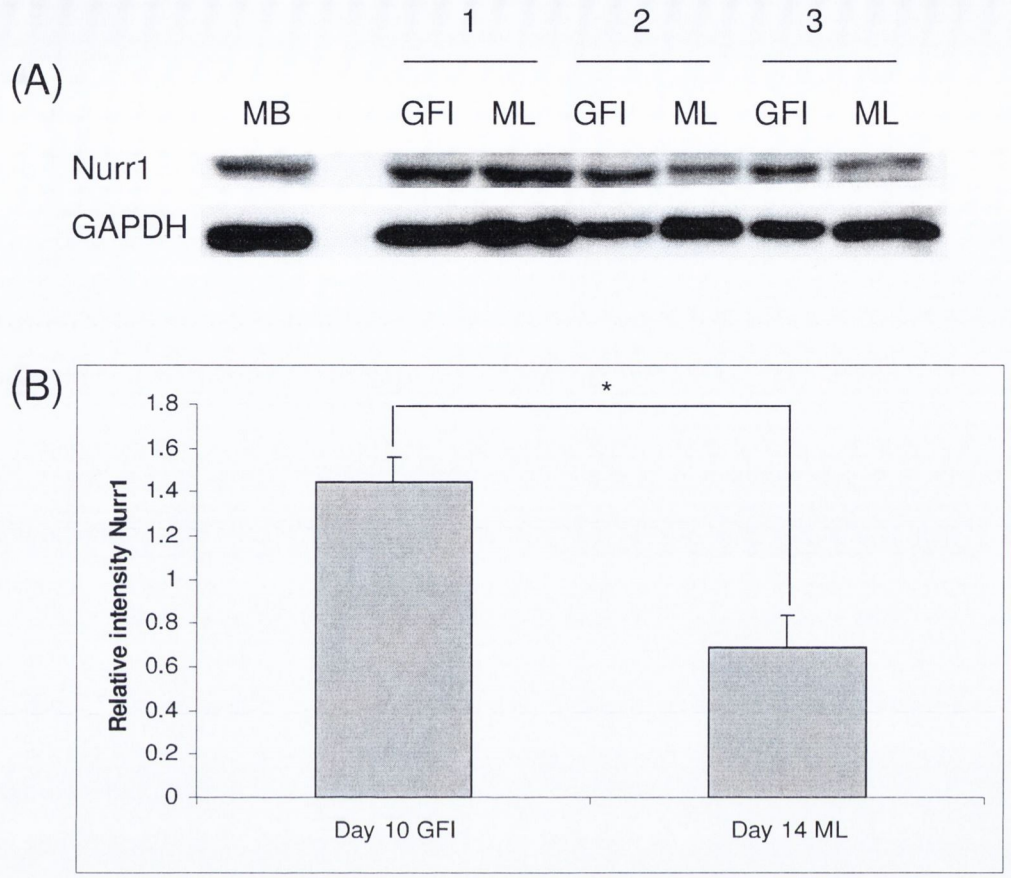

Figure 4.9: Levels of Nurr1 protein in Sox1-GFP ESC derived neurons are higher following growth factor induced (GFI) neuronal differentiation than following monolayer (ML) neuronal differentiation

The Nurr1 blot from Fig. 4.7 and its corresponding GAPDH blot (A) were processed in ImageJ to calculate the amount of Nurr1 protein in each sample on day 10 of terminal differentiation of the GFI differentiation protocol (Day 10 GFI) and day 14 of the ML differentiation protocol (Day 14 ML) relative to the amount of GAPDH protein, and are expressed as the relative intensity of Nurr1 (B). Data shown represent the mean + SEM of experiments performed in triplicates on three independent cell populations. *$p<0.05$; Student's two-tailed t-test. MB indicates mouse brain lysate; 1-3, three independent differentiation procedures; GAPDH, glyceraldehyde-3-phosphate dehydrogenase, 36 kDa; Nurr1, ~66 kDa.

The level of TH protein was relatively constant across cultures but was quite low and no statistically significant difference was detected between the different protocols (Figs 4.7, 4.10). Furthermore, TH+ cells were detected by immunofluorescence following neuronal induction by both protocols, with cells also expressing the neuronal protein Tuj1 and having a distinctive neuronal morphology (Figs 4.11, 4.12).

4.3.2 Comparison of neuronal populations derived from Sox1-GFP ESCs on day 10 and day 16 of the terminal differentiation stage of the growth factor induced differentiation procedure

As Sox1-GFP ESCs differentiated effectively to neurons using the GFI method, including expressing DA markers, it was of interest to assess if increased terminal differentiation (stage 4) using this procedure resulted in a more mature neuronal phenotype. Tuj1 positive colonies were detected at day 16 of terminal differentiation and appeared morphologically similar to those at day 10 of terminal differentiation (Fig. 4.13). However, Tuj1 staining of neurites was not as prominent at later time points, with colonies occasionally detected that did not have processes (Fig. 4.13). This was rarely observed at day 10. In addition, while no difference was detected in the number of Tuj1 positive colonies between time points (Day 10, 23.16 $\pm$ 1.42 colonies; Day 16, 21.83 $\pm$ 1.01 colonies; Fig. 4.14), increased differentiation time resulted in the diameter of colonies being significantly larger (Day 10, 158.98 $\pm$ 9.15 μm; Day 16, 250.75 $\pm$ 8.88 μm; $p<0.01$; Fig 4.15).

Western blot analysis of cellular proteins revealed the presence of neuronal markers Tuj1, NeuN and synaptophysin, and the astrocytic marker GFAP 10 and 16 days after the initiation of terminal differentiation (Fig. 4.16). Variation between three repeats at the two time points of the differentiation procedures did not appear high. Semi-quantitative densitometry revealed a significant decrease in Tuj1 protein levels with increased terminal differentiation ($p<0.05$; Fig. 4.17). However, the protein levels of the more mature neuronal marker NeuN at day 16 of terminal differentiation was not significantly different than day 10 (Fig. 4.18). Furthermore, although the level of the pre-synaptic protein synaptophysin was typically low, it appeared to be higher at day 10 of terminal differentiation (Fig. 4.16).

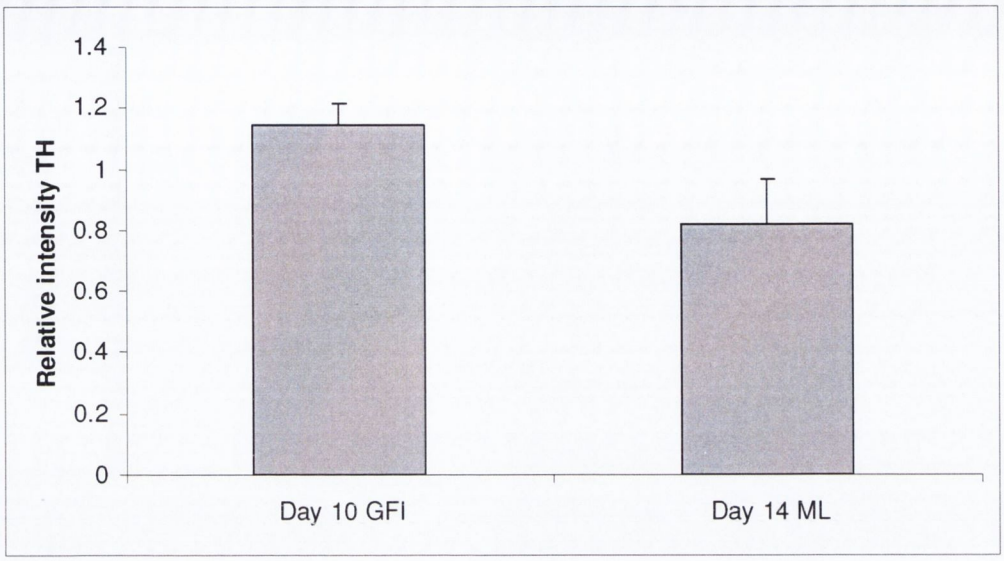

Figure 4.10: Levels of TH protein in Sox1-GFP ESC derived neurons are similar following growth factor induced (GFI) and monolayer (ML) neuronal differentiation procedures

The TH and GAPDH blots from Fig. 4.7 were processed in ImageJ to calculate the amount of TH protein in each sample on day 10 of terminal differentiation of the GFI differentiation protocol (Day 10 GFI) and day 14 of the ML differentiation protocol (Day 14 ML) relative to the amount of GAPDH protein, and are expressed as the relative intensity of TH. Data shown represent the mean + SEM of experiments performed in triplicates on three independent cell populations. TH indicates tyrosine hydroxylase.

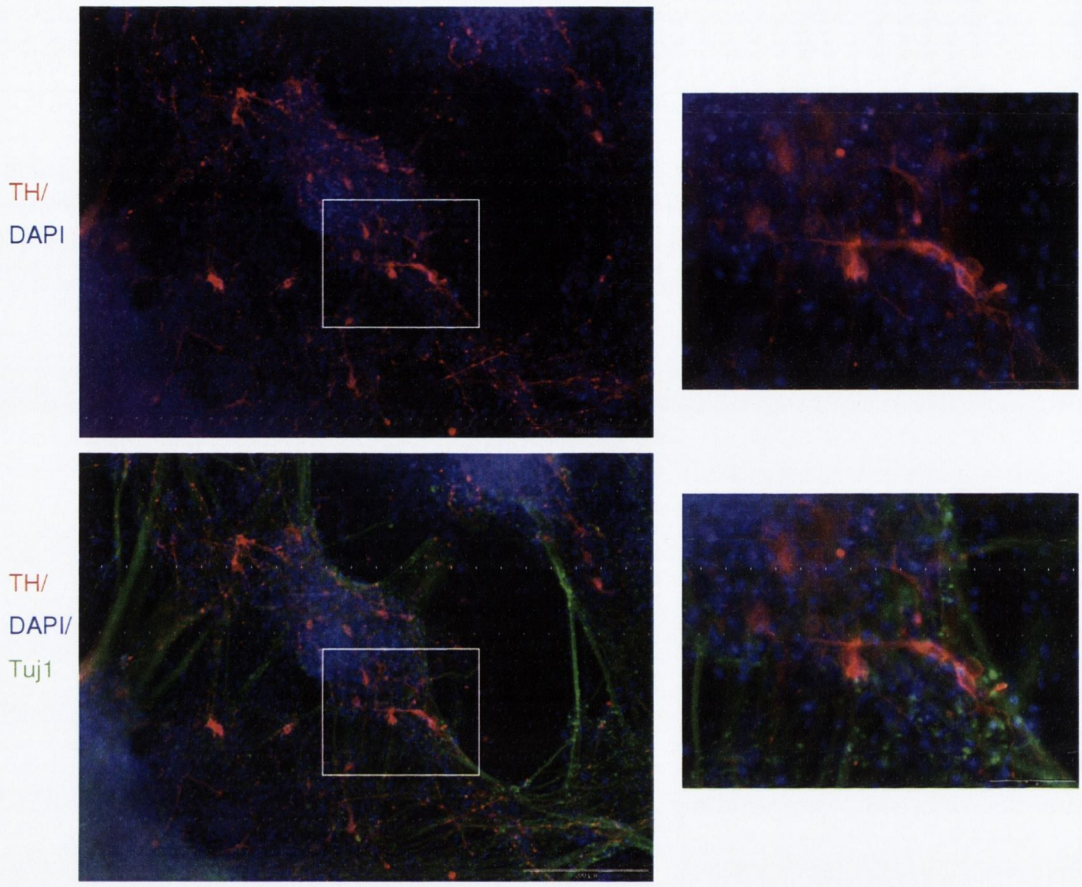

Figure 4.11: Visualisation of tyrosine hydroxylase positive neurons derived from Sox1-GFP ESCs following growth factor induced (GFI) neuronal differentiation

Sox1-GFP ESCs were fixed and stained for Tuj1 (green) and TH (red) expression on day 10 of terminal differentiation of the growth factor induced (GFI) neuronal differentiation procedure, as indicated. Nuclei were counterstained with DAPI (blue). Samples were analysed with an Olympus IX81-long focal length fluorescent microscopy using DAPI, Cy3 and GFP filters and images were captured at 10 x. The boxed area in each image on the left represents the enlarged image on the right hand side obtained at 40 x objective. TH indicates tyrosine hydroxylase. Scale bar: 200 µm (10 x); 50 µm (40 x).

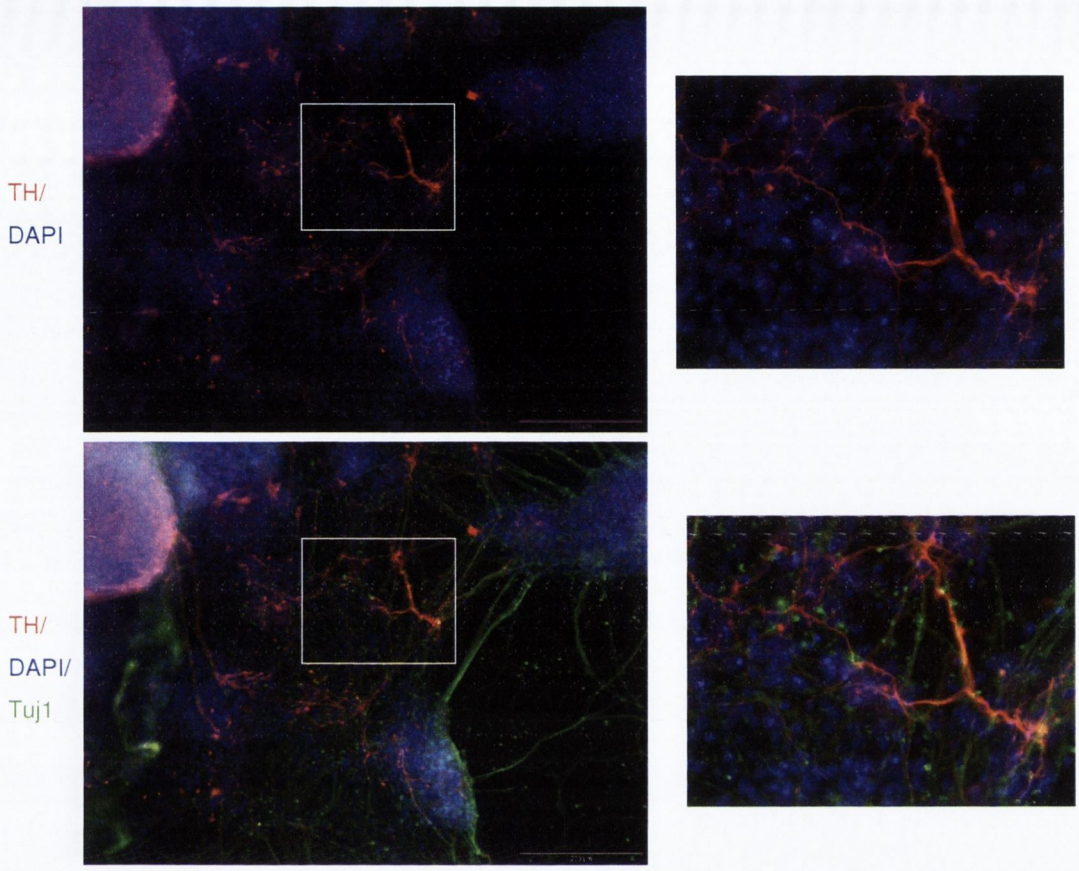

Figure 4.12: Visualisation of tyrosine hydroxylase positive neurons derived from Sox1-GFP ESCs following monolayer (ML) neuronal differentiation

Sox1-GFP ESCs were fixed and stained for Tuj1 (green) and TH (red) expression on day 14 of monolayer (ML) neuronal differentiation, as indicated. Nuclei were counterstained with DAPI (blue). Samples were analysed with an Olympus IX81-long focal length fluorescent microscopy using DAPI, Cy3 and GFP filters and images were captured at 10 x. The boxed area in each image on the left represents the enlarged image on the right hand side obtained at 40 x objective. TH indicates tyrosine hydroxylase. Scale bar: 200 µm (10 x); 50 µm (40 x).

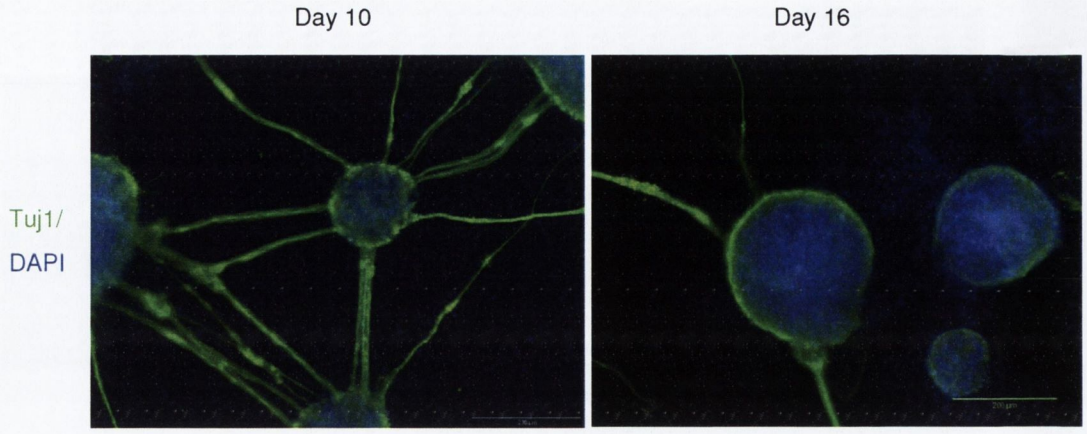

Figure 4.13: Tuj1 positive colonies derived from Sox1-GFP ESCs appear morphologically similar on day 10 and day 16 of the terminal differentiation stage of growth factor induced (GFI) differentiation but neurite extensions are less prominent at day 16

Sox1-GFP ESCs were fixed and stained for Tuj1 expression (green) on day 10 and day 16 of the terminal differentiation stage of GFI neuronal differentiation, as indicated. Nuclei were counterstained with DAPI (blue). Samples were analysed using an Olympus IX81-long focal length fluorescent microscopy using DAPI and GFP filters and images were captured at 10 x objective with an F-View II digital camera. Scale bar: 200 µm.

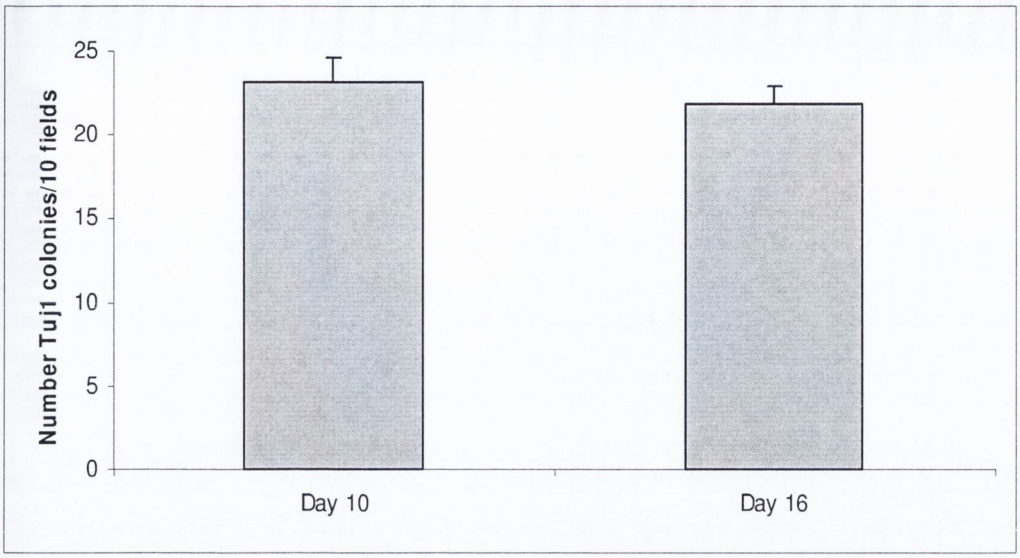

Figure 4.14: Increased terminal differentiation time has no effect on the number of Tuj1 positive colonies derived from Sox1-GFP ESCs following growth factor induced (GFI) differentiation

Sox1-GFP ESCs were fixed and stained for Tuj1 expression on day 10 and day 16 of the terminal differentiation stage of the GFI differentiation procedure, as indicated. Ten randomly selected images were taken per well and the number of Tuj1 positive colonies was counted. Data shown represent the mean + SEM of experiments performed in duplicates on three cell populations.

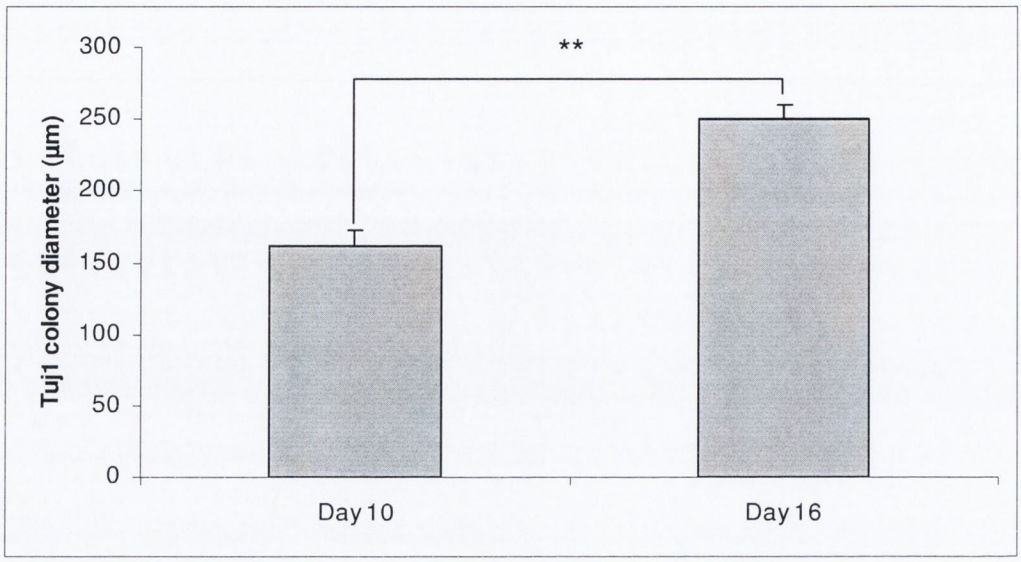

Figure 4.15: The diameter of Tuj1 positive colonies derived from Sox1-GFP ESCs following growth factor induced (GFI) neuronal differentiation are larger at day 16 of terminal differentiation than at day 10

Sox1-GFP ESCs were fixed and stained for Tuj1 expression on day 10 and day 16 of the terminal differentiation stage of the GFI neuronal differentiation procedure, as indicated. Ten randomly selected images were taken of Tuj1 positive colonies per well and the diameters were measured in ImageJ. Data shown represent the mean + SEM of experiments performed in duplicates on three cell populations. **$p<0.01$; Student's two-tailed t-test.

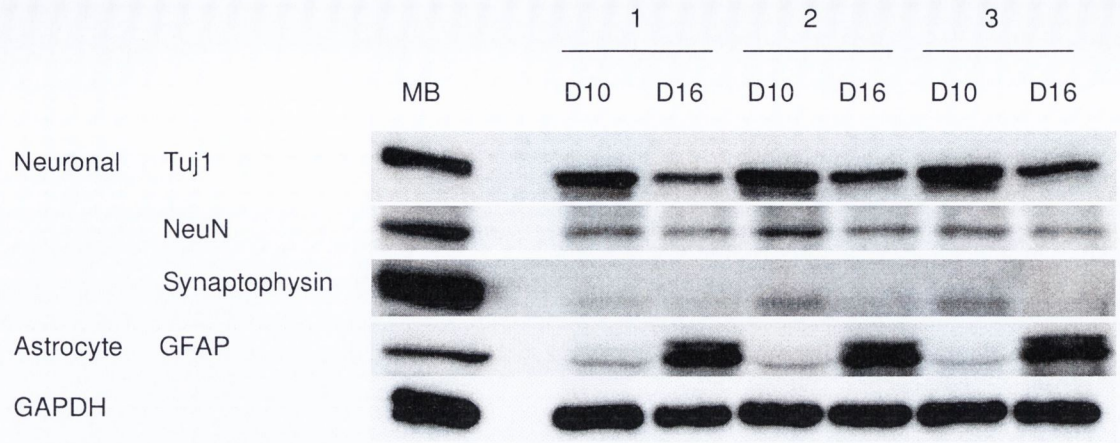

Figure 4.16: Sox1-GFP ESCs express neuronal and astrocytic markers on day 10 and day 16 of the terminal differentiation stage of the growth factor induced (GFI) neuronal differentiation procedure

Protein was extracted from Sox1-GFP ESCs on day 10 (D10) and day 16 (D16) of the terminal differentiation stage of the GFI neuronal differentiation procedure and 20 µg (GFAP, Tuj1) or 30 µg (NeuN, synaptophysin) was run on 10% SDS-PAGE gels. Mouse brain lysate (MB) was run as positive control to identify the presence of neuronal proteins. Membranes were probed with antibodies as indicated. GAPDH was analysed to verify equal loading and a representative blot is shown. GFAP indicates glial fibrillary acidic protein, 50 kDa; GAPDH, glyceraldehyde-3-phosphate dehydrogenase, 36 kDa; NeuN, neuronal nuclei, ~46 kDa; synaptophysin, 38 kDa; Tuj1, 50 kDa; 1-3, three independent differentiation procedures.

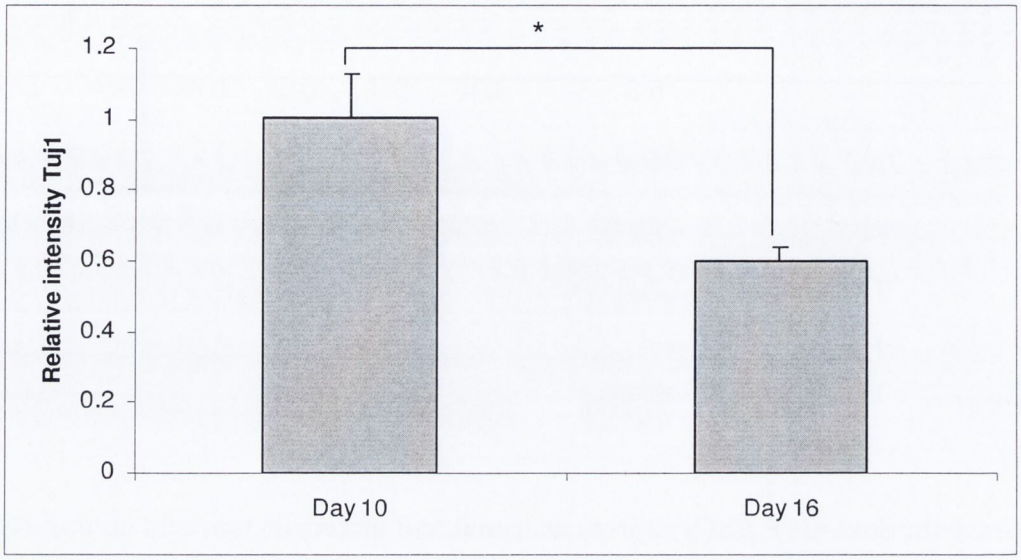

Figure 4.17: Levels of Tuj1 protein in Sox1-GFP ESC derived neurons are higher on day 10 than day 16 of the terminal differentiation stage of the growth factor induced (GFI) neuronal differentiation procedure

The Tuj1 and GAPDH blots from Fig. 4.16 were processed in ImageJ to calculate the amount of Tuj1 protein in each sample at day 10 and day 16 of terminal differentiation relative to the amount of GAPDH protein, and are expressed as the relative intensity of Tuj1. Data shown represent the mean + SEM of experiments performed in triplicates on three independent cell populations. *$p<0.05$; Student's two-tailed t-test.

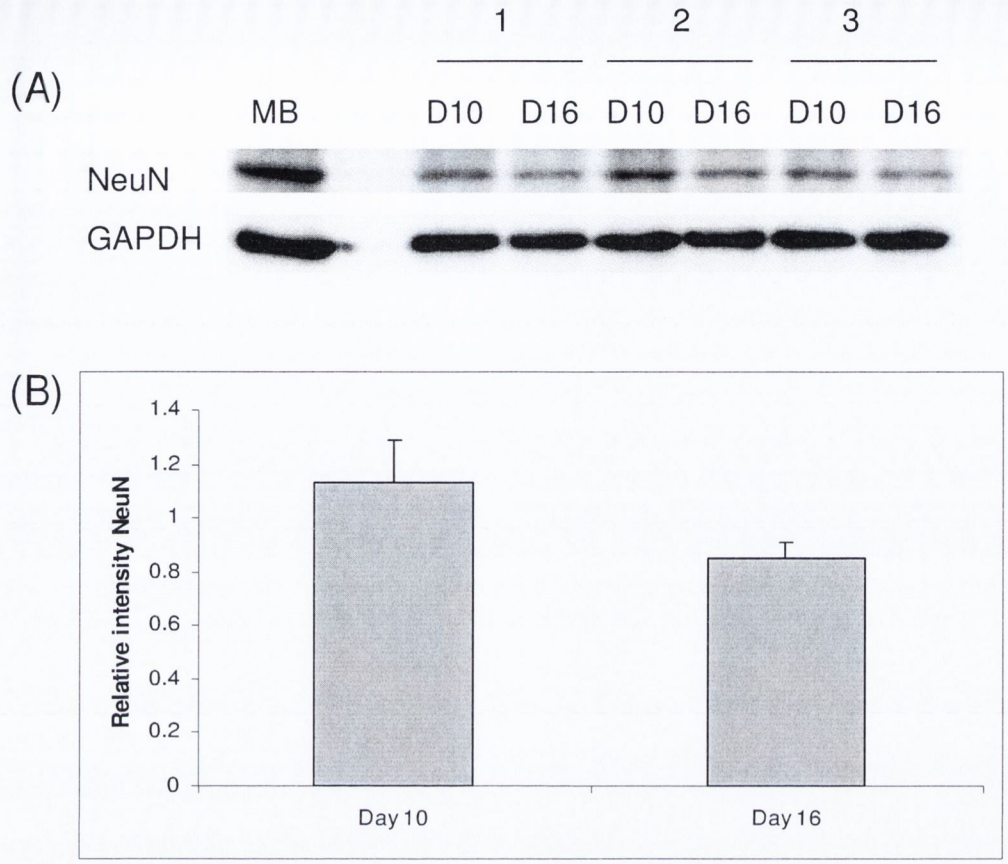

Figure 4.18: Levels of NeuN protein in Sox1-GFP ESC derived neurons are similar on day 10 and day 16 of the terminal differentiation stage of the growth factor induced (GFI) neuronal differentiation procedure

The NeuN blot from Fig. 4.16 and its corresponding GAPDH blot (A) were processed in ImageJ to calculate the amount of NeuN protein in each sample at day 10 (D10) and day 16 (D16) of terminal differentiation relative to the amount of GAPDH protein, and are expressed as the relative intensity of NeuN (B). Data shown represent the mean + SEM of experiments performed in triplicates on three independent cell populations. MB indicates mouse brain lysate; 1-3, three independent differentiation procedures; GAPDH, glyceraldehyde-3-phosphate dehydrogenase, 36 kDa; NeuN, neuronal nuclei, ~46 kDa.

Increased terminal differentiation resulted in a significant increase in the protein level of the astrocytic marker GFAP ($p<0.001$; Fig. 4.19). This finding was mirrored by cellular staining for GFAP expression, with abundant astrocytes present at day 16 but only sparse staining at day 10 (Fig. 4.20).

Markers for the same neuronal subtypes were detected at day 10 and 16 of terminal differentiation, namely for the GABAergic (GAD), serotonergic (SERT) and dopaminergic (DAT, Nurr1, TH) systems (Fig. 4.21). Markers of the noradrenergic (NAT) and glutamatergic (EAAC1) systems were not present (Fig. 4.21). Protein levels of the dopaminergic markers DAT and Nurr1 were significantly reduced at day 16 of terminal differentiation when compared to the levels at day 10 ($p<0.01$ for both; Figs 4.22, 4.23). TH protein expression was variable across independent differentiation procedures at both time points and no difference was detected in protein levels at day 10 and day 16 by semi-quantitative densitometry (Figs 4.21, 4.24). Protein levels of both isoforms of GAD, GAD65 and GAD67, were also significantly diminished at day 16 of terminal differentiation (GAD65, $p<0.05$, GAD67, $p<0.01$, Fig. 4.25). No difference was detected in the level of SERT protein between day 10 and day 16 of terminal differentiation, with expression being relatively constant in all samples analysed (Fig. 4.26). Thus, as increased culture time had a negative effect on the neuronal population, day 10 of terminal differentiation was chosen as the end point for all subsequent experiments.

4.3.3 Comparison of Sox1-GFP expression during growth factor induced and monolayer differentiation procedures

In order to facilitate sorting of Sox1-GFP NPs, GFP fluorescence was analysed in Sox1-GFP ESCs during the process of neuronal differentiation by fluorescent microscopy and FACS. Cells were analysed simultaneously during both ML and GFI differentiation, using cells from ML cultures as a control to assess activation of the *Sox1* gene. No Sox1-GFP fluorescence was detected in NSSs during suspension culture of GFI differentiation (stage 2, Fig. 2.1; Fig. 4.27). Sox1-GFP expression was first visualised at day 4 of the neural proliferation stage of GFI differentiation (stage 3; Fig. 4.27) and at day 4 during ML differentiation (Fig. 4.28).

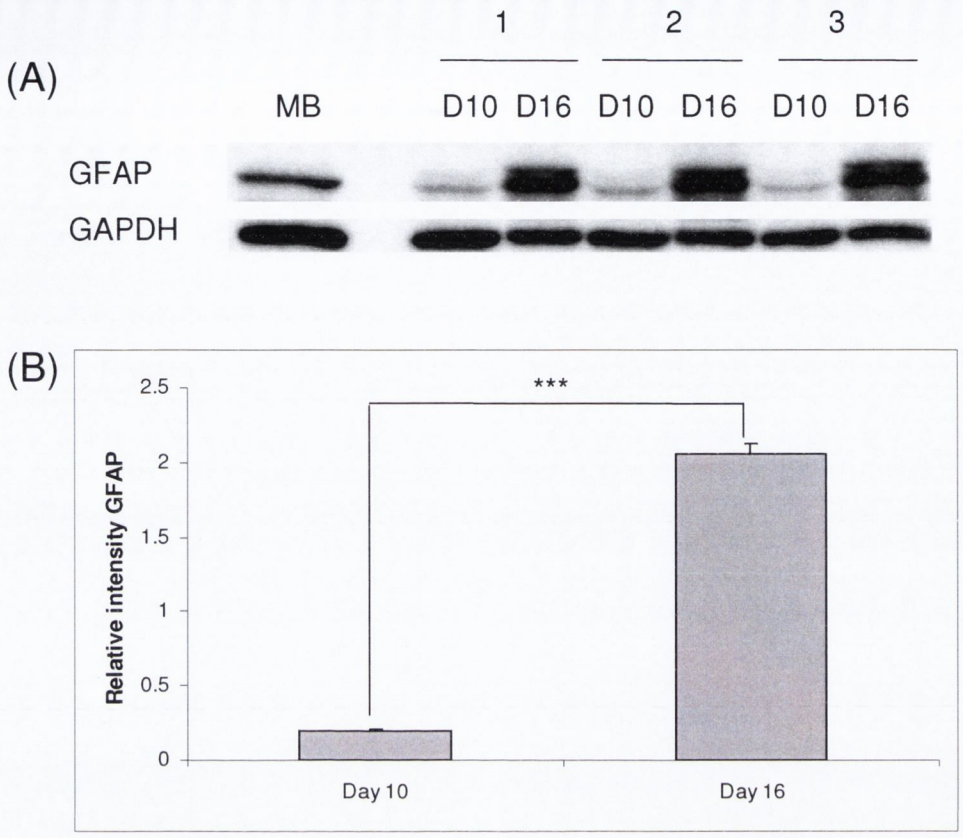

Figure 4.19: Levels of GFAP protein in Sox1-GFP ESC derived cultures are higher on day 16 than day 10 of the terminal differentiation stage of the growth factor induced (GFI) neuronal differentiation procedure

The GFAP blot from Fig. 4.16 and its corresponding GAPDH blot (A) were processed in ImageJ to calculate the amount of GFAP protein in each sample on day 10 (D10) and day 16 (D16) of terminal differentiation relative to the amount of GAPDH protein, and are expressed as the relative intensity of GFAP (B). Data shown represent the mean + SEM of experiments performed in triplicates on three independent cell populations. ***$p<0.001$; Student's two-tailed t-test. MB indicates mouse brain lysate; 1-3, three independent differentiation procedures; GAPDH, glyceraldehyde-3-phosphate dehydrogenase, 36 kDa; GFAP, glial fibrillary acidic protein, 50 kDa.

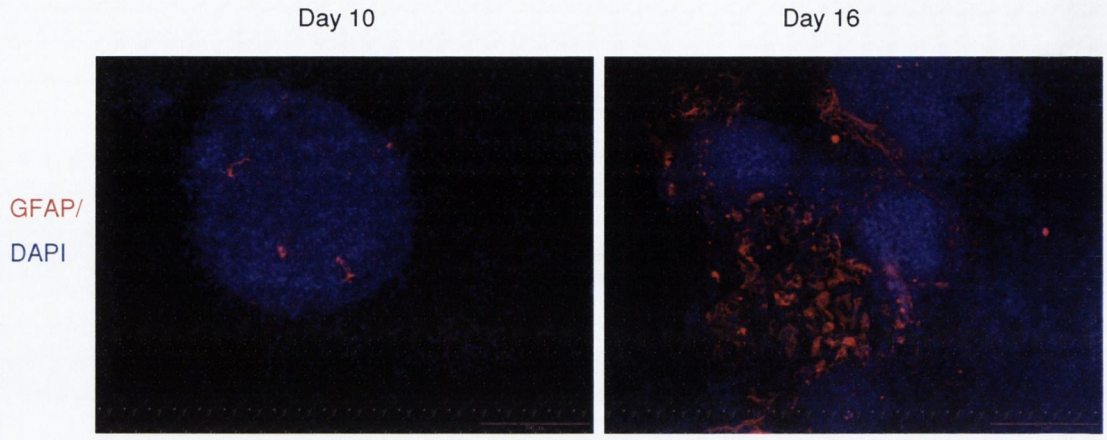

Figure 4.20: Astrocytes derived from Sox1-GFP ESCs are more abundant on day 16 than day 10 of the terminal differentiation stage of the growth factor induced (GFI) differentiation procedure

Sox1-GFP ESCs were fixed and stained for GFAP expression (red) on day 10 or 16 of terminal differentiation of the GFI differentiation procedure, as indicated. Nuclei were counterstained with DAPI (blue). Samples were analysed using an Olympus IX81-long focal length fluorescent microscopy using DAPI and Cy3 filters and images were captured at 10 x objective with an F-View II digital camera. GFAP indicates glial fibrillary acidic protein. Scale bar: 200 μm.

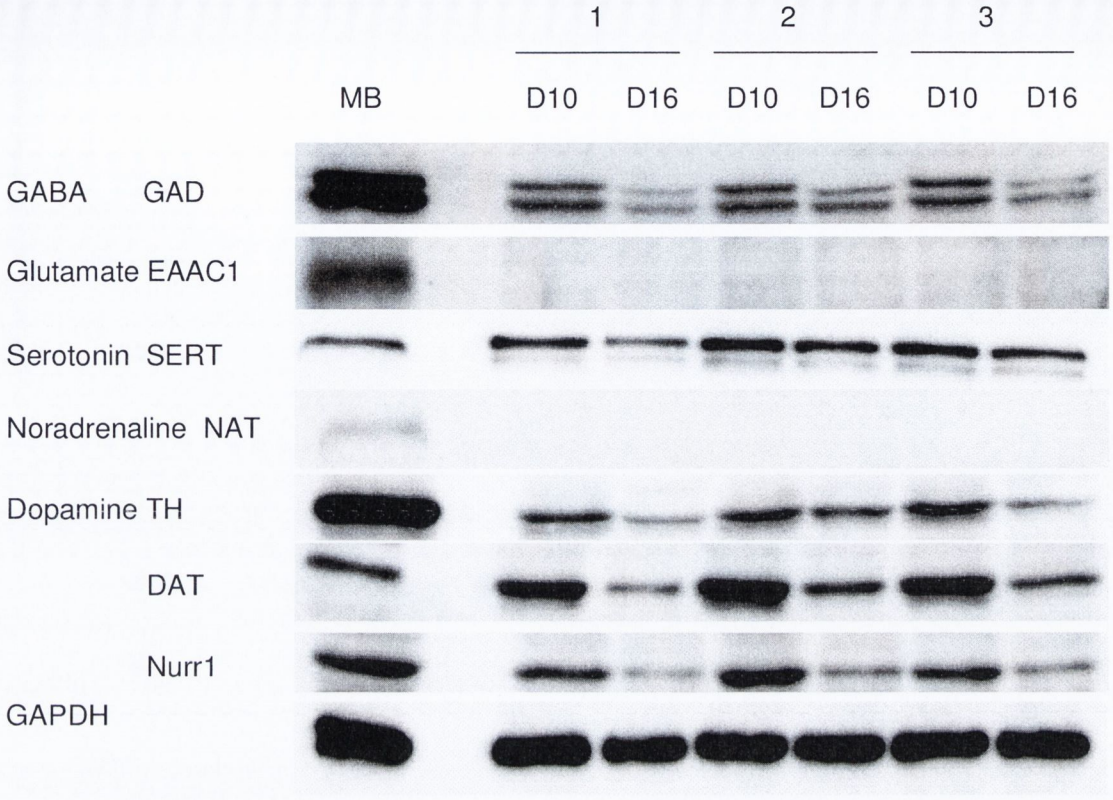

Figure 4.21: Sox1-GFP ESCs derived neurons express dopaminergic, GABAergic and serotonergic neuronal markers on day 10 and day 16 of the terminal differentiation stage of the growth factor induced neuronal differentiation procedure

Protein was extracted from Sox1-GFP ESCs on day 10 (D10) and day 16 (D16) of the terminal differentiation stage of the GFI neuronal differentiation procedure and 20 µg or 30 µg (Nurr1) was run on 10% SDS-PAGE gels. Mouse brain lysate (MB) was run as positive control to identify the presence of neuronal proteins. Membranes were probed with antibodies against each neuronal subtype as indicated. GAPDH was analysed to verify equal loading and a representative blot is shown. TH indicates tyrosine hydroxylase, ~66 kDa; DAT, dopamine transporter, ~55 kDa; GAPDH, glyeraldehyde-3-phosphate dehydrogenase, 36 kDa; GAD, glutamic acid decarboxylase, 65 and 67 kDa; NAT, noradrenergic transporter, ~80 kDa; EAAC1, excitatory amino acid carrier 1, ~69 kDa; SERT, serotonin transporter, ~100 kDa; Nurr1, 66 kDa; 1-3, three independent differentiation procedures.

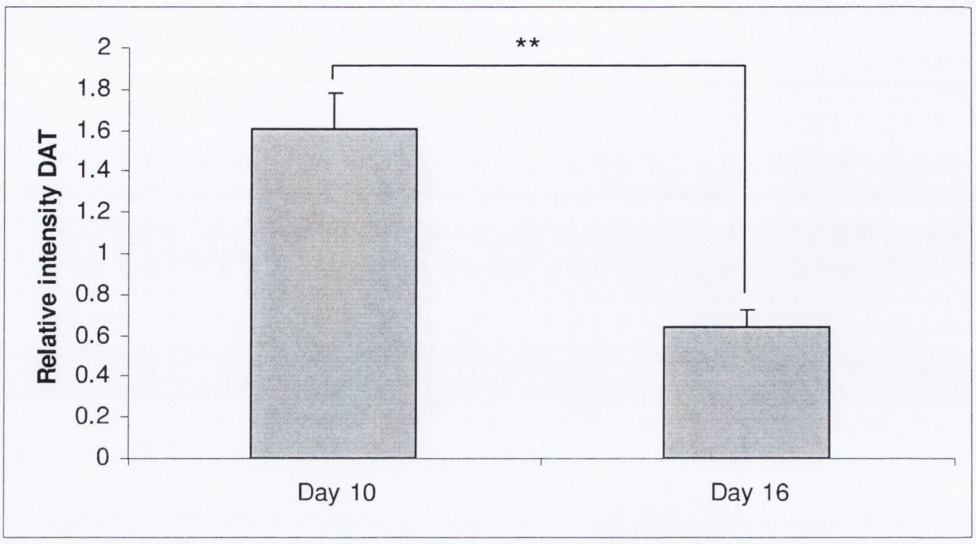

Figure 4.22: Levels of DAT protein in Sox1-GFP ESC derived neurons are higher on day 10 than day 16 of the terminal differentiation stage of the growth factor induced (GFI) neuronal differentiation procedure

The DAT and GAPDH blots from Fig. 4.21 were processed in ImageJ to calculate the amount of DAT protein in each sample on day 10 and day 16 of terminal differentiation relative to the amount of GAPDH protein, and are expressed as the relative intensity of DAT. Data shown represent the mean + SEM of experiments performed in triplicates on three independent cell populations. **$p<0.01$; Student's two-tailed t-test. DAT indicates dopamine transporter.

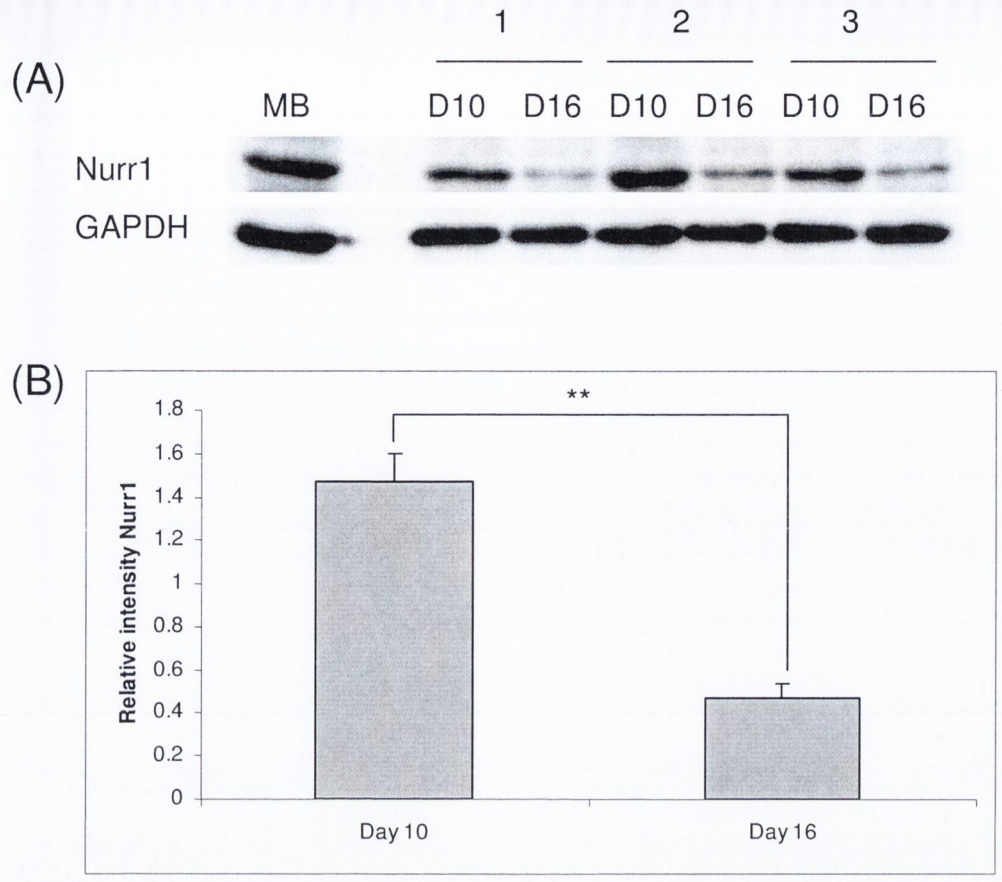

Figure 4.23: Levels of Nurr1 protein in Sox1-GFP ESC derived neurons are higher on day 10 than day 16 of the terminal differentiation stage of the growth factor induced neuronal differentiation procedure

The Nurr1 blot from Fig. 4.21 and its corresponding GAPDH blot (A) were processed in ImageJ to calculate the amount of Nurr1 protein in each sample on day 10 (D10) and day 16 (D16) of terminal differentiation relative to the amount of GAPDH protein, and are expressed as the relative intensity of Nurr1 (B). Data shown represent the mean + SEM of experiments performed in triplicates on three independent cell populations. **$p<0.01$, Student's two-tailed t-test. MB indicates mouse brain lysate; 1-3, three independent differentiation procedures; GAPDH, glyceraldehyde-3-phosphate dehydrogenase, 36 kDa; Nurr1, ~66 kDa.

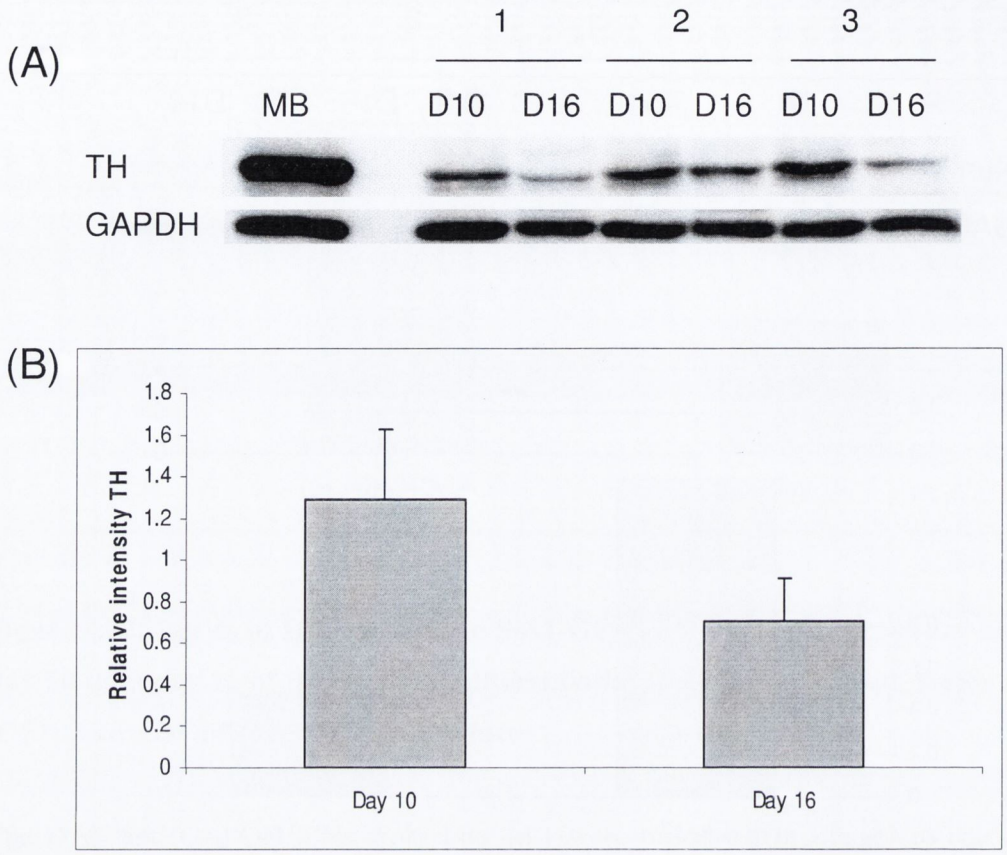

Figure 4.24: No difference exists in the levels of TH protein in Sox1-GFP ESC derived neurons on day 10 and day 16 of the terminal differentiation stage of the growth factor induced (GFI) neuronal differentiation procedure

The TH blot from Fig. 4.21 and its corresponding GAPDH blot (A) were processed in ImageJ to calculate the amount of TH protein in each sample on day 10 (D10) and day 16 (D16) of terminal differentiation relative to the amount of GAPDH protein, and are expressed as the relative intensity of TH (B). Data shown represent the mean + SEM of experiments performed in triplicates on three independent cell populations. MB indicates mouse brain lysate; 1-3, three independent differentiation procedures; GAPDH, glyceraldehyde-3-phosphate dehydrogenase, 36 kDa; TH, tyrosine hydroxylase, ~66 kDa.

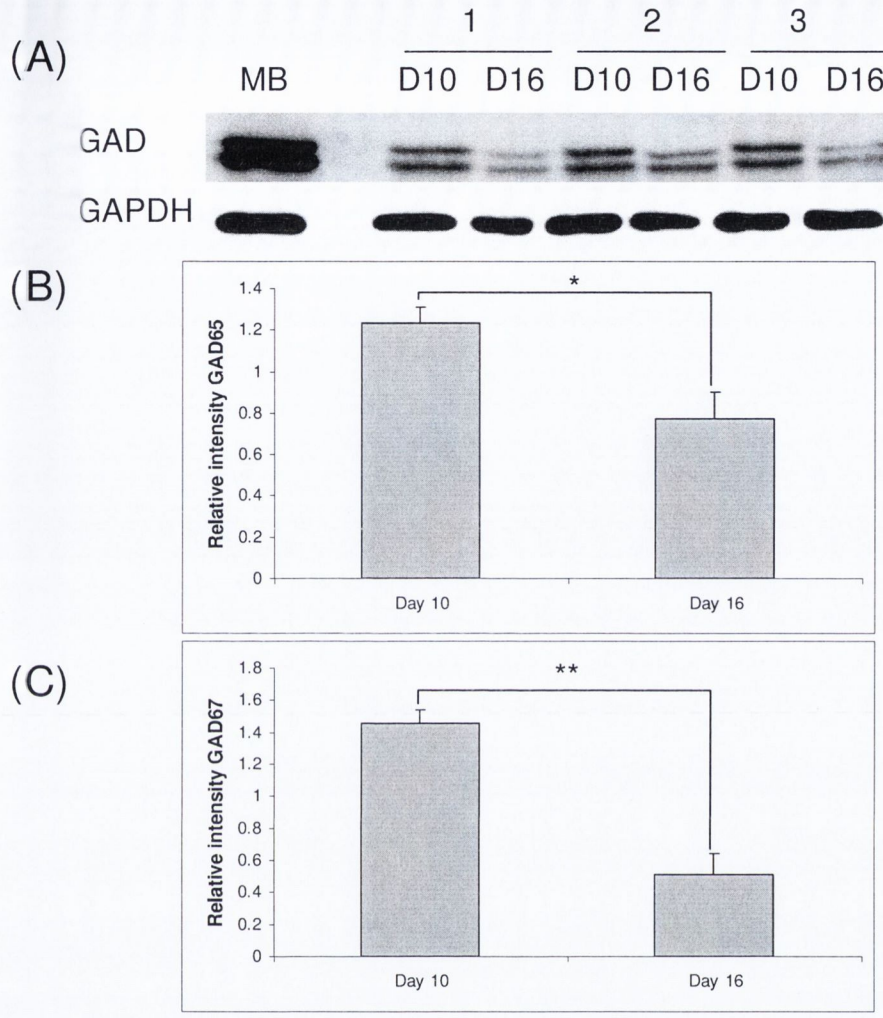

Figure 4.25: Levels of GAD65 and GAD67 in Sox1-GFP ESC derived neurons are higher on day 10 than day 16 of the terminal differentiation stage of the growth factor induced neuronal differentiation procedure

The GAD blot from Fig. 4.21 and its corresponding GAPDH blot (A) were processed in ImageJ to calculate the amount of GAD65 and GAD67 protein in each sample on day 10 (D10) and day 16 (D16) of terminal differentiation relative to the amount of GAPDH protein, and are expressed as the relative intensity of GAD65 (B) and GAD67 (C). Data shown represent the mean + SEM of experiments performed in triplicates on three independent cell populations. *$p<0.05$, **$p<0.01$; Student's two-tailed t-test. MB indicates mouse brain lysate; 1-3, three independent differentiation procedures; GAD65, glutamic acid decarboxylase, 65 kDa; GAD67, glutamic acid decarboxylase, 67 kDa; GAPDH, glyceraldehyde-3-phosphate dehydrogenase, 36 kDa.

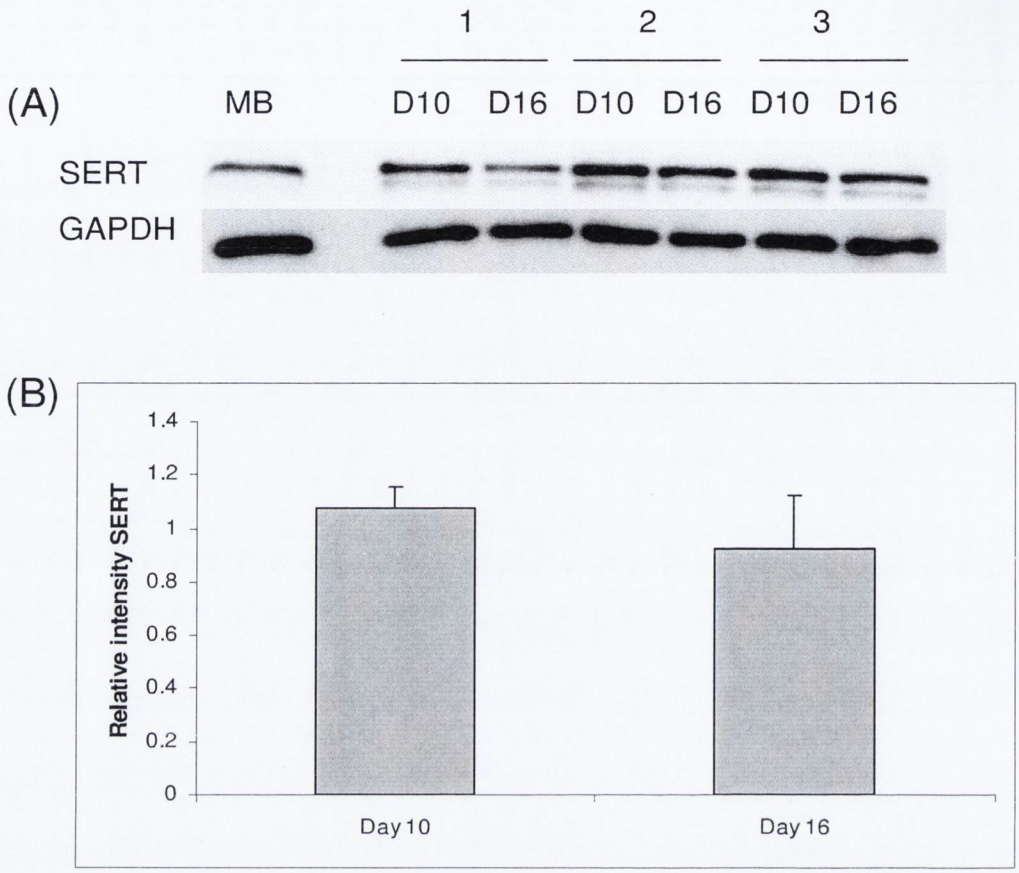

Figure 4.26: No difference exists in the levels of SERT protein in Sox1-GFP ESC derived neurons on day 10 and day 16 of the terminal differentiation stage of the growth factor induced (GFI) neuronal differentiation procedure

The SERT blot from Fig. 4.21 and its corresponding GAPDH blot (A) were processed in ImageJ to calculate the amount of SERT protein in each sample at day 10 (D10) and day 16 (D16) of terminal differentiation relative to the amount of GAPDH protein, and are expressed as the relative intensity of SERT (B). Data shown represent the mean + SEM of experiments performed in triplicates on three independent cell populations. MB indicates mouse brain lysate; 1-3, three independent differentiation procedures; GAPDH, glyceraldehyde-3-phosphate dehydrogenase, 36 kDa; SERT, serotonin transporter, ~100 kDa.

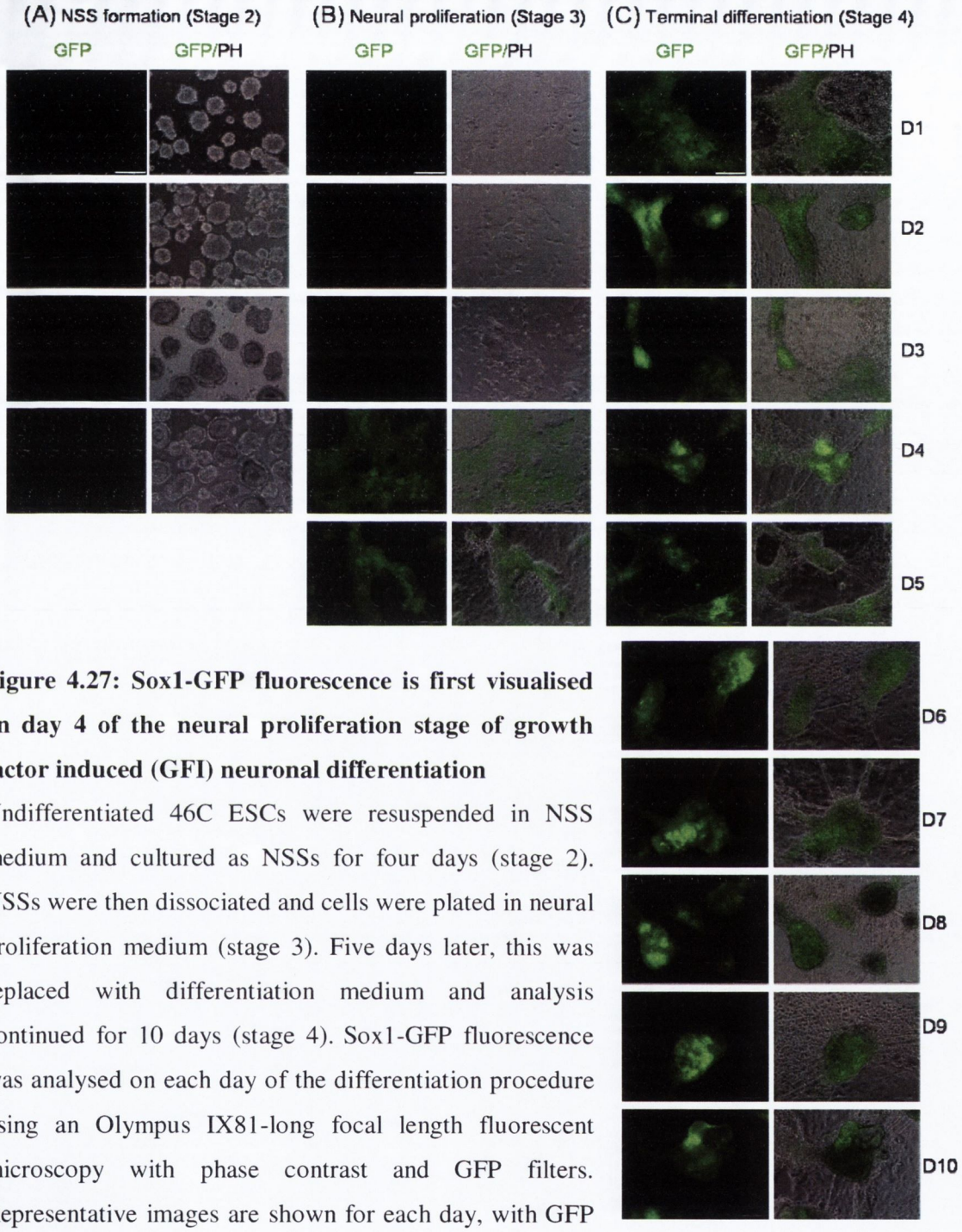

Figure 4.27: Sox1-GFP fluorescence is first visualised on day 4 of the neural proliferation stage of growth factor induced (GFI) neuronal differentiation

Undifferentiated 46C ESCs were resuspended in NSS medium and cultured as NSSs for four days (stage 2). NSSs were then dissociated and cells were plated in neural proliferation medium (stage 3). Five days later, this was replaced with differentiation medium and analysis continued for 10 days (stage 4). Sox1-GFP fluorescence was analysed on each day of the differentiation procedure using an Olympus IX81-long focal length fluorescent microscopy with phase contrast and GFP filters. Representative images are shown for each day, with GFP (green) and phase contrast (PH) as indicated. Images were captured at 10 x objective with an F-View II digital camera. NSS indicates neural stem sphere; GFP, green fluorescent protein; D, day. Scale bar: 100 μm.

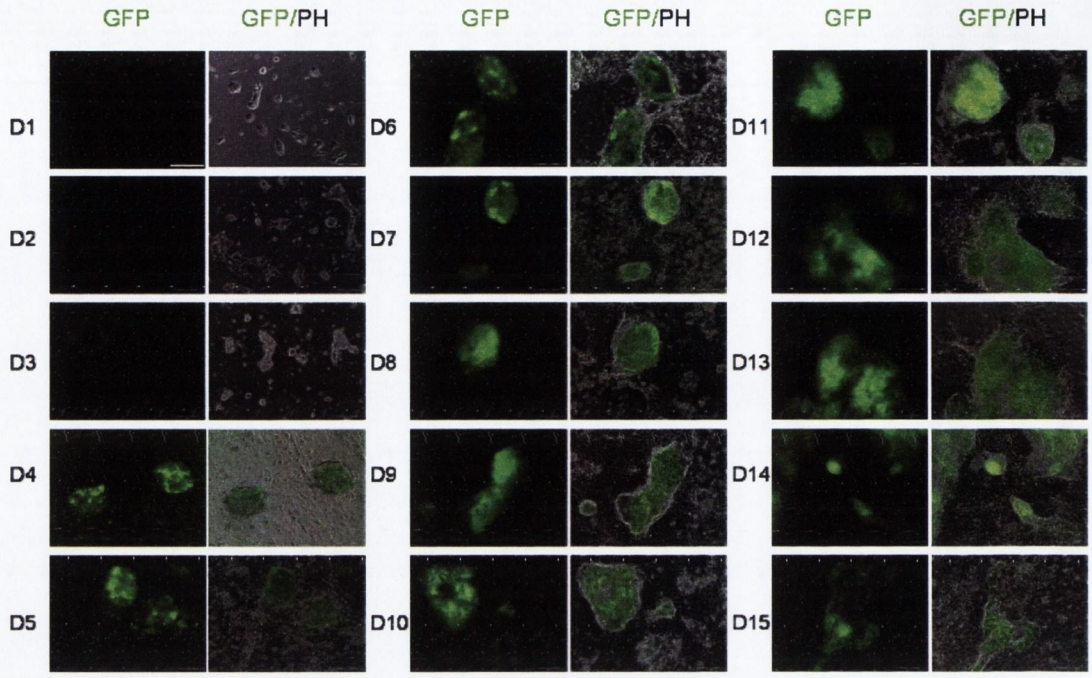

Figure 4.28: Sox1-GFP fluorescence is first visualised on day 4 of monolayer (ML) differentiation and continues throughout the entire differentiation process

Undifferentiated Sox1-GFP ESCs were plated as monolayers on gelatine coated dishes in ESC medium. The following day medium was replaced with N2B27 medium to induce differentiation. Analysis of Sox1-GFP fluorescence began the next day using an Olympus IX81-long focal length fluorescent microscopy with phase contrast and GFP filters and is indicated as day 1. Representative images are shown for each day, with GFP (green) and phase contrast (PH) as indicated. Images were captured at 10 x objective. GFP indicates green fluorescent protein; D, day. Scale bar: 100 µm.

In both instances expression was observed in cellular aggregates, indicating these cells were undergoing neural induction. In addition, Sox1-GFP expression was seen throughout the entire differentiation process in these cell clusters, indicating the continued presence of proliferating NPs (Figs 4.27, 4.28).

Analysis of the percentage of Sox1-GFP+ cells during neuronal differentiation by FACS mirrored the results obtained by fluorescent microscopy (Figs 4.29, 4.30). The percentage of Sox1-GFP+ cells began to increase on day 3 of the neural proliferation stage during GFI differentiation (Fig. 4.29A) and day 3 of ML differentiation (Fig. 4.30A), with 16.43 $\pm$ 1.43% of cells expressing Sox1-GFP in the GFI cultures by day 4 of this stage (Fig. 4.29A) and 25.56 $\pm$ 2.68% Sox1-GFP+ cells observed in ML differentiation by day 4 (Fig. 4.30A). GFP steadily increased in both cultures, with the highest levels observed on day 2 of terminal differentiation for GFI differentiation (42.49 $\pm$ 1.75% Sox1-GFP+ cells; Fig. 4.29A) and day 8 for ML differentiation (49.13 $\pm$ 1.31% Sox1-GFP+ cells; Fig. 4.30A). After these time points the percentage of GFP+ cells decreased as cells differentiated to neurons and glia. Representative flow cytometry profiles from day 2 of terminal differentiation of GFI differentiation and day 7 of ML differentiation are indicated in Figs 4.29B and 4.30B, respectively, including plots of control R1 ESCs at the same stage of differentiation, which were analysed at each time point to set background fluorescence.

4.3.4 Isolation and analysis of Sox1-GFP expressing neural precursors at the neural proliferation stage of growth factor induced neuronal differentiation

All the experiments thus far indicated that Sox1-GFP ESCs could be effectively differentiated to DA neurons using the GFI protocol. In addition, a similar pattern of Sox1-GFP expression was observed under this procedure as with the commonly used ML method. Therefore, NPs were sorted 5 days after plating NSSs (day 5 of neural proliferation, stage 3). While the percentage of Sox1-GFP+ cells did not peak until day 2 of terminal differentiation, longer time in culture typically resulted in the appearance of neurites (Fig. 4.27). Previous studies using mature DA markers such as TH and Pitx3 have indicated that dissociation of cells with neurites can result in high cell death (Yoshizaki et al., 2004; Hedlund et al., 2008).

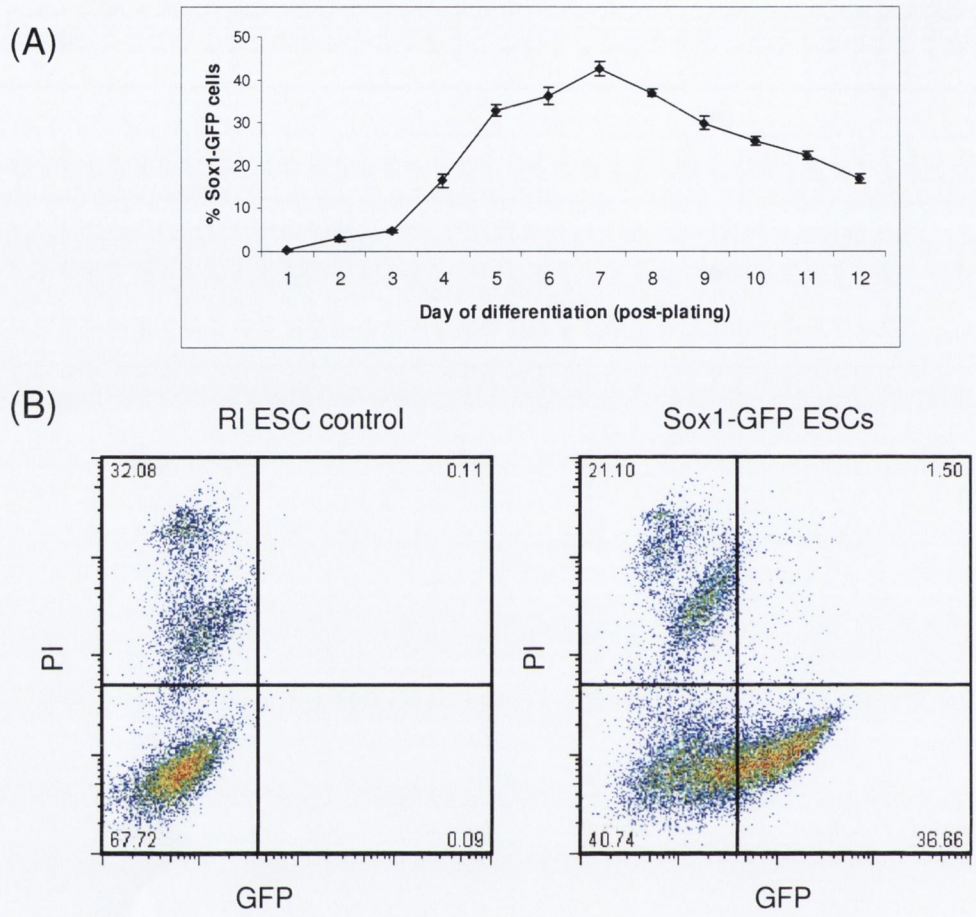

Figure 4.29: Kinetic analysis of Sox1-GFP expression during growth factor induced (GFI) neuronal differentiation

(A) FACS analysis began one day after neural proliferation (stage 3) was initiated (day 1) and continued for the next 12 days, representing 5 days of neural proliferation (stage 3) and 7 days of terminal differentiation (stage 4). Experimental details are provided in section 4.2.1. The percentage of Sox1-GFP fluorescent cells was analysed from three independent experiments using FlowJo software and represent the mean + SEM. (B) Flow cytometry profile from day 2 of terminal differentiation (7 days post-plating), showing GFP fluorescence in viable Sox1-GFP ESCs in the bottom right hand quadrant. Non-GFP expressing R1 ESCs at the same stage of differentiation were used as negative control for background fluorescence, with cells lacking GFP fluorescence observed in left quadrants, the top quadrants indicating non-viable (PI+) cells and the bottom viable cells (PI-). GFP indicates green fluorescent protein; PI, propidium iodide.

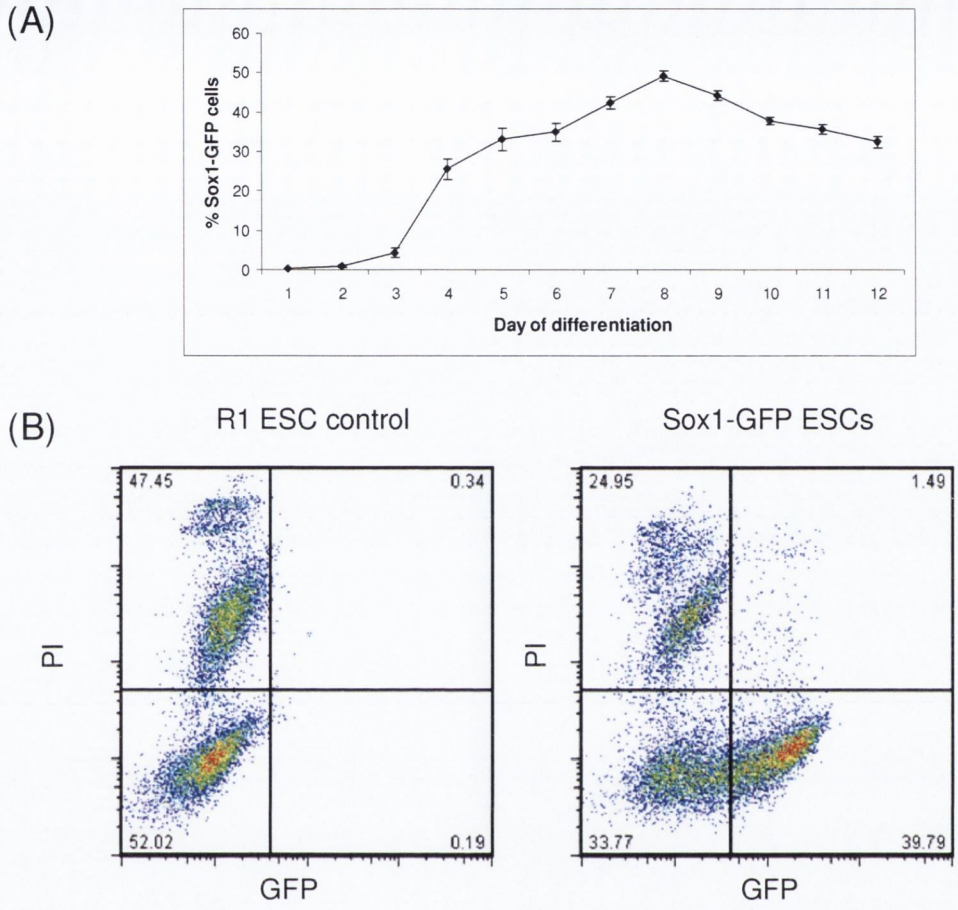

Figure 4.30: Kinetic analysis of Sox1-GFP expression during monolayer (ML) neuronal differentiation

(A) FACS analysis began one day after N2B27 medium was applied to Sox1-GFP ESCs plated in monolayers and is indicated as day 1 and the analysis continued for the next 12 days. Experimental details are provided in section 4.2.1. The percentage of Sox1-GFP fluorescent cells was analysed from three independent experiments using FlowJo software and represent the mean + SEM. (B) Flow cytometry profile from day 7 of ML differentiation, showing GFP fluorescence in viable Sox1-GFP ESCs in the bottom right hand quadrant. Non-GFP expressing R1 ESCs at the same stage of differentiation were used as negative control for background fluorescence, with cells lacking GFP fluorescence observed in left quadrants, the top quadrants indicating non-viable (PI+) cells and the bottom quadrants viable cells (PI-). GFP indicates green fluorescent protein; PI, propidium iodide.

Sox1-GFP+ and Sox1-GFP- were separated by FACS, with representative flow cytometry plots in Fig. 4.31A. Re-analysis of sorted samples confirmed that the FACS procedure resulted in a highly purified Sox1-GFP+ population (Fig. 4.31B).

RT-PCR analysis of mRNA from both populations immediately after sorting verified that the Sox1-GFP+ population had been effectively purified. mRNA encoding neuroectodermal markers Sox1 and nestin were enriched in the Sox1-GFP+ population, while those encoding pluripotent stem cell markers Oct4 and Nanog were enriched in the Sox1-GFP- population (Fig. 4.32A). Fluorescent microscopy analysis of these samples immediately after sorting also indicated that GFP expression was only present in the GFP+ population but not the GFP- population (Fig. 4.32B).

4.3.5 Analysis of Sox1-GFP sorted samples following growth factor induced neuronal differentiation

FACS purified Sox1-GFP+ NPs developed a neuronal morphology following plating of sorted cells and culturing in medium without growth factors to induce terminal differentiation (Fig. 4.33). Single cells were visible during this stage that extended neurites (Fig. 4.33). In contrast, Sox1-GFP- cells cultured in parallel did not exhibit an overt neuronal morphology at any time point examined (Fig 4.33). Analysis of sorted samples at day 10 of terminal differentiation (stage 4) of GFI differentiation with the neuronal marker Tuj1 also revealed striking differences between these two populations (Fig. 4.34). While abundant neurons were detected in the Sox1-GFP+ sample, only sparse staining was apparent in the Sox1-GFP- sample (Fig. 4.34A). This was verified by cell count analysis for Tuj1, with $65 \pm 9.9\%$ of cells staining positive for this marker in the Sox1-GFP+ population while only $1.56 \pm 0.42\%$ of cells stained positive in the Sox1-GFP- population (Fig. 4.34B). These results further established that Sox1-GFP expression could be effectively used to obtain a highly enriched neuronal population after FACS sorting.

Astrocytes were rarely detected in the Sox1-GFP+ cultures at day 10 of terminal differentiation, as indicated by sparse staining with the astrocytic marker GFAP (Fig. 4.35). No co-localisation of GFAP and the neuronal marker Tuj1were observed in these samples.

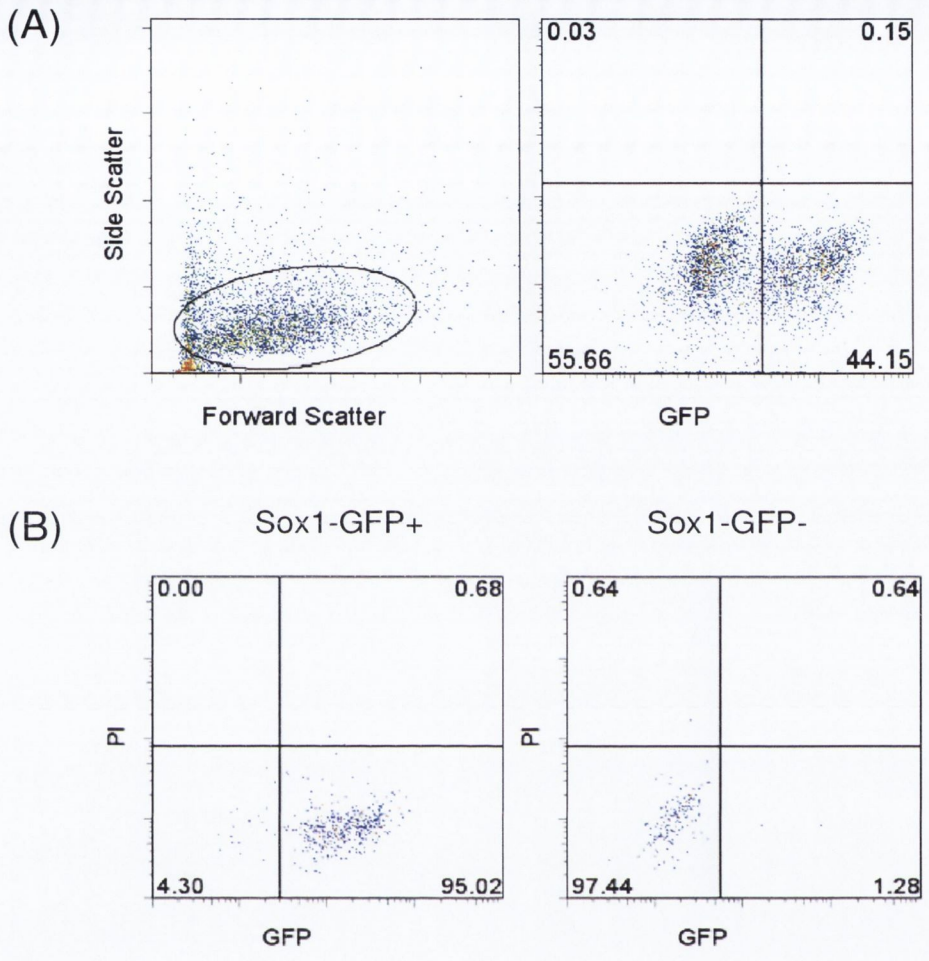

Figure 4.31: Isolation of Sox1-GFP expressing neural precursor by FACS at the neural proliferation stage of growth factor induced (GFI) neuronal differentiation

(A) Sox1-GFP ESCs were differentiated to day 5 of the neural proliferation stage (stage 3) of GFI neuronal differentiation and resuspended in ice-cold 4% FBS/1X PBS. GFP+ and GFP- populations were subsequently purified using a FACS cell sorter, with cells being first gated by forward-side scatter and within this population by GFP expression, as indicated. Non-GFP expressing R1 ESCs at the same stage of differentiation were used as negative control for background fluorescence. (B) GFP+ and GFP- samples were stained with PI and re-analysed after sorting to confirm purity and viability of samples. In the Sox1-GFP+ sample, viable GFP+ cells are present in the bottom right quadrant. GFP indicates green fluorescent protein; PI, propidium iodide.

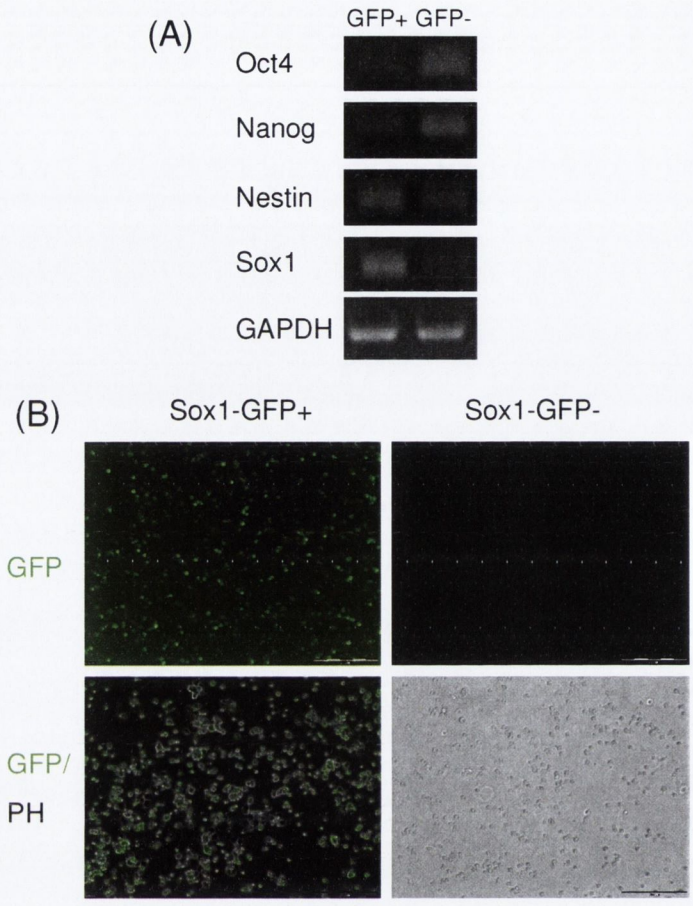

Figure 4.32: Sox1-GFP+ neural precursors can be effectively purified by FACS at the neural proliferation stage of growth factor induced neuronal differentiation

(A) Total RNA was isolated from Sox1-GFP+ (GFP+) and Sox1-GFP- (GFP-) cells immediately after sorting and used to synthesis cDNA. This was subsequently used to identify the neuroectodermal markers Sox1 and nestin and pluripotent stem cell markers Oct4 and Nanog using gene specific primers. The house keeping gene GAPDH was included to verify equality between samples. Samples were then analysed by agarose gel electrophoresis. GAPDH indicates glyceraldehyde-3-phosphate dehydrogenase, 454 bp; Oct4, 312 bp; Nanog: 363 bp; Sox1: 593 bp; Nestin: 327 bp. (B) Sox1-GFP+ and Sox1-GFP- cells were plated immediately after sorting and live cells were analysed for GFP fluorescence (green), as indicated. Images were acquired using an Olympus IX81-long focal length fluorescent microscope at 10 x objective with an F-View II digital camera. GFP indicates green fluorescent protein; PH, phase contrast. Scale bar: 200 µm.

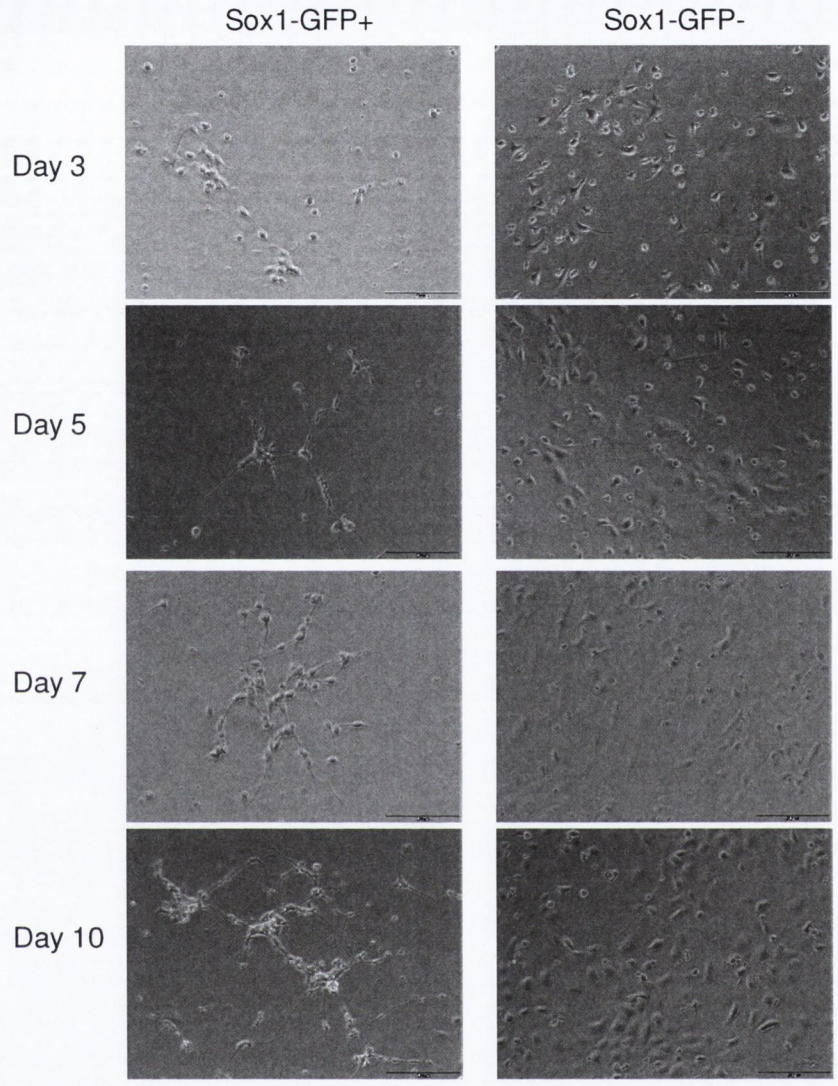

Figure 4.33: FACS purified Sox1-GFP+ neural precursors develop a neuronal morphology during terminal differentiation

FACS purified Sox1-GFP+ and Sox1-GFP- samples were plated immediately after sorting in growth factor free medium to induce terminal differentiation. Sox1-GFP+ neural precursors developed a neuronal morphology during this stage, with neurite extensions clearly visible. In contrast, Sox1-GFP- cells did not exhibit a typical neuronal morphology at any time point. Phase contrast images were obtained using an Olympus IX81-long focal length fluorescent microscope at 10 x objective with an F-View II digital camera. Scale bar: 200 μm.

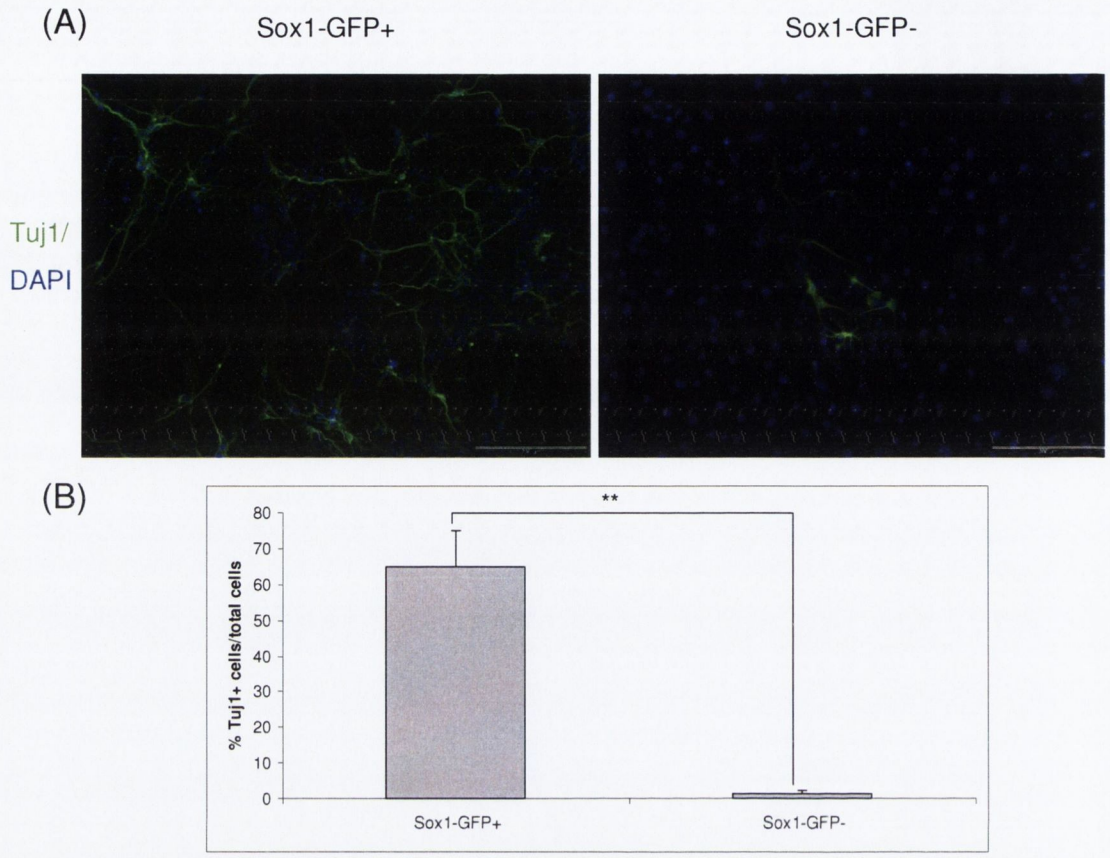

Figure 4.34: FACS purified Sox1-GFP neural precursors generate a highly enriched neuronal population following terminal differentiation of growth factor induced (GFI) neuronal differentiation

(A) Sox1-GFP+ and Sox1-GFP- cells were fixed on day 10 of terminal differentiation and stained for expression of the neuronal marker Tuj1 (green), as indicated. Nuclei were counterstained with DAPI (blue). Samples were analysed with an Olympus IX81-long focal length fluorescent microscopy using DAPI and GFP filters and images were captured at 10 x objective with an F-View II digital camera. Scale bar: 200 μm. (B) The number of Tuj1+ and DAPI+ cells from Sox1-GFP+ and Sox1-GFP- cells were counted in ten random fields per sample and the proportion of neurons was calculated by dividing the number of Tuj1+ cells by DAPI+ cells. Data shown represent the mean + SEM of experiments performed in triplicates on three cell populations. **$p<0.01$; Student's two-tailed t-test.

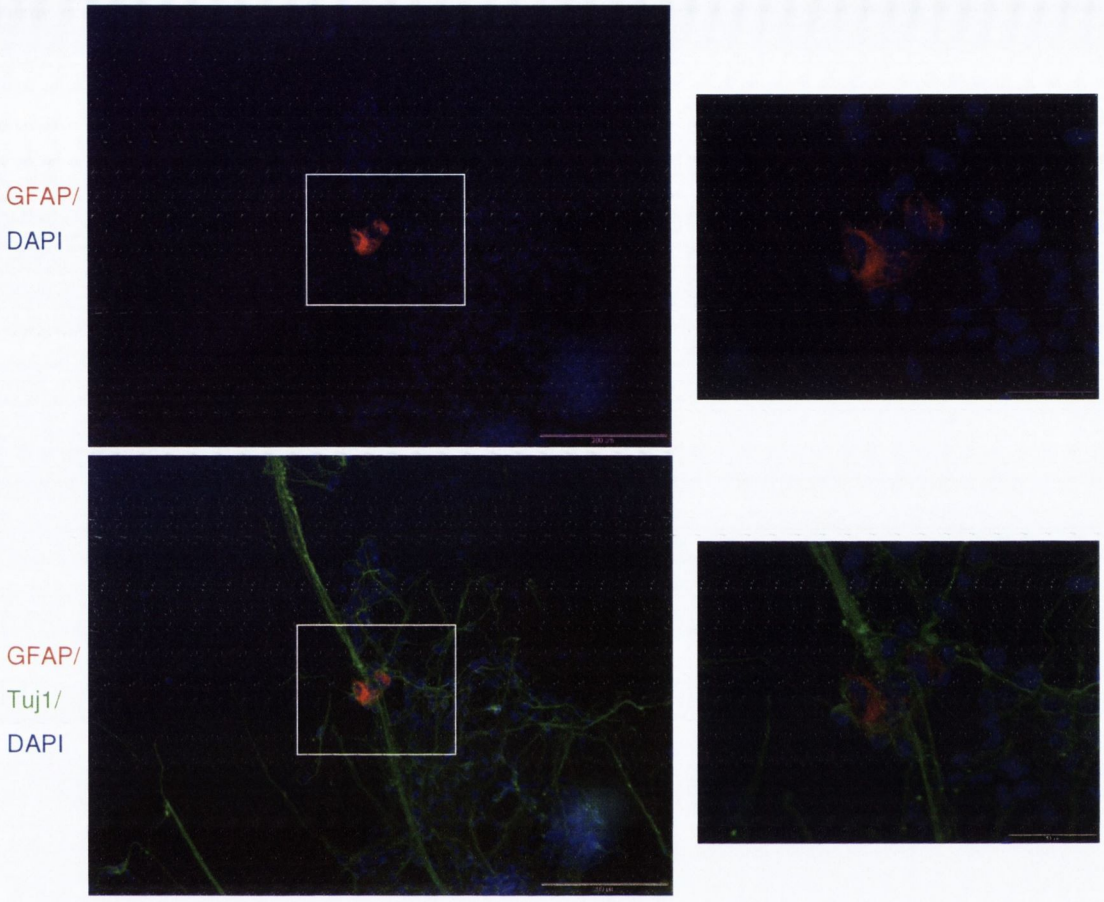

Figure 4.35: FACS purified Sox1-GFP+ neuronal precursors generate few astrocytes following growth factor induced neuronal differentiation

Sox1-GFP+ cells were fixed at day 10 of terminal differentiation of the growth factor induced differentiation procedure and stained for expression of astrocytic marker GFAP (red) and neuronal marker Tuj1 (green), as indicated. Nuclei were counterstained with DAPI (blue). Samples were analysed with an Olympus IX81-long focal length fluorescent microscopy using DAPI, Cy3 and GFP filters and images were captured at 10 x and 40 x objective with an F-View II digital camera. The boxed area in each image on the left represents the enlarged image on the right hand side obtained at 40 x objective. GFAP indicates glial fibrillary acidic protein. Scale bar: 200 µm (10 x); 50 µm (40 x).

Furthermore, purified Sox1-GFP+ cells were found to express the DA marker TH at day 10 of terminal differentiation, with TH+ cells having a typical neuronal morphology and co-expressing Tuj1 (Fig. 4.36). Both TH and Tuj1 staining was observed in the soma and neurites. However, by gross morphological analysis TH+ neurons were more abundant in unsorted cultures than Sox1-GFP+ sorted samples following terminal neuronal differentiation (Fig. 4.37). This result was mirrored by Western blotting data, in which TH protein was absent in Sox1-GFP+ sorted neuronal cultures from 3 independent sorting procedures but present in unsorted samples at day 10 of terminal differentiation (Fig. 4.38). It should be noted that while TH protein was only detected in two of three unsorted samples, it appears that GAPDH was not equivalent in all unsorted samples. In particular, the level of GAPDH was seems lower in sample 1 in which TH protein was not detected. Thus it is possible that as TH protein expression is low in sample 2 and sample 3, analysis of more protein from sample 1 may detect TH protein. As would be expected, Tuj1 protein was readily detected in all FACS purified Sox1-GFP+ samples and unsorted Sox1-GFP samples at day 10 of terminal differentiation (Fig. 4.38).

In contrast to the absence of TH protein in Sox1-GFP+ sorted samples following 10 days of terminal differentiation, DAT protein was detected from cultures derived from 3 independent differentiation procedures (Fig. 4.39A). Furthermore, no difference was observed in the level of DAT protein between unsorted samples and Sox1-GFP+ sorted samples at this time point (Fig. 4.39B).

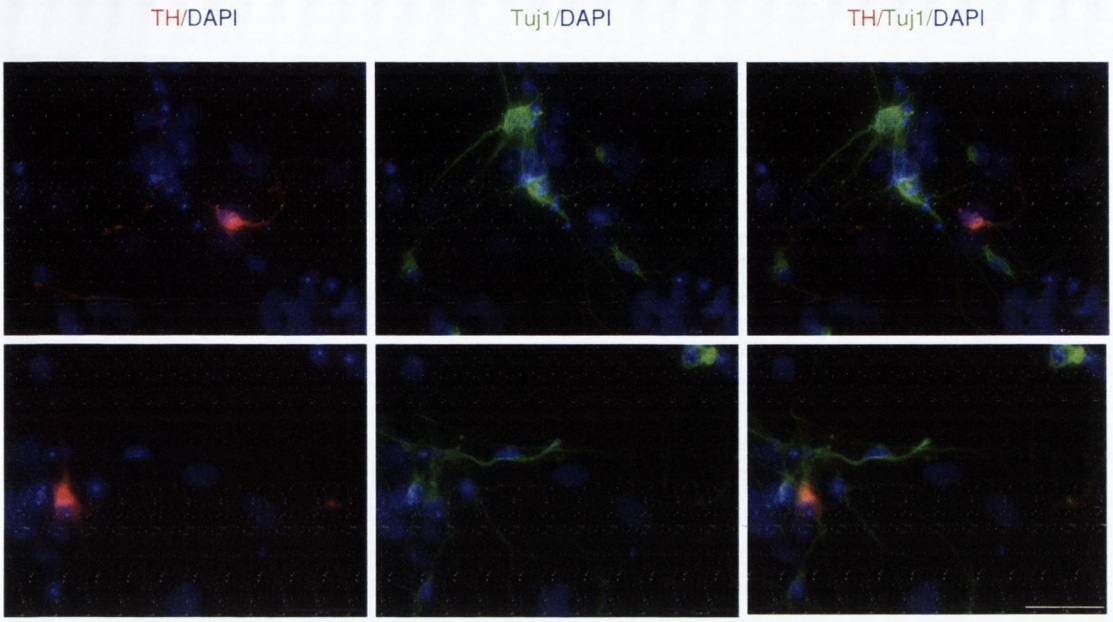

Figure 4.36: Neurons derived from FACS purified Sox1-GFP+ neural precursors express the dopaminergic marker tyrosine hydroxylase following growth factor induced (GFI) neuronal differentiation

Sox1-GFP+ cells were fixed at day 10 of the terminal differentiation stage of GFI differentiation and stained for expression of TH (red) and Tuj1 (green), as indicated. Nuclei were counterstained with DAPI (blue). Samples were analysed with an Olympus IX81-long focal length fluorescent microscopy using DAPI, Cy3 and GFP filters and images were captured at 40 x objective with an F-View II digital camera. Scale bar: 50 µm. TH indicates tyrosine hydroxylase.

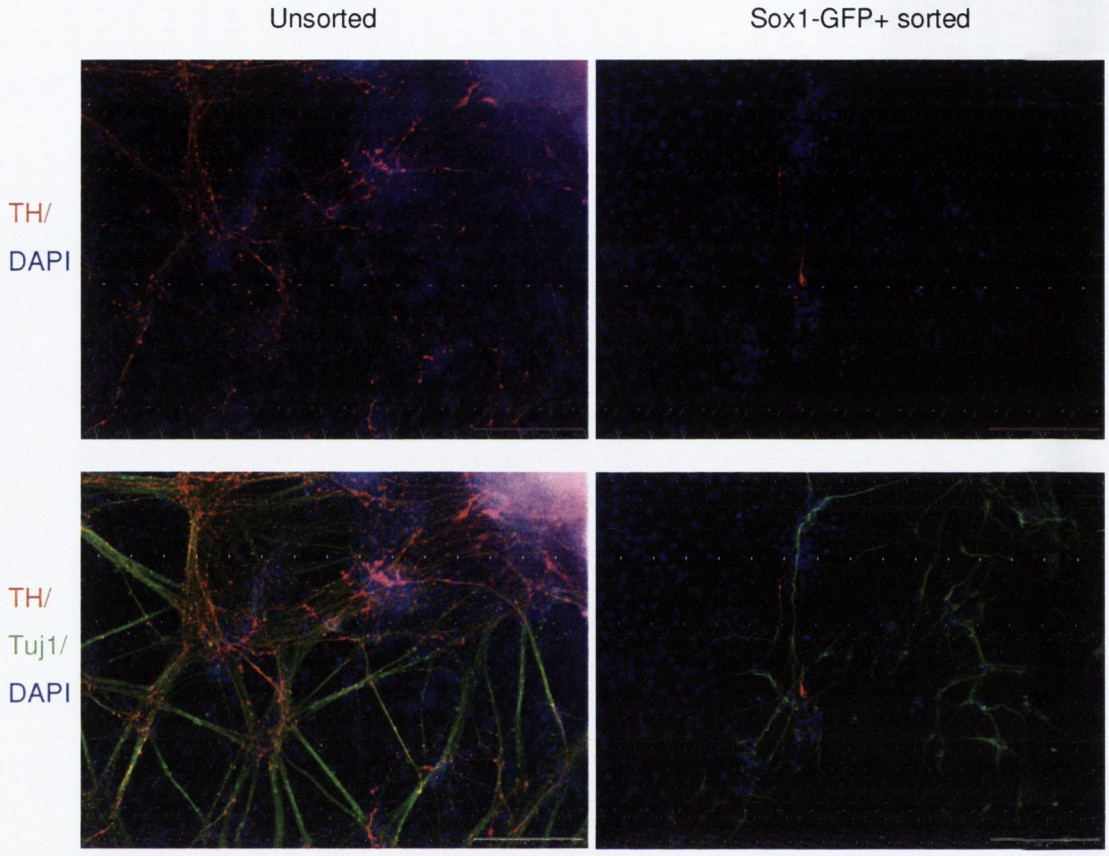

Figure 4.37: By morphological analysis tyrosine hydroxylase positive neurons are more abundant in unsorted Sox1-GFP ESCs than in FAC purified Sox1-GFP+ neural precursors following growth factor induced neuronal differentiation

Unsorted Sox1-GFP+ ESCs and FACS purified Sox1-GFP+ neural precursors were fixed at day 10 of terminal differentiation of the growth factor induced neuronal differentiation procedure and stained for co-expression of TH (red) and Tuj1 (green), as indicated. Nuclei were counterstained with DAPI (blue). Samples were analysed with an Olympus IX81-long focal length fluorescent microscopy using DAPI, Cy3 and GFP filters and images were captured at 10 x objective with an F-View II digital camera. TH indicates tyrosine hydroxylase. Scale bar: 200 µm.

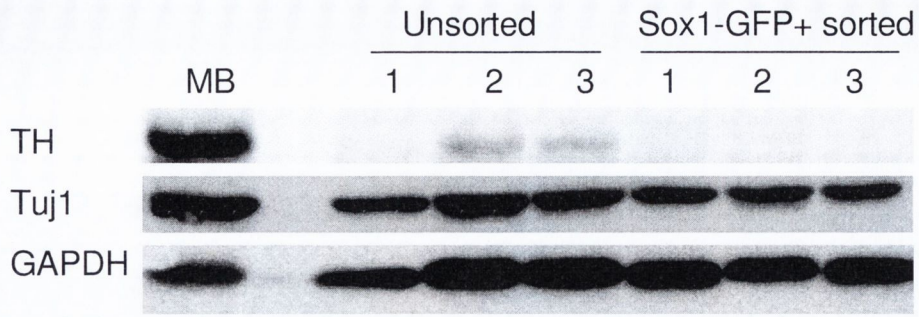

Figure 4.38: The level of TH protein is higher in neurons derived from unsorted Sox1-GFP ESCs compared to FACS purified Sox1-GFP+ neural precursors at day 10 of terminal differentiation

Protein was extracted from unsorted Sox1-GFP cells and FACS purified Sox1-GFP+ cells on day 10 of terminal differentiation of the growth factor induced neuronal differentiation procedure. 20 µg of each sample was run on a 10% SDS-PAGE gel. Mouse brain lysate (MB) was run as positive control. Membranes were probed with antibodies as indicated in the figure. GAPDH was analysed to verify equal loading and a representative blot is shown. TH indicates tyrosine hydroxylase, ~66 kDa; GAPDH, glyceraldehyde-3-phosphate dehydrogenase, 36 kDa; Tuj1, 50 kDa; 1-3, three independent differentiation procedures.

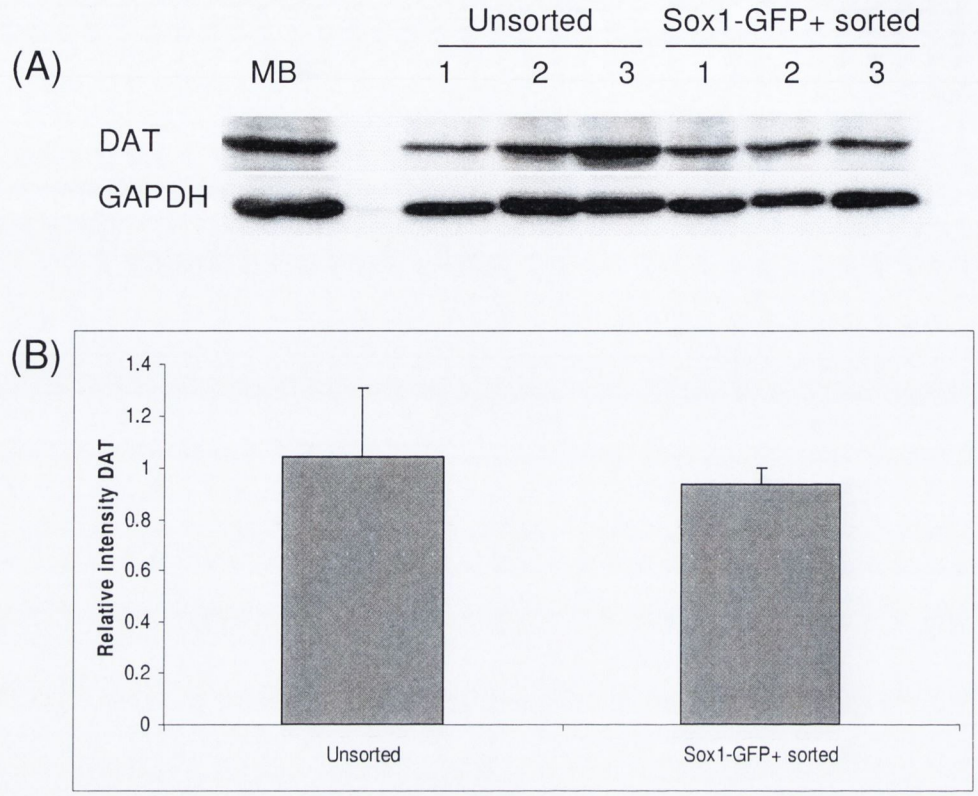

Figure 4.39: No difference was detected in the levels of DAT protein in neurons derived from unsorted Sox1-GFP ESCs and FACS purified Sox1-GFP+ neural precursors at day 10 of terminal differentiation of growth factor induced (GFI) differentiation

(A) Protein was extracted from unsorted Sox1-GFP ESCs and FACS purified Sox1-GFP+ neural precursors on day 10 of terminal differentiation of GFI neuronal differentiation. 20 µg of each sample was run on a 10% SDS-PAGE gel. Mouse brain lysate (MB) was run as positive control. Membranes were probed for DAT and GAPDH expression with anti-DAT and anti-GAPDH antibodies, as indicated. DAT indicates dopamine transporter, ~55 kDa; GAPDH, glyceraldehyde-3-phosphate dehydrogenase, 36 kDa; 1-3, three independent differentiation procedures. (B) Blots were processed in ImageJ to calculate the amount of DAT protein in each sample relative to the amount of GAPDH, and are expressed as relative intensity of DAT.

4.4 Discussion

Extracellular matrix proteins, such as laminin, fibronectin and collagen, provide key extracellular cues in the development of the nervous system (Letourneau et al., 1994). These proteins have also been reported to support *in vitro* neuronal differentiation of ESCs (Li et al., 1998; Lee et al., 2000; Ying and Smith, 2003; Goetz et al., 2006; Lau et al., 2006). Thus as 46C Sox1-GFP ESCs had not previously been differentiated by the GFI method, a simple assay was performed to assess the attachment and neuronal differentiation of dissociated NSSs plated on commonly used substrates, including laminin, fibronectin, PDL, PLO, gelatin and combinations thereof (Fig. 4.1). Cells were also plated at two densities ($5x10^4$ cells/cm^2, $1x10^5$ cells/cm^2), as plating density has been reported to be an important factor in neuronal differentiation of ESCs (Ying and Smith, 2003; Lorincz, 2006), with low cell densities often resulting in poor cell survival, while high cell densities may promote differentiation to non-neuronal lineages (Ying and Smith, 2003; Lorincz, 2006). Gross morphological analysis of cells one day after plating by light microscopy demonstrated that all substrates promoted cell attachment at both densities analysed (Fig. 4.1). Further neuronal differentiation resulted in the generation of small spherical Tuj1 positive colonies at both cell densities and on all substrates examined (Fig. 4.1). Numerous single cells which did not stain with Tuj1 were also apparent in all cultures. Neurite extensions were more prominent at lower densities, possibly due to fewer cells in these cultures. Thus it was determined that all substrates supported attachment and differentiation.

Previous studies have suggested that variation can exist in the neuronal differentiation potential of the same ESC line using different differentiation methods (Zhao et al., 2004; Chung et al., 2006; Fukuda et al., 2006; Hedlund et al., 2007; Parmar and Li, 2007; Hedlund et al., 2008). Thus prior to use of 46C Sox1-GFP ESCs for sorting by the GFI method, a comparative study was performed to assess if the GFI method supported robust neuronal differentiation, as has been reported for this cell line following ML differentiation (Ying and Smith, 2003; Ying et al., 2003). Tuj1 positive colonies were readily derived from Sox1-GFP ESCs by both methods, with colonies of various sizes being generated and extending networks of neurites (Fig. 4.2). Analysis of these colonies revealed that they

were more numerous following GFI differentiation (Fig. 4.3) and that the mean diameter was larger following ML differentiation (Fig. 4.4). As terminal neuronal differentiation was initiated in the GFI method by withdrawal of growth factors, it is possible that this decreased proliferation of NPs within colonies, limiting their size. This is supported by the finding that at day 12 of ML differentiation and day 7 of terminal differentiation of GFI differentiation, which was the final time point at which Sox1-GFP expression was analysed by FACS, 32.36 $\pm$ 1.4% of cells expressed GFP in ML differentiated cultures (Fig. 4.30) while only 17.5 $\pm$ 1.6% of cells expressed GFP in GFI differentiated cultures (Fig. 4.29).

Examination of neurite length revealed that those extending from Tuj1 colonies in GFI cultures were longer than those formed in the ML cultures (Fig. 4.5). This may be due, in part, to the fact that cells were cultured on different substrates, with PDL/laminin used in the GFI differentiation method and gelatine in the ML differentiation method, which is not the optimal substratum for neuronal differentiation (Ying and Smith, 2003). Gelatine was used to support attachment of ESCs for ML differentiation as it has previously been reported that other substrates, such as laminin and fibronectin, can promote differentiation to non-neural lineages (Ying et al., 2003). This result may be clarified by re-plating Sox1-GFP cells on laminin coated dishes during the process of ML differentiation (Ying et al., 2003) to determine if it is the specific substrate used or differentiation method applied that affects neurite length. Thus, while morphological differences were detected in the neuronal populations generated by these protocols, the GFI method induced robust neuronal differentiation of Sox1-GFP ESCs.

It was also of interest to examine the neuronal subtypes generated from both protocols and to identify if differences existed after differentiation. As demonstrated in Fig. 4.2, neuronal differentiation by both procedures results in the formation of three-dimensional colonies with individual cells being difficult to discern (Lorincz, 2006; Hedlund et al., 2008), thus making immunocytochemical analysis challenging. Therefore analysis was performed by Western blotting. In accordance with immunocytochemistry results (Fig. 4.2), Tuj1 protein expression was readily detected following differentiation of Sox1-GFP ESCs by both methods in three independent procedures (Fig. 4.6). While high levels of the pre-synaptic protein synaptophysin were detected in mouse brain lysate (positive control), only low

levels were present in *in vitro* generated neuronal cultures, with expression being almost exclusively restricted to cells differentiated by the GFI protocol (Fig. 4.6). As synaptophysin is a major intrinsic membrane protein of synaptic vesicles that is widely expressed in presynaptic nerve terminals in the brain (Marqueze-Pouey et al., 1991; Fykse et al., 1993) and has been correlated with synapse formation and maturation (Knaus et al., 1986), it suggests that ML differentiation may not support these processes, while they may be supported by GFI differentiation. Alternatively, it is possible that synapses have not yet developed by day 14 of ML differentiation when samples were harvested or that a small subset of neurons expresses synaptophysin and it is below the level of detection by Western blotting. This is intriguing as it has previously been reported that post-mitotic neurons can already be identified four days after the initiation of the ML differentiation (Ying et al., 2003). However, it has recently been published that ML differentiation does not support the development of fully mature and functional neuronal networks from mouse ESCs, even after long-term culturing (Illes et al., 2009). In contrast, the same study found that differentiation of mouse ESCs in neural aggregates supported these processes, and the authors suggested that heterogeneous cell populations within aggregates provide factors which support the generation of functional neuronal networks (Illes et al., 2009). Therefore, neurons derived from Sox1-GFP ESCs following GFI differentiation may more closely recapitulate the properties of functionally mature neurons, which is of significance when these properties are required by *in vitro* differentiated neurons.

GFAP was only detected in GFI cultures, with this level being low and detected twice (Fig. 4.6). This suggests that differentiation by these methods may not promote gliogenesis or that astrocytes have not formed by the time point at which cells were collected. As GFAP is a marker of differentiated astrocytes, it may be of interest to analyse cultures for the presence of an earlier astrocytic marker such as CD44, which is expressed by astrocyte precursor cells (Liu et al., 2004). Interestingly, Ying et al. (2003) reported that ML differentiation does, in fact, support the development of astrocytes, with these cells being apparent already 10 days after initiation of the differentiation process. Thus it is possible that only few astrocytes are present in differentiated cultures, as suggested by cellular staining of cells at day 10 of terminal differentiation of the GFI method (Fig. 4.20), which may have been below the level of detection by Western blotting.

Further analysis of cellular proteins revealed that the same neuronal subtypes were present in Sox1-GFP ESCs neuronal cultures differentiated by GFI and ML methods, with markers of the dopaminergic (DAT, TH, Nurr1), GABAergic (GAD) and serotonergic (SERT) systems being detected (Fig. 4.7). However, it should be noted that variability existed in the expression of specific markers in independent samples from both differentiation procedures. No protein expression was detected for glutamatergic or noradrenergic neurons, as determined by their transporter proteins EAAC1 and NAT, respectively, indicating that these neuronal subtypes were absent or represented only a small fraction of the total cell population after differentiation, which was below the level of detection by Western blotting. A definitive assessment of their presence or absence in differentiated cultures may be provided by performing immunocytochemistry. The presence of GABAergic neurons in the differentiated population is in agreement with previous reports regarding ML differentiation of this ESC line (Ying and Smith, 2003; Ying et al., 2003).

The presence of dopaminergic neurons is also in agreement with previous reports (Lau et al., 2006; Parmar and Li, 2007) and markers were expressed relatively consistently across cultures. Interestingly, semi-quantitative analysis revealed that significantly higher levels of DAT and Nurr1 protein were present in cultures differentiated by the GFI method (Figs 4.8, Fig. 4.9). This result is not unexpected as the application of the Shh, FGF8 and L-AA has been reported to support the generation of DA neurons from ESCs (Lee et al., 2000; Lau et al., 2006). However, there was no difference in the level of TH protein between differentiation procedures (Fig. 4.10). Furthermore, TH expressing neurons were readily detected by immunocytochemistry following differentiation by both protocols (Figs 4.11, 4.12). As discussed previously, Nurr1 is a transcription factor required for the induction of the mDA phenotype in the developing embryo, with *Null*$^{-/-}$ mutants failing to express TH and DAT (Zetterstrom et al., 1997; Castillo et al., 1998; Saucedo-Cardenas et al., 1998; Wallen et al., 1999). Therefore, the increased level of Nurr1 protein following GFI differentiation without an apparent increase in TH protein is somewhat surprising (Figs 4.9, 4.10). However, recent research indicates that Nurr1 may be particularly required for DAT expression (Kadkhodaei et al., 2009). Kadkhodaei et al. (2009) found that inactivation of *Nurr1* in late embryonic development in mice resulted in a progressive decline in mDA markers, including TH, VMAT2 and AADC. In contrast, DAT was completely absent in

mDA neurons soon after ablation (Kadkhodaei et al., 2009). Furthermore, Nurr1 has been found to enhance transcription of the *DAT* gene (Sacchetti et al., 1999; Sacchetti et al., 2001). In addition, while it has been reported that ML differentiation supports the generation of TH positive neurons without the application of Shh and FGF8, the percentage of TH positive neurons increased from 16 to 26% on their addition (Parmar and Li, 2007). Thus it is possible that these growth factors enhance the acquisition of a dopaminergic phenotype and increase the expression of DAT and Nurr1.

Serotonergic neurons were also present in these cultures, as indicated by detection of the transport protein SERT (Fig. 4.6). This is expected as Shh and FGF8 are inductive signals for ventral mDA neurons and rostral hindbrain serotonin neurons during embryonic development (Ye et al., 1998), and Lee et al. (2000) reported that around 10% of neurons derived from ESCs following application of these factors expressed serotonin. Furthermore, it has also been recently reported that up to 25% of neurons generated by ML differentiation are serotonergic (Friling et al., 2009).

Therefore, this comparative analysis of differentiation methods suggested that Sox1-GFP ESCs could be effectively differentiated to neurons using the GFI procedure, and that these neurons expressed DA markers. As this method is abbreviated in comparison to other published reports regarding DA differentiation of mouse ESCs (Lee et al., 2000; Rolletschek et al., 2001), it was of interest to analyse if a more mature neuronal phenotype could be obtained following extended neuronal differentiation, such as expression of synaptophysin (Wernig et al., 2002). Therefore cells were maintained at the terminal differentiation stage (stage 4) for an extra 6 days, thus being in differentiation medium for a total of 16 days. Tuj1 positive colonies were detected at this time point and appeared morphologically similar to colonies at day 10 (Fig. 4.13). However, neurites were not as prominent at later time points, suggesting that additional factors may be required to support their maintenance. In addition, while no difference was detected in the number of colonies between the two time points (Fig. 4.14), those present on day 16 were found to be larger in size (Fig. 4.15). As discussed above, NPs are still present in colonies at day 10 of differentiation, as assessed by GFP expression (Fig. 4.27), and thus may account for this observation. In agreement with immunocytochemical analysis of cells, Tuj1 protein levels

were found to be reduced at day 16 when compared to day 10 (Figs 4.16, 4.17). However, protein levels of the more mature marker NeuN, which labels neuronal nuclei, did not change with increased differentiation (Figs 4.16, 4.18), suggesting that while Tuj1 positive neurite extension may have been reduced at day 16 of terminal differentiation, the number of neurons at both time points was similar. Expression of synaptophysin was almost undetectable at day 16 of terminal differentiation (Fig. 4.16). This is surprising as expression of this protein has previously been reported to increase at later stages of neuronal differentiation of ESCs (Wernig et al., 2002) and may be related to the general decrease in neurite extensions at day 16 (Fig. 4.13).

Extended terminal differentiation significantly increased protein expression of the astrocyte specific intermediate filament GFAP (Fig. 4.19). Immunocytochemical analysis of cells mirrored this finding, with abundant GFAP staining at day 16 of differentiation (Fig. 4.20). This result is not unexpected as neurogenesis precedes gliogenesis in the developing nervous system and astrocytes have previously been reported to arise at later time points during *in vitro* neuronal differentiation of ESCs (Rolletschek et al., 2001; Barberi et al., 2003). Markers of GABAergic (GAD), serotonergic (SERT) and dopaminergic (TH, DAT, Nurr1) neurons were detected at both time points of differentiation (Fig. 4.21). However, markers of glutamatergic and noradrenergic neurons were not detected in any cultures (Fig. 4.21). As discussed above, this may suggest that these neuronal subtypes are absent or represent only a small fraction of the total cell population after differentiation, which was below the level of detection by Western blotting, and their presence in differentiated cultures may be conclusively determined by performing immunocytochemistry.

Increased terminal differentiation time had a negative effect on dopaminergic and GABAergic neurons, with protein expression of DAT, Nurr1 and GAD being significantly reduced at day 16 of differentiation (Figs 4.22, 4.23, 4.25). Interestingly, SERT was expressed relatively consistently at both time points across cultures, with no difference in protein levels being detected (Fig. 4.26). This suggests that increased time in the terminal differentiation stage of GFI neuronal differentiation may selectively affect particularly neuronal subtypes, namely dopaminergic and GABAergic, while serotonergic neurons are relatively spared. This is somewhat surprising as a previous published report suggested that

all three neuronal subtypes may be maintained for at least 16 days after the withdrawal of growth factors in the absence of any additional trophic factors (Rolletschek et al., 2001). Thus as increased terminal differentiation time had a general negative affect of the neuronal population, day 10 was selected as the end point for subsequent experiments.

All the studies thus far indicated that DA neurons could be effectively generated from this Sox1-GFP ESC line using the fast and efficient protocol of Lau et al. (2006), and were in accordance with previous published reports (Chung et al., 2006; Fukuda et al., 2006; Parmar and Li, 2007). In order to determine the optimal time point for sorting NPs, Sox1-GFP expression was analysed daily during suspension cultures of NSSs (stage 2), neural proliferation (stage 3) and terminal differentiation (stage 4). Sox1-GFP expression was first detected by fluorescent microscopy on day 4 during the neural proliferation stage of GFI differentiation (Fig. 4.27), and day 3 of this stage by FACS analysis (Fig. 4.29). Interestingly, Sox1-GFP expression was also initially detected at these time points during ML differentiation (Figs 4.28, 4.30). This suggests that NPs are first generated at a similar time using independent methods to differentiate ESCs to neurons. In agreement with previous reports (Ying et al., 2003; Chung et al., 2006), Sox1-GFP expression decreased as differentiation proceeded (Figs 4.29, 4.30) due to down-regulation of *Sox1* (Ying et al., 2003). However, even at later stages of differentiation Sox1-GFP expression was detected in both GFI (Figs 4.27, 4.29) and ML (Figs 4.28, 4.30) differentiated cultures, indicating the continued presence of NPs, which was also reported by Ying et al. (2003). As GFP is a relatively stable protein, its expression may also continue in cells which have already down-regulated *Sox1*, as previously reported (Barraud et al., 2005). From this data day 5 of the neural proliferation stage of GFI differentiation was determined as the optimal time point to sort cells as robust Sox1-GFP expression was observed at this time point (Figs 4.27, 4.29) but neurites had not yet developed (Fig. 4.29). This is of particular significance as more mature neurons have been reported to be vulnerable to dissociation and FACS (Yoshizaki et al., 2004; Hedlund et al., 2008).

In agreement with previous reports (Chung et al., 2006; Fukuda et al., 2006), NPs could be effectively sorted to purity by FACS using Sox1-GFP expression (Figs 4.31, 4.32). While undifferentiated stem cell markers (Oct4 and Nanog) were enriched in the Sox1-GFP-

population after sorting, neuroectodermal markers (Sox1 and nestin) were enriched in the Sox1-GFP+ population (Fig. 4.32A). Further *in vitro* terminal differentiation of these Sox1-GFP+ and Sox1-GFP- cells supported this finding, with 65 ± 9.9% and 1.56 ± 0.42% Tuj1+ neurons per total cells generated in each population, respectively (Fig. 4.34). Thus these results established that Sox1-GFP expression could be effectively used to purify NPs at day 5 of the neural proliferation stage of GFI differentiation and that terminal differentiation of Sox1-GFP+ samples generated a highly enriched neuronal population.

Comparison of the Sox1-GFP+ population generated by this method and those from previous studies (Chung et al., 2006; Fukuda et al., 2006) indicates it is at least as effective in obtaining an enriched neuronal population. The percentage of Tuj1+ cells generated in this study (65 ± 9.9%) is higher than that reported by Chung et al. (2006), in which 44.29 ± 7.93% of cells expressed Tuj1, and lower than that reported by Fukuda et al. (2006), in which ~95% of cells expressed Tuj1. However, Chung et al. (2006) differentiated Sox1-GFP ESCs using the multi-stage protocol by Lee et al. (2000), with Fukuda et al. (2006) differentiating Sox1-GFP ESCs on PA6 stromal cells (Kawasaki et al., 2000), and thus more closely resembles the method used in this study. Furthermore, plating of Sox1-GFP+ NPs on these stromal cells may hinder *in vitro* studies following terminal neuronal differentiation due to the largely undetermined affect of this cell layer. A difference was observed in relation to the generation of astrocytes in the present study and that of Chung et al. (2006). While only sparse GFAP staining was observed in the sorted Sox1-GFP+ population in this report after terminal differentiation (Fig. 4.35), Chung et al. (2006) reported that astrocytes comprised 22.94 ± 2.07% of total cells after differentiation of Sox1-GFP+ cells. Immunocytochemical analysis of unsorted Sox1-GFP samples after GFI differentiation indicates that this method does not support the generation of astrocytes until later stages of terminal differentiation (Fig. 4.20), and while cells were also analysed ten days after withdrawal of growth factors in the report of Chung et al. (2006), the overall increase in culturing time using the method of Lee et al. (2000) may have allowed for the generation of glial cells.

In accordance with previous studies, TH+ neurons were detected in Sox1-GFP+ sorted samples by immunocytochemistry following terminal neuronal differentiation (Fig. 4.36)

(Chung et al., 2006; Fukuda et al., 2006; Parmar and Li, 2007). However, by gross morphological analysis TH+ neurons appeared more abundant in unsorted samples at day 10 of differentiation than Sox1-GFP+ sorted samples (Fig. 4.37). TH protein was also absent from independent Sox1-GFP+ sorted cultures following terminal differentiation as determined by Western blotting (Fig. 4.38). In contrast, TH protein was detected in unsorted neuronal cultures at the same time point of differentiation (Fig. 4.38). This difference in TH expression between sorted and unsorted neuronal cultures after terminal differentiation is in agreement with results published by Chung et al (2006), with higher expression of TH observed in unsorted samples. As stated previously, Chung et al. (2006) used a multi-stage differentiation procedure to obtain DA neurons for sorted and unsorted Sox1-GFP ESCs (Lee et al., 2000) which was similar to the differentiation procedure used in the present study. On the contrary, Parmar and Li (2007) reported that the proportion of TH+ neurons was indistinguishable in sorted and unsorted samples (14 $\pm$ 2% versus 16 $\pm$ 3%) following ML neuronal differentiation. In addition, the proportion of TH+ neurons has also been reported to be comparable in sorted and unsorted samples following differentiation on PA6 stromal cells (Fukuda et al. (2006); sorted Sox1-GFP+ sample 22 $\pm$ 6% TH+ neurons, unsorted sample 25 $\pm$ 5% TH+ neurons).

Interestingly, while it has been reported that Sox1 is expressed at early stages of neural development in all progenitor cells (Pevny et al., 1998), Barraud et al. (2005) have found, using the same Sox1-GFP reporter in transgenic mice, that Sox1-GFP fluorescence and endogenous Sox1 protein were conspicuously absent from the ventral aspects of the midbrain and rostral hindbrain at mid-embryogenesis during neural development. Furthermore, in the ventral midbrain, Sox1-GFP fluorescence and endogenous Sox1 protein were completely absent from the area that contains the precursors for dopaminergic neurons (Barraud et al., 2005). The authors suggested that Sox1-GFP expression cannot be used to identify and isolate neural stem cells from all areas of the developing CNS and an alternative reporter is likely required for identification and isolation of corresponding ventral midbrain precursors (Barraud et al., 2005). Thus in light of these finding, it is possible that application of growth factors at early stages of the differentiation process in the present study resulted in a subset of cells, namely DA precursors, not expressing Sox1-

GFP at the time point of sorting, resulting in higher expression of TH in unsorted samples following terminal differentiation (Figs 4.37, 4.38).

This hypothesis is corroborated by previously published data (Chung et al., 2006). In particular, it has been reported that TH+ neurons represented 19.44 $\pm$ 6.02% of the Sox1-GFP- neuronal population after sorting and terminal differentiation, and that this was significantly higher than TH+ neurons in the Sox1-GFP+ population. Furthermore, Sox1-GFP- samples were found to release DA upon depolarisation (Chung et al., 2006). It was also observed that mixing Sox1-GFP+ and Sox1-GFP- samples after sorting and differentiating the cells together did not have an additive effect in terms of dopaminergic differentiation (Chung et al., 2006). Thus the authors concluded from these results that some NPs that can generate DA neurons are not expressing Sox1 and thus, are Sox1-GFP-, rather than there being DA-inducing, factor releasing cells in the Sox1-GFP- population (Chung et al., 2006).

In contrast to the absence of TH protein in Sox1-GFP+ sorted samples by Western blotting following terminal differentiation (Fig. 4.38), DAT protein was observed in these samples (Fig. 4.39). Furthermore, no difference was detected in DAT protein levels between unsorted and sorted samples (Fig. 4.39). As DAT is expressed exclusively in DA neurons in the brain (Augood et al., 1993; Turiault et al., 2007), it suggests that differences may exist in the expression of DA neuronal markers by Sox1-GFP+ sorted neurons. This is of importance as TH is the most widely used marker of DA neurons following *in vitro* differentiation of ESCs and suggests that different protein markers may not be equivalent in detection of DA neurons. These findings also advocate the use of more than one marker for definitive assessment of the presence of DA neurons in *in vitro* neuronal cultures. Further studies are required to assess the number of TH+ and DAT+ neurons in Sox1-GFP+ samples following GFI neuronal differentiation. The presence of other markers of the DA system is in agreement with previous studies, in which DAT and AADC were detected in Sox1-GFP+ samples following neuronal differentiation (Chung et al., 2006).

In conclusion, the results presented in this chapter demonstrate that the GFI differentiation method supports robust neuronal differentiation of the Sox1-GFP ESC line, which is

accompanied by expression of dopaminergic markers and the pre-synaptic protein synaptophysin. Furthermore, Sox1-GFP+ NPs can be effectively FACS sorted during the process of GFI differentiation, which generate enriched neuronal populations following terminal differentiation. However, TH expression was more abundant in unsorted neuronal cultures than Sox1-GFP+ sorted samples at day 10 of terminal differentiation, and with results from previous studies (Chung et al., 2006; Fukuda et al., 2006; Parmar and Li, 2007), may suggest that the use of Sox1-GFP expression to sort NPs and generate an enriched dopaminergic population may be influenced by the neuronal differentiation method used.

Chapter 5

Comparison of neural populations derived from embryonic and induced pluripotent stem cells

5.1 Introduction

The generation of iPSCs from somatic cells has opened remarkable avenues for basic research and regenerative medicine (for review, see Takahashi and Yamanaka, 2006; Yamanaka, 2009). This is of particular relevance to diseases of the central nervous system, the underlying disease mechanisms of which are largely unknown and due in part to the limited access to human nerve cells (for reviews, see Kim, 2010; Wichterle and Przedborski, 2010). Thus the generation of disease specific iPSCs and differentiation to the relevant neuronal subtype may elucidate mechanisms of disease pathogenesis, allowing the creation of more faithful disease models which may facilitate the development of efficacious therapies (for reviews, see Yamanaka, 2009; Kim, 2010; Wichterle and Przedborski, 2010).

While much research is focused on the methodology related to the generation of iPSCs, for the promise of iPSCs to be realised, it is necessary to ask if and how effectively they may be differentiated to functional cells of various lineages (Hu et al., 2010). This question can be answered by direct comparison with ESCs, as iPSCs should, by definition, behave like ESCs in their self-renewal and lineage differentiation (Hu et al., 2010). Undifferentiated mouse ESCs have several characteristic features, including relatively short generation time of ~12-15 hours with a short G_1 cell cycle phase (Rohwedel et al., 1996; for review, see Wobus and Boheler, 2005), expression of undifferentiated pluripotent stem cell surface markers, such as SSEA1 (Solter and Knowles, 1978), and undifferentiated pluripotent stem cell transcription factors, such as Oct4 and Nanog (Niwa et al., 2000; Chambers et al., 2003; Mitsui et al., 2003). Thus iPSCs should display similar characteristics (Takahashi and Yamanaka, 2006). ESCs are also characterised by pluripotency, meaning that they can generate the three germ layers, mesoderm, ectoderm and endoderm, in both *in vitro* and *in vivo* assays. This is often assessed *in vitro* by the spontaneous formation of embryoid bodies (EBs) in suspension culture, with EBs being suggested as an *in vitro* model of mouse embryogenesis (Leahy et al., 1999; for review, see Desbaillets et al., 2000). Pluripotency may also be investigates by *in vivo* assays such as teratoma formation upon injection of ESCs or iPSCs into immunodeficient mice, tetraploid complementation and formation of chimeric mice (for review, see Stadtfeld and Hochedlinger, 2010).

It is also essential to carefully evaluate the ability of iPSCs to undergo differentiation to specific lineages and characterise the properties of differentiated cells (Zhang et al., 2009; Hu et al., 2010). It has recently been reported that while human iPSCs followed the same temporal course during neural specification as human ESCs, iPSCs exhibited lower and more variable neuroepithelial and neuronal differentiation efficiencies (Hu et al., 2010). However, a more extensive study was subsequently published which concluded that iPSCs gave rise to functional motor neurons with efficiencies similar to that of ESCs (Boulting et al., 2011). Importantly, both reports suggested that the method used to generate iPSC clones did not negatively affect the neural differentiation propensity of these cells (Hu et al., 2010; Boulting et al., 2011). Recent evidence indicates that differences may exist in the reprogramming process between human and mouse cells (Maherali et al., 2007; Stadtfeld and Hochedlinger, 2010; Tchieu et al., 2010). Thus as human iPSCs and ESCs are derived from an outbred population, it may be of interest to analyse the neural differentiation efficiency of mouse iPSCs in comparison to mouse ESCs. As mouse iPSCs can be easily compared to ESCs derived from the same mouse strain it may control background variability and allow differences between the cell types to be identified. Therefore the aim of this study was to analyse and compare the formation of neural stem spheres (NSSs) by iPSCs and ESCs from the mouse strain in suspension culture (Lau et al., 2006), so as to determine if iPSCs exhibited similar neural differentiation efficiency as ESCs. This was also evaluated by the formation of neurons using a procedure in which differentiation is induced by culturing cells as monolayers in chemically defined medium in the absence of LIF, in which autocrine signalling is required for neural conversion (Ying and Smith, 2003; Ying et al., 2003). The iPSC clone used was initially validated by analysis of key pluripotent stem cell markers and formation of EBs in suspension culture, in comparison to ESCs.

5.2 Methods

5.2.1 Cell proliferation and population doubling time

V6.5 mouse ESCs and V6.5 mouse iPSCs were obtained as a kind gift from Dr Stephen Sullivan. iPSCs were derived from MEFs by retroviral transfection with c-Myc, Oct-4,

Sox-2 and Klf-4. To determine the growth characteristics and population doubling time of undifferentiated ESCs and iPSCs, $1.92x10^5$ cells (passage number 24) were plated per well of a 6-well plate in duplicate (initial cell density of $2x10^4$ cells/cm^2). Cell counts were performed 24, 48 and 72 hours after plating and cell viability was determined using the Trypan blue exclusion assay as described in Section 2.7.5, with unstained cells being used for analysis. The population doubling rate was determined after 48 hours to ensure exponential growth was maintained. This was calculated by first performing a natural logarithmic transformation of viable cell number at 0, 24 and 48 hours, to establish a linear relationship between variables. These values were subsequently used as the response variable in simple linear regression analysis, with the time in hours as the predictor variable. The slope of the regression equation was used to calculate population doubling time with the following formula:

Doubling time (Hours) = ln 2/slope

5.2.2 Embryoid body and neural stem sphere assay

Undifferentiated ESCs and iPSCs (passage number 24) were trypsinised and resuspended at a density of $3x10^5$ cells/ml in 10 ml embryoid body (EB) medium (KO-DMEM, 10% (v/v) ESC qualified FBS, 1X pen/strep, 2 mM L-glutamine, 1X NEAA, 0.1 mM β-MeOH) or NSS medium (KO-DMEM supplemented with 10% (v/v) ESC qualified FBS, 1X NEAA, 1X pen/strep, 2 mM L-glutamine with 20 ng/ml EGF, 20 ng/ml bFGF added freshly prior to use; Lau et al. (2006)) and plated in non-adherent bacteriological dishes to form EBs and NSSs in suspension culture, respectively. Culturing was performed in the absence of LIF to induce differentiation. Colonies were analysed at the same time point each day over the next four days and 20 randomly selected images per dish were obtained using an Olympus IX81-long focal length fluorescent microscope set to 10 x objective with an F-View II digital camera. Colonies were counted in each image and the diameter of 50 randomly selected colonies was measured using ImageJ. To maintain consistency, colonies were only counted and measured if they were round and had well-defined borders.

Differences between the number and diameter of EBs derived from ESCs and iPSCs, and the number and diameter of NSSs derived from ESCs and iPSCs, were analysed using two-way repeated measure ANOVA. In both cases the cell type and day were the independent variables. When a statistical significance relationship was found between the day and cell type, a Student's unpaired two-tailed t-test was performed for ESCs and iPSCs on day 1, day 2, day 3 and day 4. When statistical significance was found for the day, this was further investigated for ESCs and iPSCs separately using one-way repeated measure ANOVA with pairwise comparison and post-hoc Bonferroni significant test. Significance was set to 0.05 for all tests.

5.3 Results

5.3.1 Undifferentiated iPSCs express characteristic features of pluripotent stem cells and show no difference to ESCs

Undifferentiated iPSCs expressed the cell surface antigen SSEA1, with morphology similar to that of undifferentiated ESCs (Fig. 5.1). In addition, Oct4 and Nanog gene expression was detected in both cell types (Fig. 5.2). ESCs and iPSCs displayed similar growth characteristics when plated at low density, with no significant difference in cell number being observed at 24 (ESCs, $0.68 \pm 0.06 \times 10^6$ cells; iPSCs, $0.58 \pm 0.08 \times 10^6$ cells), 48 (ESC, $1.87 \pm 0.06 \times 10^6$ cells; iPSCs, $1.6 \pm 0.22 \times 10^6$ cells) or 72 (ESCs, $3.46 \pm 0.29 \times 10^6$ cells; iPSCs, $3.26 \pm 0.29 \times 10^6$ cells) hours post-plating (Fig. 5.3). Similarly, ESCs and iPSCs exhibited comparable population doubling times of 14.7 hours and 15.7 hours, respectively.

5.3.2 iPSCs form embryoid bodies in suspension culture and show overall similarities to ESCs

The ability of stem cells to form EBs is a common test of pluripotency and was examined in undifferentiated iPSCs by growth in non-adherent bacteriological dishes in the absence of LIF. Under this system, iPSCs formed three-dimensional colonies that increased in size and were morphologically comparable to ESC derived EBs over a 4 day culture period (Fig. 5.4).

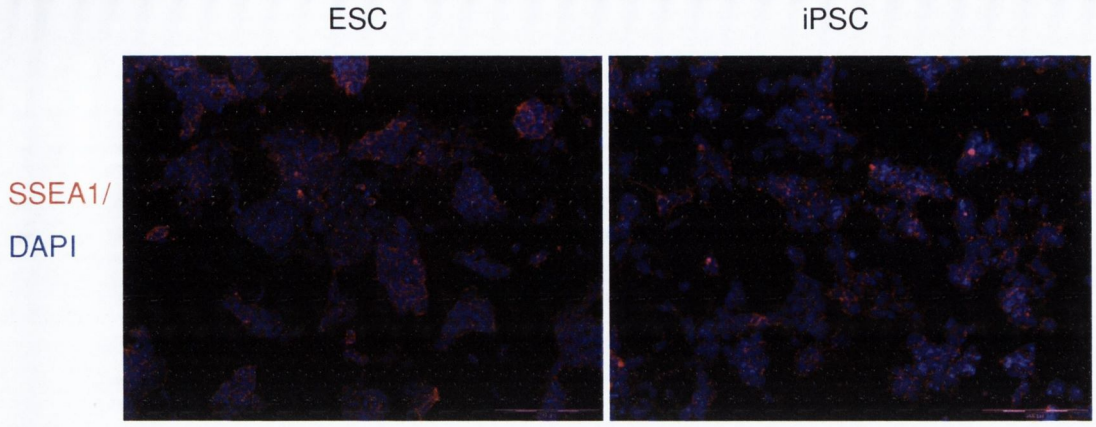

Figure 5.1: Undifferentiated ESCs and iPSCs express the pluripotent stem cell surface marker SSEA1

Undifferentiated ESCs and iPSCs were fixed and stained for expression of SSEA1 (red), as indicated. Nuclei were counterstained with DAPI (blue). Samples were analysed using an Olympus IX81-long focal length fluorescent microscopy using DAPI and Cy3 filters and images were obtained at 10 x objective with an F-View II digital camera. SSEA1 indicates stage specific embryonic antigen 1; ESC, embryonic stem cells; iPSC, induced pluripotent stem cells. Scale bar: 200 μm.

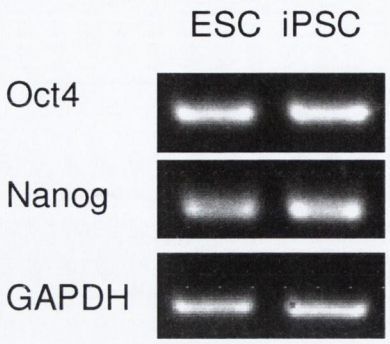

Figure 5.2: Undifferentiated ESCs and iPSCs express the pluripotent stem cell transcription factors Oct4 and Nanog

Total RNA was isolated from undifferentiated ESCs and iPSCs and used to synthesis cDNA. One-twentieth of the reaction (1 µl) was subsequently used to identify pluripotent transcription factors Oct4 and Nanog using gene specific primers, as indicated. The house keeping gene GAPDH was included to verify equality between samples. Samples were analysed by agarose gel electrophoresis. ESC indicates embryonic stem cells; iPSC, induced pluripotent stem cells; GAPDH, glyceraldehyde-3-phosphate dehydrogenase, 454 bp; Oct4, 312 bp; Nanog, 363 bp.

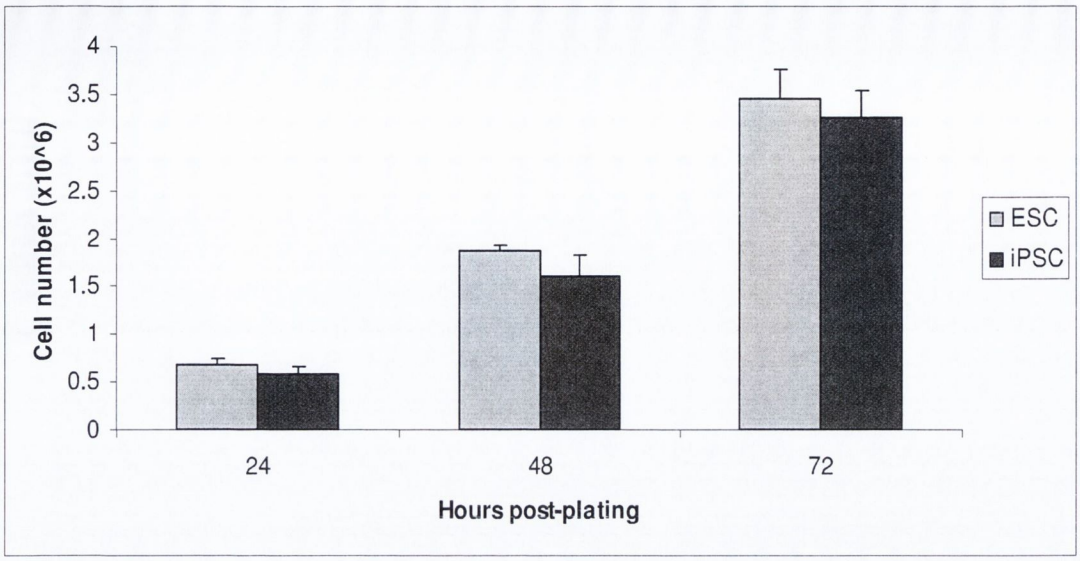

Figure 5.3: Undifferentiated ESCs and iPSCs exhibit similar growth characteristics

Undifferentiated ESCs and iPSCs were plated in duplicate at a density of $2x10^4$ cells/cm^2 in 6-well plates ($1.92x10^5$ cells/well) and analysed 24, 48 and 72 hours later by cell counts. Cell viability was determined using Trypan blue exclusion assay and only unstained cells were included in the analysis. Data represents the mean + SEM of experiments performed on four cell populations.

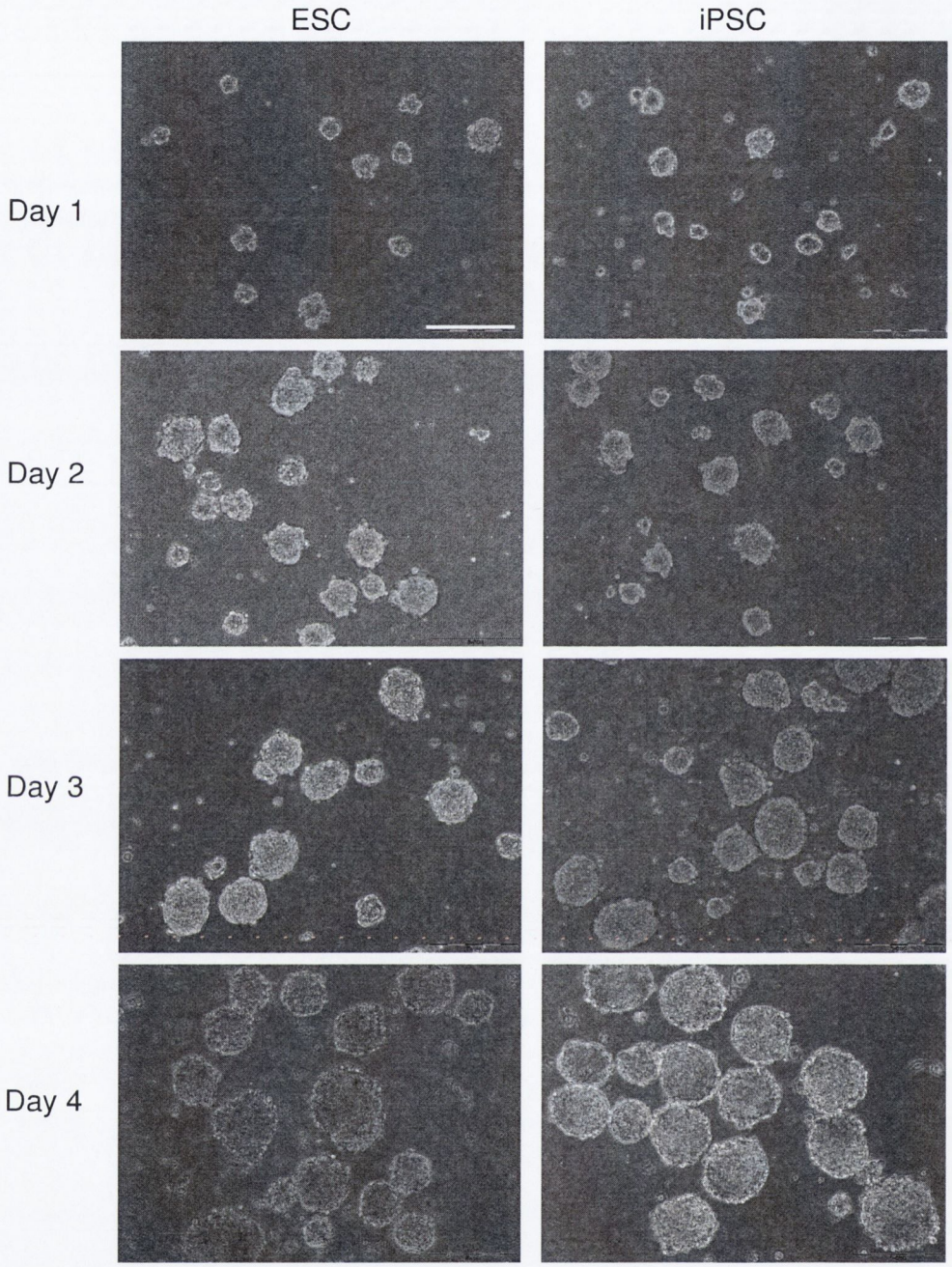

Figure 5.4: ESCs and iPSCs form morphologically similar embryoid bodies following growth in suspension cultures

Undifferentiated ESCs and iPSCs were resuspended in EB medium in the absence of LIF and induced to form EBs in suspension culture. Phase contrast images were obtained 1, 2, 3 and 4 days post plating, as indicated, using an Olympus IX81-long focal length fluorescent microscope at 10 x objective with an F-View II digital camera. ESC indicates embryonic stem cells; iPSC, induced pluripotent stem cells. Scale bar: 200 μm.

The number of EBs formed by both cell types showed a time dependent decrease and was similar (Figs 5.5). However, significant differences were detected in the number of ESC- and iPSC-derived EBs on day 1 of culturing, with more iPSC derived EBs being observed (ESCs, 299.4 ± 22.15 EBs; iPSCs, 396.4 ± 35.47 EBs; $p<0.05$; Fig. 5.5A). Using the same data to analyse each cell type individually, ESC-derived EBs were more abundant on day 1 (299.4 ± 22.15 EBs) when compared with day 4 (109.2 ± 22.54 EBs; $p<0.01$), day 2 (289.8 ± 27.06 EBs) compared with day 4 ($p<0.05$), and day 3 (190.4 ± 31.63 EBs) compared with day 4 ($p<0.05$; Fig. 5.5B). Interestingly, iPSCs derived EBs were also more numerous on day 1 (396.4 ± 35.47 EBs) compared with day 3 (191 ± 35.76 EBs; $p<0.001$) and 4 (145.8 ± 16.79 EBs; $p<0.01$; Fig. 5.5C).

The diameter of floating colonies were also examined on each successive day of the assay and found to increase significantly with time (Figs 5.6). Whilst the diameter of EBs appeared remarkably similar on day 1 of culturing for both cell type, ESC derived EBs subsequently appeared larger, with those formed on day 4 being significantly bigger than EBs formed from iPSCs (ESCs, 142.85 ± 3.4 μm; iPSCs, 123.68 ± 3.88 μm; $p<0.01$; Fig. 5.6A). Using the same data to analyse each cell type separately, both ESC and iPSC derived-EBs showed a stepwise increase in diameter that was remarkably similar, with significantly larger colonies being observed for both cell types on each day (Fig. 5.6B, C).

Analysis of EBs derived from ESCs and iPSCs across three independent cultures revealed expression of pluripotent stem cell and germ layer genes (Fig. 5.7). Four days after plating EBs, expression of the neuroectodermal marker nestin and the mesodermal marker BMP4 was detected in all samples derived from ESCs and iPSCs. However, the endodermal marker AFP was only detected in one culture derived from ESCs, with it being absent in other cultures. Furthermore, the pluripotent stem cell markers Oct4 and Nanog were still present at the gene level at this stage and were detected in EBs derived from both ESCs and iPSCs. GAPDH was also analysed to verify equal loading between samples.

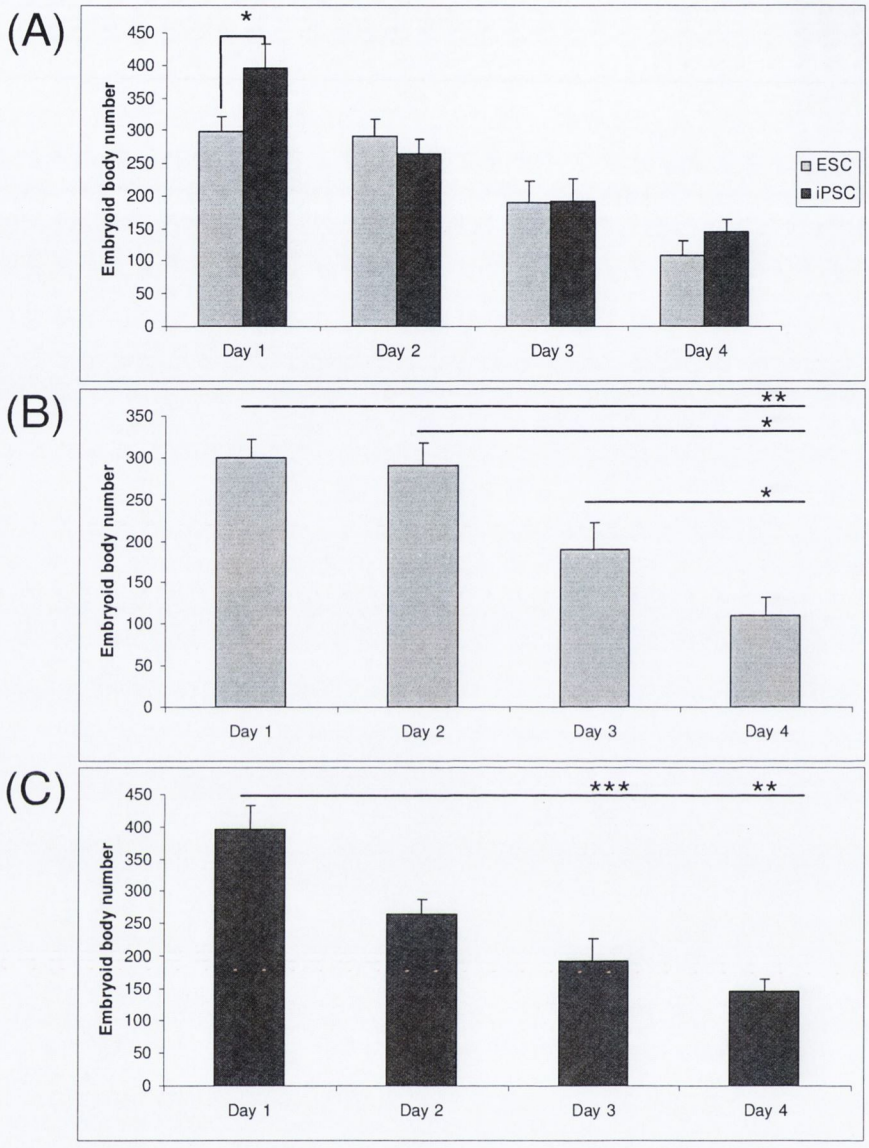

Figure 5.5: EBs derived from iPSCs are more numerous than those derived from ESCs on day 1 of 4 day culture period, while the number derived from each cell type decreases with increased culturing time

Undifferentiated ESCs and iPSCs were resuspended in EB medium in the absence of LIF and induced to form EBs in suspension culture. 20 randomly selected images were taken on each day over the next 4 days and the number of colonies present was counted in ImageJ. (A) Comparison of EB number between ESCs and iPSCs. Using the same data the number of EBs derived from ESCs (B) and iPSCs (C) were analysed separately. Data represents the mean + SEM of experiments performed on 5 independent cell populations. *$p<0.05$, **$p<0.01$, ***$p<0.001$. (A) One-way repeated measure ANOVA; (B), (C) Student's t-test.

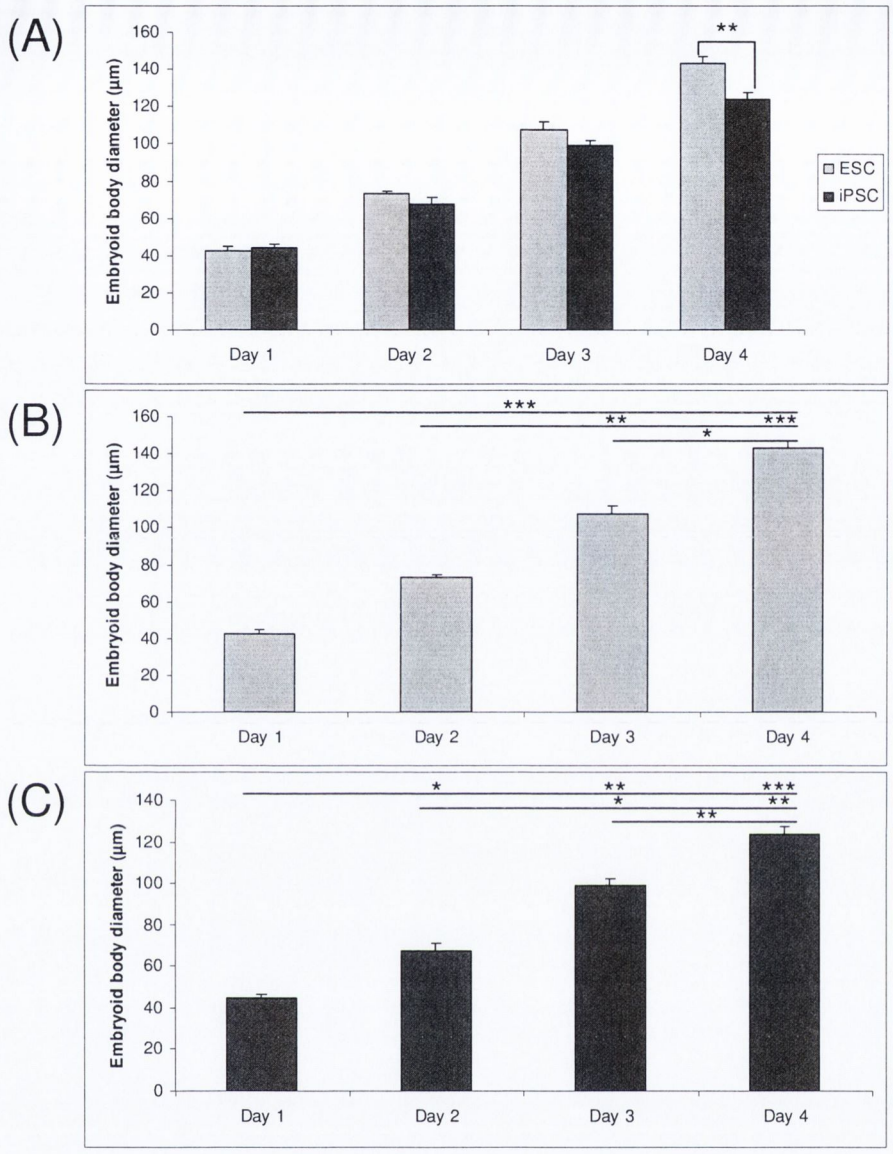

Figure 5.6: The diameter of ESC derived EBs are larger than those derived from iPSCs on day 4 of 4 day culture period, while the diameter of EBs derived from each cell type increases significantly in a step-wise fashion with time

Undifferentiated ESCs and iPSCs were resuspended in EB medium in the absence of LIF and induced to form EBs in suspension culture. Images were obtained of 50 randomly selected colonies each day over the next 4 days and diameters were measured using ImageJ. (A) Comparison of EB diameter between ESCs and iPSCs. Using the same data diameter of EBs derived from ESCs (B) and iPSCs (C) were analysed separately. Data represents mean + SEM of experiments performed on 5 independent cell populations. *$p<0.05$, **$p<0.01$, ***$p<0.001$. (A) One-way repeated measure ANOVA; (B), (C) Student's t-test.

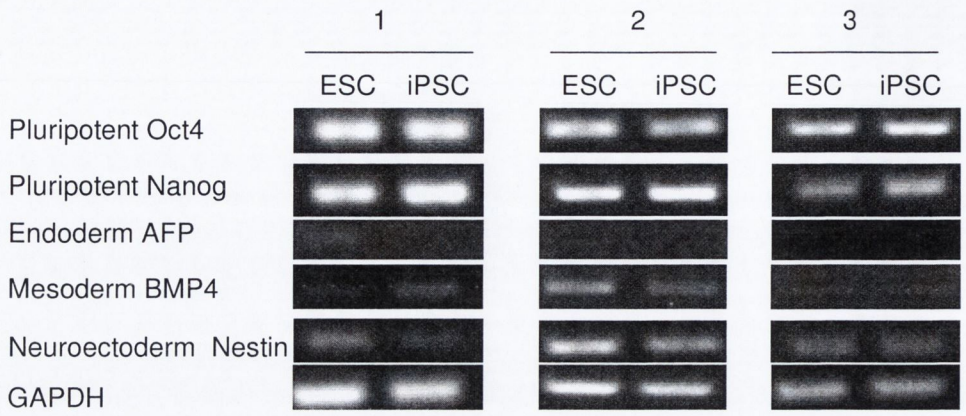

Figure 5.7: Embryoid bodies derived from ESCs and iPSCs express pluripotent stem cell and germ layer genes after 4 days in suspension culture

Total RNA was extracted from three independent cultures of EBs (1-3, as indicated) derived from ESCs and iPSCs 4 days after plating, and used to synthesis cDNA. One-twentieth of the reaction (1 µl) was subsequently used to investigate the presence of mesoderm (BMP4), neuroectoderm (nestin), endoderm (AFP) and pluripotent stem cell (Oct4, Nanog) mRNA. GAPDH was included to verify equality between samples. Samples were subsequently analysed by agarose gel electrophoresis. EB indicates embryoid body; ESC, embryonic stem cells; iPSC, induced pluripotent stem cells; BMP4, morphogenic protein 4, 398 bp; AFP, alpha fetoprotein, 252 bp, GAPDH, glyceraldehyde-3-phosphate dehydrogenase, 454 bp; Oct4, 312 bp; Nanog, 363 bp; Nestin, 327 bp.

5.3.3 iPSCs form neural stem spheres in suspension culture with a similar efficiency as ESCs

As neural differentiation is of particular importance, the ability of iPSCs to form NSSs was examined by growth in suspension culture in the presence of EGF and bFGF, with LIF being removed at this stage to induce differentiation. Undifferentiated iPSCs plated in non-adherent bacteriological dishes formed three dimensional colonies that increased in size and were morphologically similar to those formed by ESCs over a 4 day culture period (Fig. 5.8). The number of NSSs decreased for both cell types in a stepwise manner with increasing time (Figs 5.9). Comparison of the number of NSSs derived from iPSCs and ESCs revealed significantly fewer ESC derived NSSs on day 2 of culturing (ESCs, 211.8 $\pm$ 15.63 NSSs; iPSCs, 326 $\pm$ 42.34 NSSs; $p<0.05$; Fig. 5.9A).

Using the same data, examination of each cell type separately revealed that there was significantly less NSSs derived from ESCs on day 4 (102 $\pm$ 24.73 NSSs) when compared with the number on day 2 (211.8 $\pm$ 15.63 NSSs; $p<0.05$; Fig. 5.9B). Similarly, there was significantly less NSSs derived from iPSCs on day 4 (177.7 $\pm$ 22.18 NSSs; $p<0.05$) when compared to the number on day 1 (341.7 $\pm$ 30.24 NSSs; Fig. 5.9C).

In contrast to decreasing NSSs number with time in culture, the diameter of colonies was found to incrementally get larger on each day for both cell types (Figs 5.10). Although the diameter of NSSs was similar on day one of culturing for ESCs and iPSCs, differences in size where thereafter observed, with ESC derived NSSs becoming significantly larger on day 3 (ESCs, 113.18 $\pm$ 2.13 μm; iPSCs, 95 $\pm$ 3.02 μm; $p<0.01$) and day 4 (ESCs, 129.51 $\pm$ 3.05 μm; iPSCs, 106.39 $\pm$ 2.76 μm; $p<0.001$; Fig. 5.10A). Analysis of NSSs derived from ESCs and iPSCs individually using the same data revealed that the diameter of NSSs became significantly larger with each successive day in culture and this increase was remarkably similar for both cell types (Figs 5.10B, C).

Examination of NSSs derived from ESCs and iPSCs revealed a similar pattern of expression of neuroectodermal marker nestin on day 4 of culturing in three independent cultures (Fig. 5.11).

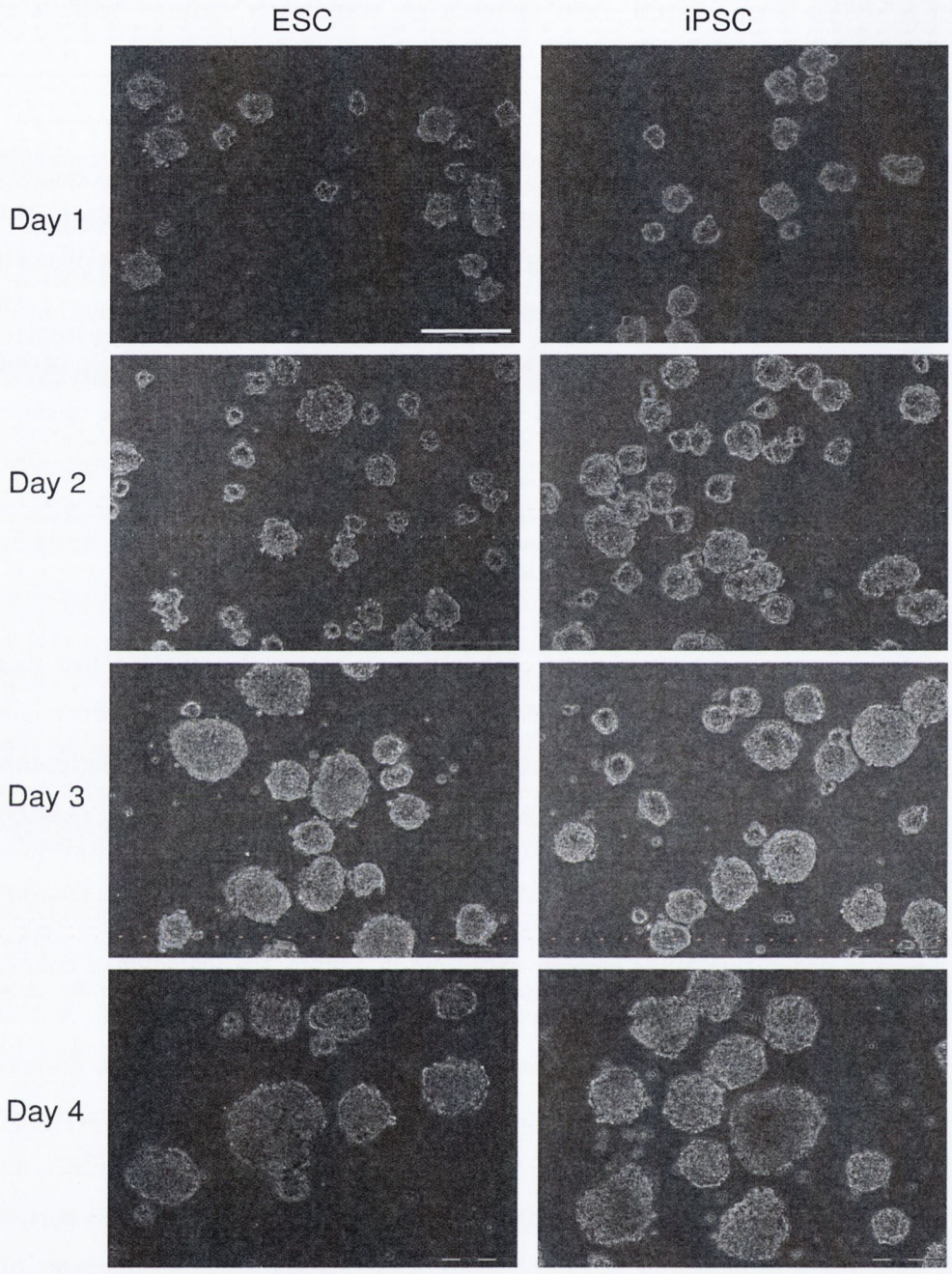

Figure 5.8: ESCs and iPSCs form morphologically similar neural stem spheres following growth in suspension cultures

Undifferentiated ESCs and iPSCs were resuspended in NSS medium in the absence of LIF and induced to form NSSs in suspension culture. Phase contrast images were obtained 1, 2, 3 and 4 days post-plating, as indicated, using an Olympus IX81-long focal length fluorescent microscope at 10 x objective with an F-View II digital camera. ESC indicates embryonic stem cells; iPSC, induced pluripotent stem cells. Scale bar: 200 μm.

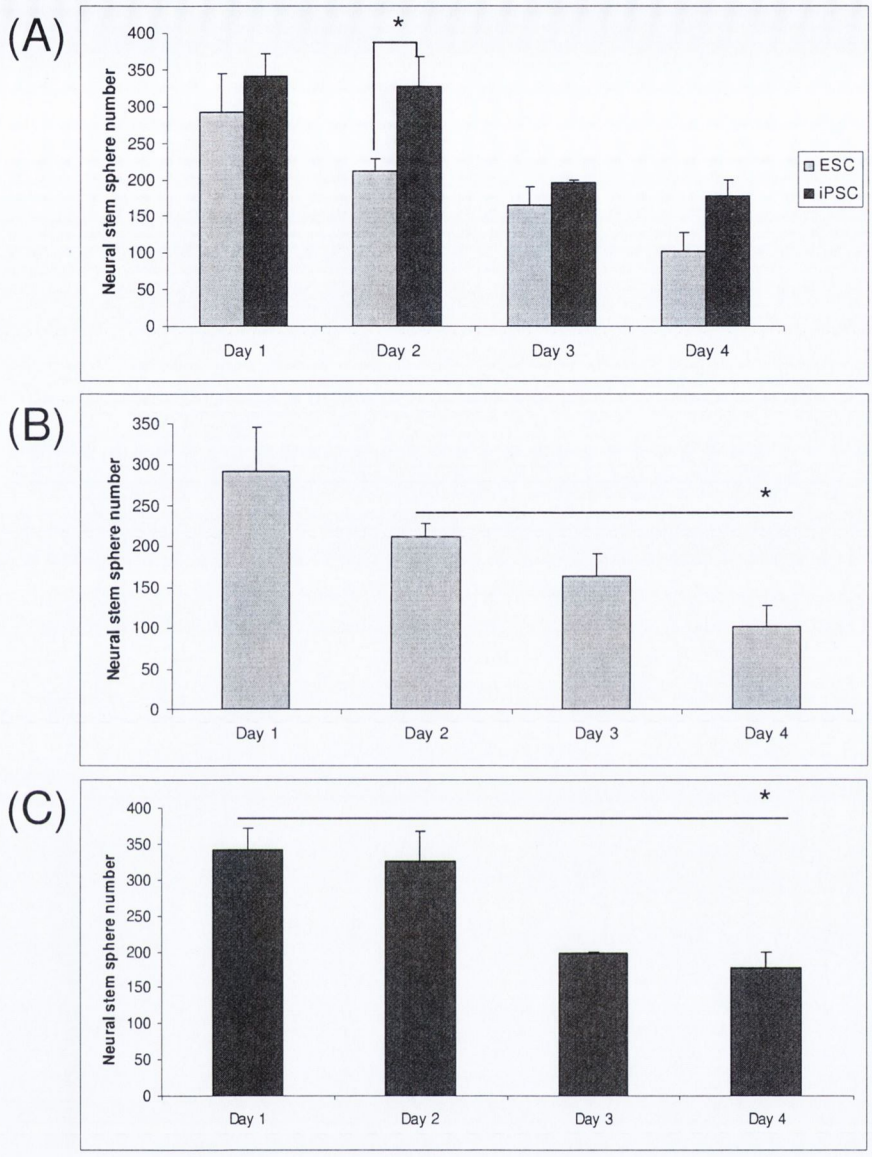

Figure 5.9: NSSs derived from iPSC are more numerous than those derived from ESCs on day 2 of 4 day culture period, while the number derived from each cell type decreases with increased culturing time

Undifferentiated ESCs and iPSCs were resuspended in NSS medium in the absence of LIF and induced to form NSSs in suspension culture. Twenty randomly selected images were taken over the next 4 days and the number of NSSs present was counted in ImageJ. (A) Comparison of NSS number between ESCs and iPSCs. Using the same data the number of NSSs derived from ESCs (B) and iPSCs (C) were analysed separately. Data represents the mean + SEM of experiments performed on 5 independent cell populations. *$p<0.05$. (A) One-way repeated measure ANOVA; (B), (C) Student's t-test.

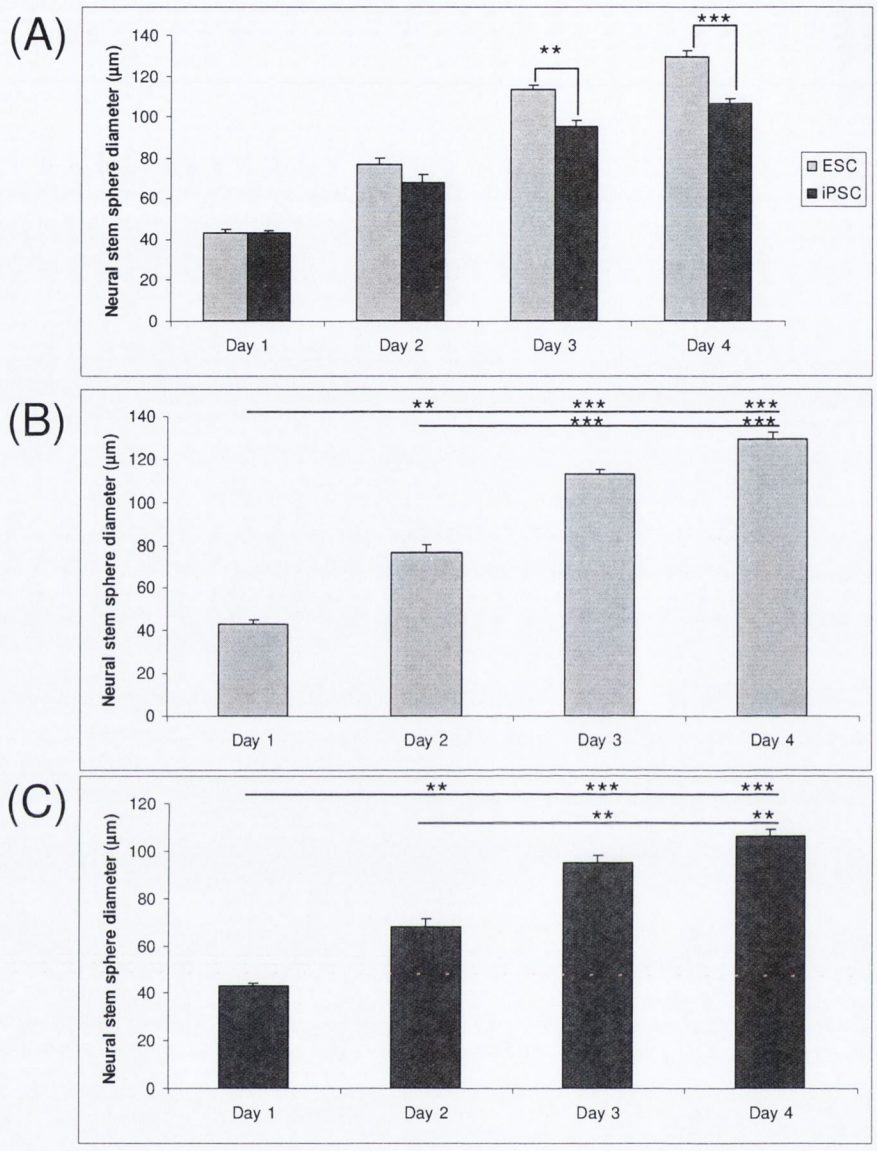

Figure 5.10: The diameter of ESC derived NSSs is larger than those derived from iPSCs on day 3 and 4 of 4 day culture period, while the diameter of colonies derived from each cell type become significantly larger with increased culturing

Undifferentiated ESCs and iPSCs were resuspended in NSS medium in the absence of LIF and induced to form NSSs in suspension culture. Images were obtained of 50 randomly selected NSSs over the next 4 days and diameters were measured using ImageJ. (A) Comparison of the diameter of NSSs derived from ESCs and iPSCs. Using the same data the diameter of NSSs derived from ESCs (B) and iPSCs (C) were analysed separately. Data represents mean + SEM of experiments performed on 5 independent cell populations **p<0.01, ***p<0.001. (A) One-way repeated measure ANOVA; (B), (C) Student's t-test.

NSSs derived from both cell types also expressed the neuronal protein Tuj1, with this being present in 3 independent cultures from ESCs and iPSCs (Fig. 5.12A). Semi-quantitative densitometry revealed no difference in Tuj1 protein levels between cell types (Fig. 5.12B).

To further assess the neural differentiation capacity of NSSs derived from iPSCs, NSSs were induced to form neurons using the growth factor induced neural differentiation procedure described in section 2.7.1 (Lau et al., 2006). In particular, NSSs were dissociated after 4 days in culture and plated in neural proliferation medium (containing growth factors EGF, FGF8, Shh) on a range of commonly used extracellular matrix proteins at two cell densities ($5x10^4$ cells/cm^2, $1x10^5$ cells/cm^2). These proteins included gelatine, laminin, fibronectin, poly-D-lysine (PDL), poly-L-ornithine (PLO), and combinations thereof (Fig. 5.13, section 2.6.7). Cells were found to attach well to all substrates examined 1 day after plating at both densities for iPSCs and ESCs and neural precursors were expanded for 5 days (Fig. 5.13). Differentiation was subsequently initiated by withdrawal of growth factors from culture medium. Ten days later, samples were fixed and probed for the neuronal marker Tuj1 (Fig. 5.13). By gross morphological analysis, Tuj1 positive colonies were formed by both ESCs (Fig. 5.13A, C) and iPSCs (Fig. 5.13B, D) on all substrates analysed at the two cells densities, with neurite extensions typically being more prominent at the lower cell density.

5.3.4 iPSCs form neurons with a similar efficiency as ESCs following neural differentiation in monolayer cultures

In order to investigate if iPSCs differentiated to neurons with a similar efficiency as ESCs, cells were plated at low density as a monolayer on gelatine coated plastic in chemically defined N2B27 medium in the absence of LIF (Section 2.7.2) (Ying and Smith, 2003; Ying et al., 2003). It has been reported that autocrine signalling is required for neural conversion in this system (Ying et al., 2003). Therefore it could be determined if the intrinsic mechanisms governing differentiation were similar in both cell types. In addition, this protocol facilitates the visualisation of the process of neural differentiation, which is circumvented when multicellular aggregates such as EBs and NSSs or co-culture with other cell types is used (Ying et al., 2003).

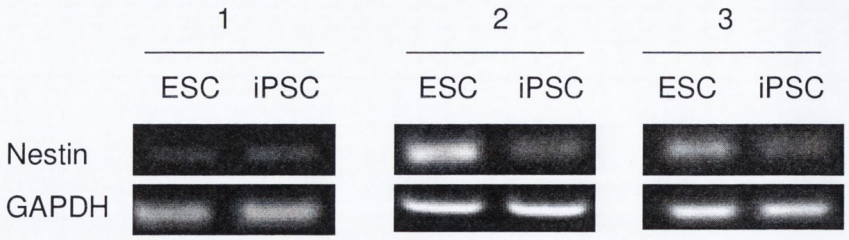

Figure 5.11: ESC and iPSC derived neural stem spheres express neuroectodermal marker nestin after four days in culture

Total RNA was extracted from three independent cultures of NSSs (1-3, as indicated) at day four of the culture period and used to synthesis cDNA. One-twentieth of the reaction (1 µl) was subsequently used to investigate the presence of the nestin mRNA. GAPDH was included to verify equality between samples. Samples were analysed agarose gel electrophoresis. ESC indicated embryonic stem cells; iPSC, induced pluripotent stem cells; GAPDH, glyceraldehyde-3-phosphate dehydrogenase, 454 bp; Nestin, 327 bp.

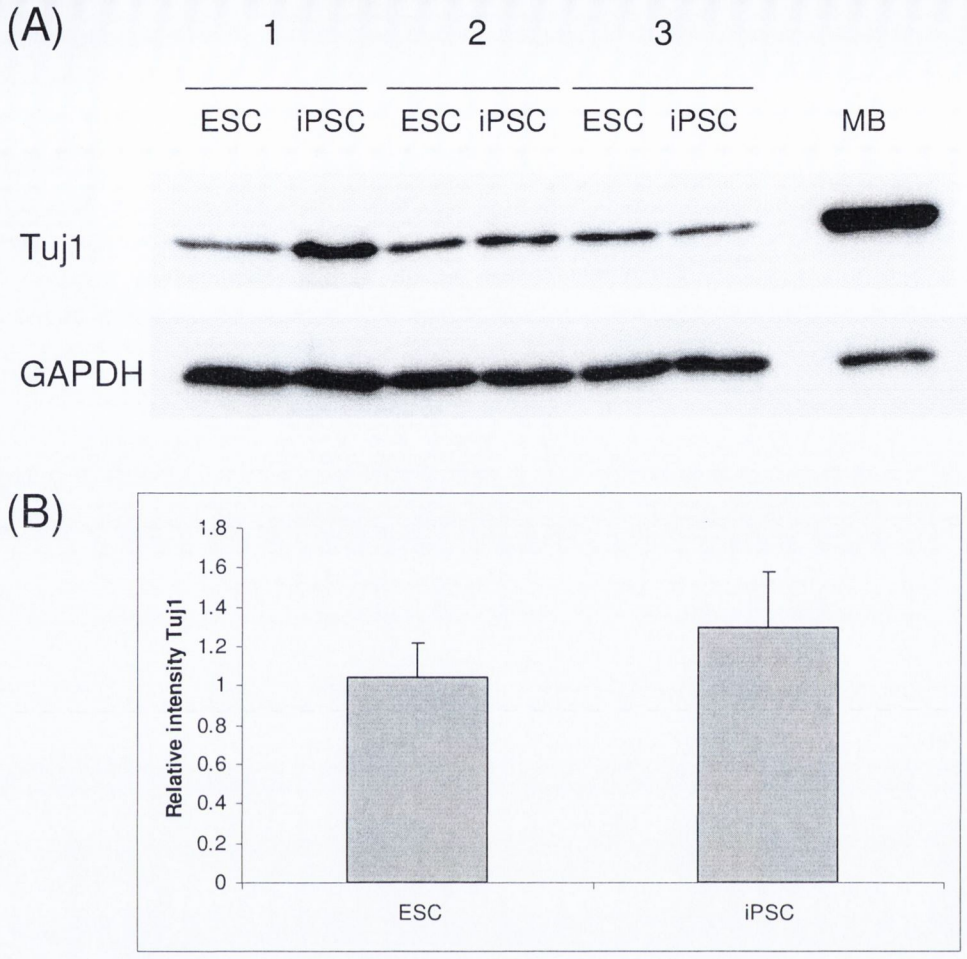

Figure 5.12: ESC and iPSC derived neural stem spheres express similar levels of the neuronal protein Tuj1 after 4 days of suspension culture

Protein was extracted from ESC and iPSC derived NSS on day 4 of culture and 30 µg from 3 independent cultures (1-3, as indicated) were run on a 12% SDS PAGE gel. Mouse brain lysate (MB) was run as positive control to identify the presence of Tuj1 protein. (A) Membranes were probed sequentially with anti-Tuj1 and anti-GAPDH antibodies. (B) Digital images were subsequently processed in ImageJ to calculate the amount of Tuj1 protein in each sample relative to GAPDH protein. Data represents the mean + SEM of experiments performed on 3 independent cell populations. ESC indicates embryonic stem cells; iPSC, induced pluripotent stem cells; GAPDH, glyceraldehyde-3-phosphate dehydrogenase, 36 kDa; Tuj1, 50 kDa.

Figure 5.13: ESC and iPSC derived neural stem spheres differentiate to neurons on a range of commonly used extracellular matrix proteins

Following 4 days of suspension culture, NSSs derived from ESCs and iPSCs were dissociated and plated at $5x10^4$ cells/cm^2 ((A) ESC , (B) iPSC) and $1x10^5$ cells/cm^2 ((C) ESC, (D) iPSC) on gelatine/laminin (Gel/Lam), poly-D-lysine/laminin (PDL/Lam), poly-D-lysine/fibronection (PDL/Fib), poly-L-ornithine/laminin (PLO/Lam), poly-L-ornithine/fibronectin (PLO/Fib), poly-L-ornititine/fibronectin/laminin (PLO/Fib/Lam), as indicated, in neural proliferation medium containing growth factors. Cell attachment was assessed one day later, as observed in phase contrast images for each substrate (Prolif Day 1). Terminal differentiation was induced 5 days later by removal of growth factors from proliferation medium. Samples were fixed and stained for Tuj1 (red) expression after 10 days and nuclei were counterstained with DAPI (blue). Phase contrast images were also obtained at this time point (Diff D10 PH). Samples were analysed using Olympus IX81-long focal length fluorescent microscopy using phase contrast, DAPI and Cy3 filters. Images were obtained at 10 x objective with an F-View II digital camera. Scale bar: 100 µm.

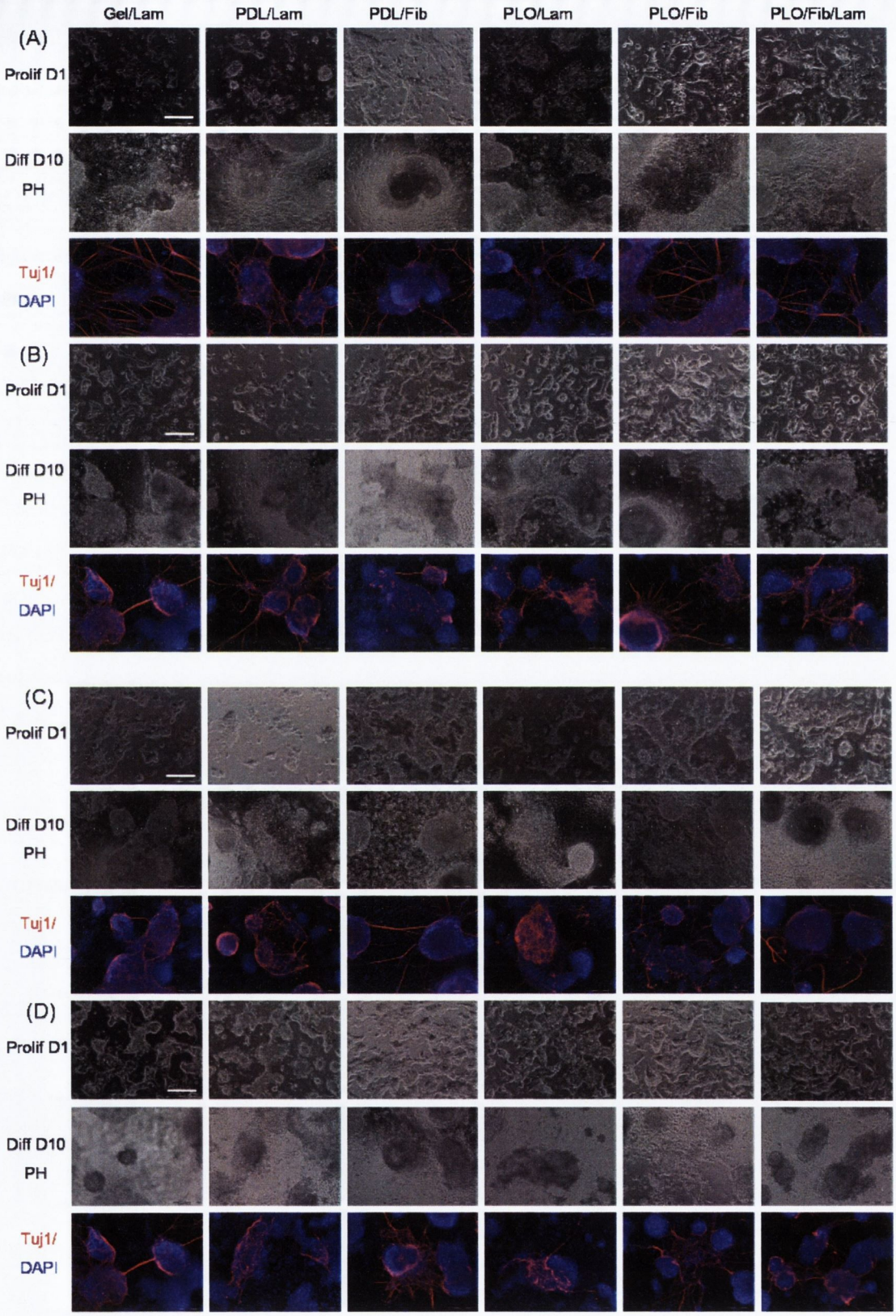
Gel/Lam
PDL/Lam
PDL/Fib
PLO/Lam
PLO/Fib
PLO/Fib/Lam
(A)
Prolif D1
Diff D10
PH
Tuj1/
DAPI
(B)
Prolif D1
Diff D10
PH
Tuj1/
DAPI
(C)
Prolif D1
Diff D10
PH
Tuj1/
DAPI
(D)
Prolif D1
Diff D10
PH
Tuj1/
DAPI

Daily microscopy analysis of ESCs and iPSCs during the process of differentiation revealed that they differentiated as colonies which were morphologically similar and typically increased in size with culture time (Fig. 5.14). For both cell types, the time point of neurite extension typically varied between independent culture procedures and often occurred around 10 days after the initiation of differentiation. In addition, this differentiation method appeared to support the long-term survival of both ESCs and iPSCs, with colonies extending neurites still present 24 days after differentiation was initiated (Fig. 5.14). Day 16 of differentiation was chosen as the time point to perform all subsequent analysis.

Staining of cultures at day 16 of differentiation revealed the presence of numerous Tuj1 positive colonies that appeared to be morphologically similar in both cell types (Fig. 5.15). In particular, Tuj1 colonies of varied size were typically detected that displayed extensive neurite branching (Fig. 5.15). Indeed, analysis of Tuj1 colony number and diameter revealed no significant difference between ESCs and iPSCs (ESCs, 9.78 $\pm$ 0.78 colonies; iPSCs, 8 $\pm$ 0.58 colonies; Fig. 5.16; ESCs, 344.79 $\pm$ 13.08 µm; iPSCs, 366.24 $\pm$ 27.95 µm; Fig. 5.17). Tuj1 colonies from both ESCs and iPSCs were also found to extend very long neurites after differentiation which again appeared similar for both ESCs and iPSCs by gross morphological analysis (Fig. 5.18). In fact, no difference was detected in the mean neurite length between ESCs and iPSCs (Fig. 5.19).

Analysis of cellular proteins at day 16 of differentiation showed a similar pattern of expression in both cell types (Fig. 5.20). However, high variability existed across different cultures. This is evidenced by inconsistent expression of Tuj1 protein from independent differentiation procedures. Synaptophysin protein was detected at low levels in one ESC preparation only, with iPSCs not expressing this pre-synaptic protein marker after any differentiation procedures. DAT protein was detected in all samples but expression levels were variable.

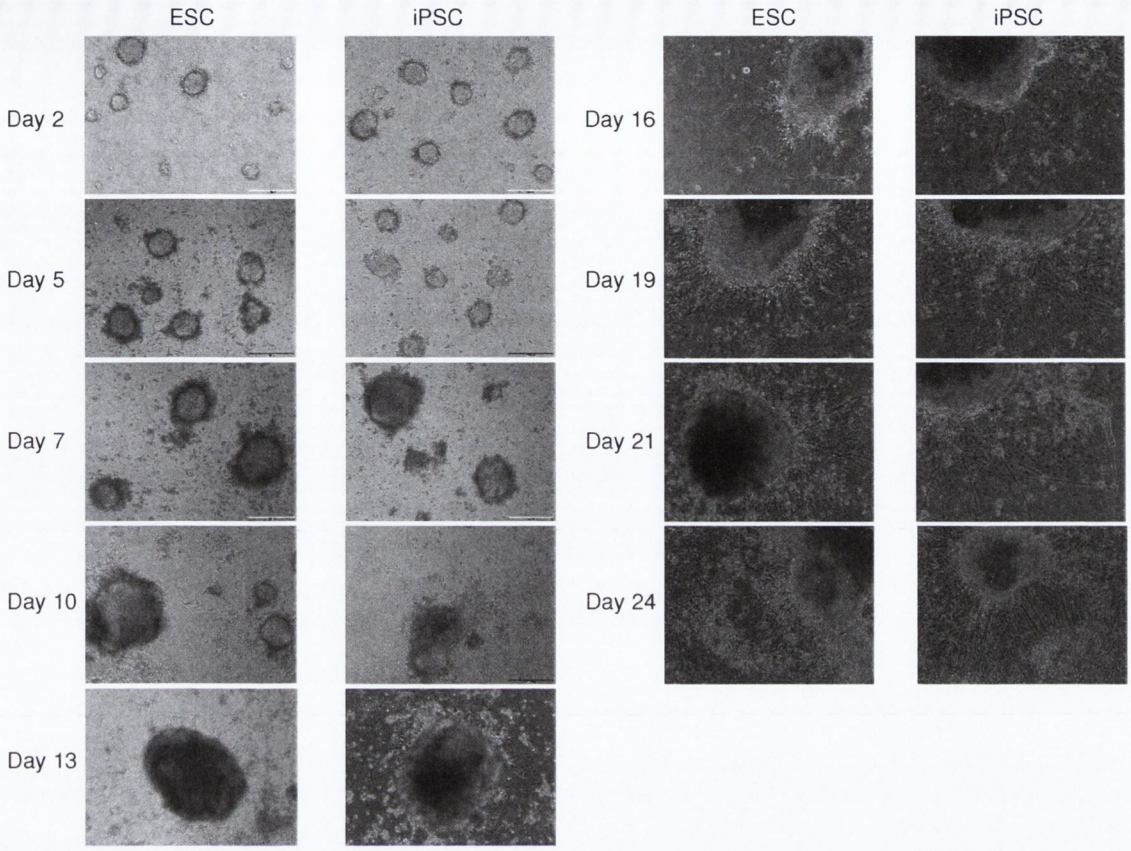

Fig. 5.14: ESCs and iPSCs appear morphologically similar during the process of monolayer neuronal differentiation, with colonies becoming larger and extending neurites with increased culturing time

ESCs and iPSCs were plated at a density of $1.5x10^4$ cells/cm^2 on plastic in embryonic stem cell medium. The following day, medium was changed to N2B27 medium and thereafter changed every two days. The morphology of cells was analysed with an Olympus IX81-long focal length fluorescent microscopy at phase contrast on the indicated days. Images were obtained at 10 x objective with an F-View II digital camera at indicated time points. ESC indicates embryonic stem cells; iPSC, induced pluripotent stem cells. Scale bar: 200 µm.

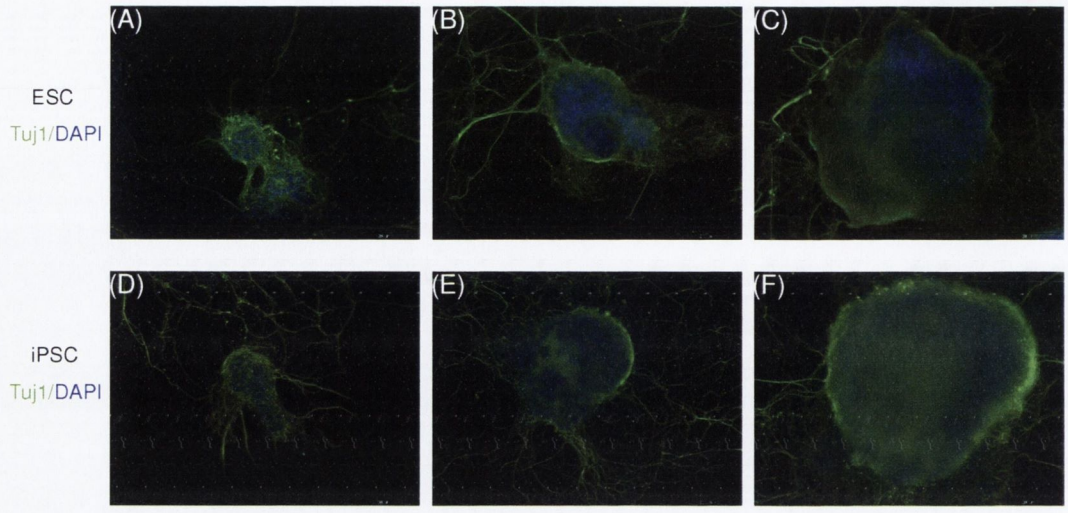

Figure 5.15: ESCs and iPSCs form Tuj1 positive colonies of different sizes with extensive branching after 16 days of monolayer neuronal differentiation

Cells were fixed and stained for Tuj1 (green) expression at day 16 of monolayer neuronal differentiation. Nuclei were counterstained with DAPI (blue). Representative images of ESCs (A, B, C) and iPSCs (D, E, F) from a single culture are shown illustrating Tuj1 colonies of different sizes. Samples were analysed using Olympus IX81-long focal length fluorescent microscopy using DAPI and GFP filters and images were captured at 10 x objective with an F-View II digital camera. Scale bar: 200 μm.

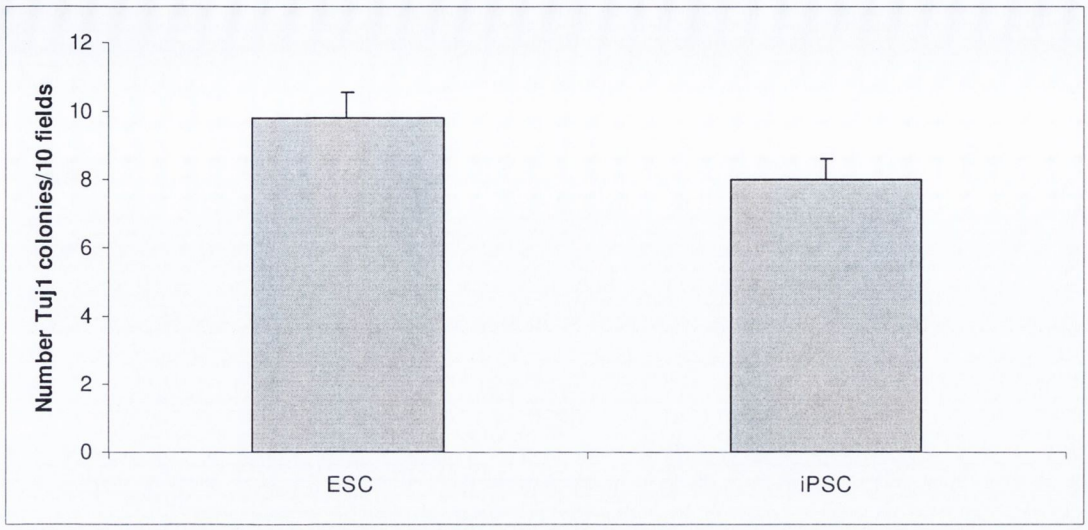

Figure 5.16: A similar number of Tuj1 positive colonies are derived from ESCs and iPSCs after 16 days of monolayer neuronal differentiation

ESCs and iPSCs were fixed and stained for Tuj1 expression at day 16 of monolayer neuronal differentiation. Ten randomly selected images were taken per well and the number of Tuj1 positive colonies was counted. Data shown represent the mean + SEM of experiments performed in triplicates on three cell populations.

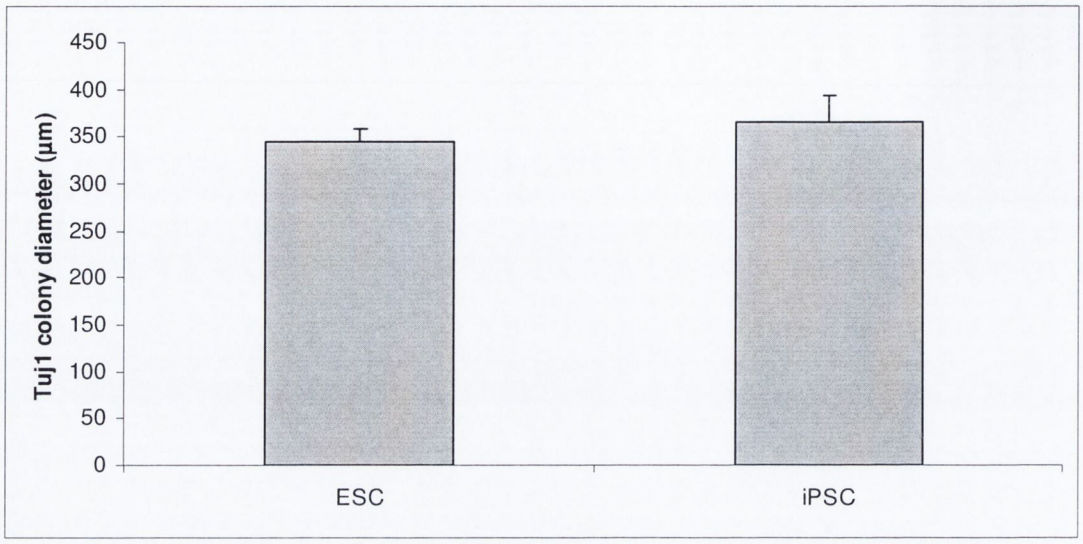

Figure 5.17: The diameter of Tuj1 positive colonies derived from ESCs and iPSCs is similar size following 16 days of monolayer neuronal differentiation

ESCs and iPSCs were fixed and stained for Tuj1 expression at day 16 of monolayer neuronal differentiation. Ten randomly selected images were taken of Tuj1 positive colonies per well for each cell type and the diameter of these colonies was measured in ImageJ. Data shown represent the mean + SEM of experiments performed in triplicates on three cell populations.

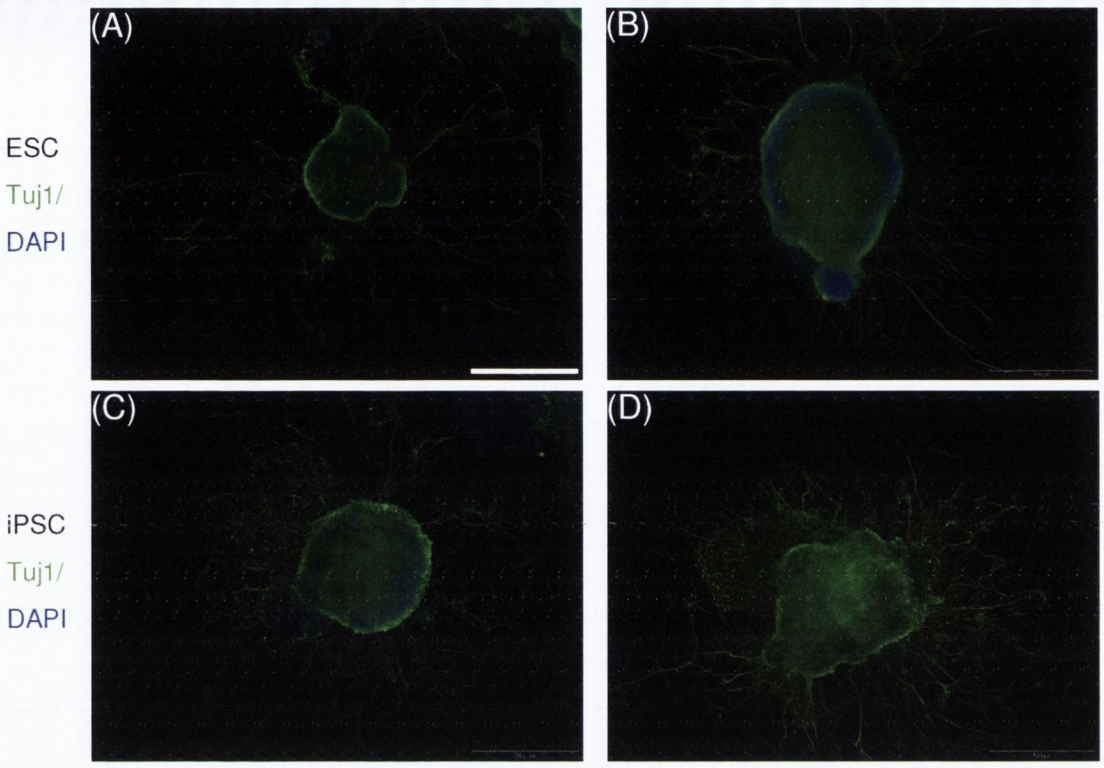

Figure 5.18: Tuj1 positive colonies derived from ESCs and iPSCs project extensive neurites after 16 days of monolayer neuronal differentiation

ESCs (A, B) and iPSCs (C, D) were fixed and stained for Tuj1 (green) expression at day 16 of monolayer neuronal differentiation. Nuclei were counterstained with DAPI (DAPI). Samples were analysed using Olympus IX81-long focal length fluorescent microscopy using DAPI and GFP filters and images were captured at 4 x objective with an F-View II digital camera. Scale bar: 500 µm.

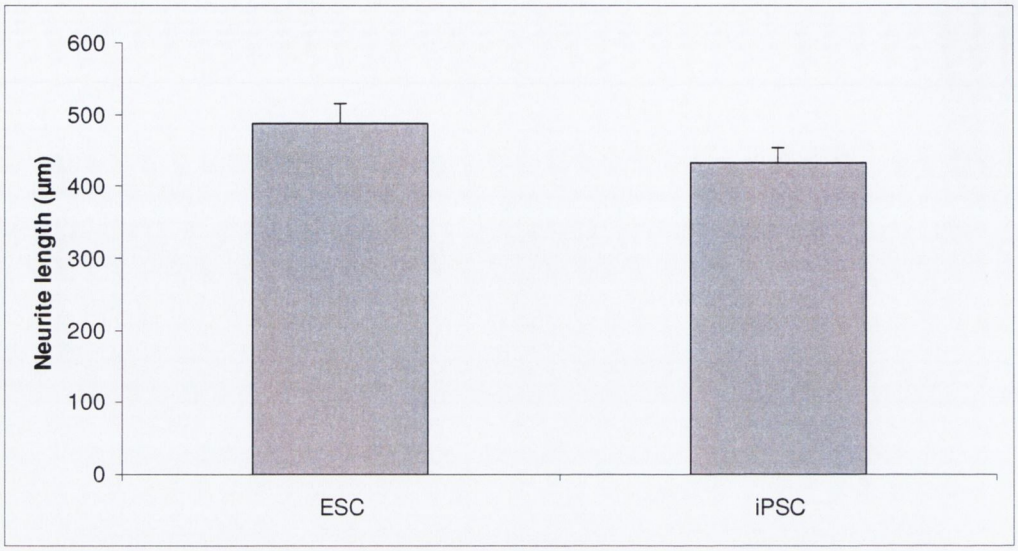

Figure 5.19: No difference exists between neurite length of ESC and iPSC derived Tuj1 positive colonies following 16 days of monolayer neuronal differentiation

ESCs and iPSCs were fixed and stained for Tuj1 expression on day 16 of monolayer neuronal differentiation. Five Tuj1 positive colonies were randomly selected per well and the length of 10 randomly selected neurites per colony was measured using the NeuronJ application of ImageJ. Data shown represent the mean neurite length + SEM of experiments performed in duplicates on three populations.

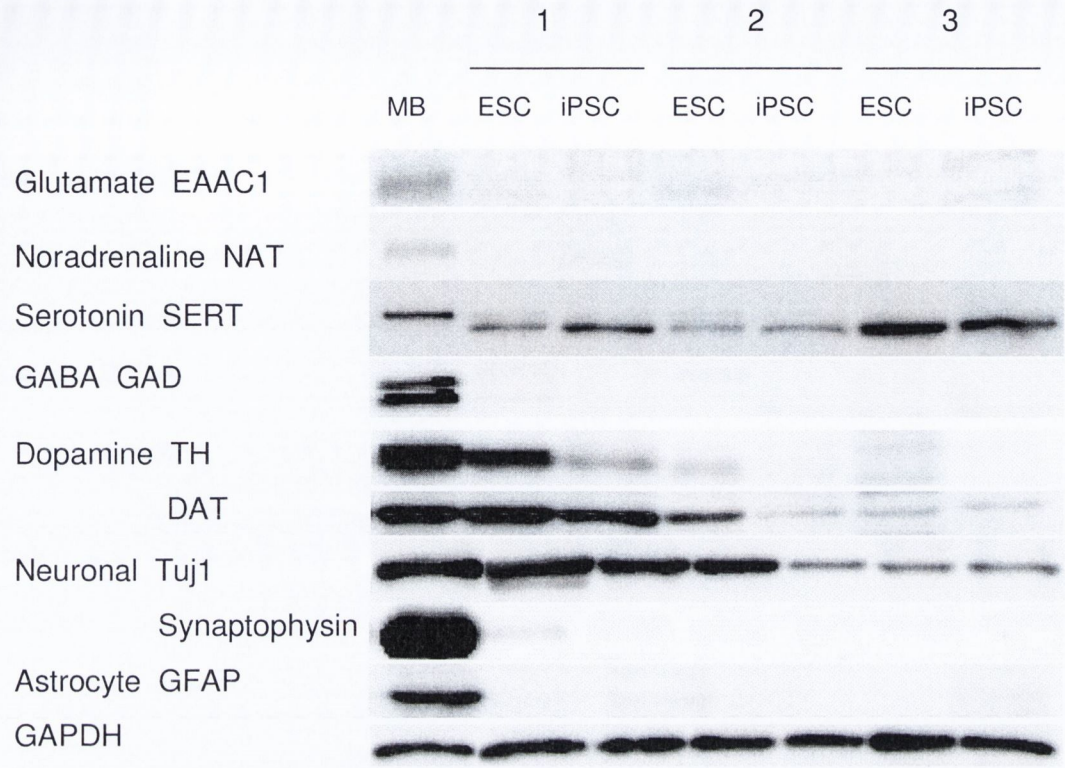

Figure 5.21: High variability exists in the expression levels of neuronal proteins derived from ESCs and iPSCs following 16 days of monolayer neuronal differentiation

Protein was extracted from ESCs and iPSCs 16 days after the induction of monolayer differentiation in three independent cultures (1-3, as indicated) and 20 µg was run on 10% SDS-PAGE gels. Mouse brain lysate (MB) was run as positive control to identify the presence of neuronal proteins. Membranes were probed with antibodies for each neuronal subtype, as indicated. GAPDH was analysed to verify equal loading and a representative blot is shown. ESC indicates embryonic stem cells; iPSC, induced pluripotent stem cells; GAPDH, glyceraldehyde-3-phosphate dehydrogenase, 36 kDa; Tuj1, 50 kDa; synaptophysin, 38 kDa; GFAP, glial fibrillary acidic protein, 50 kDa; TH, tyrosine hydroxylase, ~66 kDa; DAT, dopamine transporter, ~55 kDa; GAD, glutamic acid decarboxylase, 65 and 67 kDa; NAT, noradrenergic transporter, ~80 kDa; EAAC1, excitatory amino acid transporter, ~69 kDa; SERT, serotonin transporter, ~100 kDa.

DAT was also detected by immunocytochemistry in differentiated populations for both cell types, with neurites and cell soma typically stained in ESCs and iPSCs (Fig. 5.21). TH was detected in one ESC sample and one iPSC sample. TH was also analysed at the cellular level by immunocytochemistry and a similar pattern of staining was observed for both cell types (Fig. 5.23). Protein markers typical of the GABAergic (GAD), serotonergic (SERT), glutamatergic (EAAC1) and noradrenergic (NAT) systems were absent. The band detected with the SERT antibody is lower than the mouse brain positive control and as this antibody was highly specific it is presumed to be a cleavage product. GFAP protein was also missing from both cell types, indicating the absence of astrocytes in these differentiated populations.

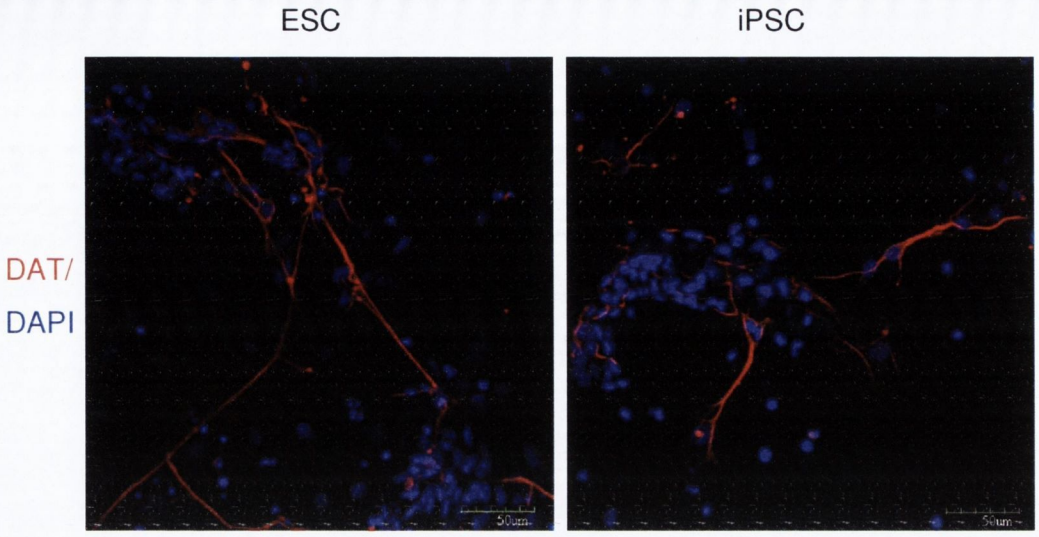

Figure 5.21: Visualisation of dopamine transporter positive cells derived from ESCs and iPSCs following 16 days of monolayer neuronal differentiation

ESCs and iPSCs were fixed and stained for DAT (red) expression on day 16 of monolayer neuronal differentiation, as indicated. Nuclei were counterstained with DAPI (blue). Images were acquired with an Olympus FV1000 laser scanning confocal microscope set to UPlanSAPO 40 x oil objective. ESC indicates embryonic stem cells; iPSC, induced pluripotent stem cells; DAT, dopamine transporter. Scale bar: 50 µm.

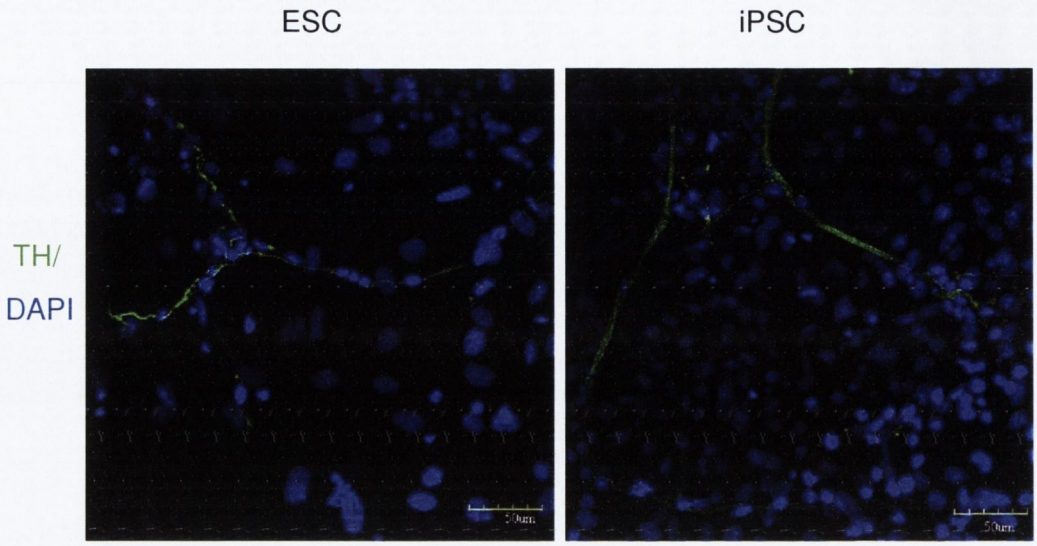

Figure 5.22: Visualisation of tyrosine hydroxylase positive cells derived from ESCs and iPSCs following 16 days of monolayer neuronal differentiation

ESCs and iPSCs were fixed and stained for TH (green) expression on day 16 of monolayer neuronal differentiation, as indicated. Nuclei were counterstained with DAPI (blue). Images were acquired with an Olympus FV1000 laser scanning confocal microscope set to UPlanSAPO 40 x oil objective. ESC indicates embryonic stem cells; iPSC, induced pluripotent stem cells; TH, tyrosine hydroxylase. Scale bar: 50 µm.

5.4 Discussion

It is of the utmost importance to validate iPSC clones prior to use in experimentation (Takahashi and Yamanaka, 2006). Therefore the iPSC clone selected for investigation in this chapter was first examined for the expression of key markers of undifferentiated pluripotent stem cells, and no differences were detected when compared with ESCs. In particular, iPSCs expressed the undifferentiated pluripotent stem cell surface antigen SSEA1 and appeared morphologically similar to ESCs (Fig. 5.1). iPSCs also expressed the pluripotent transcription factors Oct4 and Nanog, with levels comparable to ESCs (Fig. 5.2). The presence of Nanog is of particular importance as Oct4 was one of the four reprogramming genes used to derive iPSCs from fibroblasts and thus shows that endogenous pluripotent stem cell genes have been activated. iPSCs also displayed similar growth characteristics as ESCs, with population doubling rate of 15.7 hours and 14.7 hours, respectively (Fig. 5.3). This also roughly corresponds with the typically generation time for ESCs of ~12-15 hours (Rohwedel et al., 1996).

The pluripotency of the iPSC clone was tested by formation of EBs in suspension in the absence of LIF (Takahashi and Yamanaka, 2006). EBs derived from iPSCs were morphologically similar to those derived from ESCs, forming three-dimensional cellular aggregates that remained suspended in culture medium over the 4 day culture period (Fig. 5.4). In agreement with previous reports regarding growth of EBs in static culture (Khoo et al., 2005; Cameron et al., 2006), EBs decreased in number and increased in size in a step-wise fashion with time for both cell types (Figs 5.5, 5.6). EBs derived from iPSCs was found to be more numerous than those derived from ESC on day 1 of the culture period (Fig. 5.5A). Furthermore, the diameter of EBs derived from iPSCs was smaller than those derived from ESC on day 4 (Fig. 5.6A). Thus, while the overall morphology of EBs derived from iPSCs was similar to ESCs, time dependent differences in EB number and size existed. Differentiation of EBs has previously been shown to be characterised by a progressive maturation that mirrors molecular events during normal embryonic development, with the stages equivalent to embryogenesis between implantation and the beginning of gastrulation (E4.5-6.5 in mouse embryo) occurring within the first two days of EB differentiation (Leahy et al., 1999). Between days 3 and 5, EBs contain cell lineages

found in embryos during gastrulation at E6.5 to 7.0, and after day 6 in culture, EBs are equivalent to early organogenesis-stage embryos (E7.5) (Leahy et al., 1999). Similarities were observed in expression of germ layer and pluripotent stem cell markers between ESCs and iPSCs, as determined by RT-PCR (Fig. 5.7). EBs derived from both cell types expressed the pluripotent stem cells makers Oct4 and Nanog over three independent cultures, which has previously been reported to be expressed in EBs derived from ESCs (Mogi et al., 2009). This indicates that not all cells in the floating colonies had initiated differentiation at the time point of the assay. Nestin was analysed as a marker for neuroectoderm (Kawaguchi et al., 2001) and have also been detected in ESC and iPSC derived EBs in all cultures analysed, as previously described for ESC derived EBs (Mogi et al., 2009). BMP4 is recognised as a marker of early mesodermal differentiation (Winnier et al., 1995; Aubert et al., 2003) and was present in all EBs derived from ESCs and iPSCs, in agreement with previous analysis of EBs formed from ESCs (Choi et al., 2010). Low levels of the endodermal marker AFP (Kwon et al., 2006) were detected in one EB culture derived from ESCs but not the other two cultures. Furthermore it was not detected in EBs derived from iPSCs. Expression of AFP has previously been reported to be detected in EBs at day 5 of suspension culture and increase thereafter (Abe et al., 1996), and this may explain the results observed here. Further insight may be garnered by analysis of an earlier endodermal marker, such as Foxa2, which has been detected in ESC derived EBs at this stage (Mogi et al., 2009). In conclusion, EBs derived from iPSCs are highly comparable to those derived from ESCs based on morphology and gene expression analysis.

The neural differentiation efficiency of iPSCs was analysed by the formation of NSSs in floating culture in the presence of EGF and bFGF, as described by Lau et al. (2006). Colonies derived from iPSCs were morphologically similar to those derived from ESCs and were found to decrease in number and to increase in size with increased culture time (Figs 5.8-5.10), as preciously reported (Lau et al., 2006). Of particular note, NSSs derived from iPSCs were found to be more numerous than those derived from ESCs on day 2 (Fig. 5.9A), while the diameter of NSSs derived from ESCs were larger than those derived from iPSCs on day 3 and 4 (Fig. 5.10A).

Analysis of neuroectodermal marker nestin in NSSs at day 4 of differentiation by RT-PCR revealed similarities between both cell types, with it being detected in three cultures from ESCs and iPSCs (Fig. 5.11). The neuronal marker Tuj1 was also detected at this stage in NSSs derived from both ESCs and iPSCs (Fig. 5.12). In addition, no difference in Tuj1 protein levels were detected between samples (Fig. 5.12). It has been reported that Tuj1 expression is initiated either during or immediately after terminal mitosis of newly born neurons (Lee et al., 1990) and therefore suggests that post-mitotic neurons are already formed at this early stage during the differentiation process.

Extracellular matrix proteins, such as laminin, fibronectin and collagen, provide key extracellular cues in the development of the nervous system (Letourneau et al., 1994). These proteins have also been reported to support *in vitro* neuronal differentiation of ESCs (Li et al., 1998; Lee et al., 2000; Ying and Smith, 2003; Goetz et al., 2006; Lau et al., 2006). Therefore, a simple assay was performed to assess the attachment and neuronal differentiation efficiency of dissociated NSSs derived from both ESCs and iPSCs on a range of commonly used substrates (Fig. 5.13). These included laminin, fibronectin, PLO, PDL, gelatine and combinations thereof. In addition, cells were plated at two densities ($5x10^4$ cells/cm^2, $1x10^5$ cells/cm^2) as plating density has been reported to be an important factor in neuronal differentiation of ESCs (Ying and Smith, 2003; Lorincz, 2006), with low cell densities often resulting in poor cell survival, while high cell densities may promote differentiation to non-neuronal lineages (Ying and Smith, 2003; Lorincz, 2006). Gross morphological analysis of cells one day after plating by light microscopy demonstrated that all substrates promoted cell attachment at both densities for ESCs (Fig. 5.13A, C) and iPSCs (Fig. 5.13B, D). Further neuronal differentiation resulted in the generation of small spherical Tuj1 positive colonies at both cell densities and on all substrates examined (Fig. 5.13). By gross morphological analysis it was determined that these colonies appeared similar for ESCs and iPSCs, with neurite extensions typically being more prominent at lower densities, possibly due to fewer cells in these cultures. Thus, from these experiments it was concluded that iPSCs could differentiate to a neurons with a similar efficiency as ESCs.

The neural differentiation efficiency of iPSCs was also investigated by the formation of neurons using a monolayer differentiation procedure. In this method neural conversion is induced by culturing cells in monolayers in chemically defined medium in the absence of extrinsic growth factors (Ying et al., 2003). It has been reported that autocrine FGF signalling is required for this process (Ying et al., 2003), with inhibition of FGF signalling preventing neural specification by ESCs upon LIF withdrawal. Thus it can be assessed if the intrinsic regulatory mechanisms governing differentiation are similar in both cell types. Differentiation in this manner also facilitates the visualisation of the process of neural conversion, which is circumvented when multicellular aggregates such as EBs and NSSs or co-culture with other cell types is used (Ying et al., 2003). ESCs and iPSCs differentiated as colonies using this method, which typically increased in size with time in culture and appeared morphologically similar (Fig. 5.14). The time point at which neurites extended from colonies typically varied between different culture procedures. This is not unexpected as it has previously been noted that not all cells behave identically in cultures, with neural conversion being an asynchronous and stochastic process (Ying et al., 2003)

As stated, cells differentiated primarily as colonies and therefore Tuj1 staining was performed to analyse if similarities, or differences, existed between the neuronal populations derived from both cell types. Interestingly, Tuj1 positive colonies of different sizes were observed in differentiated populations from ESCs and iPSCs, which were morphologically comparable (Fig. 5.15). Indeed, no differences were found between cells in relation to the number or diameter of Tuj1 colonies across differentiation procedures (Figs 5.16, 5.17). Furthermore, extensive neurites projected from Tuj1 colonies derived from ESCs and iPSCs, which often formed branched structures (Fig. 5.18). Analysis of the mean length of randomly selected neurites across differentiation procedures did not detect any differences between the cell types (Fig. 5.19).

Analysis of the neuronal subtypes generated after differentiation also revealed similarities between ESCs and iPSCs (Fig. 5.20). However, high variability existed across cultures, with inconsistent expression of the neuronal protein Tuj1 in both ESCs and iPSCs. As the number of Tuj1 positive colonies remained relatively constant across cultures for both cell types (Fig. 5.16), it is possible that even using this differentiation procedure which has been

reported to robustly generate neurons (Ying et al., 2003) that cells also differentiated to alternative lineages and thus the proportion of neuronal proteins in the total cellular protein lysate may be variable. Indeed, the generation of heterogeneous cell population after differentiation of ESCs has been widely reported (Stavridis and Smith, 2003; Pruszak et al., 2007) and, as discussed in previously chapters, is a significant hurdle to overcome in the use of ESCs.

Surprisingly the GABAergic marker GAD were absent from neurons derived from both ESCs and iPSCs at day 16 of monolayer differentiation (Fig. 5.20), even though this neuronal subtype has been reported to be readily generated by this differentiation procedure (Ying et al., 2003). In addition, no GFAP protein was detected in any samples (Fig. 5.20), suggesting that this method does not support the robust development of astrocytes from pluripotent stem cells, at least by day 16 analysed here. This finding is in agreement with results in chapter 4, in which GFAP protein was not detected in any samples of 46C ESCs following monolayer differentiation (Fig. 4.6). Importantly, as GFAP was absent from differentiated populations of both cell types it suggests that iPSCs may still have the potential to generate astrocytes but alternative culturing conditions are required to induce their formation, such as increased differentiation time or application of specific growth factors (Brustle et al., 1999; Barberi et al., 2003).

Protein expression of the DA markers TH and DAT was also found to be inconsistent across cultures, but DAT protein was detected, at least at low levels, in each independent sample for both cell types (Fig. 5.20). TH protein was also detected in one neuronal culture derived from iPSCs and two derived from ESCs (Fig. 5.20). The generation of DA neurons by this differentiation procedure is in agreement with previous reports suggesting that this neuronal subtype can form in the absence of extrinsic growth factors (Parmar and Li, 2007; Friling et al., 2009). In addition, TH and DAT were detected at the cellular level at day 16 of differentiation for both ESCs and iPSCs (Figs 5.21, 5.22). Wernig et al. (2008) have also recently shown that TH+ neurons can be derived from numerous mouse iPSC clones (generated by retroviral transfection with Oct4, c-Myc, Klf4 and Sox2) following neuronal differentiation and treatment with high concentration of SHH and FGF8, with these TH+

cells also expressing markers typical of midbrain DA neurons such as Pitx3 and Nurr1. However, no comparison was made to ESCs in this study.

The pre-synaptic vesicular protein synaptophysin was absent in all but one ESC sample, with expression very low in this sample, and all iPSC samples (Fig. 5.21). As synaptophysin is missing in both ESCs and iPSCs, it indicates that a deficiency is not inherent to iPSC derived neurons. Furthermore, this absence of synaptophysin expression is in agreement with the results of chapter 4 in which synaptophysin was not detected in samples differentiated by this method (Fig. 4.6). As synaptophysin is a major intrinsic membrane protein of synaptic vesicles that is widely expressed in presynaptic nerve terminals in the brain (Marqueze-Pouey et al., 1991; Fykse et al., 1993) and has been correlated with synapse formation and maturation (Knaus et al., 1986), it absence suggests that monolayer neuronal differentiation may not support these processes, or that they have not yet developed by day 16 of differentiation when samples were harvested. However, as both iPSCs and ESCs differentiated to Tuj1 positive colonies that extended long branching neurites (Fig. 5.18), it indicates that the extracellular guidance cues and intracellular signalling events regulating neurite outgrowth (for reviews, see Dickson, 2002; Henley and Poo, 2004; Hansen et al., 2008) are present in these cultures but the intrinsic signals or extracellular factors governing synapse formation (for review, see Waites et al., 2005) are not. Alternatively, it is possible that a small subset of cells have developed mature nerve terminals and synaptophysin protein levels are too low in total cellular protein to be detected. This may be clarified by performing immunocytochemistry to analyse expression of this protein at the cellular level.

It is important to note that recent studies suggest that iPSCs have the potential to form functionally mature neurons (Wernig et al., 2008; Hu et al., 2010). Wernig et al. (2008) reported that implantation of neural cells derived from three iPSC clones into the brain of mouse embryos *in utero* displayed electrophysiological properties of mature functional neurons when analysed in the adult brain. However, no functional analysis of *in vitro* differentiated neurons was performed by Wernig et al. (2008). Hu et al. (2010) have also reported that human iPSC-derived neurons extend long Tuj1 process that express the presynaptic protein synapsin and become electrophysiologically active after extended

culturing (Hu et al., 2010). Thus as iPSCs formed extensive Tuj1-positive neurites in this study (Fig. 5.18), it is possible that increased differentiation time or culturing with astrocytes, which are thought to play a role in synaptogenesis (for reviews, see Eroglu and Barres, 2010; Pfrieger, 2010) and have been shown to significantly accelerate the onset of synaptic activity in human ESC-derived neurons (Johnson et al., 2007), may result in the formation or maturation of synapses in iPSC derived neurons.

In conclusion, the experiments performed here suggest that the neural differentiation capacity of iPSCs is comparable to that of ESCs, based on the formation of NSSs and neurons, and expression of neuroectodermal and neuronal markers. This is in agreement with data regarding the cardiomyocyte differentiation potential of mouse iPSCs, which was found to be comparable to mouse ESCs (Narazaki et al., 2008; Schenke-Layland et al., 2008). However, as only one iPSC clone was analysed in this study and only a small number of clones were evaluated in the reports of Narazaki et al. (2008) and Schenke-Layland et al. (2008), further studies are required to rigorously assess if this is a general phenomenon of mouse iPSCs.

Chapter 6

General discussion

6.1 Discussion

DA neurons have several fundamental functions in the brain, dysfunction or degeneration of which are implicated in a myriad of neurological and psychiatric disorders, including PD, schizophrenia and ADHD (for review, see Greengard, 2001). ESCs may provide an unlimited source of DA neurons as they can be propagated indefinitely in culture in an undifferentiated state while retaining pluripotency (Evans and Kaufman, 1981; Thomson et al., 1998) and protocols have been established to direct differentiation of mouse (Kawasaki et al., 2000; Lee et al., 2000; Rolletschek et al., 2001; Lau et al., 2006) and human (Perrier et al., 2004; Zeng et al., 2004; Sonntag et al., 2007; Cooper et al., 2010) ESCs to this neuronal subtype. However, due to the developmental potency of ESCs it is not possible to synchronise the birth and development of cell populations to the extent seen in normal development, and consequently cells at different stages of maturation and of non-neural lineages are present in such cultures, causing cellular heterogeneity and often variability across differentiation procedures (for review, see Stavridis and Smith, 2003; Hedlund et al., 2007; Pruszak et al., 2007). This greatly impedes the experimental and clinical utility of such cells, which would benefit greatly from a large homogenous cell population (for review, see Stavridis and Smith, 2003; Pruszak et al., 2007). This obstacle may be partly or wholly overcome by introducing a reporter cassette, such as EGFP, into a locus with restricted expression in a specific cell type, effectively labelling the cell of interest (Stavridis and Smith, 2003; Murry and Keller, 2008). Alternatively, it may be possible to label cells with surface markers expressed on the desired cell population (Pruszak et al., 2007). This would allow the selection of a particular cell type from a mixed cell population by FACS, enabling the study of a pure cell population which would otherwise be impossible (Pruszak et al., 2007; Hedlund et al., 2008; Placantonakis et al., 2009). In the case of labelling cells with EGFP, differentiation could also be followed *in vitro* in real time in live cells, greatly enhancing our ability to study gene regulation and lineage choice during development (Tomishima et al., 2007).

However, the results reported here (Chapters 3 and 4) and those from published studies discussed thus far (Chung et al., 2006; Hedlund et al., 2007; Hedlund et al., 2008; Zhou et al., 2009b) emphasis the difficulty with using fluorescent reporter gene expression systems to label dopaminergic neurons and obtain enriched dopaminergic neuronal populations after

purification. Expression of EGFP from promoters specific to post-mitotic DA neurons clearly has the benefit of labelling the cell type of interest. Nevertheless, this approach in itself has encountered problems (Fukuda et al., 2006; Hedlund et al., 2007). For example, use of a TH promoter fragment thought to be sufficient to drive transgene expression in DA neurons resulted in labelling of immature cell populations (Hedlund et al., 2007). Therefore, it was anticipated that the use of a BAC to drive EGFP expression from the DAT promoter in mouse ESCs would allow specific and faithful transgene expression in DA neurons following differentiation, overcoming the limitations associated with the use of short promoter elements, such as mosaic transgene expression (Hedlund et al., 2007), and knock-in strategies, which are labour-intensive and may disrupt normal cellular function (Tomishima et al., 2007). However, following careful design and construction of such a vector (Figs 3.1, 3.2, 3.4-3.6), and transfection and selection of ESCs (Fig. 3.7), this reporter system did not successfully label DA neurons (Figs 3.8-3.12). This highlights the technical difficulties associated with constructing such targeting vectors. Nevertheless, this approach may still have merit as GFP expressed from neural specific promoters contained within BACs have been reported to faithfully label both mouse and human ESCs during the process of neural differentiation (Tomishima et al., 2007; Placantonakis et al., 2009). Furthermore, motor neurons derived from such human ESCs (expressing GFP from motor neuron specific HB9 promoter) could be enriched from a mixed cell population and further differentiated and analysed (Placantonakis et al., 2009).

In light of the difficulty in obtaining DAT-EGFP neurons from ESCs, an alternative approach using Sox1-GFP ESCs was implemented to obtain an enriched DA neuronal population. Sox1 is the earliest known specific marker of the neuroectoderm in the mouse embryo (Wood and Episkopou, 1999), being first expressed in the neural plate and subsequently maintained in neuroepithelial cells throughout the entire neuroaxis (Pevny et al., 1998; Ying et al., 2003). In addition, as its expression is downregulated during neuronal and glial differentiation, it provides an ideal marker for neural precursors (NPs) (Pevny et al., 1998; Ying et al., 2003). Selection of ESCs at early stages of neural differentiation by targeting GFP to neural specific promoters, such as Sox1, is an attractive option, as it allows NPs to be further amplified and differentiated *in vitro* (Ying et al., 2003). Thus, this may over-come problems associated with the use of more mature markers to label DA

neurons, such as high cell death after dissociation of post-mitotic neurons (Fukuda et al., 2006; Hedlund et al., 2008) and DA neurons representing only a small proportion of the differentiated cell population (Hedlund et al., 2008). However, the results from Chapter 4 suggest that even the use of the Sox1-GFP reporter to label and purify NPs is not without limitations. Considering the findings of this study and those in the literature using the Sox1-GFP reporter system (Chung et al., 2006; Fukuda et al., 2006; Parmar and Li, 2007), it would seem that the specific differentiation method used to direct Sox1-GFP+ NPs to a dopaminergic fate influences the generation of DA (TH+) neurons.

In the present study, ESCs were differentiated to DA neurons using the protocol published by Lau et al. (2006; referred to as growth factor induced differentiation method throughout this thesis), which generates DA neurons in a shorter time period than alternative differentiation procedures (Lee et al., 2000; Rolletschek et al., 2001) and thus is advantageous. This is achieved in a four stage process (Fig. 2.1). Stage 1 involves expansion of undifferentiated ESCs in the presence of LIF. Neural stem spheres (NSSs) are then generated from these ESCs in suspension culture in the presence of EGF, bFGF and L-ascorbic acid (L-AA) for 4 days (stage 2). Stage 3 is initiated by dissociation and plating of these spheres, with NPs being induced to proliferate in medium containing Shh, FGF8, EGF and L-AA. After 5 days, terminal differentiation of precursors occurs by withdrawal of growth factors from culture medium, but still in the presence of L-AA, and continues for 10 days (stage 4). A highly enriched neuronal population was obtained following sorting of Sox1-GFP+ NPs at day 5 of stage 3 and further differentiation (65 $\pm$ 9.9% Tuj1+ neurons; Fig. 4.34). Furthermore, while TH expression was more abundant in unsorted neuronal cultures than Sox1-GFP+ NPs following terminal differentiation (Figs 4.37, 4.38), the level of DAT protein was indistinguishable between Sox1-GFP+ sorted and unsorted samples (Fig. 3.39). Thus additional studies are required to further clarify the ability of Sox1-GFP+ NPs to generate enriched DA neuronal populations.

Chung et al. (2006) also reported higher expression of TH in unsorted neuronal cultures than Sox1-GFP+ NPs following terminal differentiation. Furthermore, while the sorted Sox1-GFP+ neuronal population contained ~6.5 $\pm$ 1% TH+ neurons after differentiation by the multi-stage method of Lee et al. (2000), TH+ neurons were more abundant in the Sox1-

GFP- population (19.4 ± 6% TH+ neurons) (Chung et al., 2006). This method is comparable to the one used in the present study, with DA neurons being formed by a five stage process. In the protocol by Lee et al. (2000), undifferentiated ESCs are first expanded in the presence of LIF (stage 1), with embryoid bodies (EBs) generated from these ESCs by growth in suspension for 4 days (stage 2). NPs are then selected by plating of EBs and culturing in neural specific medium for 10 days (stage 3). NPs are subsequently expanded in the presence of bFGF, Shh and FGF8 for 6 days (stage 4), and terminal differentiation (stage 5) is induced by withdrawal of growth factors and addition to L-AA to growth medium, with this stage continuing for 10 days (Lee et al., 2000). In the report by Chung et al. (2006), NPs were sorted at day 2 of stage 4.

Interestingly, differentiation of sorted Sox1-GFP+ NPs on PA6 stromal cells has been reported to generate 22 ± 6% TH+ neurons, with this figure comparable to unsorted neuronal cultures (25 ± 6% TH+ neurons) (Fukuda et al., 2006). This differentiation procedure involves culturing ESCs on a layer of PA6 stromal cells for 14 days (Kawasaki et al., 2000). By differentiating Sox1-GFP ESCs using a monolayer system, Parmar and Li (2007) reported that the sorted Sox1-GFP+ NP population contained 14 ± 2% TH+ neurons at the end of the differentiation process (Parmar and Li, 2007). Again this percentage was indistinguishable from unsorted neuronal cultures (16 ± 3% TH+ neurons) (Parmar and Li, 2007). In this method, undifferentiated ESCs are plated onto gelatine coated dishes and cultured in chemically defined N2B27 medium in the absence of extrinsic factors for 14 days (Ying and Smith, 2003; Ying et al., 2003). Therefore, it would seem from these reports that the Sox1-GFP ESC reporter line may not by widely applicable to the generation of enriched TH+ neurons from selected Sox1-GFP+ NPs, with this enrichment possibly influenced by the neuronal differentiation procedure used.

An alternative approach which has been investigated to increase the number and/or specificity of DA neurons derived from ESCs has been genetic manipulation of these cells to express transcription factors implicated in the *in vivo* development of mDA neurons, as discussed previously, and including Nurr1, Pitx3 and Lmx1a (Chung et al., 2002; Chung et al., 2005; Andersson et al., 2006b; Hedlund et al., 2007; Friling et al., 2009). Nurr1 has been shown to have a critical role in the differentiation and survival of mDA neurons at

later stages of embryonic developmental (Zetterstrom et al., 1997; Castillo et al., 1998; Saucedo-Cardenas et al., 1998; Wallen et al., 1999; Kadkhodaei et al., 2009). Reports suggest that over-expression of Nurr1 in mouse ESCs can induce a four-to-five fold increase in the percentage of TH+ neurons, in comparison to wild-type cells after treatment with Shh and FGF8, with this also being associated with an increase in the expression of midbrain specific transcription factors such as En1 and Pitx3, and DA phenotypic markers such as DAT and AADC (Chung et al., 2002; Kim et al., 2002). Interestingly, over-expression of the transcription factor Pitx3, which is thought to be specifically required for differentiation of mDA neurons in the SNpc (Hwang et al., 2003; Nunes et al., 2003; van den Munckhof et al., 2003; Smidt et al., 2004; Maxwell et al., 2005), increased expression of markers specific for the SNpc such as aldehyde dehydrogenase 2 and the G protein-gated inwardly rectifying K^+ channel Girk2, without increasing the total number of TH+ neurons (Chung et al., 2005). Furthermore, co-expression of Nurr1 and Pitx3 synergistically promoted terminal differentiation to the mDA phenotype in both mouse and human ESC cultures, with evidence suggesting that these factors cooperatively activate transcription of mDA neuron specific genes (Martinat et al., 2006).

Lmx1a is a transcription factor induced early during neural development, possibly by Shh and/or Wnt1, which appears to have a role in establishment of mDA progenitor domain and specification of mDA neuronal fate in these precursors (Andersson et al., 2006b; Chung et al., 2009). It has recently been reported that expression of this transcription factor in neural progenitors derived from mouse ESCs effectively promoted the generation of functional mDA neurons, with 75-95% of all neurons expressing TH, and almost complete over-lap between TH+ neurons and other mDA markers, including Pitx3, Nurr1, En1/2 and Lmx1b (Friling et al., 2009). In fact, recent studies suggest that Lmx1a directly binds Pitx3 and Nurr1 promoter elements and regulates their expression (Chung et al., 2009). Furthermore, over-expression of Lmx1a had a similar effect on human ESCs (Friling et al., 2009). However, while these strategies can increase the proportion of neurons which express dopaminergic markers, differentiated ESC cultures always contain a heterogeneous cell population, as indicated in Chapter 4, and thus, depending on the application of these cells, selection techniques may still be required (Hedlund et al., 2007).

It has also recently been published that co-culture of ESCs with astrocytes can increase the number of DA neurons derived from ESCs in the differentiated neuronal population (Roy et al., 2006). In particular, Roy et al. (2006) reported that immortalised human midbrain astrocytes specifically potentiated DA neuron induction and maintenance from human ESCs, significantly increasing the proportion of TH+ neurons and the proportion of TH+ neurons that co-expressed markers of the SNpc such as Girk2. Interestingly, while human cortical astrocytes enhanced neuronal maturation and survival in differentiated cultures to a similar extent as midbrain astrocytes, they had no effect on the proportion of TH+ neurons, suggesting that competency of astrocytes to induce DA neurons is region specific (Roy et al., 2006). These striking results suggest that further work on the dependency of differentiating ESCs on glial cells is required. However, it should be noted that even though co-culture with astrocytes greatly enhanced the percentage of DA neurons in the differentiated population in this study, these cultures were still typically heterogeneous and the authors suggested the need for isolating terminally differentiated phenotypes, or their fate restricted progenitors, prior to further application (Roy et al., 2006). The experiments in chapter 4 addressed this need, and although TH+ neurons were generated from Sox1-GFP ESCs following sorting of Sox1-GFP NPs, the cultures still contained a heterogeneous neuronal population, highlighting that further work is required to obtain highly enriched dopaminergic neurons from ESCs.

Astrocytes are now, in fact, recognised as having a fundamental role in proper neuronal development and are particularly implicated in synapse formation and maturation (for review, see Eroglu and Barres, 2010). Indeed, the close structural and functional association of astrocytic processes with the synapse has given rise to the concept of the 'tripartite synapse', in which synapses are defined as being composed of the presynaptic and postsynaptic specialisation of the neurons and the glial process that ensheaths them (for reviews, see Araque et al., 1999; Eroglu and Barres, 2010). It has been demonstrated that not only are synapses generated concurrently with glial cells *in vivo* but that isolated CNS neurons cultured *in vitro* show little spontaneous synaptic activity and form few synapses in the absence of astrocytes (for review, see Pfrieger and Barres, 1997; Ullian et al., 2001; Eroglu and Barres, 2010). However, this deficit is overcome by co-culture with either an astrocytic monolayer or astrocyte-conditioned medium (for review, see Pfrieger and Barres,

1997; Ullian et al., 2001; Eroglu and Barres, 2010). It is now thought that astrocytes secrete factors that act pre- and postsynaptically to induce the proper formation and activity of synapses (Mauch et al., 2001; Christopherson et al., 2005; for review, see Eroglu and Barres, 2010). In addition, evidence also suggests that astrocytes regulate synapse formation by contact mediated mechanisms (Barker et al., 2008). Importantly, astrocytes have also been shown to be necessary for inducing synapse formation by human ESC derived neurons (Johnson et al., 2007), suggesting that applications requiring functional neurons *in vitro* may necessitate co-culture of ESCs with these cells.

As previously discussed, the generation of iPSCs from somatic cells has opened remarkable avenues for basic research and regenerative medicine (Takahashi and Yamanaka, 2006; Yamanaka, 2009). The application of iPSCs is of particular relevance to neurodegenerative and psychiatric disorders (for reviews, see Kim, 2010; Wichterle and Przedborski, 2010), subsets of which may be caused by dysfunction of the DA system (for review, see Greengard, 2001). In both cases the underlying pathogenic mechanisms are largely unknown, with cellular models of these disorders being extremely limited and rational treatments are lacking in most cases (for reviews, see Kim, 2010; Wichterle and Przedborski, 2010). This is of particular relevance to neurodegenerative diseases, with current medications having only a symptomatic effect and unable to halt or retard the degenerative process (for review, see Wichterle and Przedborski, 2010). Thus the derivation of disease specific iPSCs from individuals suffering from these disorders and the directed differentiation to the neuronal subtype implicated in the disease may elucidate mechanisms of disease pathogenesis, allowing the creation of more faithful disease models which may facilitate the development of efficacious therapies (for reviews, see Yamanaka, 2009; Kim, 2010; Wichterle and Przedborski, 2010). It should be noted, however, that no disease-related phenotypes have been reported for sporadic late-onset diseases, such as PD, suggesting that these phenotypes may only manifest themselves after challenging neural cells with stressors and that an additional level of complexity may be involved in effective disease modelling (Soldner et al., 2009; Hargus et al., 2010; Wichterle and Przedborski, 2010).

Clearly, for the potential of iPSCs to be realised, it is necessary to ask if and how effectively they may be differentiated to functional neurons, which can be answered by direct comparison to ESCs (Hu et al., 2010). Using a monolayer procedure in which differentiation is induced by culturing cells at low density in chemically defined medium (Ying and Smith, 2003; Ying et al., 2003), it was observed that mouse iPSCs differentiated to neurons with efficiency comparable to that of ESCs (Figs 5.15-5.17), including the generation of DA neurons (Figs 5.22, 5.23). This is of importance as autocrine signalling is required for neural conversion in this system (Ying et al., 2003) and thus suggests that intrinsic mechanisms governing differentiation are similar in both iPSCs and ESCs. However, variability was observed in both cell types in relation to neuronal subtype marker expression (Fig. 5.21). Furthermore, NSSs derived from iPSCs were found to be comparable to those derived from ESCs based on morphology (Figs 5.8-5.11), neuroectodermal (Fig. 5.11) and neuronal marker expression (Fig. 5.12).

Two studies recently published regarding the neural differentiation capacity of human iPSCs resulted in different conclusions (Hu et al., 2010; Boulting et al., 2011). While Hu et al. (2010) reported that human iPSCs followed the same temporal course during neural specification as human ESCs, iPSCs exhibited lower and more variable neuroepithelial and neuronal differentiation efficiencies (Hu et al., 2010). However, Boulting et al (2011) reported that iPSCs gave rise to functional motor neurons with a range of efficiencies similar to that of ESCs. This study is of significance as more iPSC and ESC lines were compared (Boulting et al., 2011). Thus it is possible that the analysis of more mouse iPSCs clones would identify differences in comparison to ESCs. Conversely it is possible that differences exist between mouse and human iPSCs. Indeed, differences have recently emerged between the cell types in relation to reprogrammed female fibroblasts (Maherali et al., 2007; Tchieu et al., 2010). Mouse iPSCs derived from female fibroblasts effectively reactivated the inactive X chromosome after reprogramming and subsequent differentiation resulted in random X chromosome inactivation, as observed in mouse ESCs (Maherali et al., 2007). In contrast, human iPSCs derived from female fibroblasts failed to reactivate the silenced X chromosome and kept the same X chromosome inactivated in differentiated cells (Tchieu et al., 2010). As mouse iPSCs can be easily compared to genetically matched ESCs, which may reduce background differences between cells, and can undergo stringent

tests of pluripotency, analysis of the differentiated progeny of mouse cells may facilitate the further identification of similarities, or differences, between these cell types.

6.2 Future work

After the studies performed in Chapter 3 to target EGFP to the DAT promoter were completed, GENSAT reported the creation of transgenic mice faithfully expressing EGFP from the DAT promoter (GENSAT, 2010). Due to the difficulties in labelling mature DA neurons (Chapter 3; Hedlund et al., 2007) and obtaining enriched populations of DA neurons (Chapter 4; Chung et al., 2006), this may still be an attractive area of investigation. However, while the BAC vectors generated by GENSAT do not include a selection gene required to create an ESC line stably expressing EGFP, previous studies indicate that the vector backbone can be readily retrofitted with such a cassette (Tomishima et al., 2007; Placantonakis et al., 2009). Furthermore, using neural specific promoters these studies successfully labelled mouse and human ESC-derived neural progeny during the process of neural induction (Tomishima et al., 2007; Placantonakis et al., 2009). In addition, motor neurons derived from human ESCs were also effectively tagged and sorted, thus generating a purified motor neuron population which was further differentiated and analysed in vitro (Placantonakis et al., 2009). These studies highlight the feasibility and tremendous application of this technique.

As discussed previously, co-culture of human ESCs with midbrain astrocytes potentiated the induction and maintenance of DA neurons (Roy et al., 2006). Thus it may be of interest to analyse if midbrain astrocytes similarly effect mouse ESCs during the process of differentiation, and if the competency of midbrain astrocytes to induce DA neurons is regionally specific, as in the human system (Roy et al., 2006), with the target of obtaining enriched DA neuronal populations. In addition, it is now widely recognised that astrocytes are required for proper synapse formation and maturation (Eroglu and Barres, 2010), with astrocytes also inducing synapse formation in neurons derived from human ESCs (Johnson et al., 2007; Wu et al., 2007). Thus the question may arise as to whether regional specificity exists in the ability of astrocytes to induce synapse formation in ESC derived DA neurons. This analysis in itself would be greatly enhanced by the use of a reporter system to label

mature postmitotic DA neurons, such as DAT-EGFP, thus allowing these cells to be rapidly localised and visualised. The ease of handling mouse ESCs and the short neuronal differentiation time of these cells (in comparison to human ESCs) make them an attractive choice.

The results presented here suggest that mouse iPSCs generate neurons with a similar efficiency as mouse ESCs. However, as only one clone was analysed it is important to extend this work to investigate if the results are clone specific. In addition, as DA neurons are of particular interest it is important to analyse if iPSCs can reproducibly differentiate to this neuronal subtype, and if they exhibit an efficiency that is comparable to that of ESCs. While an end point of neuronal differentiation was investigated here, it is clearly of relevance to examine if iPSCs display characteristic neural/neuronal markers during the process of differentiation and if the sequence and timing of these markers is similar in ESCs, as suggested by recent work (Hu et al., 2010). In particular, markers of dopaminergic differentiation should be examined including ADH2, Lmx1a, Pitx3 and Nurr1 (as discussed previously).

Due to the enormous potential of iPSCs, it should also be investigated if these cells can generate mature functional DA neurons, with evidence that functional motor neurons can be derived from human iPSCs (Hu et al., 2010; Boulting et al., 2011), and if this requires culturing with astrocytes, as discussed above. Furthermore, as co-culturing of human ESCs with midbrain astrocytes biased the DA neurons generated to a nigral fate (Roy et al., 2006), it may be of interest to analyse if this effect is replicated when iPSCs are differentiated by a similar manner. This will have particular relevance in relation to disease specific PD iPSCs, as this subset of DA neurons is particularly vulnerable during the disease process, and thus far no disease related phenotype has been identified in DA neurons derived from these cells (Soldner et al., 2009; Cooper et al., 2010; Hargus et al., 2010). While ultimately studies must be performed with human ESCs and iPSCs, the easy of handling mouse cells and the ability to easily genetically match mouse ESCs and iPSCs, make these cells an attractive option to determine if differences exist between the cell types.

Finally, even if iPSCs can reproducibly differentiate to DA neurons with a similar efficiency as ESCs, the problem of heterogeneous cell populations post-differentiation will still persist. Therefore, it is likely, depending on the final application, that differentiated DA neurons, or their fate restricted progenitors, will need to be sorted from the mixed cell population to facilitate reproducibility across differentiation procedure. Thus markers which have been identified that allow DA neurons derived from ESCs to be successfully labelled and isolated will most likely be translated to iPSCs derived DA neurons, highlighting the importance of the work of this thesis.

Bibliography

Abe, K., Niwa, H., Iwase, K., Takiguchi, M., Mori, M., Abe, S.I. and Yamamura, K.I. Endoderm-specific gene expression in embryonic stem cells differentiated to embryoid bodies. *Exp Cell Res* **229** (1996), pp. 27-34.

Abi-Dargham, A., Gil, R., Krystal, J., Baldwin, R.M., Seibyl, J.P., Bowers, M., van Dyck, C.H., Charney, D.S., Innis, R.B. and Laruelle, M. Increased striatal dopamine transmission in schizophrenia: confirmation in a second cohort. *Am J Psychiatry* **155** (1998), pp. 761-7.

Abi-Dargham, A. and Laruelle, M. Mechanisms of action of second generation antipsychotic drugs in schizophrenia: insights from brain imaging studies. *Eur Psychiatry* **20** (2005), pp. 15-27.

Abi-Dargham, A., Rodenhiser, J., Printz, D., Zea-Ponce, Y., Gil, R., Kegeles, L.S., Weiss, R., Cooper, T.B., Mann, J.J., Van Heertum, R.L., Gorman, J.M. and Laruelle, M. Increased baseline occupancy of D2 receptors by dopamine in schizophrenia. *Proc Natl Acad Sci U S A* **97** (2000), pp. 8104-9.

Adams, K.A., Maida, J.M., Golden, J.A. and Riddle, R.D. The transcription factor Lmx1b maintains Wnt1 expression within the isthmic organizer. *Development* **127** (2000), pp. 1857-67.

Alavian, K.N., Scholz, C. and Simon, H.H. Transcriptional regulation of mesencephalic dopaminergic neurons: the full circle of life and death. *Mov Disord* **23** (2008), pp. 319-28.

Alberi, L., Sgado, P. and Simon, H.H. Engrailed genes are cell-autonomously required to prevent apoptosis in mesencephalic dopaminergic neurons. *Development* **131** (2004), pp. 3229-36.

Albin, R.L., Young, A.B. and Penney, J.B. The functional anatomy of basal ganglia disorders. *Trends Neurosci* **12** (1989), pp. 366-75.

Amit, M., Carpenter, M.K., Inokuma, M.S., Chiu, C.P., Harris, C.P., Waknitz, M.A., Itskovitz-Eldor, J. and Thomson, J.A. Clonally derived human embryonic stem cell lines

maintain pluripotency and proliferative potential for prolonged periods of culture. *Dev Biol* **227** (2000), pp. 271-8.

Andersson, E., Jensen, J.B., Parmar, M., Guillemot, F. and Bjorklund, A. Development of the mesencephalic dopaminergic neuron system is compromised in the absence of neurogenin 2. *Development* **133** (2006a), pp. 507-16.

Andersson, E., Tryggvason, U., Deng, Q., Friling, S., Alekseenko, Z., Robert, B., Perlmann, T. and Ericson, J. Identification of intrinsic determinants of midbrain dopamine neurons. *Cell* **124** (2006b), pp. 393-405.

Andressen, C., Stocker, E., Klinz, F.J., Lenka, N., Hescheler, J., Fleischmann, B., Arnhold, S. and Addicks, K. Nestin-specific green fluorescent protein expression in embryonic stem cell-derived neural precursor cells used for transplantation. *Stem Cells* **19** (2001), pp. 419-24.

Aoi, T., Yae, K., Nakagawa, M., Ichisaka, T., Okita, K., Takahashi, K., Chiba, T. and Yamanaka, S. Generation of pluripotent stem cells from adult mouse liver and stomach cells. *Science* **321** (2008), pp. 699-702.

Araque, A., Parpura, V., Sanzgiri, R.P. and Haydon, P.G. Tripartite synapses: glia, the unacknowledged partner. *Trends Neurosci* **22** (1999), pp. 208-15.

Arnsten, A.F. and Li, B.M. Neurobiology of executive functions: catecholamine influences on prefrontal cortical functions. *Biol Psychiatry* **57** (2005), pp. 1377-84.

Astradsson, A., Cooper, O., Vinuela, A. and Isacson, O. Recent advances in cell-based therapy for Parkinson disease. *Neurosurg Focus* **24** (2008), p. E6.

Aubert, J., Stavridis, M.P., Tweedie, S., O'Reilly, M., Vierlinger, K., Li, M., Ghazal, P., Pratt, T., Mason, J.O., Roy, D. and Smith, A. Screening for mammalian neural genes via fluorescence-activated cell sorter purification of neural precursors from Sox1-gfp knock-in mice. *Proc Natl Acad Sci U S A* **100 Suppl 1** (2003), pp. 11836-41.

Augood, S.J., Westmore, K., McKenna, P.J. and Emson, P.C. Co-expression of dopamine transporter mRNA and tyrosine hydroxylase mRNA in ventral mesencephalic neurones. *Brain Res Mol Brain Res* **20** (1993), pp. 328-34.

Backman, C.M., Malik, N., Zhang, Y., Shan, L., Grinberg, A., Hoffer, B.J., Westphal, H. and Tomac, A.C. Characterization of a mouse strain expressing Cre recombinase from the 3' untranslated region of the dopamine transporter locus. *Genesis* **44** (2006), pp. 383-90.

Bannon, M.J., Michelhaugh, S.K., Wang, J. and Sacchetti, P. The human dopamine transporter gene: gene organization, transcriptional regulation, and potential involvement in neuropsychiatric disorders. *Eur Neuropsychopharmacol* **11** (2001), pp. 449-55.

Barberi, T., Klivenyi, P., Calingasan, N.Y., Lee, H., Kawamata, H., Loonam, K., Perrier, A.L., Bruses, J., Rubio, M.E., Topf, N., Tabar, V., Harrison, N.L., Beal, M.F., Moore, M.A. and Studer, L. Neural subtype specification of fertilization and nuclear transfer embryonic stem cells and application in parkinsonian mice. *Nat Biotechnol* **21** (2003), pp. 1200-7.

Barker, A.J., Koch, S.M., Reed, J., Barres, B.A. and Ullian, E.M. Developmental control of synaptic receptivity. *J Neurosci* **28** (2008), pp. 8150-60.

Barr, C.L., Xu, C., Kroft, J., Feng, Y., Wigg, K., Zai, G., Tannock, R., Schachar, R., Malone, M., Roberts, W., Nothen, M.M., Grunhage, F., Vandenbergh, D.J., Uhl, G., Sunohara, G., King, N. and Kennedy, J.L. Haplotype study of three polymorphisms at the dopamine transporter locus confirm linkage to attention-deficit/hyperactivity disorder. *Biol Psychiatry* **49** (2001), pp. 333-9.

Barraud, P., Thompson, L., Kirik, D., Bjorklund, A. and Parmar, M. Isolation and characterization of neural precursor cells from the Sox1-GFP reporter mouse. *Eur J Neurosci* **22** (2005), pp. 1555-69.

Beal, M.F. Parkinson's disease: a model dilemma. *Nature* **466** (2010), pp. S8-10.

Ben-Jonathan, N. and Hnasko, R. Dopamine as a prolactin (PRL) inhibitor. *Endocr Rev* **22** (2001), pp. 724-63.

Benoit-Marand, M., Borrelli, E. and Gonon, F. Inhibition of dopamine release via presynaptic D2 receptors: time course and functional characteristics in vivo. *J Neurosci* **21** (2001), pp. 9134-41.

Bergman, H., Wichmann, T. and DeLong, M.R. Reversal of experimental parkinsonism by lesions of the subthalamic nucleus. *Science* **249** (1990), pp. 1436-8.

Bertorello, A.M., Hopfield, J.F., Aperia, A. and Greengard, P. Inhibition by dopamine of (Na(+)+K+)ATPase activity in neostriatal neurons through D1 and D2 dopamine receptor synergism. *Nature* **347** (1990), pp. 386-8.

Blaess, S., Corrales, J.D. and Joyner, A.L. Sonic hedgehog regulates Gli activator and repressor functions with spatial and temporal precision in the mid/hindbrain region. *Development* **133** (2006), pp. 1799-809.

Bian, Q. and Belmont, A.S. BAC TG-EMBED: one-step method for high-level, copy-number-dependent, position-independent transgene expression. *Nucleic Acids Res* **38** (2010), p. e127.

Biederman, J. Attention-deficit/hyperactivity disorder: a selective overview. *Biol Psychiatry* **57** (2005), pp. 1215-20.

Boland, M.J., Hazen, J.L., Nazor, K.L., Rodriguez, A.R., Gifford, W., Martin, G., Kupriyanov, S. and Baldwin, K.K. Adult mice generated from induced pluripotent stem cells. *Nature* **461** (2009), pp. 91-4.

Boulting, G.L., Kiskinis, E., Croft, G.F., Amoroso, M.W., Oakley, D.H., Wainger, B.J., Williams, D.J., Kahler, D.J., Yamaki, M., Davidow, L., Rodolfa, C.T., Dimos, J.T., Mikkilineni, S., Macdermott, A.B., Woolf, C.J., Henderson, C.E., Wichterle, H. and Eggan,

K. A functionally characterized test set of human induced pluripotent stem cells. *Nat Biotechnol* **29** (2011), pp. 279-86.

Brambrink, T., Foreman, R., Welstead, G.G., Lengner, C.J., Wernig, M., Suh, H. and Jaenisch, R. Sequential expression of pluripotency markers during direct reprogramming of mouse somatic cells. *Cell Stem Cell* **2** (2008), pp. 151-9.

Broccoli, V., Boncinelli, E. and Wurst, W. The caudal limit of Otx2 expression positions the isthmic organizer. *Nature* **401** (1999), pp. 164-8.

Brodski, C., Weisenhorn, D.M., Signore, M., Sillaber, I., Oesterheld, M., Broccoli, V., Acampora, D., Simeone, A. and Wurst, W. Location and size of dopaminergic and serotonergic cell populations are controlled by the position of the midbrain-hindbrain organizer. *J Neurosci* **23** (2003), pp. 4199-207.

Brozoski, T.J., Brown, R.M., Rosvold, H.E. and Goldman, P.S. Cognitive deficit caused by regional depletion of dopamine in prefrontal cortex of rhesus monkey. *Science* **205** (1979), pp. 929-32.

Brustle, O., Jones, K.N., Learish, R.D., Karram, K., Choudhary, K., Wiestler, O.D., Duncan, I.D. and McKay, R.D. Embryonic stem cell-derived glial precursors: a source of myelinating transplants. *Science* **285** (1999), pp. 754-6.

Bymaster, F.P., Katner, J.S., Nelson, D.L., Hemrick-Luecke, S.K., Threlkeld, P.G., Heiligenstein, J.H., Morin, S.M., Gehlert, D.R. and Perry, K.W. Atomoxetine increases extracellular levels of norepinephrine and dopamine in prefrontal cortex of rat: a potential mechanism for efficacy in attention deficit/hyperactivity disorder. *Neuropsychopharmacology* **27** (2002), pp. 699-711.

Cai, J., Yang, M., Poremsky, E., Kidd, S., Schneider, J.S. and Iacovitti, L. Dopaminergic neurons derived from human induced pluripotent stem cells survive and integrate into 6-OHDA-lesioned rats. *Stem Cells Dev* **19** (2010), pp. 1017-23.

Cameron, C.M., Hu, W.S. and Kaufman, D.S. Improved development of human embryonic stem cell-derived embryoid bodies by stirred vessel cultivation. *Biotechnol Bioeng* **94** (2006), pp. 938-48.

Carboni, E., Tanda, G.L., Frau, R. and Di Chiara, G. Blockade of the noradrenaline carrier increases extracellular dopamine concentrations in the prefrontal cortex: evidence that dopamine is taken up in vivo by noradrenergic terminals. *J Neurochem* **55** (1990), pp. 1067-70.

Carey, B.W., Markoulaki, S., Beard, C., Hanna, J. and Jaenisch, R. Single-gene transgenic mouse strains for reprogramming adult somatic cells. *Nat Methods* **7** (2010), pp. 56-9.

Carey, B.W., Markoulaki, S., Hanna, J., Saha, K., Gao, Q., Mitalipova, M. and Jaenisch, R. Reprogramming of murine and human somatic cells using a single polycistronic vector. *Proc Natl Acad Sci U S A* **106** (2009), pp. 157-62.

Carlsson, A. and Lindqvist, M. Effect of Chlorpromazine or Haloperidol on Formation of 3methoxytyramine and Normetanephrine in Mouse Brain. *Acta Pharmacol Toxicol (Copenh)* **20** (1963), pp. 140-4.

Carlsson, A., Lindqvist, M. and Magnusson, T. 3,4-Dihydroxyphenylalanine and 5-hydroxytryptophan as reserpine antagonists. *Nature* **180** (1957), p. 1200.

Castillo, S.O., Baffi, J.S., Palkovits, M., Goldstein, D.S., Kopin, I.J., Witta, J., Magnuson, M.A. and Nikodem, V.M. Dopamine biosynthesis is selectively abolished in substantia nigra/ventral tegmental area but not in hypothalamic neurons in mice with targeted disruption of the Nurr1 gene. *Mol Cell Neurosci* **11** (1998), pp. 36-46.

Chambers, I., Colby, D., Robertson, M., Nichols, J., Lee, S., Tweedie, S. and Smith, A. Functional expression cloning of Nanog, a pluripotency sustaining factor in embryonic stem cells. *Cell* **113** (2003), pp. 643-55.

Chiang, C.H., Su, Y., Wen, Z., Yoritomo, N., Ross, C.A., Margolis, R.L., Song, H. and Ming, G.L. Integration-free induced pluripotent stem cells derived from schizophrenia patients with a DISC1 mutation. *Mol Psychiatry* (2011).

Choi, Y.Y., Chung, B.G., Lee, D.H., Khademhosseini, A., Kim, J.H. and Lee, S.H. Controlled-size embryoid body formation in concave microwell arrays. *Biomaterials* **31** (2010), pp. 4296-303.

Christopherson, K.S., Ullian, E.M., Stokes, C.C., Mullowney, C.E., Hell, J.W., Agah, A., Lawler, J., Mosher, D.F., Bornstein, P. and Barres, B.A. Thrombospondins are astrocyte-secreted proteins that promote CNS synaptogenesis. *Cell* **120** (2005), pp. 421-33.

Chung, S., Leung, A., Han, B.S., Chang, M.Y., Moon, J.I., Kim, C.H., Hong, S., Pruszak, J., Isacson, O. and Kim, K.S. Wnt1-lmx1a forms a novel autoregulatory loop and controls midbrain dopaminergic differentiation synergistically with the SHH-FoxA2 pathway. *Cell Stem Cell* **5** (2009), pp. 646-58.

Chung, S., Shin, B.S., Hedlund, E., Pruszak, J., Ferree, A., Kang, U.J., Isacson, O. and Kim, K.S. Genetic selection of sox1GFP-expressing neural precursors removes residual tumorigenic pluripotent stem cells and attenuates tumor formation after transplantation. *J Neurochem* **97** (2006), pp. 1467-80.

Chung, S., Sonntag, K.C., Andersson, T., Bjorklund, L.M., Park, J.J., Kim, D.W., Kang, U.J., Isacson, O. and Kim, K.S. Genetic engineering of mouse embryonic stem cells by Nurr1 enhances differentiation and maturation into dopaminergic neurons. *Eur J Neurosci* **16** (2002), pp. 1829-38.

Ciliax, B.J., Heilman, C., Demchyshyn, L.L., Pristupa, Z.B., Ince, E., Hersch, S.M., Niznik, H.B. and Levey, A.I. The dopamine transporter: immunochemical characterization and localization in brain. *J Neurosci* **15** (1995), pp. 1714-23.

Cooper, O., Hargus, G., Deleidi, M., Blak, A., Osborn, T., Marlow, E., Lee, K., Levy, A., Perez-Torres, E., Yow, A. and Isacson, O. Differentiation of human ES and Parkinson's

disease iPS cells into ventral midbrain dopaminergic neurons requires a high activity form of SHH, FGF8a and specific regionalization by retinoic acid. *Mol Cell Neurosci* **45** (2010), pp. 258-66.

Craggs, T.D. Green fluorescent protein: structure, folding and chromophore maturation. *Chem Soc Rev* **38** (2009), pp. 2865-75.

Crossley, P.H., Martinez, S. and Martin, G.R. Midbrain development induced by FGF8 in the chick embryo. *Nature* **380** (1996), pp. 66-8.

Daly, G., Hawi, Z., Fitzgerald, M. and Gill, M. Mapping susceptibility loci in attention deficit hyperactivity disorder: preferential transmission of parental alleles at DAT1, DBH and DRD5 to affected children. *Mol Psychiatry* **4** (1999), pp. 192-6.

David, V., Durkin, T.P. and Cazala, P. Self-administration of the GABAA antagonist bicuculline into the ventral tegmental area in mice: dependence on D2 dopaminergic mechanisms. *Psychopharmacology (Berl)* **130** (1997), pp. 85-90.

David, V., Durkin, T.P. and Cazala, P. Differential effects of the dopamine D2/D3 receptor antagonist sulpiride on self-administration of morphine into the ventral tegmental area or the nucleus accumbens. *Psychopharmacology (Berl)* **160** (2002), pp. 307-17.

Davila, N.G., Blakemore, L.J. and Trombley, P.Q. Dopamine modulates synaptic transmission between rat olfactory bulb neurons in culture. *J Neurophysiol* **90** (2003), pp. 395-404.

Davis, K.L., Kahn, R.S., Ko, G. and Davidson, M. Dopamine in schizophrenia: a review and reconceptualization. *Am J Psychiatry* **148** (1991), pp. 1474-86.

DeLong, M.R. and Wichmann, T. Circuits and circuit disorders of the basal ganglia. *Arch Neurol* **64** (2007), pp. 20-4.

Desbaillets, I., Ziegler, U., Groscurth, P. and Gassmann, M. Embryoid bodies: an in vitro model of mouse embryogenesis. *Exp Physiol* **85** (2000), pp. 645-51.

Desponts, C. and Ding, S. Using small molecules to improve generation of induced pluripotent stem cells from somatic cells. *Methods Mol Biol* **636** (2010), pp. 207-18.

Devine, D.P. and Wise, R.A. Self-administration of morphine, DAMGO, and DPDPE into the ventral tegmental area of rats. *J Neurosci* **14** (1994), pp. 1978-84.

Di Chiara, G. and Imperato, A. Drugs abused by humans preferentially increase synaptic dopamine concentrations in the mesolimbic system of freely moving rats. *Proc Natl Acad Sci U S A* **85** (1988), pp. 5274-8.

Dickson, B.J. Molecular mechanisms of axon guidance. *Science* **298** (2002), pp. 1959-64.

Dimos, J.T., Rodolfa, K.T., Niakan, K.K., Weisenthal, L.M., Mitsumoto, H., Chung, W., Croft, G.F., Saphier, G., Leibel, R., Goland, R., Wichterle, H., Henderson, C.E. and Eggan, K. Induced pluripotent stem cells generated from patients with ALS can be differentiated into motor neurons. *Science* **321** (2008), pp. 1218-21.

Donovan, D.M., Vandenbergh, D.J., Perry, M.P., Bird, G.S., Ingersoll, R., Nanthakumar, E. and Uhl, G.R. Human and mouse dopamine transporter genes: conservation of 5'-flanking sequence elements and gene structures. *Brain Res Mol Brain Res* **30** (1995), pp. 327-35.

Ebert, A.D., Yu, J., Rose, F.F., Jr., Mattis, V.B., Lorson, C.L., Thomson, J.A. and Svendsen, C.N. Induced pluripotent stem cells from a spinal muscular atrophy patient. *Nature* **457** (2009), pp. 277-80.

Eisenhofer, G., Kopin, I.J. and Goldstein, D.S. Catecholamine metabolism: a contemporary view with implications for physiology and medicine. *Pharmacol Rev* **56** (2004), pp. 331-49.

Ekstrand, M.I., Terzioglu, M., Galter, D., Zhu, S., Hofstetter, C., Lindqvist, E., Thams, S., Bergstrand, A., Hansson, F.S., Trifunovic, A., Hoffer, B., Cullheim, S., Mohammed, A.H., Olson, L. and Larsson, N.G. Progressive parkinsonism in mice with respiratory-chain-deficient dopamine neurons. *Proc Natl Acad Sci U S A* **104** (2007), pp. 1325-30.

Eminli, S., Utikal, J., Arnold, K., Jaenisch, R. and Hochedlinger, K. Reprogramming of neural progenitor cells into induced pluripotent stem cells in the absence of exogenous Sox2 expression. *Stem Cells* **26** (2008), pp. 2467-74.

Ernst, M., Zametkin, A.J., Matochik, J.A., Jons, P.H. and Cohen, R.M. DOPA decarboxylase activity in attention deficit hyperactivity disorder adults. A [fluorine-18]fluorodopa positron emission tomographic study. *J Neurosci* **18** (1998), pp. 5901-7.

Eroglu, C. and Barres, B.A. Regulation of synaptic connectivity by glia. *Nature* **468** (2010), pp. 223-31.

Evans, M.J. and Kaufman, M.H. Establishment in culture of pluripotential cells from mouse embryos. *Nature* **292** (1981), pp. 154-6.

Faraone, S.V., Perlis, R.H., Doyle, A.E., Smoller, J.W., Goralnick, J.J., Holmgren, M.A. and Sklar, P. Molecular genetics of attention-deficit/hyperactivity disorder. *Biol Psychiatry* **57** (2005), pp. 1313-23.

Faraone, S.V., Sergeant, J., Gillberg, C. and Biederman, J. The worldwide prevalence of ADHD: is it an American condition? *World Psychiatry* **2** (2003), pp. 104-13.

Fienberg, A.A., Hiroi, N., Mermelstein, P.G., Song, W., Snyder, G.L., Nishi, A., Cheramy, A., O'Callaghan, J.P., Miller, D.B., Cole, D.G., Corbett, R., Haile, C.N., Cooper, D.C., Onn, S.P., Grace, A.A., Ouimet, C.C., White, F.J., Hyman, S.E., Surmeier, D.J., Girault, J., Nestler, E.J. and Greengard, P. DARPP-32: regulator of the efficacy of dopaminergic neurotransmission. *Science* **281** (1998), pp. 838-42.

Fiorino, D.F., Coury, A., Fibiger, H.C. and Phillips, A.G. Electrical stimulation of reward sites in the ventral tegmental area increases dopamine transmission in the nucleus accumbens of the rat. *Behav Brain Res* **55** (1993), pp. 131-41.

Fouriezos, G., Hansson, P. and Wise, R.A. Neuroleptic-induced attenuation of brain stimulation reward in rats. *J Comp Physiol Psychol* **92** (1978), pp. 661-71.

Franklin, K.B. and McCoy, S.N. Pimozide-induced extinction in rats: stimulus control of responding rules out motor deficit. *Pharmacol Biochem Behav* **11** (1979), pp. 71-5.

Friling, S., Andersson, E., Thompson, L.H., Jonsson, M.E., Hebsgaard, J.B., Nanou, E., Alekseenko, Z., Marklund, U., Kjellander, S., Volakakis, N., Hovatta, O., El Manira, A., Bjorklund, A., Perlmann, T. and Ericson, J. Efficient production of mesencephalic dopamine neurons by Lmx1a expression in embryonic stem cells. *Proc Natl Acad Sci U S A* **106** (2009), pp. 7613-8.

Fukuda, H., Arai, M. and Kuwajima, K. Folding of green fluorescent protein and the cycle3 mutant. *Biochemistry* **39** (2000), pp. 12025-32.

Fukuda, H., Takahashi, J., Watanabe, K., Hayashi, H., Morizane, A., Koyanagi, M., Sasai, Y. and Hashimoto, N. Fluorescence-activated cell sorting-based purification of embryonic stem cell-derived neural precursors averts tumor formation after transplantation. *Stem Cells* **24** (2006), pp. 763-71.

Fusaki, N., Ban, H., Nishiyama, A., Saeki, K. and Hasegawa, M. Efficient induction of transgene-free human pluripotent stem cells using a vector based on Sendai virus, an RNA virus that does not integrate into the host genome. *Proc Jpn Acad Ser B Phys Biol Sci* **85** (2009), pp. 348-62.

Fykse, E.M., Takei, K., Walch-Solimena, C., Geppert, M., Jahn, R., De Camilli, P. and Sudhof, T.C. Relative properties and localizations of synaptic vesicle protein isoforms: the case of the synaptophysins. *J Neurosci* **13** (1993), pp. 4997-5007.

GENSAT: The Gene Expression Nervous System Atlas (GENSAT) Project, NINDS Contracts N01NS02331 & HHSN271200723701C to The Rockefeller University (New York, NY) (2010).

Gerber, G.J., Sing, J. and Wise, R.A. Pimozide attenuates lever pressing for water reinforcement in rats. *Pharmacol Biochem Behav* **14** (1981), pp. 201-5.

Gerrits, M.A. and Van Ree, J.M. Effect of nucleus accumbens dopamine depletion on motivational aspects involved in initiation of cocaine and heroin self-administration in rats. *Brain Res* **713** (1996), pp. 114-24.

Girault, J.A. and Greengard, P. The neurobiology of dopamine signaling. *Arch Neurol* **61** (2004), pp. 641-4.

Goetz, A.K., Scheffler, B., Chen, H.X., Wang, S., Suslov, O., Xiang, H., Brustle, O., Roper, S.N. and Steindler, D.A. Temporally restricted substrate interactions direct fate and specification of neural precursors derived from embryonic stem cells. *Proc Natl Acad Sci U S A* **103** (2006), pp. 11063-8.

Goldberg, A.L. Protein degradation and protection against misfolded or damaged proteins. *Nature* **426** (2003), pp. 895-9.

Goldman-Rakic, P.S., Muly, E.C., 3rd and Williams, G.V. D(1) receptors in prefrontal cells and circuits. *Brain Res Brain Res Rev* **31** (2000), pp. 295-301.

Greengard, P. The neurobiology of slow synaptic transmission. *Science* **294** (2001), pp. 1024-30.

Greif, G.J., Lin, Y.J., Liu, J.C. and Freedman, J.E. Dopamine-modulated potassium channels on rat striatal neurons: specific activation and cellular expression. *J Neurosci* **15** (1995), pp. 4533-44.

Guhaniyogi, J. and Brewer, G. Regulation of mRNA stability in mammalian cells. *Gene* **265** (2001), pp. 11-23.

Hansen, S.M., Berezin, V. and Bock, E. Signaling mechanisms of neurite outgrowth induced by the cell adhesion molecules NCAM and N-cadherin. *Cell Mol Life Sci* **65** (2008), pp. 3809-21.

Hargus, G., Cooper, O., Deleidi, M., Levy, A., Lee, K., Marlow, E., Yow, A., Soldner, F., Hockemeyer, D., Hallett, P.J., Osborn, T., Jaenisch, R. and Isacson, O. Differentiated

Parkinson patient-derived induced pluripotent stem cells grow in the adult rodent brain and reduce motor asymmetry in Parkinsonian rats. *Proc Natl Acad Sci U S A* **107** (2010), pp. 15921-6.

Hawi, Z., Lowe, N., Kirley, A., Gruenhage, F., Nothen, M., Greenwood, T., Kelsoe, J., Fitzgerald, M. and Gill, M. Linkage disequilibrium mapping at DAT1, DRD5 and DBH narrows the search for ADHD susceptibility alleles at these loci. *Mol Psychiatry* **8** (2003), pp. 299-308.

Hedlund, E., Pruszak, J., Ferree, A., Vinuela, A., Hong, S., Isacson, O. and Kim, K.S. Selection of embryonic stem cell-derived enhanced green fluorescent protein-positive dopamine neurons using the tyrosine hydroxylase promoter is confounded by reporter gene expression in immature cell populations. *Stem Cells* **25** (2007), pp. 1126-35.

Hedlund, E., Pruszak, J., Lardaro, T., Ludwig, W., Vinuela, A., Kim, K.S. and Isacson, O. Embryonic stem cell-derived Pitx3-enhanced green fluorescent protein midbrain dopamine neurons survive enrichment by fluorescence-activated cell sorting and function in an animal model of Parkinson's disease. *Stem Cells* **26** (2008), pp. 1526-36.

Hemmings, H.C., Jr., Greengard, P., Tung, H.Y. and Cohen, P. DARPP-32, a dopamine-regulated neuronal phosphoprotein, is a potent inhibitor of protein phosphatase-1. *Nature* **310** (1984a), pp. 503-5.

Hemmings, H.C., Jr., Nairn, A.C. and Greengard, P. DARPP-32, a dopamine- and adenosine 3':5'-monophosphate-regulated neuronal phosphoprotein. II. Comparison of the kinetics of phosphorylation of DARPP-32 and phosphatase inhibitor 1. *J Biol Chem* **259** (1984b), pp. 14491-7.

Henley, J. and Poo, M.M. Guiding neuronal growth cones using Ca2+ signals. *Trends Cell Biol* **14** (2004), pp. 320-30.

Hernandez, L. and Hoebel, B.G. Food reward and cocaine increase extracellular dopamine in the nucleus accumbens as measured by microdialysis. *Life Sci* **42** (1988), pp. 1705-12.

Hernandez-Lopez, S., Tkatch, T., Perez-Garci, E., Galarraga, E., Bargas, J., Hamm, H. and Surmeier, D.J. D2 dopamine receptors in striatal medium spiny neurons reduce L-type Ca2+ currents and excitability via a novel PLC[beta]1-IP3-calcineurin-signaling cascade. *J Neurosci* **20** (2000), pp. 8987-95.

Hersch, S.M., Yi, H., Heilman, C.J., Edwards, R.H. and Levey, A.I. Subcellular localization and molecular topology of the dopamine transporter in the striatum and substantia nigra. *J Comp Neurol* **388** (1997), pp. 211-27.

Hill, D.E., Yeo, R.A., Campbell, R.A., Hart, B., Vigil, J. and Brooks, W. Magnetic resonance imaging correlates of attention-deficit/hyperactivity disorder in children. *Neuropsychology* **17** (2003), pp. 496-506.

Hu, B.Y., Weick, J.P., Yu, J., Ma, L.X., Zhang, X.Q., Thomson, J.A. and Zhang, S.C. Neural differentiation of human induced pluripotent stem cells follows developmental principles but with variable potency. *Proc Natl Acad Sci U S A* **107** (2010), pp. 4335-40.

Hwang, D.Y., Ardayfio, P., Kang, U.J., Semina, E.V. and Kim, K.S. Selective loss of dopaminergic neurons in the substantia nigra of Pitx3-deficient aphakia mice. *Brain Res Mol Brain Res* **114** (2003), pp. 123-31.

Hwang, D.Y., Hong, S., Jeong, J.W., Choi, S., Kim, H., Kim, J. and Kim, K.S. Vesicular monoamine transporter 2 and dopamine transporter are molecular targets of Pitx3 in the ventral midbrain dopamine neurons. *J Neurochem* **111** (2009), pp. 1202-12.

Hynes, M., Stone, D.M., Dowd, M., Pitts-Meek, S., Goddard, A., Gurney, A. and Rosenthal, A. Control of cell pattern in the neural tube by the zinc finger transcription factor and oncogene Gli-1. *Neuron* **19** (1997), pp. 15-26.

Ikemoto, S., McBride, W.J., Murphy, J.M., Lumeng, L. and Li, T.K. 6-OHDA-lesions of the nucleus accumbens disrupt the acquisition but not the maintenance of ethanol

consumption in the alcohol-preferring P line of rats. *Alcohol Clin Exp Res* **21** (1997), pp. 1042-6.

Ikemoto, S. and Wise, R.A. Rewarding effects of the cholinergic agents carbachol and neostigmine in the posterior ventral tegmental area. *J Neurosci* **22** (2002), pp. 9895-904.

Illes, S., Theiss, S., Hartung, H.P., Siebler, M. and Dihne, M. Niche-dependent development of functional neuronal networks from embryonic stem cell-derived neural populations. *BMC Neurosci* **10** (2009), p. 93.

Inoue, H., Nojima, H. and Okayama, H. High efficiency transformation of Escherichia coli with plasmids. *Gene* **96** (1990), pp. 23-8.

Jacobs, F.M., van Erp, S., van der Linden, A.J., von Oerthel, L., Burbach, J.P. and Smidt, M.P. Pitx3 potentiates Nurr1 in dopamine neuron terminal differentiation through release of SMRT-mediated repression. *Development* **136** (2009), pp. 531-40.

Jaskiw, G.E., Karoum, F.K. and Weinberger, D.R. Persistent elevations in dopamine and its metabolites in the nucleus accumbens after mild subchronic stress in rats with ibotenic acid lesions of the medial prefrontal cortex. *Brain Res* **534** (1990), pp. 321-3.

Johnson, M.A., Weick, J.P., Pearce, R.A. and Zhang, S.C. Functional neural development from human embryonic stem cells: accelerated synaptic activity via astrocyte coculture. *J Neurosci* **27** (2007), pp. 3069-77.

Jones, S.R., Gainetdinov, R.R., Jaber, M., Giros, B., Wightman, R.M. and Caron, M.G. Profound neuronal plasticity in response to inactivation of the dopamine transporter. *Proc Natl Acad Sci U S A* **95** (1998), pp. 4029-34.

Joseph, J.D., Wang, Y.M., Miles, P.R., Budygin, E.A., Picetti, R., Gainetdinov, R.R., Caron, M.G. and Wightman, R.M. Dopamine autoreceptor regulation of release and uptake in mouse brain slices in the absence of D(3) receptors. *Neuroscience* **112** (2002), pp. 39-49.

Kadkhodaei, B., Ito, T., Joodmardi, E., Mattsson, B., Rouillard, C., Carta, M., Muramatsu, S., Sumi-Ichinose, C., Nomura, T., Metzger, D., Chambon, P., Lindqvist, E., Larsson, N.G., Olson, L., Bjorklund, A., Ichinose, H. and Perlmann, T. Nurr1 is required for maintenance of maturing and adult midbrain dopamine neurons. *J Neurosci* **29** (2009), pp. 15923-32.

Kalir, H.H. and Mytilineou, C. Ascorbic acid in mesencephalic cultures: effects on dopaminergic neuron development. *J Neurochem* **57** (1991), pp. 458-64.

Kang, L., Wang, J., Zhang, Y., Kou, Z. and Gao, S. iPS cells can support full-term development of tetraploid blastocyst-complemented embryos. *Cell Stem Cell* **5** (2009), pp. 135-8.

Kawaguchi, A., Miyata, T., Sawamoto, K., Takashita, N., Murayama, A., Akamatsu, W., Ogawa, M., Okabe, M., Tano, Y., Goldman, S.A. and Okano, H. Nestin-EGFP transgenic mice: visualization of the self-renewal and multipotency of CNS stem cells. *Mol Cell Neurosci* **17** (2001), pp. 259-73.

Kawasaki, H., Mizuseki, K., Nishikawa, S., Kaneko, S., Kuwana, Y., Nakanishi, S., Nishikawa, S.I. and Sasai, Y. Induction of midbrain dopaminergic neurons from ES cells by stromal cell-derived inducing activity. *Neuron* **28** (2000), pp. 31-40.

Kawasaki, H., Suemori, H., Mizuseki, K., Watanabe, K., Urano, F., Ichinose, H., Haruta, M., Takahashi, M., Yoshikawa, K., Nishikawa, S., Nakatsuji, N. and Sasai, Y. Generation of dopaminergic neurons and pigmented epithelia from primate ES cells by stromal cell-derived inducing activity. *Proc Natl Acad Sci U S A* **99** (2002), pp. 1580-5.

Kebabian, J.W., Petzold, G.L. and Greengard, P. Dopamine-sensitive adenylate cyclase in caudate nucleus of rat brain, and its similarity to the "dopamine receptor". *Proc Natl Acad Sci U S A* **69** (1972), pp. 2145-9.

Khan, Z.U., Mrzljak, L., Gutierrez, A., de la Calle, A. and Goldman-Rakic, P.S. Prominence of the dopamine D2 short isoform in dopaminergic pathways. *Proc Natl Acad Sci U S A* **95** (1998), pp. 7731-6.

Khoo, M.L., McQuade, L.R., Smith, M.S., Lees, J.G., Sidhu, K.S. and Tuch, B.E. Growth and differentiation of embryoid bodies derived from human embryonic stem cells: effect of glucose and basic fibroblast growth factor. *Biol Reprod* **73** (2005), pp. 1147-56.

Kim, D., Kim, C.H., Moon, J.I., Chung, Y.G., Chang, M.Y., Han, B.S., Ko, S., Yang, E., Cha, K.Y., Lanza, R. and Kim, K.S. Generation of human induced pluripotent stem cells by direct delivery of reprogramming proteins. *Cell Stem Cell* **4** (2009), pp. 472-6.

Kim, J.H., Auerbach, J.M., Rodriguez-Gomez, J.A., Velasco, I., Gavin, D., Lumelsky, N., Lee, S.H., Nguyen, J., Sanchez-Pernaute, R., Bankiewicz, K. and McKay, R. Dopamine neurons derived from embryonic stem cells function in an animal model of Parkinson's disease. *Nature* **418** (2002), pp. 50-6.

Kim, K.S. Induced pluripotent stem (iPS) cells and their future in psychiatry. *Neuropsychopharmacology* **35** (2010), pp. 346-8.

Knaus, P., Betz, H. and Rehm, H. Expression of synaptophysin during postnatal development of the mouse brain. *J Neurochem* **47** (1986), pp. 1302-4.

Kurosawa, H. Methods for inducing embryoid body formation: in vitro differentiation system of embryonic stem cells. *J Biosci Bioeng* **103** (2007), pp. 389-98.

Kwon, G.S., Fraser, S.T., Eakin, G.S., Mangano, M., Isern, J., Sahr, K.E., Hadjantonakis, A.K. and Baron, M.H. Tg(Afp-GFP) expression marks primitive and definitive endoderm lineages during mouse development. *Dev Dyn* **235** (2006), pp. 2549-58.

Lacey, M.G., Mercuri, N.B. and North, R.A. Dopamine acts on D2 receptors to increase potassium conductance in neurones of the rat substantia nigra zona compacta. *J Physiol* **392** (1987), pp. 397-416.

Lau, T., Adam, S. and Schloss, P. Rapid and efficient differentiation of dopaminergic neurons from mouse embryonic stem cells. *Neuroreport* **17** (2006), pp. 975-9.

Leahy, A., Xiong, J.W., Kuhnert, F. and Stuhlmann, H. Use of developmental marker genes to define temporal and spatial patterns of differentiation during embryoid body formation. *J Exp Zool* **284** (1999), pp. 67-81.

Lecomte, F.J., Ismail, N. and High, S. Making membrane proteins at the mammalian endoplasmic reticulum. *Biochem Soc Trans* **31** (2003), pp. 1248-52.

Lee, E.C., Yu, D., Martinez de Velasco, J., Tessarollo, L., Swing, D.A., Court, D.L., Jenkins, N.A. and Copeland, N.G. A highly efficient Escherichia coli-based chromosome engineering system adapted for recombinogenic targeting and subcloning of BAC DNA. *Genomics* **73** (2001), pp. 56-65.

Lee, G., Papapetrou, E.P., Kim, H., Chambers, S.M., Tomishima, M.J., Fasano, C.A., Ganat, Y.M., Menon, J., Shimizu, F., Viale, A., Tabar, V., Sadelain, M. and Studer, L. Modelling pathogenesis and treatment of familial dysautonomia using patient-specific iPSCs. *Nature* **461** (2009), pp. 402-6.

Lee, M.K., Tuttle, J.B., Rebhun, L.I., Cleveland, D.W. and Frankfurter, A. The expression and posttranslational modification of a neuron-specific beta-tubulin isotype during chick embryogenesis. *Cell Motil Cytoskeleton* **17** (1990), pp. 118-32.

Lee, S.H., Lumelsky, N., Studer, L., Auerbach, J.M. and McKay, R.D. Efficient generation of midbrain and hindbrain neurons from mouse embryonic stem cells. *Nat Biotechnol* **18** (2000), pp. 675-9.

Lee, S.M., Danielian, P.S., Fritzsch, B. and McMahon, A.P. Evidence that FGF8 signalling from the midbrain-hindbrain junction regulates growth and polarity in the developing midbrain. *Development* **124** (1997), pp. 959-69

Lendahl, U., Zimmerman, L.B. and McKay, R.D. CNS stem cells express a new class of intermediate filament protein. *Cell* **60** (1990), pp. 585-95.

Letourneau, P.C., Condic, M.L. and Snow, D.M. Interactions of developing neurons with the extracellular matrix. *J Neurosci* **14** (1994), pp. 915-28.

Li, M., Pevny, L., Lovell-Badge, R. and Smith, A. Generation of purified neural precursors from embryonic stem cells by lineage selection. *Curr Biol* **8** (1998), pp. 971-4.

Li, W. and Ding, S. Small molecules that modulate embryonic stem cell fate and somatic cell reprogramming. *Trends Pharmacol Sci* **31** (2010), pp. 36-45.

Lidow, M.S., Koh, P.O. and Arnsten, A.F. D1 dopamine receptors in the mouse prefrontal cortex: Immunocytochemical and cognitive neuropharmacological analyses. *Synapse* **47** (2003), pp. 101-8.

Limousin, P., Krack, P., Pollak, P., Benazzouz, A., Ardouin, C., Hoffmann, D. and Benabid, A.L. Electrical stimulation of the subthalamic nucleus in advanced Parkinson's disease. *N Engl J Med* **339** (1998), pp. 1105-11.

Liu, A. and Joyner, A.L. EN and GBX2 play essential roles downstream of FGF8 in patterning the mouse mid/hindbrain region. *Development* **128** (2001), pp. 181-91.

Liu, P., Jenkins, N.A. and Copeland, N.G. A highly efficient recombineering-based method for generating conditional knockout mutations. *Genome Res* **13** (2003), pp. 476-84.

Liu, Y., Han, S.S., Wu, Y., Tuohy, T.M., Xue, H., Cai, J., Back, S.A., Sherman, L.S., Fischer, I. and Rao, M.S. CD44 expression identifies astrocyte-restricted precursor cells. *Dev Biol* **276** (2004), pp. 31-46.

Lorincz, M.T. Optimized neuronal differentiation of murine embryonic stem cells: role of cell density. *Methods Mol Biol* **330** (2006), pp. 55-69.

Lu, X.H., Fleming, S.M., Meurers, B., Ackerson, L.C., Mortazavi, F., Lo, V., Hernandez, D., Sulzer, D., Jackson, G.R., Maidment, N.T., Chesselet, M.F. and Yang, X.W. Bacterial artificial chromosome transgenic mice expressing a truncated mutant parkin exhibit age-

dependent hypokinetic motor deficits, dopaminergic neuron degeneration, and accumulation of proteinase K-resistant alpha-synuclein. *J Neurosci* **29** (2009), pp. 1962-76.

Ma, S.Y., Rinne, J.O., Collan, Y., Roytta, M. and Rinne, U.K. A quantitative morphometrical study of neuron degeneration in the substantia nigra in Parkinson's disease. *J Neurol Sci* **140** (1996), pp. 40-5.

Maherali, N., Sridharan, R., Xie, W., Utikal, J., Eminli, S., Arnold, K., Stadtfeld, M., Yachechko, R., Tchieu, J., Jaenisch, R., Plath, K. and Hochedlinger, K. Directly reprogrammed fibroblasts show global epigenetic remodeling and widespread tissue contribution. *Cell Stem Cell* **1** (2007), pp. 55-70.

Marchetto, M.C., Carromeu, C., Acab, A., Yu, D., Yeo, G.W., Mu, Y., Chen, G., Gage, F.H. and Muotri, A.R. A model for neural development and treatment of Rett syndrome using human induced pluripotent stem cells. *Cell* **143** (2010), pp. 527-39.

Marqueze-Pouey, B., Wisden, W., Malosio, M.L. and Betz, H. Differential expression of synaptophysin and synaptoporin mRNAs in the postnatal rat central nervous system. *J Neurosci* **11** (1991), pp. 3388-97.

Martin, G.R. Isolation of a pluripotent cell line from early mouse embryos cultured in medium conditioned by teratocarcinoma stem cells. *Proc Natl Acad Sci U S A* **78** (1981), pp. 7634-8.

Martinat, C., Bacci, J.J., Leete, T., Kim, J., Vanti, W.B., Newman, A.H., Cha, J.H., Gether, U., Wang, H. and Abeliovich, A. Cooperative transcription activation by Nurr1 and Pitx3 induces embryonic stem cell maturation to the midbrain dopamine neuron phenotype. *Proc Natl Acad Sci U S A* **103** (2006), pp. 2874-9.

Martinat, C., Shendelman, S., Jonason, A., Leete, T., Beal, M.F., Yang, L., Floss, T. and Abeliovich, A. Sensitivity to oxidative stress in DJ-1-deficient dopamine neurons: an ES-derived cell model of primary Parkinsonism. *PLoS Biol* **2** (2004), p. e327.

Martinez, S., Crossley, P.H., Cobos, I., Rubenstein, J.L. and Martin, G.R. FGF8 induces formation of an ectopic isthmic organizer and isthmocerebellar development via a repressive effect on Otx2 expression. *Development* **126** (1999), pp. 1189-200.

Mauch, D.H., Nagler, K., Schumacher, S., Goritz, C., Muller, E.C., Otto, A. and Pfrieger, F.W. CNS synaptogenesis promoted by glia-derived cholesterol. *Science* **294** (2001), pp. 1354-7.

Maxwell, S.L., Ho, H.Y., Kuehner, E., Zhao, S. and Li, M. Pitx3 regulates tyrosine hydroxylase expression in the substantia nigra and identifies a subgroup of mesencephalic dopaminergic progenitor neurons during mouse development. *Dev Biol* **282** (2005), pp. 467-79.

Mercuri, N.B., Saiardi, A., Bonci, A., Picetti, R., Calabresi, P., Bernardi, G. and Borrelli, E. Loss of autoreceptor function in dopaminergic neurons from dopamine D2 receptor deficient mice. *Neuroscience* **79** (1997), pp. 323-7.

Millet, S., Campbell, K., Epstein, D.J., Losos, K., Harris, E. and Joyner, A.L. A role for Gbx2 in repression of Otx2 and positioning the mid/hindbrain organizer. *Nature* **401** (1999), pp. 161-4.

Mitsui, K., Tokuzawa, Y., Itoh, H., Segawa, K., Murakami, M., Takahashi, K., Maruyama, M., Maeda, M. and Yamanaka, S. The homeoprotein Nanog is required for maintenance of pluripotency in mouse epiblast and ES cells. *Cell* **113** (2003), pp. 631-42.

Mizoguchi, K., Shoji, H., Tanaka, Y., Maruyama, W. and Tabira, T. Age-related spatial working memory impairment is caused by prefrontal cortical dopaminergic dysfunction in rats. *Neuroscience* **162** (2009), pp. 1192-201.

Mizoguchi, K., Yuzurihara, M., Ishige, A., Sasaki, H., Chui, D.H. and Tabira, T. Chronic stress induces impairment of spatial working memory because of prefrontal dopaminergic dysfunction. *J Neurosci* **20** (2000), pp. 1568-74.

Mogi, A., Ichikawa, H., Matsumoto, C., Hieda, T., Tomotsune, D., Sakaki, S., Yamada, S. and Sasaki, K. The method of mouse embryoid body establishment affects structure and developmental gene expression. *Tissue Cell* **41** (2009), pp. 79-84.

Moron, J.A., Brockington, A., Wise, R.A., Rocha, B.A. and Hope, B.T. Dopamine uptake through the norepinephrine transporter in brain regions with low levels of the dopamine transporter: evidence from knock-out mouse lines. *J Neurosci* **22** (2002), pp. 389-95.

Morrison, S.L. Transformation of E. coli by electroporation. *Curr Protoc Immunol* **Appendix 3** (2001), p. Appendix 3N.

Murphy, M., Drago, J. and Bartlett, P.F. Fibroblast growth factor stimulates the proliferation and differentiation of neural precursor cells in vitro. *J Neurosci Res* **25** (1990), pp. 463-75.

Neisser, U., Cognitive Psychology. Prentice-Hall, Englewood Cliffs, NJ (1967).

Nelson, E.L., Liang, C.L., Sinton, C.M. and German, D.C. Midbrain dopaminergic neurons in the mouse: computer-assisted mapping. *J Comp Neurol* **369** (1996), pp. 361-71.

Nguyen, H.N., Byers, B., Cord, B., Shcheglovitov, A., Byrne, J., Gujar, P., Kee, K., Schüle, B., Dolmetsch, R.E., Langston, W., Palmer, T.D. and Pera, R.R. LRRK2 Mutant iPSC-Derived DA Neurons Demonstrate Increased Susceptibility to Oxidative Stress. *Cell Stem Cell* **8** (2011), pp. 267-80.

Nishi, A., Snyder, G.L. and Greengard, P. Bidirectional regulation of DARPP-32 phosphorylation by dopamine. *J Neurosci* **17** (1997), pp. 8147-55.

Niwa, H., Miyazaki, J. and Smith, A.G. Quantitative expression of Oct-3/4 defines differentiation, dedifferentiation or self-renewal of ES cells. *Nat Genet* **24** (2000), pp. 372-6.

Nunes, I., Tovmasian, L.T., Silva, R.M., Burke, R.E. and Goff, S.P. Pitx3 is required for development of substantia nigra dopaminergic neurons. *Proc Natl Acad Sci U S A* **100** (2003), pp. 4245-50.

Olanow, C.W. The scientific basis for the current treatment of Parkinson's disease. *Annu Rev Med* **55** (2004), pp. 41-60.

Okabe, S., Forsberg-Nilsson, K., Spiro, A.C., Segal, M. and McKay, R.D. Development of neuronal precursor cells and functional postmitotic neurons from embryonic stem cells in vitro. *Mech Dev* **59** (1996), pp. 89-102.

Okita, K., Ichisaka, T. and Yamanaka, S. Generation of germline-competent induced pluripotent stem cells. *Nature* **448** (2007), pp. 313-7.

Okita, K., Nakagawa, M., Hyenjong, H., Ichisaka, T. and Yamanaka, S. Generation of mouse induced pluripotent stem cells without viral vectors. *Science* **322** (2008), pp. 949-53.

Ormo, M., Cubitt, A.B., Kallio, K., Gross, L.A., Tsien, R.Y. and Remington, S.J. Crystal structure of the Aequorea victoria green fluorescent protein. *Science* **273** (1996), pp. 1392-5.

Park, I.H., Arora, N., Huo, H., Maherali, N., Ahfeldt, T., Shimamura, A., Lensch, M.W., Cowan, C., Hochedlinger, K. and Daley, G.Q. Disease-specific induced pluripotent stem cells. *Cell* **134** (2008a), pp. 877-86.

Park, I.H., Zhao, R., West, J.A., Yabuuchi, A., Huo, H., Ince, T.A., Lerou, P.H., Lensch, M.W. and Daley, G.Q. Reprogramming of human somatic cells to pluripotency with defined factors. *Nature* **451** (2008b), pp. 141-6.

Parmar, M. and Li, M. Early specification of dopaminergic phenotype during ES cell differentiation. *BMC Dev Biol* **7** (2007), p. 86.

Parsons, S.M. Transport mechanisms in acetylcholine and monoamine storage. *FASEB J* **14** (2000), pp. 2423-34.

Pettit, H.O., Ettenberg, A., Bloom, F.E. and Koob, G.F. Destruction of dopamine in the nucleus accumbens selectively attenuates cocaine but not heroin self-administration in rats. *Psychopharmacology (Berl)* **84** (1984), pp. 167-73.

Perrier, A.L., Tabar, V., Barberi, T., Rubio, M.E., Bruses, J., Topf, N., Harrison, N.L. and Studer, L. Derivation of midbrain dopamine neurons from human embryonic stem cells. *Proc Natl Acad Sci U S A* **101** (2004), pp. 12543-8.

Pevny, L.H., Sockanathan, S., Placzek, M. and Lovell-Badge, R. A role for SOX1 in neural determination. *Development* **125** (1998), pp. 1967-78.

Pfaus, J.G., Damsma, G., Wenkstern, D. and Fibiger, H.C. Sexual activity increases dopamine transmission in the nucleus accumbens and striatum of female rats. *Brain Res* **693** (1995), pp. 21-30.

Pfrieger, F.W. and Barres, B.A. Synaptic efficacy enhanced by glial cells in vitro. *Science* **277** (1997), pp. 1684-7.

Pickering, B.M. and Willis, A.E. The implications of structured 5' untranslated regions on translation and disease. *Semin Cell Dev Biol* **16** (2005), pp. 39-47.

Pierce, R.C. and Kumaresan, V. The mesolimbic dopamine system: the final common pathway for the reinforcing effect of drugs of abuse? *Neurosci Biobehav Rev* **30** (2006), pp. 215-38.

Placantonakis, D.G., Tomishima, M.J., Lafaille, F., Desbordes, S.C., Jia, F., Socci, N.D., Viale, A., Lee, H., Harrison, N., Tabar, V. and Studer, L. BAC transgenesis in human embryonic stem cells as a novel tool to define the human neural lineage. *Stem Cells* **27** (2009), pp. 521-32.

Pontieri, F.E., Tanda, G. and Di Chiara, G. Intravenous cocaine, morphine, and amphetamine preferentially increase extracellular dopamine in the "shell" as compared with the "core" of the rat nucleus accumbens. *Proc Natl Acad Sci U S A* **92** (1995), pp. 12304-8.

Prakash, N., Brodski, C., Naserke, T., Puelles, E., Gogoi, R., Hall, A., Panhuysen, M., Echevarria, D., Sussel, L., Weisenhorn, D.M., Martinez, S., Arenas, E., Simeone, A. and Wurst, W. A Wnt1-regulated genetic network controls the identity and fate of midbrain-dopaminergic progenitors in vivo. *Development* **133** (2006), pp. 89-98.

Prakash, N. and Wurst, W. Development of dopaminergic neurons in the mammalian brain. *Cell Mol Life Sci* **63** (2006a), pp. 187-206.

Prakash, N. and Wurst, W. Genetic networks controlling the development of midbrain dopaminergic neurons. *J Physiol* **575** (2006b), pp. 403-10.

Pruszak, J., Sonntag, K.C., Aung, M.H., Sanchez-Pernaute, R. and Isacson, O. Markers and methods for cell sorting of human embryonic stem cell-derived neural cell populations. *Stem Cells* **25** (2007), pp. 2257-68.

Pycock, C.J., Kerwin, R.W. and Carter, C.J. Effect of lesion of cortical dopamine terminals on subcortical dopamine receptors in rats. *Nature* **286** (1980), pp. 74-6.

Reid, B.G. and Flynn, G.C. Chromophore formation in green fluorescent protein. *Biochemistry* **36** (1997), pp. 6786-91.

Rohwedel, J., Sehlmeyer, U., Shan, J., Meister, A. and Wobus, A.M. Primordial germ cell-derived mouse embryonic germ (EG) cells in vitro resemble undifferentiated stem cells with respect to differentiation capacity and cell cycle distribution. *Cell Biol Int* **20** (1996), pp. 579-87.

Rolletschek, A., Blyszczuk, P. and Wobus, A.M. Embryonic stem cell-derived cardiac, neuronal and pancreatic cells as model systems to study toxicological effects. *Toxicol Lett* **149** (2004), pp. 361-9.

Rolletschek, A., Chang, H., Guan, K., Czyz, J., Meyer, M. and Wobus, A.M. Differentiation of embryonic stem cell-derived dopaminergic neurons is enhanced by survival-promoting factors. *Mech Dev* **105** (2001), pp. 93-104.

Rondou, P., Haegeman, G. and Van Craenenbroeck, K. The dopamine D4 receptor: biochemical and signalling properties. *Cell Mol Life Sci* **67** (2010), pp. 1971-86.

Roy, N.S., Cleren, C., Singh, S.K., Yang, L., Beal, M.F. and Goldman, S.A. Functional engraftment of human ES cell-derived dopaminergic neurons enriched by coculture with telomerase-immortalized midbrain astrocytes. *Nat Med* **12** (2006), pp. 1259-68.

Rubia, K., Overmeyer, S., Taylor, E., Brammer, M., Williams, S.C., Simmons, A. and Bullmore, E.T. Hypofrontality in attention deficit hyperactivity disorder during higher-order motor control: a study with functional MRI. *Am J Psychiatry* **156** (1999), pp. 891-6.

Rubin, L.L. Stem cells and drug discovery: the beginning of a new era? *Cell* **132** (2008), pp. 549-52.

Sacchetti, P., Brownschidle, L.A., Granneman, J.G. and Bannon, M.J. Characterization of the 5'-flanking region of the human dopamine transporter gene. *Brain Res Mol Brain Res* **74** (1999), pp. 167-74.

Sacchetti, P., Mitchell, T.R., Granneman, J.G. and Bannon, M.J. Nurr1 enhances transcription of the human dopamine transporter gene through a novel mechanism. *J Neurochem* **76** (2001), pp. 1565-72.

Santa-Olalla, J. and Covarrubias, L. Epidermal growth factor (EGF), transforming growth factor-alpha (TGF-alpha), and basic fibroblast growth factor (bFGF) differentially influence neural precursor cells of mouse embryonic mesencephalon. *J Neurosci Res* **42** (1995), pp. 172-83.

Saucedo-Cardenas, O., Quintana-Hau, J.D., Le, W.D., Smidt, M.P., Cox, J.J., De Mayo, F., Burbach, J.P. and Conneely, O.M. Nurr1 is essential for the induction of the dopaminergic phenotype and the survival of ventral mesencephalic late dopaminergic precursor neurons. *Proc Natl Acad Sci U S A* **95** (1998), pp. 4013-8.

Savelieva, K.V., Caudle, W.M., Findlay, G.S., Caron, M.G. and Miller, G.W. Decreased ethanol preference and consumption in dopamine transporter female knock-out mice. *Alcohol Clin Exp Res* **26** (2002), pp. 758-64.

Schenke-Layland, K., Rhodes, K.E., Angelis, E., Butylkova, Y., Heydarkhan-Hagvall, S., Gekas, C., Zhang, R., Goldhaber, J.I., Mikkola, H.K., Plath, K. and MacLellan, W.R. Reprogrammed mouse fibroblasts differentiate into cells of the cardiovascular and hematopoietic lineages. *Stem Cells* **26** (2008), pp. 1537-46.

Seeman, P., Lee, T., Chau-Wong, M. and Wong, K. Antipsychotic drug doses and neuroleptic/dopamine receptors. *Nature* **261** (1976), pp. 717-9.

Simon, H.H., Saueressig, H., Wurst, W., Goulding, M.D. and O'Leary, D.D. Fate of midbrain dopaminergic neurons controlled by the engrailed genes. *J Neurosci* **21** (2001), pp. 3126-34.

Smidt, M.P., Asbreuk, C.H., Cox, J.J., Chen, H., Johnson, R.L. and Burbach, J.P. A second independent pathway for development of mesencephalic dopaminergic neurons requires Lmx1b. *Nat Neurosci* **3** (2000), pp. 337-41.

Smidt, M.P., Smits, S.M., Bouwmeester, H., Hamers, F.P., van der Linden, A.J., Hellemons, A.J., Graw, J. and Burbach, J.P. Early developmental failure of substantia nigra dopamine neurons in mice lacking the homeodomain gene Pitx3. *Development* **131** (2004), pp. 1145-55.

Smidt, M.P., van Schaick, H.S., Lanctot, C., Tremblay, J.J., Cox, J.J., van der Kleij, A.A., Wolterink, G., Drouin, J. and Burbach, J.P. A homeodomain gene Ptx3 has highly restricted brain expression in mesencephalic dopaminergic neurons. *Proc Natl Acad Sci U S A* **94** (1997), pp. 13305-10.

Smits, S.M., Ponnio, T., Conneely, O.M., Burbach, J.P. and Smidt, M.P. Involvement of Nurr1 in specifying the neurotransmitter identity of ventral midbrain dopaminergic neurons. *Eur J Neurosci* **18** (2003), pp. 1731-8.

Snyder, G.L., Fienberg, A.A., Huganir, R.L. and Greengard, P. A dopamine/D1 receptor/protein kinase A/dopamine- and cAMP-regulated phosphoprotein (Mr 32 kDa)/protein phosphatase-1 pathway regulates dephosphorylation of the NMDA receptor. *J Neurosci* **18** (1998), pp. 10297-303.

Soldner, F., Hockemeyer, D., Beard, C., Gao, Q., Bell, G.W., Cook, E.G., Hargus, G., Blak, A., Cooper, O., Mitalipova, M., Isacson, O. and Jaenisch, R. Parkinson's disease patient-derived induced pluripotent stem cells free of viral reprogramming factors. *Cell* **136** (2009), pp. 964-77.

Solter, D. and Knowles, B.B. Monoclonal antibody defining a stage-specific mouse embryonic antigen (SSEA-1). *Proc Natl Acad Sci U S A* **75** (1978), pp. 5565-9.

Sommer, C.A., Sommer, A.G., Longmire, T.A., Christodoulou, C., Thomas, D.D., Gostissa, M., Alt, F.W., Murphy, G.J., Kotton, D.N. and Mostoslavsky, G. Excision of reprogramming transgenes improves the differentiation potential of iPS cells generated with a single excisable vector. *Stem Cells* **28** (2010), pp. 64-74.

Sommer, C.A., Stadtfeld, M., Murphy, G.J., Hochedlinger, K., Kotton, D.N. and Mostoslavsky, G. Induced pluripotent stem cell generation using a single lentiviral stem cell cassette. *Stem Cells* **27** (2009), pp. 543-9.

Sonntag, K.C., Pruszak, J., Yoshizaki, T., van Arensbergen, J., Sanchez-Pernaute, R. and Isacson, O. Enhanced yield of neuroepithelial precursors and midbrain-like dopaminergic neurons from human embryonic stem cells using the bone morphogenic protein antagonist noggin. *Stem Cells* **25** (2007), pp. 411-8.

Spielewoy, C., Biala, G., Roubert, C., Hamon, M., Betancur, C. and Giros, B. Hypolocomotor effects of acute and daily d-amphetamine in mice lacking the dopamine transporter. *Psychopharmacology (Berl)* **159** (2001), pp. 2-9.

Spielewoy, C., Gonon, F., Roubert, C., Fauchey, V., Jaber, M., Caron, M.G., Roques, B.P., Hamon, M., Betancur, C., Maldonado, R. and Giros, B. Increased rewarding properties of morphine in dopamine-transporter knockout mice. *Eur J Neurosci* **12** (2000), pp. 1827-37.

Stadtfeld, M., Apostolou, E., Akutsu, H., Fukuda, A., Follett, P., Natesan, S., Kono, T., Shioda, T. and Hochedlinger, K. Aberrant silencing of imprinted genes on chromosome 12qF1 in mouse induced pluripotent stem cells. *Nature* **465** (2010a), pp. 175-81.

Stadtfeld, M. and Hochedlinger, K. Induced pluripotency: history, mechanisms, and applications. *Genes Dev* **24** (2010), pp. 2239-63.

Stadtfeld, M., Maherali, N., Borkent, M. and Hochedlinger, K. A reprogrammable mouse strain from gene-targeted embryonic stem cells. *Nat Methods* **7** (2010b), pp. 53-5.

Stadtfeld, M., Maherali, N., Breault, D.T. and Hochedlinger, K. Defining molecular cornerstones during fibroblast to iPS cell reprogramming in mouse. *Cell Stem Cell* **2** (2008a), pp. 230-40.

Stadtfeld, M., Nagaya, M., Utikal, J., Weir, G. and Hochedlinger, K. Induced pluripotent stem cells generated without viral integration. *Science* **322** (2008b), pp. 945-9.

Stavridis, M.P. and Smith, A.G. Neural differentiation of mouse embryonic stem cells. *Biochem Soc Trans* **31** (2003), pp. 45-9.

Stoof, J.C. and Kebabian, J.W. Opposing roles for D-1 and D-2 dopamine receptors in efflux of cyclic AMP from rat neostriatum. *Nature* **294** (1981), pp. 366-8.

Surmeier, D.J., Bargas, J., Hemmings, H.C., Jr., Nairn, A.C. and Greengard, P. Modulation of calcium currents by a D1 dopaminergic protein kinase/phosphatase cascade in rat neostriatal neurons. *Neuron* **14** (1995), pp. 385-97.

Surmeier, D.J., Eberwine, J., Wilson, C.J., Cao, Y., Stefani, A. and Kitai, S.T. Dopamine receptor subtypes colocalize in rat striatonigral neurons. *Proc Natl Acad Sci U S A* **89** (1992), pp. 10178-82.

Takahashi, K. and Yamanaka, S. Induction of pluripotent stem cells from mouse embryonic and adult fibroblast cultures by defined factors. *Cell* **126** (2006), pp. 663-76.

Tchieu, J., Kuoy, E., Chin, M.H., Trinh, H., Patterson, M., Sherman, S.P., Aimiuwu, O., Lindgren, A., Hakimian, S., Zack, J.A., Clark, A.T., Pyle, A.D., Lowry, W.E. and Plath, K. Female human iPSCs retain an inactive X chromosome. *Cell Stem Cell* **7** (2010), pp. 329-42.

Thomson, J.A., Itskovitz-Eldor, J., Shapiro, S.S., Waknitz, M.A., Swiergiel, J.J., Marshall, V.S. and Jones, J.M. Embryonic stem cell lines derived from human blastocysts. *Science* **282** (1998), pp. 1145-7.

Thomson, J.A., Kalishman, J., Golos, T.G., Durning, M., Harris, C.P., Becker, R.A. and Hearn, J.P. Isolation of a primate embryonic stem cell line. *Proc Natl Acad Sci U S A* **92** (1995), pp. 7844-8.

Tomishima, M.J., Hadjantonakis, A.K., Gong, S. and Studer, L. Production of green fluorescent protein transgenic embryonic stem cells using the GENSAT bacterial artificial chromosome library. *Stem Cells* **25** (2007), pp. 39-45.

Tompers, D.M. and Labosky, P.A. Electroporation of murine embryonic stem cells: a step-by-step guide. *Stem Cells* **22** (2004), pp. 243-9.

Torres, G.E., Gainetdinov, R.R. and Caron, M.G. Plasma membrane monoamine transporters: structure, regulation and function. *Nat Rev Neurosci* **4** (2003), pp. 13-25.

Trokovic, R., Trokovic, N., Hernesniemi, S., Pirvola, U., Vogt Weisenhorn, D.M., Rossant, J., McMahon, A.P., Wurst, W. and Partanen, J. FGFR1 is independently required in both developing mid- and hindbrain for sustained response to isthmic signals. *EMBO J* **22** (2003), pp. 1811-23.

Tsien, R.Y. The green fluorescent protein. *Annu Rev Biochem* **67** (1998), pp. 509-44.

Tunbridge, E.M., Bannerman, D.M., Sharp, T. and Harrison, P.J. Catechol-o-methyltransferase inhibition improves set-shifting performance and elevates stimulated dopamine release in the rat prefrontal cortex. *J Neurosci* **24** (2004), pp. 5331-5.

Tunbridge, E.M., Harrison, P.J. and Weinberger, D.R. Catechol-o-methyltransferase, cognition, and psychosis: Val158Met and beyond. *Biol Psychiatry* **60** (2006), pp. 141-51.

Turiault, M., Parnaudeau, S., Milet, A., Parlato, R., Rouzeau, J.D., Lazar, M. and Tronche, F. Analysis of dopamine transporter gene expression pattern -- generation of DAT-iCre transgenic mice. *FEBS J* **274** (2007), pp. 3568-77.

Utikal, J., Maherali, N., Kulalert, W. and Hochedlinger, K. Sox2 is dispensable for the reprogramming of melanocytes and melanoma cells into induced pluripotent stem cells. *J Cell Sci* **122** (2009), pp. 3502-10.

van den Munckhof, P., Luk, K.C., Ste-Marie, L., Montgomery, J., Blanchet, P.J., Sadikot, A.F. and Drouin, J. Pitx3 is required for motor activity and for survival of a subset of midbrain dopaminergic neurons. *Development* **130** (2003), pp. 2535-42.

Vazin, T., Chen, J., Lee, C.T., Amable, R. and Freed, W.J. Assessment of stromal-derived inducing activity in the generation of dopaminergic neurons from human embryonic stem cells. *Stem Cells* **26** (2008), pp. 1517-25.

Vembar, S.S. and Brodsky, J.L. One step at a time: endoplasmic reticulum-associated degradation. *Nat Rev Mol Cell Biol* **9** (2008), pp. 944-57.

Vernay, B., Koch, M., Vaccarino, F., Briscoe, J., Simeone, A., Kageyama, R. and Ang, S.L. Otx2 regulates subtype specification and neurogenesis in the midbrain. *J Neurosci* **25** (2005), pp. 4856-67.

Vial, D. and Piomelli, D. Dopamine D2 receptors potentiate arachidonate release via activation of cytosolic, arachidonate-specific phospholipase A2. *J Neurochem* **64** (1995), pp. 2765-72.

Vijayraghavan, S., Wang, M., Birnbaum, S.G., Williams, G.V. and Arnsten, A.F. Inverted-U dopamine D1 receptor actions on prefrontal neurons engaged in working memory. *Nat Neurosci* **10** (2007), pp. 376-84.

Volkow, N.D., Wang, G., Fowler, J.S., Logan, J., Gerasimov, M., Maynard, L., Ding, Y., Gatley, S.J., Gifford, A. and Franceschi, D. Therapeutic doses of oral methylphenidate significantly increase extracellular dopamine in the human brain. *J Neurosci* **21** (2001), p. RC121.

Volkow, N.D., Wang, G.J., Fowler, J.S., Gatley, S.J., Logan, J., Ding, Y.S., Hitzemann, R. and Pappas, N. Dopamine transporter occupancies in the human brain induced by therapeutic doses of oral methylphenidate. *Am J Psychiatry* **155** (1998), pp. 1325-31.

Waites, C.L., Craig, A.M. and Garner, C.C. Mechanisms of vertebrate synaptogenesis. *Annu Rev Neurosci* **28** (2005), pp. 251-74.

Wallen, A., Zetterstrom, R.H., Solomin, L., Arvidsson, M., Olson, L. and Perlmann, T. Fate of mesencephalic AHD2-expressing dopamine progenitor cells in NURR1 mutant mice. *Exp Cell Res* **253** (1999), pp. 737-46.

Wallen, A.A., Castro, D.S., Zetterstrom, R.H., Karlen, M., Olson, L., Ericson, J. and Perlmann, T. Orphan nuclear receptor Nurr1 is essential for Ret expression in midbrain dopamine neurons and in the brain stem. *Mol Cell Neurosci* **18** (2001), pp. 649-63.

Warren, L., Manos, P.D., Ahfeldt, T., Loh, Y.H., Li, H., Lau, F., Ebina, W., Mandal, P.K., Smith, Z.D., Meissner, A., Daley, G.Q., Brack, A.S., Collins, J.J., Cowan, C., Schlaeger, T.M. and Rossi, D.J. Highly efficient reprogramming to pluripotency and directed differentiation of human cells with synthetic modified mRNA. *Cell Stem Cell* **7** (2010), pp. 618-30.

Wernig, M., Meissner, A., Foreman, R., Brambrink, T., Ku, M., Hochedlinger, K., Bernstein, B.E. and Jaenisch, R. In vitro reprogramming of fibroblasts into a pluripotent ES-cell-like state. *Nature* **448** (2007), pp. 318-24.

Wernig, M., Tucker, K.L., Gornik, V., Schneiders, A., Buschwald, R., Wiestler, O.D., Barde, Y.A. and Brustle, O. Tau EGFP embryonic stem cells: an efficient tool for neuronal lineage selection and transplantation. *J Neurosci Res* **69** (2002), pp. 918-24.

Wernig, M., Zhao, J.P., Pruszak, J., Hedlund, E., Fu, D., Soldner, F., Broccoli, V., Constantine-Paton, M., Isacson, O. and Jaenisch, R. Neurons derived from reprogrammed fibroblasts functionally integrate into the fetal brain and improve symptoms of rats with Parkinson's disease. *Proc Natl Acad Sci U S A* **105** (2008), pp. 5856-61.

Weinberger, D.R. Implications of normal brain development for the pathogenesis of schizophrenia. *Arch Gen Psychiatry* **44** (1987), pp. 660-9.

Wenkstern, D., Pfaus, J.G. and Fibiger, H.C. Dopamine transmission increases in the nucleus accumbens of male rats during their first exposure to sexually receptive female rats. *Brain Res* **618** (1993), pp. 41-6.

Wichterle, H. and Przedborski, S. What can pluripotent stem cells teach us about neurodegenerative diseases? *Nat Neurosci* **13** (2010), pp. 800-4.

Wiese, C., Rolletschek, A., Kania, G., Blyszczuk, P., Tarasov, K.V., Tarasova, Y., Wersto, R.P., Boheler, K.R. and Wobus, A.M. Nestin expression--a property of multi-lineage progenitor cells? *Cell Mol Life Sci* **61** (2004), pp. 2510-22.

Winnier, G., Blessing, M., Labosky, P.A. and Hogan, B.L. Bone morphogenetic protein-4 is required for mesoderm formation and patterning in the mouse. *Genes Dev* **9** (1995), pp. 2105-16.

Winterer, G. and Weinberger, D.R. Genes, dopamine and cortical signal-to-noise ratio in schizophrenia. *Trends Neurosci* **27** (2004), pp. 683-90.

Wise, R.A. Brain reward circuitry: insights from unsensed incentives. *Neuron* **36** (2002), pp. 229-40.

Wise, R.A. Dopamine, learning and motivation. *Nat Rev Neurosci* **5** (2004), pp. 483-94.

Wise, R.A. Roles for nigrostriatal--not just mesocorticolimbic--dopamine in reward and addiction. *Trends Neurosci* **32** (2009), pp. 517-24.

Wise, R.A. and Schwartz, H.V. Pimozide attenuates acquisition of lever-pressing for food in rats. *Pharmacol Biochem Behav* **15** (1981), pp. 655-6.

Wise, R.A., Spindler, J., deWit, H. and Gerberg, G.J. Neuroleptic-induced "anhedonia" in rats: pimozide blocks reward quality of food. *Science* **201** (1978), pp. 262-4.

Witkovsky, P. Dopamine and retinal function. *Doc Ophthalmol* **108** (2004), pp. 17-40.

Wobus, A.M. and Boheler, K.R. Embryonic stem cells: prospects for developmental biology and cell therapy. *Physiol Rev* **85** (2005), pp. 635-78.

Wood, H.B. and Episkopou, V. Comparative expression of the mouse Sox1, Sox2 and Sox3 genes from pre-gastrulation to early somite stages. *Mech Dev* **86** (1999), pp. 197-201.

Wu, H., Xu, J., Pang, Z.P., Ge, W., Kim, K.J., Blanchi, B., Chen, C., Sudhof, T.C. and Sun, Y.E. Integrative genomic and functional analyses reveal neuronal subtype differentiation bias in human embryonic stem cell lines. *Proc Natl Acad Sci U S A* **104** (2007), pp. 13821-6.

Yamanaka, S. A fresh look at iPS cells. *Cell* **137** (2009), pp. 13-7.

Ye, W., Shimamura, K., Rubenstein, J.L., Hynes, M.A. and Rosenthal, A. FGF and Shh signals control dopaminergic and serotonergic cell fate in the anterior neural plate. *Cell* **93** (1998), pp. 755-66.

Ying, Q.L. and Smith, A.G. Defined conditions for neural commitment and differentiation. *Methods Enzymol* **365** (2003), pp. 327-41.

Ying, Q.L., Stavridis, M., Griffiths, D., Li, M. and Smith, A. Conversion of embryonic stem cells into neuroectodermal precursors in adherent monoculture. *Nat Biotechnol* **21** (2003), pp. 183-6.

Yoshizaki, T., Inaji, M., Kouike, H., Shimazaki, T., Sawamoto, K., Ando, K., Date, I., Kobayashi, K., Suhara, T., Uchiyama, Y. and Okano, H. Isolation and transplantation of dopaminergic neurons generated from mouse embryonic stem cells. *Neurosci Lett* **363** (2004), pp. 33-7.

Yu, D., Ellis, H.M., Lee, E.C., Jenkins, N.A., Copeland, N.G. and Court, D.L. An efficient recombination system for chromosome engineering in Escherichia coli. *Proc Natl Acad Sci U S A* **97** (2000), pp. 5978-83.

Yu, J., Hu, K., Smuga-Otto, K., Tian, S., Stewart, R., Slukvin, II and Thomson, J.A. Human induced pluripotent stem cells free of vector and transgene sequences. *Science* **324** (2009), pp. 797-801.

Yu, J., Vodyanik, M.A., Smuga-Otto, K., Antosiewicz-Bourget, J., Frane, J.L., Tian, S., Nie, J., Jonsdottir, G.A., Ruotti, V., Stewart, R., Slukvin, II and Thomson, J.A. Induced pluripotent stem cell lines derived from human somatic cells. *Science* **318** (2007), pp. 1917-20.

Zahrt, J., Taylor, J.R., Mathew, R.G. and Arnsten, A.F. Supranormal stimulation of D1 dopamine receptors in the rodent prefrontal cortex impairs spatial working memory performance. *J Neurosci* **17** (1997), pp. 8528-35.

Zeng, X., Cai, J., Chen, J., Luo, Y., You, Z.B., Fotter, E., Wang, Y., Harvey, B., Miura, T., Backman, C., Chen, G.J., Rao, M.S. and Freed, W.J. Dopaminergic differentiation of human embryonic stem cells. *Stem Cells* **22** (2004), pp. 925-40.

Zetterstrom, R.H., Solomin, L., Jansson, L., Hoffer, B.J., Olson, L. and Perlmann, T. Dopamine neuron agenesis in Nurr1-deficient mice. *Science* **276** (1997), pp. 248-50.

Zetterstrom, R.H., Williams, R., Perlmann, T. and Olson, L. Cellular expression of the immediate early transcription factors Nurr1 and NGFI-B suggests a gene regulatory role in

several brain regions including the nigrostriatal dopamine system. *Brain Res Mol Brain Res* **41** (1996), pp. 111-20.

Zhang, J., Wilson, G.F., Soerens, A.G., Koonce, C.H., Yu, J., Palecek, S.P., Thomson, J.A. and Kamp, T.J. Functional cardiomyocytes derived from human induced pluripotent stem cells. *Circ Res* **104** (2009), pp. e30-41.

Zhang, X.M., Ng, A.H., Tanner, J.A., Wu, W.T., Copeland, N.G., Jenkins, N.A. and Huang, J.D. Highly restricted expression of Cre recombinase in cerebellar Purkinje cells. *Genesis* **40** (2004), pp. 45-51.

Zhao, S., Maxwell, S., Jimenez-Beristain, A., Vives, J., Kuehner, E., Zhao, J., O'Brien, C., de Felipe, C., Semina, E. and Li, M. Generation of embryonic stem cells and transgenic mice expressing green fluorescence protein in midbrain dopaminergic neurons. *Eur J Neurosci* **19** (2004), pp. 1133-40.

Zhao, X.Y., Li, W., Lv, Z., Liu, L., Tong, M., Hai, T., Hao, J., Guo, C.L., Ma, Q.W., Wang, L., Zeng, F. and Zhou, Q. iPS cells produce viable mice through tetraploid complementation. *Nature* **461** (2009), pp. 86-90.

Zhou, H., Wu, S., Joo, J.Y., Zhu, S., Han, D.W., Lin, T., Trauger, S., Bien, G., Yao, S., Zhu, Y., Siuzdak, G., Scholer, H.R., Duan, L. and Ding, S. Generation of induced pluripotent stem cells using recombinant proteins. *Cell Stem Cell* **4** (2009), pp. 381-4.

Zhou, W. and Freed, C.R. Adenoviral gene delivery can reprogram human fibroblasts to induced pluripotent stem cells. *Stem Cells* **27** (2009), pp. 2667-74.

Zhou, W., Lee, Y.M., Guy, V.C. and Freed, C.R. Embryonic stem cells with GFP knocked into the dopamine transporter yield purified dopamine neurons in vitro and from knock-in mice. *Stem Cells* **27** (2009), pp. 2952-61.

Zhuang, X., Masson, J., Gingrich, J.A., Rayport, S. and Hen, R. Targeted gene expression in dopamine and serotonin neurons of the mouse brain. *J Neurosci Methods* **143** (2005), pp. 27-32.